申报	系列：教师系列教学科研并重型
	专业：林木遗传育种
	职称：副教授

业绩成果材料

（申报人的业绩成果材料包括论文、科研项目、获奖以及其他成果等）

单　位（二级单位）：林学与风景园林学院

姓　名　　龙健梅

材料核对人：　　单位盖章：

核对时间：

华南农业大学制

目　录

一、教学研究业绩

二、科研项目

三、论文、著作等

华南农业大学文件

华南农教〔2020〕41号

关于公布华南农业大学2020年度校级质量工程和教改项目立项的通知

各学院、部处、各单位:

根据《教育部关于加快建设高水平本科教育全面提高人才培养能力的意见》(教高〔2018〕2号)和《广东省普通本科高校“十三五”教学质量与教学改革工程建设实施方案(修订)》(粤教高〔2019〕6号)精神，以及学校《关于开展2020年校级本科教学类项目申报工作的通知》等要求，为进一步推进学校教学改革，建设一流本科教育，提升人才培养质量，学校组织开展了2020年度校级质量工程和教改项目遴选工作。

经项目负责人申请、所在单位推荐、学校组织专家评审、校内公示无异议等程序，确定“新兽医人才实验班”等49个项目为2020年度校级质量工程项目；确定“基于大规模在线开放课程的线上金课建设探索--以《压花艺术》课程为例”等195个项目为2020年度校级教改项目。其中，针对学校本科人才培养改

革重点领域，本年度特设思政改革专项45项（思政课程12项，课程思政33项），金课改革专项39项，四新改革专项39项。具体立项情况详见附件1和附件2。

请各项目负责人按照项目建设任务及要求，及时开展各项工作，加快推进学校人才培养改革，并力争取得高水平的教学成果。各单位要切实加强对项目建设的督促、指导，以确保项目能如期高质量完成。

特此通知。

附件：1. 华南农业大学2020年校级质量工程立项名单

2. 华南农业大学2020年校级教改项目立项名单

华南农业大学

2020年9月1日

（联系人：曹广祥、李艳丽，电　话：85280052）

公开方式：主动公开

华南农业大学党政办公室　　2020年9月2日印发

华南农业大学2020年校级教改项目立项名单

项目编号	项目名称	申报人	项目类别	专项类别
JG20001	基于大规模在线开放课程的线上“金课”建设探索--以“压花艺术”课程为例	陈国菊	重点项目	金课改革
JG20002	数学类课程线上线下混合教学的探究与实践	江雪萍	重点项目	金课改革
JG20003	基于高阶性、创新性与挑战度“三位一体”的“金课”改革研究与实践——以《中国文学批评史》为例	孙宗美	重点项目	金课改革
JG20004	基于创新能力培养的专业实践课中混合教学模式的探索与实践--以《操作系统》实践课为例	王金凤	重点项目	金课改革
JG20005	“MOOC+线下课”教学模式的探索与实践—以《生物化学》“MOOC+线上见面课”课程教学为鉴	初志战	重点项目	金课改革
JG20006	分级教学背景下大学英语B级线上线下混合式写作教学模式研究	张雅娜	重点项目	金课改革
JG20007	大思政视域下高校思政课校内实践教学基地建设的研究与实践 ----以华南农业大学为例	叶晖有	重点项目	思政课程
JG20008	课程思政教育在《禽病学》教学中的应用与实践	贾伟新	重点项目	课程思政
JG20009	中国民族音乐课程中的思政教学探索	朱虹	重点项目	课程思政
JG20010	“三全育人”背景下《无机功能材料》课程思政的建设与实践	倪春林	重点项目	课程思政
JG20011	新工科背景下工程类人才培养中课程思政育人模式研究	李高扬	重点项目	课程思政
JG20012	“三全育人”理念下“课程思政”的向度与路径研究——以3门通识教育课的教学改革为例	陈晓梅	重点项目	课程思政
JG20013	基于混合式教学的课程思政改革探索——以《当代中国社会问题研究》课程为例	张运红	重点项目	课程思政
JG20014	“立德树人”视域下中外合作办学课程思政教学模式探索与实践——以日语专业中日合作办学项目为例	赵无忌	重点项目	课程思政
JG20015	艺术类史论课程融入课程思政的探索与实践	胡辉	重点项目	课程思政
JG20016	基于“新农科”建设的农林经济管理专业人才培养模式探索与实践	陈有华	重点项目	四新改革
JG20017	新农科背景下多学科交叉融合的园林专业人才培养模式研究与实践	翁殊斐	重点项目	四新改革
JG20018	新工科背景下基于能力培养的城乡规划专业“双线混融式”实践教学改革与创新	赵建华	重点项目	四新改革
JG20019	大数据背景下基于文本挖掘的新农科人才需求分析与人才培养模式改革研究	张建桃	重点项目	四新改革
JG20020	以新工科人才培养为导向的发酵工程实践教学模式探索	徐学锋	重点项目	四新改革
JG20021	新文科理念下应用型管理人才培养模式改革与实践——以土地资源管理专业为例	李灿	重点项目	四新改革
JG20022	新农科背景下农林院校旅游管理专业建设的内涵与提升路径	林敏慧	重点项目	四新改革
JG20023	面向新文科建设的农林院校历史专业改革与发展研究	赵飞	重点项目	四新改革
JG20024	新文科建设视域下的哲学本科人才培养模式改革研究与实践	谢翾	重点项目	四新改革
JG20025	基于创新能力培养的《养兔学》教学模式改革研究与实践	孙宝丽	重点项目	
JG20026	以传承中华优秀传统文化为特色的应用型音乐人才培养模式改革研究	郑颜文	重点项目	
JG20027	风景园林专业美术类课程群模块构建与教学创新	李静	重点项目	
JG20028	社会主义核心价值观教育融入“英美文学选读”教学的研究与实践	尹晓霞	重点项目	
JG20029	基于学生工程能力培养的机械基础实验课程改革与实践	甄文斌	重点项目	
JG20030	基于校企合作的风景园林协同育人模式探索与实践	黄东	重点项目	

JG20031	普通大学高水平运动员培养模式改革与研究----以华南农业大学为例	陈华东	重点项目	
JG20032	智慧植保导向下的精准农业人才培养体系构建	徐汉虹	重点项目	
JG20033	基于教育数据挖掘的高校学习评价方法研究	倪妙珊	重点项目	
JG20034	工程基础实践课在高校“冲一流”背景下的改革与实践	徐相华	重点项目	
JG20035	农林院校创新创业型人才培养视角下知识产权教育课程体系建设研究	张日新	重点项目	
JG20036	大规模远程在线考核关键技术研究	陈湘骥	重点项目	
JG20037	国际化视野下生态环境类人才培养的研究与实践	蔡昆争	重点项目	
JG20038	高等农业院校工程类专业“普通化学”在线开放课程建设与应用	刘海峰	重点项目	
JG20039	基于移动平台的自然地理野外实习虚拟仿真系统建设与研究	钟晓兰	重点项目	
JG20040	“植物学类专业课+古诗词+立德树人”的三全育人教学模式探索	解新明	重点项目	
JG20041	植物学虚实协同融合实验教学体系创新路径与实践	方颖	重点项目	
JG20042	法庭科学技术虚拟仿真实验项目的研究与实践	杜国明	重点项目	
JG20043	基于TPC 模式的温氏班《养牛学实训》课程改革与实践	邓铭	重点项目	
JG20044	校企协同育人下的应用型知识产权人才培养创新模式研究	王红	重点项目	
JG20045	DMap在大学英语的教学改革及研究	钟志英	重点项目	
JG20046	基于创新能力培养的遗传学实验教学资源体系改革研究	李楠	重点项目	
JG20047	产教融合视域下复合应用型旅游管理人才培养体系创新与实践	陈丽丽	重点项目	
JG20048	农业高校广播电视编导专业涉农人才培养模式研究	郑文华	重点项目	
JG20049	动画专业产教融合协同育人模式的研究	陈瑰丽	重点项目	
JG20050	基于产教深度融合的农林经济管理实践教学体系内涵建设	李巧璇	重点项目	
JG20051	高等农业院校与农业产业园合作育人模式创新研究——以华南农业大学为例	潘军	重点项目	
JG20052	核心素养助推智慧教育导向的《水产动物组织胚胎学》教学探索与实践	范兰芬	重点项目	
JG20053	“后疫情时代”线上线下混合式教学模式在病毒学课程中的应用	马金成	一般项目	金课改革
JG20054	“线上线下”混合式教学中协作学习体系的构建——基于经管专业数据分析类课程的探索与实践	李宗璋	一般项目	金课改革
JG20055	《植物生理学实验》微课的建设	钱春梅	一般项目	金课改革
JG20056	后疫情时期Orff教学法在音乐通识课“线上”教学模式研究与实践	李伟	一般项目	金课改革
JG20057	基于 MOOC+SPOC 线上线下混合模式的林学实验教学改革与实践	苏艳	一般项目	金课改革
JG20058	互联网+背景下《电工电子技术》 教学中的微课运用研究与实践	史艳玲	一般项目	金课改革
JG20059	新冠疫情后基于中国大学MOOC异步SPOC的混合式教学模式推进策略与效果评价——三个“三位一体”视野下对两门公共管理类课程的对比研究	吴法	一般项目	金课改革
JG20060	基于MOOC 的SPOC混合教学模式在《动物学》教学中应用探索	佟富春	一般项目	金课改革
JG20061	线上翻转课堂的教学模式在操舞类体育课中的应用研究	何灵捷	一般项目	金课改革
JG20062	基于网络教学平台的大学英语翻译模块课程混合式教学改革研究与构建	仇如慧	一般项目	金课改革
JG20063	“林木遗传育种学”课程的“线上”+“线下”混合式教学模式研究与实践	欧阳昆唏	一般项目	金课改革

JG20064	基于“问题引导”的《大学物理实验》课程线上线下结合教学模式改革和实践研究	王先菊	一般项目	金课改革
JG20065	“线上”和“线下”有机融合的SPOC混合式教学在模拟电子技术实验中的研究与实践	成兰仙	一般项目	金课改革
JG20066	基于“学习通+翻转课堂”的混合教学模式的创新与实践--以《数据库应用》公共课为例	郭艾侠	一般项目	金课改革
JG20067	《工程测量学》混合式教学模式研究	林观土	一般项目	金课改革
JG20068	基于SPOC的翻转教学模式的研究与实践---以数字通信原理课程为例	胡春筠	一般项目	金课改革
JG20069	《测量学》课程混合式教学改革研究	刘建滨	一般项目	金课改革
JG20070	“清洁生产与循环经济”线上和线下混合式教学研究与实践	蒋成爱	一般项目	金课改革
JG20071	大数据挖掘与可视化课程的线上线下混合教学模式应用与实践	古万荣	一般项目	金课改革
JG20072	“互联网+教育”环境下控制工程基础课程混合教学改革与实践	邢航	一般项目	金课改革
JG20073	高等数学翻转课堂探究式教学方式的创新与实践	何婧	一般项目	金课改革
JG20074	高校思政“基础”课专题式教学研究	郑萍	一般项目	思政课程
JG20075	习近平相关论述指导下高校思政课在新时代人才培养中的作用研究	王景奇	一般项目	思政课程
JG20076	以"传统文化"为切入点的课程思政融入金属工艺课程教学模式探索	潘子广	一般项目	课程思政
JG20077	课程思政下的专业课程教学设计——以生态道德教育为导向的动物学课程 “线上 +线下 ”混合教学探索	曾芳	一般项目	课程思政
JG20078	“课程思政”视域下农事训练课程与思政教育协同育人路径研究	陈娴	一般项目	课程思政
JG20079	大思政背景下的英语视听说混合式课程建设	秦建华	一般项目	课程思政
JG20080	土壤类课程思政的探索与实践：多学科与多维度之融会贯通	卫泽斌	一般项目	课程思政
JG20081	新形势下“芯”专业课程思政探索与实践	代秋芳	一般项目	课程思政
JG20082	公共基础课无机&分析化学及实验课程思政元素的挖掘与实践研究	周晓华	一般项目	课程思政
JG20083	融合思政元素和翻转课堂的线性代数教学模式探究	朱艳丽	一般项目	课程思政
JG20084	“新农科”背景下创新型融媒体人才的教学探究——以《新媒体实务》课程为例	赵娜	一般项目	四新改革
JG20085	新工科理念下“食品添加剂”的“学-研-产”纵横延拓型课程设计与实践	肖杰	一般项目	四新改革
JG20086	新农科背景下的智慧教学环境的设计研究	周恩浩	一般项目	四新改革
JG20087	云教学条件下新工科专业实践课程在线教学模式探索与实践——以家具设计与工程专业为例	宋杰	一般项目	四新改革
JG20088	新工科背景下测绘工程实践教学改革	陈俊林	一般项目	四新改革
JG20089	新农科背景下《土壤肥料学》课程思政建设和实践教学形式改革研究	徐会娟	一般项目	四新改革
JG20090	国际化新形势与新林科背景下林学专业人才培养模式改革与探索	周玮	一般项目	
JG20091	计算机基础课程线上实验平台与资源建设应用研究	李玉峰	一般项目	
JG20092	高校教师应对在线教学的教育技术应用能力提升路径探索	李玉玲	一般项目	
JG20093	十年来国内高等农林教学研究的可视化分析	杨永忠	一般项目	
JG20094	互联网背景下 “产出导向法 (POA) ”在大学英语教学中的应用研究	牛莉	一般项目	
JG20095	基于供给侧结构性改革理论的资科专业《土壤学》课程教学改革研究与实践	任宗玲	一般项目	
JG20096	模拟法庭课程建设质量评价体系研究	张艳琼	一般项目	

JG20097	基于教育大数据的高校学生学业预警机制构建研究——以华南农业大学为例	曾鸣	一般项目	
JG20098	社会工作专业学生实习选择及分化逻辑研究——基于八个年级实习材料的分析	马林芳	一般项目	
JG20099	新媒体环境下形象设计的教学改革实践	郑丽娜	一般项目	
JG20100	“课程思政”视域下图书馆与思政教育协同育人模式研究	黄承红	一般项目	
JG20101	禁毒社会工作标准化课程体系研究与实践	曾永辉	一般项目	
JG20102	新时代背景下植物与中华文化的有机结合——《植物命名与中华文化》课程教学改革与实践	单体江	一般项目	
JG20103	基于奥尔堡 PBL 模式的《小动物传染病学》实践教学创新与研究	孙海亮	一般项目	
JG20104	R语言融入统计学课程教学的探索	潘逵	一般项目	
JG20105	基于“社会—生态实践”的风景园林设计基础类课程创新改革研究	汤辉	一般项目	
JG20106	基于超星平台的大学英语智慧课堂教学模式设计与应用研究	夏妙月	一般项目	
JG20107	人工智能技术与英语交互式口语教学的融合应用研究	于玮婷	一般项目	
JG20108	虚拟现实(VR)技术在《互联网+农业》实验教学改革中的探索	张雷	一般项目	
JG20109	基于新冠肺炎疫情形势下的《植物学实验》课程教学模式改革研究	张荣京	一般项目	
JG20110	以学生为中心的遗传学实验优化与实践	刘振兰	一般项目	
JG20111	可视化植物营养学实验课程建设	喻建刚	一般项目	
JG20112	基于实践和创新的地图学教学改革研究	吴小芳	一般项目	
JG20113	数据结构在线评判系统题库的建设与应用研究	司国东	一般项目	
JG20114	《农业机器人》教学模式与创新实践	胡练	一般项目	
JG20115	“课程思政”视角下的UI设计教学改革与创新	欧阳文昱	青年项目	课程思政
JG20116	“互联网+实体课堂”线上线下混合式体育教学模式研究	周文英	青年项目	课程思政
JG20117	工科短学时课程“线上”+“线下”混合式教学模式研究与实践—以《建筑给排水工程》为例	梁瑜海	青年项目	课程思政
JG20118	课程思政视角下的《生命科学与人类文明》教学改革与初探	李培	青年项目	课程思政
JG20119	《草坪营养与施肥》线上线下翻转课堂研究与实践	钟天秀	青年项目	课程思政
JG20120	基于虚拟仿真平台的“线上+线下”教学模式在《甲壳动物实验及实习》中的应用	何玉慧	青年项目	课程思政
JG20121	基于微课的翻转课堂教学模式在动物营养学中的运用初探	谭成全	青年项目	课程思政
JG20122	新农科背景下涉农法律人才培养研究	唐穗	青年项目	四新改革
JG20123	新工科背景下的《操作系统》课程改革研究	张猜	青年项目	四新改革
JG20124	新农科背景下基于学生创新能力培养的生物化学实验教学改革研究	许燕珍	青年项目	四新改革
JG20125	新工科背景下模拟电子技术实验教学内容与考核方式改革研究	黄慧娴	青年项目	四新改革
JG20126	BOPPPS 教学模式在创新创业导向型《财务管理》中的应用	龙思颖	青年项目	
JG20127	《园艺植物种子生产原理与技术》理论与实验课程内容优化改革研究	程蛟文	青年项目	
JG20128	基于病历挖掘式实验教学模式的改革与实践——以《兽医临床病理学实验课》为例	韩庆月	青年项目	
JG20129	以《畜牧微生物学实验》为例探索专业基础实验课教学模式改革	李鸿鑫	青年项目	

JG20130	农林类院校《保险精算学》课程教学方法改革与探索	杨明旭	青年项目	
JG20131	IT类专业“1站2导3平台”创新创业实践教育模式研究	刘树鑫	青年项目	
JG20132	以建立数据库为导向提升《水产饲料添加剂学》教学效果的研究	陈世俊	青年项目	
JG20133	斑马鱼突变模型在《遗传学实验》教学实践中的应用研究	谢少林	青年项目	
JG20134	《空间数据库原理与应用》在线社区式教学创新与实践	刘轶伦	青年项目	
JG20135	基于创新能力培养的实验类教学方式改革研究与实践	毛子翎	青年项目	
JG20136	生态学野外综合实习课程改革	李荣华	青年项目	
JG20137	基于微信公众号的基础化学实验教学辅助平台的构建与实践	赖婷	青年项目	
JG20138	基于行动导向型教学模式的《汽车理论》标准化教学组织模型研究	王昱	青年项目	
JG20139	CLIL视域下“农业＋日语”课程教学改革研究	郭圣琳	青年项目	
JG20140	翻转课堂在《鱼类学》分类教学中的应用	崔科	自筹项目	金课改革
JG20141	实践课线上线下混合式教学模式改革探索——能源与环境系统工程专业《环境工程实验》	简秀梅	自筹项目	金课改革
JG20142	“线上虚拟仿真+线下光路设计”的光信息数字化实验体系改革与优化	翁嘉文	自筹项目	金课改革
JG20143	基于腾讯课堂+SPOC的《汇编语言程序设计》翻转课堂教学模式研究	吴理华	自筹项目	金课改革
JG20144	信息化条件下高等数学混合式教学模式的研究与实践	王雪琴	自筹项目	金课改革
JG20145	基于认知主义学习理论的基础日语课程线上线下混合教学模式研究	高琴	自筹项目	金课改革
JG20146	基于翻转课堂的《畜牧微生物学》理论课教学改革	孙媛	自筹项目	金课改革
JG20147	基于微课的翻转课堂模式在《园艺植物栽培学》实验教学中的创新研究	柴喜荣	自筹项目	金课改革
JG20148	基于慕课混合式教学的数学类课程评价研究	杨志程	自筹项目	金课改革
JG20149	基于云课堂的《矿物资源与宝石鉴赏》混合式教学模式研究	李博	自筹项目	金课改革
JG20150	翻转课堂在《园艺产品物流与供应链管理》 线上线下混合教学中的应用	单伟	自筹项目	金课改革
JG20151	基于雨课堂的《无机化学》课程线上线下混合式教学改革与实践	何良	自筹项目	金课改革
JG20152	中国近现代史纲要现场教学研究	赵志宇	自筹项目	思政课程
JG20153	疫情防控常态化背景下的高校思政课教学模式研究与实践	袁尔纯	自筹项目	思政课程
JG20154	“课程思政”视域下高校思政课教学与创新创业教育协同育人机制研究	林晓燕	自筹项目	思政课程
JG20155	新时代高校思政课“混合式”教学模式研究与实践	陈洁	自筹项目	思政课程
JG20156	新媒体视域下高校思想政治理论课获得感研究 ——以《思想道德修养与法律基础》为例	余喜	自筹项目	思政课程
JG20157	《中国近现代史纲要》课程主题教学整体优化研究与实践	周新华	自筹项目	思政课程
JG20158	课程思政改革的中国话语建构研究	杨琳	自筹项目	思政课程
JG20159	基于乡村振兴和新农科建设背景下《农业环境与乡村旅游》课程思政的探索与实践	吕辉雄	自筹项目	课程思政
JG20160	农林院校《大学英语》课程思政实施路径研究	杜龙鼎	自筹项目	课程思政
JG20161	《大学物理实验》课程思政教学改革与实践探索	杨小红	自筹项目	课程思政
JG20162	计算机通识教育课程中“思政”教学建设与实践研究	万华	自筹项目	课程思政

JG20163	工匠精神视域下创新人才培养与课程思政协同育人模式研究——以中国传统工艺课程为例	张静	自筹项目	课程思政
JG20164	基于“学习强国+课程思政”的大学英语写作混合式教学模式研究	苏君	自筹项目	课程思政
JG20165	商务英语专业课“课程思政”教学模式研究——以《电子商务》为例	尹静媛	自筹项目	课程思政
JG20166	将“思政”之盐融入计算机算法类课程之汤的隐性教育探索和实践	郑婵	自筹项目	课程思政
JG20167	课程思政背景下遗传学教学改革研究与实践	陈志雄	自筹项目	课程思政
JG20168	以能力为导向的《环境影响评价》教学改革及课程思政探索	陈烁娜	自筹项目	课程思政
JG20169	新农科和学分制双背景下动物科学专业课程结构调整与建设	习欠云	自筹项目	四新改革
JG20170	新农科下高等农业院校农科人才培养错位与政策优化研究	刘春桃	自筹项目	四新改革
JG20171	新工科理念下房地产开发与管理专业人才培养模式改革与实践	游珍	自筹项目	四新改革
JG20172	新农科人才培养模式下大学生农业科技英语阅读能力的培养研究	叶茂连	自筹项目	四新改革
JG20173	新农科背景下的农科院校国家一流行政管理本科课程体系创新研究	朱生伟	自筹项目	四新改革
JG20174	新工科背景下农机丁颖班创新能力培养的研究	贾瑞昌	自筹项目	四新改革
JG20175	新农科背景下《林木遗传育种学》双语教学探索与实践	龙健梅	自筹项目	四新改革
JG20176	新理工科背景下基于虚拟仿真技术的《电路实验》教学改革与实践	王建华	自筹项目	
JG20177	智能化教学模式改革研究--以证据法学在线课程设计为例	赵蕾	自筹项目	
JG20178	基于信息化技术（SCAULab of Arts 微信公众号） 在英语专业文学课教学中的融合应用研究	侯金萍	自筹项目	
JG20179	语言智能背景下机器翻译与人工翻译的对比分析在非英语专业翻译教学中的作用	刘玉花	自筹项目	
JG20180	《插画设计》课程教学模式创新与跨界研究	彭艳霞	自筹项目	
JG20181	微观结构和形貌的认知教学在工程训练中的作用研究	张殿武	自筹项目	
JG20182	深化产教融合校企合作的育人模式——以市场营销专业为例	彭思喜	自筹项目	
JG20183	新工科背景下大学生专利创新能力培养的研究与实践	何效平	自筹项目	
JG20184	基于工程教育认证的测绘工程专业综合改革研究	刘惠明	自筹项目	
JG20185	基于岭南地域文化下 “中国建筑史”课程建设研究	姜磊	自筹项目	
JG20186	移动应用开发课程体系优化研究与实践	杨春	自筹项目	
JG20187	基于创新创业能力培养的《机械装备设计》课程教学改革与实践	夏红梅	自筹项目	
JG20188	基于CDIO和智慧农业导向的农业院校复合型人才培养模式探究	杨意	自筹项目	
JG20189	“互联网+”背景下校企联合工作室教学模式探究	徐宁	自筹项目	
JG20190	以学生为中心的《基础植物病理学》课程教学内容体系改革和优化研究	饶雪琴	自筹项目	
JG20191	智能化信息化背景下数学与程序设计能力培养相结合的教学改革探索与实践	廖彬	自筹项目	
JG20192	科教融合提升生态学专业理论课教学效果的实践探索	危晖	自筹项目	
JG20193	基于新媒体平台《大学生心理健康教育》课程建设	李佳媛	自筹项目	
JG20194	兽医药理学全英教学的实践探索	于洋	自筹项目	
JG20195	科教融合背景下省级科研平台承担通识教育课程的探索与实践	阙青敏	自筹项目	

备注：“项目编号”并非项目排序，是优先项目类别、专项类别依次排列后再进行编号。

关于国家自然科学基金资助项目批准及有关事项的通知

龙健梅　先生/女士：

根据《国家自然科学基金条例》的规定和专家评审意见，国家自然科学基金委员会（以下简称自然科学基金委）决定批准资助您的申请项目。项目批准号：31800560，项目名称：黄梁木蔗糖转运蛋白NcSUTs在木材发育与形成中的功能研究，直接费用：25.00万元，项目起止年月：2019年01月至 2021年 12月，有关项目的评审意见及修改意见附后。

请尽早登录科学基金网络信息系统（https://isisn.nsfc.gov.cn），获取《国家自然科学基金资助项目计划书》（以下简称计划书）并按要求填写。对于有修改意见的项目，请按修改意见及时调整计划书相关内容；如对修改意见有异议，须在计划书电子版报送截止日期前提出。

计划书电子版通过科学基金网络信息系统（https://isisn.nsfc.gov.cn）上传，由依托单位审核后提交至自然科学基金委进行审核。审核未通过者，返回修改后再行提交；审核通过者，打印为计划书纸质版（一式两份，双面打印），由依托单位审核并加盖单位公章后报送至自然科学基金委项目材料接收工作组。计划书电子版和纸质版内容应当保证一致。向自然科学基金委提交和报送计划书截止时间节点如下：

1、提交计划书电子版截止时间为**2018年9月11日16点**（视为计划书正式提交时间）；

2、提交计划书电子修改版截止时间为**2018年9月18日16点**；

3、报送计划书纸质版截止时间为**2018年9月26日16点**。

请按照以上规定及时提交计划书电子版，并报送计划书纸质版，未说明理由且逾期不报计划书者，视为自动放弃接受资助。

附件：项目评审意见及修改意见表

国家自然科学基金委员会

生命科学部

2018年8月16日

受理编号：c23140700000217

项目编号：2023A1515030250

文件编号：粤基金字〔2023〕2号

广东省基础与应用基础研究基金项目

任务书

项目名称： 精细取样和多组学分析发掘速生黄梁木维管形成层发育的关键基因

项目类别： 广东省自然科学基金-青年提升项目

项目起止时间： 2023-01-01 至 2025-12-31

管理单位（甲方）： 广东省基础与应用基础研究基金委员会

依托单位（乙方）： 华南农业大学

通讯地址： 广东省广州市天河区五山路483号

邮政编码： 510642 **单位电话：** 020-85283435

项目负责人： 龙健梅 **联系电话：** 18820760615

（广东科技微信公众号） （查看任务书信息） （受理纸质材料二维码）

广东省基础与应用基础研究
基金委员会
二〇二〇年制

填写说明

一、项目任务书内容原则上要求与申报书相关内容保持一致，不得无故修改。

二、项目承担单位通过广东省科技业务管理阳光政务平台下载项目任务书，按要求完成签名盖章后扫描上传到广东省科技业务管理阳光政务平台。

三、签名盖章说明。请分别在单位工作分工及经费分配情况页、人员信息页、签约各方页等地方按要求签字或盖章，签章不合规或错漏将不予受理。其中，人员信息页要求所有参与人员本人亲笔签名，代签或印章无效，漏签将不予受理。

四、本任务书自签字并加盖公章之日起生效，各方均应负本任务书的法律责任，不应受机构、人事变动影响。

五、根据《广东省科学技术厅广东省则政厅关于深入推进省基础与应严础研究基金项目经费使用“负面清单+包干制”改革试点工作的通知》（粤科规范字[2022]2号），2022年度及以后立项资助的全部省基金项目（包括省自然科学基金、省市联合基金、省企联合基金项自等）均适用“负面清单+包干制”，项目提交申请书和任务书时无需编制费用明细科目预算。

一、主要研究内容和要达到的目标

本项目前期在完成黄梁木基因组测序和建立激光显微切割精细获取维管组织的技术体系下，通过精细取样和单细胞水平多组学测序发掘参与黄梁木形成层发育的关键基因，重点对黄梁木维管形成层发育活动的转录调控机制进行解析探索，主要研究内容分为两大块：（1）参与速生黄梁木维管形成层发育关键基因的挖掘。通过收集不同地点黄梁木种源，进行种源间的生长性状比较，获得生长最快与最慢两种类型黄梁木种源；以此为材料，通过黄梁木维管组织的激光显微切割体系，分别获取两种类型种源次生生长时期形成层、韧皮部和木质部细胞，提取RNA进行RNA-seq测序；同时，以进行次生生长茎节为材料，获取黄梁木维管组织的细胞核，进行单细胞RNA-seq。通过联合以上两种不同取样方式获得的RNA-seq数据深入挖掘参与速生黄梁木维管形成层发育的关键基因。（2）单细胞水平速生黄梁木形成层发育的转录调控机制。（a）构建单细胞水平速生黄梁木形成层发育的TF-target 调控网络：通过获得的黄梁木维管组织ATAC-seq，分析两种类型黄梁木种源维管形成层的染色质开放区域，通过寻找转录因子（TF）“足迹”，比较两者TF结合区域的差异，找出与黄梁木形成层相关的顺式作用元件。结合（1）获得的关键维管形成层发育的基因，通过WGCNA进行基因共表达分析网络，获得可能参与速生维管形成层发育的TF-target调控组合，在单细胞水平构建形成层发育的转录调控网络。（b）关键TF-target 调控模块表达模式与互作关系验证：基于上一步筛选到的TF-target调控组合，结合生物信息学分析与转录组表达数据，挑选4-5个关键的TF-target调控模块，进一步利用qRT-PCR 和RNA组织原位杂交分析关键TF和target的表达模式，验证其在形成层发育的时空表达模式；克隆target的启动子，利用酵母单杂交、烟草双荧光素酶瞬时表达体系和EMSA等手段验证TF与target启动子间的互作关系。（c）关键TF-target 功能解析：筛选2-3个（4）中获得的候选TF-target调控组合，通过构建TF和target的超量表达载体和RNAi载体，通过农杆菌介导法转化黄梁木，对转基因植株进行维管组织发育的生长性状评价与表型分析，重点深入分析转基因植株维管形成层发生的变化，验证TF和target 在形成层发育中的功能。综上，通过单细胞水平多组学测序等手段，获得参与速生黄梁木维管形成层发育的关键基因；构建速生黄梁木维管形成层发育TF-target 调控网络，明确其转录调控机制，为黄梁木速生机理的解析奠定基础。

二、项目预期获得的研究成果及形式

<table>
<tr><td rowspan="3">论文及专著情况</td><td colspan="2">国家统计源刊物以上刊物发表论文（篇）</td><td colspan="2">2</td><td colspan="2">科技报告（篇）</td><td colspan="2">0</td></tr>
<tr><td colspan="2">其中被SCI/EI/ISTP收录论文数（篇）</td><td colspan="2">1</td><td colspan="2">培养人才（人）</td><td colspan="2">2</td></tr>
<tr><td colspan="2">专著（册）</td><td colspan="2">0</td><td colspan="2">引进人才（人）</td><td colspan="2">0</td></tr>
<tr><td rowspan="3">专利情况(项)</td><td colspan="2">发明专利</td><td colspan="2">实用新型专利</td><td colspan="2">外观设计专利</td><td colspan="2">国外专利</td></tr>
<tr><td>申请</td><td>授权</td><td>申请</td><td>授权</td><td>申请</td><td>授权</td><td>申请</td><td>授权</td></tr>
<tr><td>0</td><td>0</td><td>0</td><td>0</td><td>0</td><td>0</td><td>0</td><td>0</td></tr>
</table>

三、项目进度和阶段目标

（一）项目起止时间： 2023-01-01 至 2025-12-31		
（二）项目实施进度及阶段主要目标:		
开始日期	结束日期	主要工作内容
2023-01-01	2023-12-31	激光显微切割获取黄梁木维管组织不同类型细胞，进行RNA-seq测序；分析RNA-seq数据，了解维管组织不同类型细胞基因表达情况，挖掘形成层发育的关键基因。建立黄梁木维管组织单细胞测序体系，进行单细胞RNA-seq和ATAC-seq测序并进行生物信息学分析。
2024-01-01	2024-12-31	ATAC-seq数据分析，比较两种类型黄梁木染色质可及性，并对不同类型细胞染色质开放区进行鉴定，分析可能参与基因表达调控的转录因子；联合单细胞RNA-seq和ATAC-seq测序数据，构建黄梁木维管形成层发育的转录调控网络；筛选关键的4-5个TF-target调控组合进行下一步表达模式与互作关系的验证；筛选2-3个TF-target调控组合，构建TF和target超表达载体和RNAi抑制载体，转化黄梁木。
2025-01-01	2025-12-31	对黄梁木转基因植株进行表型分析，比较转基因株系在维管组织发育过程中的变化，特别是形成层的变化；整理项目研究结果，参加相关学术会议，并撰写文章。

四、项目总经费及省基金委经费预算

1.省基金委经费下达总额： （大写）叁拾万圆整；（小写 ）30万元；					
2.省基金委经费年度下达计划：					
年度	2023 年	年	年	年	年
经费(万元)	30.00				

五、人员信息

项目负责人								
姓名	证件号码	年龄	性别	职称	学历	在项目中承担的任务	所在单位	签名
龙健梅	452123198908283146	34	女	讲师	博士研究生	项目负责人	华南农业大学	

项目组主要成员								
姓名	证件号码	年龄	性别	职称	学历	在项目中承担的任务	所在单位	签名
张俊杰	420683198909223168	34	女	讲师	博士研究生	黄梁木遗传转化	华南农业大学	
郭婷	411481199508255126	28	女	未取得	本科	激光显微切割获取维管组织及单细胞测序	华南农业大学	
许佐威	440682199707094355	26	男	未取得	本科	关键TF和target的互作关系验证	华南农业大学	
覃福宇	450103199701121024	26	女	未取得	本科	生物信息分析挖掘黄梁木形成层发育关键基因及调控转录因子	华南农业大学	
梁正炫	440112199811200318	25	男	未取得	本科	遗传转化与植株表型分析	华南农业大学	

六、工作分工及财政经费分配

承担/参与单位名称（盖章）	工作分工	省级财政科技资金分配（万元）
华南农业大学	负责改项目的实施，统筹整个项目，把握项目进度	30.00
	合计	30.00

七、任务书条款

第一条 甲方与乙方根据《中华人民共和国民法典》及国家有关法规和规定，按照《广东省科学技术厅关于广东省基础与应用基础研究基金（省自然科学基金、联合基金等）项目管理的实施细则（试行）》《广东省省级科技计划项目验收结题工作规程（试行）》等规定，为顺利完成（2023）年精细取样和多组学分析发掘速生黄梁木维管形成层发育的关键基因专项项目（文件编号：粤基金字〔2023〕2号 ）经协商一致，特订立本任务书，作为甲乙双方在项目实施管理过程中共同遵守的依据。

第二条 甲方的权利义务：

1.按任务书规定进行经费核拨的有关工作协调。

2.根据甲方需要，在不影响乙方工作的前提下，定期或不定期对乙方项目的实施情况和经费使用情况进行检查或抽查。

3.根据《广东省科研诚信管理办法(试行)》等规定对乙方进行科技计划信用管理。

第三条 乙方的权利义务：

1.确保落实自筹经费及有关保障条件。

2.按任务书规定，对甲方核拨的经费实行专款专用，单独列账，并随时配合甲方进行监督检查。

3.应按照国家和省有关规定，制定经费使用“包干制”内部管理规定；项目经费支出应实际用于研发活动相关支出，使用范围限于设备费、材料费、测试化验加工费、燃料动力费、差旅/会议/国际合作与交流费、出版/文献/信息传播/知识产权事务费、劳务费、专家咨询费、依托单位管理费用、绩效支出以及其他合理支出；管理费用根据实际管理支出情况与项目负责人协商确定；绩效支出由项目负责人根据实际科研需要和相关薪酬标准自主确定，单位按照现行工资制度进行管理；其余用途经费无额度限制，由项目负责人根据实际需要自主决定使用；项目验收时应提交经费决算表。

4.对项目负责人按计划开展项目研究和规范使用资金进行监督管理，经费使用按照《广东省财政厅 广东省审计厅关于省级财政科研项目资金的管理监督办法》等规定进行管理。

5.使用财政资金采购设备、原材料等，按照《广东省实施〈中华人民共和国招标投标法〉办法》有关规定，符合招标条件的须进行招标。

6.项目任务书任务完成后，或任务书规定的任务、指标及经费投入等提前完成的，乙方可提出验收结题申请，并按甲方要求做好项目验收结题工作。

7.若项目发生需要终止结题的情况，乙方须提出终止结题申请，并按甲方要求做好项目终止结题工作。

8.在每年规定时间内向甲方如实提交上年度工作情况报告，报告内容包含上年度项目进展情况、经费决算和取得的成果等。

9.按照国家和省有关规定，提交科技报告及其他材料。

10.利用甲方的经费获得的研究成果，项目负责人和参与者应当注明获得“广东省基础与应用基础研究基金（英文：Guangdong Basic and Applied Basic Research Foundation）（项目编号）”资助或作有关说明。

11.乙方要恪守科学道德准则，遵守科研活动规范，践行科研诚信要求，不得抄袭、剽窃他人科研成果或者伪造、篡改研究数据、研究结论；不得购买、代写、代投论文，虚构同行评议专家及评议意见；不得违反论文署名规范，擅自标注或虚假标注获得科技计划（专项、基金等）等资助；不得弄虚作假，骗取科技计划（专项、基金等）项目、科研经费以及奖励、荣誉等；不得有其他违背科研诚信要求的行为。

12.确保本项目开展的研究工作符合我国科研伦理管理相关规定。

第四条 在履行本任务书的过程中，如出现广东省相关政策法规重大改变等不可抗力情况，甲方有权对所核拨经费的数量和时间进行相应调整。

第五条 在履行本任务书的过程中，当事人一方发现可能导致项目整体或部分失败的情形时，应及时通知另一方，并采取适当措施减少损失，没有及时通知并采取适当措施，致使损失扩大的，应当就扩大的损失承担责任。

第六条 本项目技术成果的归属、转让和实施技术成果所产生的经济利益的分享，除双方另有约定外，按国家和广东省有关法规执行。

第七条 根据项目具体情况，经双方另行协商订立的附加条款，作为本任务书正式内容的一部分，与本任务书具有同等效力。

第八条 本任务书一式三份，各份具有同等效力。甲、乙方及项负责人各执一份，三方签字、盖章后即生效，有效期至项目结题后一年内。各方均应负任务书的法律责任，不应受机构、人事变动的影响。

第九条 乙方必须接受甲方聘请的本项目任务书监理单位的监督和管理。监理单位按照甲方赋予的权利对本项目任务书的履行进行审核、进度调查，对项目任务书变更、经费使用情况进行监督管理及组织项目验收。

说明：1.本任务书中，凡是当事人约定无需填写的内容，应在空白处划（/）。

2.委托代理人签订本任务书的，应出具合法、有效的委托书。

八、本任务书签约各方

管理单位（甲方）：　　广东省基础与应用基础研究基金委员会　（盖章）

法定代表人（或法人代理）：　曾路　（签章）

2023 年　02 月　14 日

依托单位（乙方）：　华南农业大学　（盖章）

法定代表人（或法人代理）：　刘雅红　（签章）

联系人（项目主管）姓名：　倪慧群　（签章）

Email：　kjcgxk@scau.edu.cn

电话：　020-85283435　/　15920301530

开户单位名称：　华南农业大学

开户银行名称：　广东广州工行五山支行

开户银行帐号：　3602002609000310520

年　月　日

联系人（项目负责人）姓名：　龙健梅　（签名）

Email：　longjianmei@scau.edu.cn

电话：　18820760615

年　月　日

受理编号：c21140500002565

项目编号：2021A1515010816

文件编号：粤基金字〔2021〕4号

广东省基础与应用基础研究基金项目

合同书

项目名称： 黄梁木蔗糖转运蛋白NcSUT1在木材发育中的作用及其机制研究

项目类别： 广东省自然科学基金-面上项目

项目起止时间： 2021-01-01 至 2023-12-31

管理单位（甲方）： 广东省基础与应用基础研究基金委员会

依托单位（乙方）： 华南农业大学

通讯地址： 广东省广州市天河区五山路483号

邮政编码： 510642 **单位电话：** 020-85283435

项目负责人： 龙健梅 **联系电话：** 18820760615

（广东科技微信公众号） （查看合同书信息） （受理纸质材料二维码）

广东省基础与应用基础研究
基金委员会
二〇二〇年制

填写说明

一、项目合同书/任务书内容原则上要求与申报书相关内容保持一致，不得无故修改。

二、项目承担单位通过广东省科技业务管理阳光政务平台下载项目合同书/任务书，按要求完成签名盖章后提交至省科技厅受理窗口。

三、签名盖章说明。请分别在单位工作分工及经费分配情况页、人员信息页、签约各方页等地方按要求签字或盖章，签章不合规或错漏将不予受理。其中，人员信息页要求所有参与人员本人亲笔签名，代签或印章无效，漏签将不予受理。

四、本合同书/任务书自签字并加盖公章之日起生效，各方均应负本合同书/任务书的法律责任，不应受机构、人事变动影响。

一、主要研究内容和要达到的目标

本项目前期通过黄梁木激光显微切割体系获取不同时期维管组织细胞并进行转录组测序，通过分析发现NcSUT1在黄梁木木质部和韧皮部中高度表达，在该基础上进一步对NcSUT1 的具体功能及其作用机制进行深入分析，研究内容如下：（1）组织定位与亚细胞定位分析：利用免疫荧光定位分析NcSUT1在黄梁木维管组织（木质部、韧皮部和形成层）在不同发育过程中的表达定位情况，明确NcSUT1在黄梁木韧皮部与木质部发育过程中的具体作用时期；利用黄梁木原生质体瞬时表达体系验证NcSUT1在亚细胞的定位情况，为解析其功能奠定基础。（2）转运蔗糖活性分析：利用酵母蔗糖吸收功能突变体SEY6210进行功能互补实验，验证NcSUT1的蔗糖转运活性。（3）NcSUT1功能鉴定：构建NcSUT1超量表达及CRISPR/Cas9（用于定点敲除NcSUT1）基因编辑载体，转化黄梁木组培苗茎段，获得NcSUT1超量表达及敲除转基因株系；对各转基因株系进行表型和各生理指标分析，包括生长发育状况、不同组织糖分组成与含量分析、光合测定及木材特性相关指标测定，明确NcSUT1在黄梁木木材发育与形成中的具体功能。（4）转录组分析：利用RNA-seq对转基因株系（包括NcSUT1超表达和基因敲除株系）和未转化黄梁木植株木质部及韧皮部进行测序，分析这些材料间差异表达基因，并挖掘生显著变化的代谢途径与生物过程。（5）上游调控因子筛选与鉴定：克隆NcSUT1启动子，通过酵母单杂交文库初步筛选与NcSUT1启动子互作的上游调控转录因子，并通过双荧光素酶瞬时表达体系与EMSA共同验证其互作关系。（6）NcSUT1互作蛋白鉴定：通过酵母双杂文库筛选及BiFC验证NcSUT1的互作蛋白。综上，通过在黄梁木中分别超量表达和敲除NcSUT1，验证其在黄梁木木质部发育过程中的相关功能；通过分别筛选并验证NcSUT1上游调控转录因子及下游互作蛋白，挖掘NcSUT1参与木材形成的分子调控网络，解析NcSUT1在黄梁木木材形成过程中的分子机制，为林木生长发育与木材品质的遗传改良提供重要的理论依据和候选基因。

二、项目预期获得的研究成果及形式

<table>
<tr><td rowspan="3">论文及专著情况</td><td colspan="2">国家统计源刊物以上刊物发表论文（篇）</td><td colspan="2">2</td><td colspan="2">科技报告（篇）</td><td colspan="2">1</td></tr>
<tr><td colspan="2">其中被SCI/EI/ISTP收录论文数（篇）</td><td colspan="2">1</td><td colspan="2">培养人才（人）</td><td colspan="2">2</td></tr>
<tr><td colspan="2">专著（册）</td><td colspan="2">0</td><td colspan="2">引进人才（人）</td><td colspan="2">0</td></tr>
<tr><td rowspan="3">专利情况(项)</td><td colspan="2">发明专利</td><td colspan="2">实用新型专利</td><td colspan="2">外观设计专利</td><td colspan="2">国外专利</td></tr>
<tr><td>申请</td><td>授权</td><td>申请</td><td>授权</td><td>申请</td><td>授权</td><td>申请</td><td>授权</td></tr>
<tr><td>0</td><td>0</td><td>0</td><td>0</td><td>0</td><td>0</td><td>0</td><td>0</td></tr>
</table>

三、项目进度和阶段目标

（一）项目起止时间： 2021-01-01 至 2023-12-31		
（二）项目实施进度及阶段主要目标:		
开始日期	结束日期	主要工作内容
2021-01-01	2021-12-31	免疫荧光定位分析NcSUT1在不同发育时期木质部和韧皮部的表达情况；利用黄梁木原生质体瞬时表达体系进行NcSUT1亚细胞定位分析；NcSUT1转化酵母突变体，验证NcSUT1的蔗糖转运活性；NcSUT1超量表达载体与CRISPR/Cas9载体构建并进行黄梁木遗传转化。
2022-01-01	2022-12-31	NcSUT1转基因植株筛选与相关表型鉴定；转录组分析转基因植株基因表达变化；通过酵母双杂交系统筛选NcSUT1互作蛋白并通过BiFC验证；酵母单杂交初步筛选NcSUT1上游的调控转录因子。
2023-01-01	2023-12-31	双荧光素酶瞬时表达与EMSA验证Y1H初步筛选获得的转录因子与NcSUT1启动子互作情况；整理数据，总结NcSUT1在木材发育与形成中的功能及其作用机制，撰写并发表论文，完成项目结题。

四、项目总经费及省基金委经费预算

1.省基金委经费下达总额： （大写）壹拾万圆整；（小写 ）10万元；

2.省基金委经费年度下达计划：

年度	2021 年	年	年	年	年
经费(万元)	10.00				

3.总经费及省基金委经费开支预算计划：

经费筹集情况： （单位：万元）

省基金委经费	自筹资金				合计
	自有资金	贷款	地方政府投入	其它	
10.00	0	0	0	0	10.00

政府部门、境外资金及其他资金投入情况说明：	

与本项目相关的其他经费来源	（单位：万元）
其他计划资助经费：	0
单位配套经费：	0
其他经费资助：	0
其他经费来源合计：	0.00

五、人员信息

项目负责人								
姓名	证件号码	年龄	性别	职称	学历	在项目中承担的任务	所在单位	签名
龙健梅	452123198908283146	32	女	讲师	博士研究生	项目负责人	华南农业大学	

项目组主要成员								
姓名	证件号码	年龄	性别	职称	学历	在项目中承担的任务	所在单位	签名
刘朝阳	410182198706153352	34	男	讲师	博士研究生	上游调控因子筛选与鉴定	华南农业大学	
刘思雯	152921199010051124	31	女	未取得	硕士研究生	互作蛋白筛选与验证	华南农业大学	
陈鑫	411327199605160029	25	女	未取得	本科	超表达及基因编辑载体构建与黄梁木遗传转化及表型分析	华南农业大学	
高佳钰	372328199310081547	28	女	未取得	本科	组织定位与亚细胞定位分析	华南农业大学	
杨舒琦	420802199604280628	25	女	未取得	本科	蔗糖转运活性验证及转基因植株RNA-seq分析	华南农业大学	

六、工作分工及经费分配

承担/参与单位名称（盖章）	工作分工	总经费分摊（万元）	省基金委经费分配（万元）
华南农业大学	本人负责整个项目的运行，包括项目研究内容制定，人员的分工与相关具体实验的统筹实施。经费将全部用于该项目所需的材料费、测试化验加工费，会议费及研究生的劳务费等。	10.00	10.00
	合计	10.00	10.00

七、合同条款

第一条 甲方与乙方根据《中华人民共和国合同法》及国家有关法规和规定，为顺利完成（2021）年黄梁木蔗糖转运蛋白NcSUT1在木材发育中的作用及其机制研究 专项项目（文件编号： 粤基金字〔2021〕4号）经协商一致，特订立本合同，作为甲乙双方在项目实施管理过程中共同遵守的依据。

第二条 甲方的权利义务：

1.按合同书规定进行经费核拨的有关工作协调。

2.根据甲方需要，在不影响乙方工作的前提下，定期或不定期对乙方项目的实施情况和经费使用情况进行检查或抽查。

3.根据《广东省科技计划项目信用管理办法(试行)》对乙方进行科技计划信用管理。

第三条 乙方的权利义务：

1.确保落实自筹经费及有关保障条件。

2.乙方是项目资金管理的责任主体，应当建立健全科研项目资金管理制度，严格按照省科技经费使用范围和有关规定管好用好财政资金；应当按合同书规定，对甲方核拨的经费实行专款专用，单独列账，并随时配合甲方进行监督检查。

3.实施“包干制”的面上项目及青年基金项目，依托单位应参照国家杰出青年科学基金试点项目经费使用“包干制”要求，制定经费使用“包干制”内部管理规定。项目经费支出应实际用于研发活动相关支出，使用范围限于设备费、材料费、测试化验加工费、燃料动力费、差旅/会议/国际合作与交流费、出版/文献/信息传播/知识产权事务费、劳务费、专家咨询费、依托单位管理费用、绩效支出以及其他合理支出。依托单位管理费用由依托单位根据实际管理支出情况与项目负责人协商确定。绩效支出由项目负责人根据实际科研需要和相关薪酬标准自主确定，依托单位按照现行工资制度进行管理。其余用途经费无额度限制，由项目负责人根据实际需要自主决定使用。项目验收时应提交经费决算表。

4.项目负责人是项目资金使用的直接责任人，对资金使用的合规性、合理性、真实性和相关性承担法律责任。

5.使用财政资金采购设备、原材料等，按照《广东省实施〈中华人民共和国招标投标法〉办法》有关规定，符合招标条件的须进行招标。

6.项目合同任务完成后，或合同书规定的任务、指标及经费投入等提前完成的，乙方可按照《广东省省级科技计划项目结题管理实施细则（试行）》提出验收结题申请，并按甲方要求做好项目验收结题工作。

7.若项目发生需要终止结题的情况，乙方须按照《广东省省级科技计划项目结题管理的实施细则（试行）》提出终止结题申请，并按甲方要求做好项目终止结题工作。

8.在每年规定时间内向甲方如实提交上年度工作情况报告，报告内容包含上年度项目进展情况、经费决算和取得的成果等。

9.按照国家和省有关规定，提交科技报告及其他材料。

10.利用甲方的经费获得的研究成果，项目负责人和参与者应当注明获得“广东省基础与应用基础研究基金（英文：Guangdong Basic and Applied Basic Research Foundation）（项目编号）”资助或作有关说明。

11.乙方要恪守科学道德准则，遵守科研活动规范，践行科研诚信要求，不得抄袭、剽窃他人科研成果或者伪造、篡改研究数据、研究结论；不得购买、代写、代投论文，虚构同行评议专家及评议意见；不得违反论文署名规范，擅自标注或虚假标注获得科技计划（专项、基金等）等资助；不得弄虚作假，骗取科技计划（专项、基金等）项目、科研经费以及奖励、荣誉等；不得有其他违背科研诚信要求的行为。

12.确保本项目开展的研究工作符合我国科研伦理管理相关规定。

第四条 在履行本合同的过程中，如出现广东省相关政策法规重大改变等不可抗力情况，甲方有权对所核拨经费的数量和时间进行相应调整。

第五条 在履行本合同的过程中，当事人一方发现可能导致项目整体或部分失败的情形时，应及时通知另一方，并采取适当措施减少损失，没有及时通知并采取适当措施，致使损失扩大的，应当就扩大的损失承担责任。

第六条 本项目技术成果的归属、转让和实施技术成果所产生的经济利益的分享，除双方另有约定外，按国家和广东省有关法规执行。

第七条 根据项目具体情况，经双方另行协商订立的附加条款，作为本合同正式内容的一部分，与本合同具有同等效力。

第八条 本合同一式三份，各份具有同等效力。甲、乙方及项目负责人各执一份，三方签字、盖章后即生效，有效期至项目结题后一年内。各方均应负合同的法律责任，不应受机构、人事变动的影响。

第九条 乙方必须接受甲方聘请的本项目合同监理单位的监督和管理。监理单位按照甲方赋予的权利对本项目合同的履行进行审核、进度调查，对项目合同变更、经费使用情况进行监督管理及组织项目验收。

说明：1.本合同书中，凡是当事人约定无需填写的内容，应在空白处划（/）。

2.委托代理人签订本合同书的，应出具合法、有效的委托书。

八、本合同签约各方

管理单位（甲方）：　　广东省基础与应用基础研究基金委员会　（盖章）

法定代表人（或法人代理）：　曾路　（签章）

2021 年　03 月　25 日

依托单位（乙方）：　华南农业大学　（盖章）

法定代表人（或法人代理）：　刘雅红　（签章）

联系人（项目主管）姓名：　安沛（基金类基础科、成果登记成果科、实验室平台办、海外名师人事处）　（签章）

Email：　414484016@qq.com

电话：　020-85283435　/　13535577893

开户单位名称：　华南农业大学

开户银行名称：　广东广州工行五山支行

开户银行帐号：　3602002609000310520

年　月　日

联系人（项目负责人）姓名：　龙健梅　（签名）

Email：　longjianmei@scau.edu.cn

电话：　18820760615

年　月　日

项目编号： 202102020505

广州市科技计划项目

合同书

项目名称： 黄粱木糖转运蛋白NcSWEET1b调控木材形成的功能解析

计划类别： 基础研究计划

专题名称： 基础与应用基础研究项目（博士青年科技人员类）

起止时间： 2021年04月01日 至 2023年03月31日

承担单位： 华南农业大学

组织单位： 华南农业大学

责任处室： 基础研究处

填表日期： 2021年04月11日

广州市科学技术局制

（2021年版）

填 写 说 明

一、本合同书的项目编号由市科学技术局（以下简称市科技局）统一确定。

二、本合同书由申报书在后台自动转换生成，如有错漏之处需修正，请联系市科技局项目责任处室退回承担单位修正。

三、本项目如涉及多家（包含两家）单位参加，乙方应在签订本合同书前与合作单位就任务分工、经费和知识产权分配等问题签订有关合同或协议，作为本合同书的附件。

四、本合同书适用于广州市事前资助类科技计划项目，有特殊要求另行制定的除外。

一、项目基本信息

项目名称	黄粱木糖转运蛋白NcSWEET1b调控木材形成的功能解析			
技术领域	农业与食品-林业-种植与遗传育种			
承担单位	名　　称	华南农业大学		
	通信地址	广东省广州市天河区五山路483号		
	邮政编码	510642	传　　真	85281885
	单位特性		单位类型	高等院校
	统一社会信用代码或组织机构代码	124400004554165634		
	法定代表人	刘雅红	电子邮箱	gale@scau.edu.cn
	联系人	侯建国	联系电话	02038632413

二、项目组人员信息

项目负责人	姓名	龙健梅	证件类型	身份证	证件号码	452123198908283146	性别	女
	出生年月	1989年08月28日	民族	汉族	国籍	中国	学历	博士研究生
	学位	博士	学位授予国家（或地区）	中国	职务	无	职称	讲师(高校)
	所学专业	果树学	手机号码	18820760615	办公电话	18820760615	电子邮箱	longjianmei@scau.edu.cn

项目组成员（含项目负责人）

序号	姓名	证件类型	证件号码	年龄	性别	职务	职称	学历	现从事专业	分工	所在单位
1	龙健梅	身份证	452123198908283146	30	女	无	讲师(高校)	博士研究生	林木遗传育种	项目负责人	华南农业大学
2	张建霞	身份证	422425197805064126	42	女	无	副研究员	博士研究生	植物遗传育种	组织定位与亚细胞定位分析	华南农业大学
3	高佳钰	身份证	372328199310081547	26	女	无	未取得	本科	林木遗传育种	载体构建与遗传转化	华南农业大学
4	陈鑫	身份证	411327199605160029	24	女	无	未取得	本科	林木遗传育种	上游调控因子与互作蛋白挖掘	华南农业大学

三、项目实施内容

（一）项目概述

本项目拟通过分析速生树种黄粱木次生维管组织细胞高丰度表达的NcSWEET1b在木材发育中的功能，进一步挖掘以其为中心的分子调控网络，明晰其在黄粱木木材形成中的作用及调控机理。项目的实施为深入阐明糖转运蛋白参与木材产量及品质形成的分子机制奠定基础，为林木生长发育与木材品质的遗传改良提供有效的候选基因。

（二）项目研究内容

1. 研究目标：

通过在黄粱木中分别超量表达和敲除NcSWEET1b，验证其在黄粱木木质部发育过程中的相关功能；通过分别筛选并验证上游调控NcSWEET1b转录因子及下游与其互作的蛋白，挖掘NcSWEET1b参与木材形成的分子调控网络，解析NcSWEET1b在黄粱木木材形成过程中的分子机制，为林木产量及品质遗传改良奠定理论基础。

2. 研究内容

（1）组织定位与亚细胞定位分析：利用免疫荧光定位分析NcSWEET1b在黄粱木维管组织（木质部、韧皮部和形成层）在不同发育过程中的定位情况；利用黄粱木原生质体瞬时表达体系验证NcSWEET1b在亚细胞的定位情况。（2）转运底物特性分析：利用酵母己糖吸收功能突变体进行功能互补实验，验证NcSWEET1b的糖转运能力。（3）NcSWEET1b功能鉴定：通过遗传转化获得超表达及敲除转基因株系并进行表型和生理指标分析。（4）调控机制解析：转录组分析挖掘发生显著变化的分子路径，筛选验证NcSWEET1b的互作蛋白；筛选验证NcSWEET1b的上游调控转录因子。

3. 拟解决的关键技术问题

针对目前黄粱木中糖转运蛋白的功能还未有相关报道，且对SWEETs在糖的运输和分配的研究相对缺乏。基于前期研究表明NcSWEET1b可能与黄粱木的次生木质部发育密切相关，进而影响木材的发育与形成。本研究拟通过分析NcSWEET1b的表达与定位特征及转运底物特性并验证其功能，解析NcSWEET1b在黄粱木木材形成中的作用，重点深入挖掘以NcSWEET1b为中心的分子调控网络，为阐明NcSWEET1b在黄粱木次生生长发育中的作用提供研究基础。

4. 主要创新点

（1）研究材料有特色

黄粱木是我国南方生长迅速的阔叶树种，材质优良，是研究木材发育和形成的理想材料。目前对糖运输及转运蛋白的功能研究目前仅在北方林木树种杨树进行，在南方林木尚未开展。因此，利用具有速生且木材优质的黄粱木为研究材料，探索糖转运蛋白的功能与调控机制，可为其他木本植物提供研究借鉴，也为创造更多速生、优质的阔叶树种新种质提供新的理论依据。

（2）选题科学意义具有创新性

目前SWEET的功能研究仅在草本植物中进行，还未在木本植物中探讨。木材作为林木植物最重要的器官，糖类如何参与调控木质部发育，特别是细胞分化及细胞腔内容物的填充等方面目前还缺乏科学证据。因此以黄粱木为研究对象本项目将在前人的研究基础上深入挖掘SWEET在木材发育与形成过程中的具体调控作用，加深对SWEET与木材发育关系的理解，为木本植物速生性状与木材品质的遗传改良奠定基础。

5. 采用的方法

（1）NcSWEET1b组织定位分析：选择NcSWEET1b特异蛋白区段，合成后制备抗体。取木材发育不同阶段的茎节（初生生长时期、初生向次生生长时期及次生生长时期）进行石蜡切片，与抗体孵育后于荧光显微镜下观察。

（2）亚细胞定位：将NcSWEET1b基因与YFP基因融合，利用黄粱木叶片原生质体瞬时表达体系观察YFP蛋白发光情况。

（3）转运底物特性分析：PCR扩增NcSWEET1b全长，连入酵母表达载体pDR195中，转化酵母己糖吸收功能突变体，观察酵母生长状况在不同碳源培养基上生长情况。

（4）功能验证：克隆NcSWEET1b基因全长，连接到超量表达载体pK7WG2D。设计针对特定靶位点的接头，插入pYLsgRNA载体sgRNA表达盒，将带有把序列的sgRNA表达盒组装到终载体pYLCRISPR/Cas9中。这两个载体分别转化黄粱木，获得NcSWEET1b超量表达及敲除转基因株系；对各转基因株系进行表型和各生理指标分析，测量转基因植株的株高、叶片大小，地径等方面；对木质部进行组织切片观察；采用GC-MS检测糖分组成与含量分析、Klason法检测茎中木材的木质素含量；Updegraff法测定木材中纤维素含量。

（5）调控机制解析：选取NcSWEET1b超量表达株系、基因敲除株系及野生型植株进行转录组测序，挖掘发

生显著变化的分子路径；通过分裂泛素化酵母双杂文库筛选及BiFC验证NcSWEET1b的互作蛋白；通过酵母单杂交文库筛选及双荧光素酶瞬时表达体系与EMSA验证NcSWEET1b的上游调控转录因子。

（三）项目预期风险及规避措施

预期风险：本项目所涉及的技术体系在本实验室应用成熟，实验室平台仪器齐全，可保证项目的正常开展，预期风险较小。因黄粱木不耐低温，可能的风险在于广州地区可能会出现的台风或极端低温等天气对植株造成的伤害。
规避措施：在项目实施过程中如遇到极端天气，提前将转基因及野生型的黄粱木放置于本单位现有的玻璃温室中，保证其不受极端天气影响，能够正常生长发育。

四、项目主要验收指标

（一）主要技术指标

发表SCI论文1篇；培养研究生2名；参加林学相关学术会议1次。

（二）主要技术成果

序号	成果形式		成果数量
1	新产品（或新材料、新装备、新品种/系）	无	0
2	新工艺（或新方法、新模式、新技术、新服务）	无	0
3	发明专利（件）	申请	0
		授权	0
4	实用新型专利（件）	申请	0
		授权	0
5	外观设计专利（件）	申请	0
		授权	0
6	国外专利（件）	PCT受理	0
		授权	0
7	技术标准制定（个）	牵头	0
		参与	0
8	软件著作权（项）		0
9	论文论著（篇）	SCI/EI/ISTP	1
		其他	0
10	创新平台（载体）项目	技术服务数量（项）	0
		服务企业数量（家）	0
11	获得国家级奖项（项）		0
12	获得省级奖项（项）		0
13	科技人才奖励（人）		0
14	引进人才（人）		0
15	培养人才（人）	博士	0
		硕士	2

其他成果及形式说明（新药证书、动植物新品种、创新特色、成果宣传推介措施等）

无

（三）主要经济指标及社会效益

序号	指标名称	指标值
1	实施期内项目销售收入（万元）	/
2	实施期内项目出口创汇（万美元）	/
3	实施期内项目新增就业人数（人）	/

其他经济指标及社会效益说明
无

五、项目经费预算

（单位：万元）

项目经费： 5.00				
资金来源	小计	市科技局经费	其他财政经费	自筹资金
2021年	5.00	5.00	0.00	0.00
2022年	0.00	0.00	0.00	0.00
2023年	0.00	0.00	0.00	0.00
合计	5.00	5.00	0.00	0.00

注：项目经费实行“包干制”，经费使用按项目承担单位或组织单位相关科研项目经费管理办法执行。

六、共同条款

第一条　甲、乙、丙三方根据《中华人民共和国科学技术进步法》《广东省自主创新促进条例》《广州市科技创新促进条例》及《中华人民共和国民法典》等国家有关法规和规定，经协商一致，特订立本合同，作为甲、乙、丙三方在合同执行中共同遵守的依据。

第二条　甲、乙、丙三方应当严格履行《广州市科技计划项目管理办法》《广州市级财政科研项目资金绩效提升和管理监督办法》《广州市科技创新发展专项资金管理办法》《广州市科技计划项目经费“包干制”改革试点工作方案》《广州市科技创新发展专项项目全过程管理简政放权改革试点工作方案》的规定要求。

第三条　甲方应：

1.根据财政经费预算安排，及时拨付项目经费。

2.赋予乙方和丙方广州市科技业务管理阳光政务平台（以下简称阳光政务平台）的使用权限，保障丙方进行项目全过程管理的使用需求。

3.按时拨付项目经费。

4.审核丙方提交的年度工作报告，制定下一年度的资金切块方案。

5.对丙方进行周期绩效考核和检查评估，重新评估丙方资格。

第四条　乙方应：

1.作为项目具体组织实施的责任主体，为本单位提供的与本项目有关的全部材料真实、合法、有效性负责；

2.按照《合同书》规定的内容组织实施项目，接受并配合甲方、丙方以及各级财政、审计部门，或上述部门委托的机构进行评估、稽查、审计、检查和绩效评价，并按要求提供项目任务与预算执行情况和有关财务资料；

3.按照市财政科技经费管理“包干制”相关要求对项目经费单独设账，专款专用；

4.保证自筹资金按时到位和其它配套条件的落实；

5.在项目研究开发过程中优先考虑使用“广东省科技资源共享服务平台”的仪器设备，项目购置的设备仪器若符合入网条件应及时办理入网手续对社会共用共享，提高设备仪器的使用率。按照《中华人民共和国采购法》要求，对符合政府采购范围的设备仪器，执行政府采购；

6.项目合同执行期内需进行变更的，按照《广州市科技计划项目管理办法》《广州市级财政科研项目资金绩效提升和管理监督办法》《广州市科技创新发展专项资金管理办法》《广州市科技创新发展专项项目全过程管理简政放权改革试点工作方案》相关程序办理；

7.项目合同执行期满后3个月内向丙方提出验收申请，提前完成合同规定任务的可提前申请验收；

8.按照相关规定，在项目验收时提交科技报告，办理《验收证书》和科技成果登记手续；

9.配合甲方开展对财政资金绩效的跟踪，在项目实施期内及实施期结束后按照甲方要求提供相关信息和数据；

10.对合作单位承担监管责任，与合作单位签署合作协议，作为本合同的附件，因合作单位违反合作协议或其他导致本合同书项目建设未能按约定完成的行为，应向甲方承担违约责任。

第五条　丙方应：

1.明确项目管理依据的管理办法或管理规程，承担项目全过程管理职责；

2.自主安排立项评审和结题验收工作，充分利用阳光政务平台，推进项目全过程管理的网络化电子化，主动配合推行合同电子签章；

3.严格落实信息公开制度，公示遴选和结题验收结果，并及时处理异议；

4.及时报送相关材料，按广州市科学技术局要求，每年按时提交拟立项项目清单，报送年度工作总结；

5.按广州市科学技术局要求配合开展绩效评价和监督检查工作；

6.主动追回终止项目未使用和不合规支出的市财政科技经费；

7.按照本单位相关项目管理办法组织项目验收工作，并按相关规定做好存档工作；

8.协助甲方对项目的实施过程进行跟踪、检查和提供相关信息，并对所提供信息的客观真实性负责；

9.负责监管乙方严格遵守《合同书》规定的任务；

10.督促乙方按时到位自筹资金并保证和落实其他配套条件。

第六条　甲方同意给予乙方人民币（¥5.00万）的资助，立项后一次性拨付。

第七条　合同终止：

1.项目因故无法继续进行的，按照相关规定实施合同终止。

2.发现存在以下情况之一的，立即启动终止程序：

①因不可抗拒因素导致项目无法继续进行、没有必要继续进行或无法完成合同预期目标任务的；

②不接受项目监督检查、检查不合格限期整改后仍未通过的或拒不配合项目验收工作的；

③无正当理由项目合同执行期满后3个月以后仍未提交验收申请的；

④项目承担单位已迁出本市，或已停止经营活动，或已注销的；

⑤发现在项目申报、实施过程中有违法、欺骗等事实的；

⑥存在其他导致项目不能正常实施的原因。

3.合同终止由乙方提出申请，丙方审定。也可由丙方强制实施。

4.合同终止后，乙方应停止使用该项目财政经费；上缴尚未使用和使用不符合规定的财政经费。

第八条 对合同正常执行期及项目整改期之外的经费开支，不属于财政项目经费列支范围。

第九条　在履行本合同的过程中，乙方发现可能导致项目失败或部分失败的情形时，应及时通知甲方和丙方，并采取适当措施减少损失，没有及时通知并采取适当措施，致使损失扩大的，应当就扩大的损失承担责任。

第十条　在履行本合同的过程中，如遇到市财政计划改变等不可抗力情况，甲方对所核拔经费的数量和时间可进行相应变更。

第十一条　成果转化：本项目技术成果及知识产权的归属、转让和实施技术成果所产生的经济利益的分享，除另有约定外，按国家和省、市有关规定执行；正式发表的论文、论著应标注“广州市科技计划项目资助”字样及项目编号；项目所取得的技术成果和知识产权应优先广州产业化或推广转让。

第十二条　属技术保密的项目，经协商订立如下技术保密条款：

1.本合同书保密内容范围为：本合同及其补充协议和附件、乙方因履行本合同所接触或知晓的甲方工作秘密（包括但不限于甲方的任何技术性资料、以及甲方为完成本合同提供的任何其他信息资料并且在提供时未说明是公开信息的）；

2.本合同书保密期限为 ：\；

3.乙方（包括但不限于乙方雇员、代理人、顾问等人员，下同）采取有效的保密措施以避免泄露给任何第三方；在本合同有效存续期间及合同终止后，未经甲方事先的书面同意，不得以任何方式公布、发表、公开、披露、散播、复制此种保密信息的任何部分，或对其加以任何形式的利用或使用；如甲方要求，乙方必须签署甲方提供的保密协议。乙方应与可能知悉保密内容的人员签订技术保密保护协议，保密义务不得低于本合同书的约定；

4.双方应建立技术保密制度；

5.属技术保密的项目必须经市负责技术保密部门审查后,方可确定可否发表或用于国际合作与交流。

第十三条　廉洁责任

甲方、丙方、评审机构及其工作人员不得索取、收受利益相关方财物或其他不正当利益，严格遵守中央八项规定精神及其实施细则。

乙方应严格遵守国家、省、市关于科技专项经费使用的有关法律、法规，相关政策以及廉洁建设的各项规定，积极开展人员廉洁从业教育，防范科技项目组成员在科研活动中出现出现“法律、行政法规、部门规章或规范性文件规定的其他相关违规行为。

第十四条 科研诚信和科技伦理要求

乙方应建立健全促进科研诚信和科技伦理的规章制度，落实以下职责：

1.建立健全本单位学术论文发表诚信承诺制度、科研过程可追溯制度、科研成果检查和报告制度等成果管理制度。对本项目形成的科研成果的署名、研究数据真实性、实验可重复性等进行诚信审核和学术把关。防范科技项目组成员在项目申报、研发过程中提供虚假信息或材料，抄袭、剽窃他人科研成果，捏造、变造或篡改科研数据；

2.加强对科技项目参加人员的科研诚信和科技伦理教育,督促科技项目组成员恪守科学道德准则,遵守科研活动规范。对在科研诚信和科技伦理方面存在问题情节较严重的,应及时调整出项目团队并及时以书面形式报告甲方；

3.加强对项目合作单位的科研诚信管理,正确履行管理、指导、监督职责,全面落实科研诚信和科技伦理要求；

4.乙方或项目合作单位及其相关人员被纳入科研严重失信行为记录或相关社会领域信用“黑名单”， 乙方应及时以书面形式报告甲方；

在项目实施过程中,对乙方或项目合作单位及其相关人员有严重违背科研诚信和科技伦理要求的行为,甲方和相关部门可对乙方采取约谈主要负责人、停拨或核减经费、记入科研诚信严重失信行为数据库、将不良行为向社会公开、移送至有管理权限的纪检监察部门等处理处罚措施。

第十五条　争议解决

因本合同书所产生的争议，各方应友好协商解决；协商不成的，各方同意由本合同签订地人民法院管辖。

第十六条　书面通知与送达

甲方在本合同履行过程中向乙方或丙方发出或者提供的所有书面通知、文件、文书、资料等，均以本合同所列明的乙方或丙方地址送达。乙方或丙方如果迁址，应当书面通知甲方；未履行书面通知义务的，甲方按原地址邮寄相关材料即视为已履行送达义务。

本合同一式四份，各份具有同等效力。甲方和丙方各存一份，乙方存二份。本合同签订各方均负有相应的法律责任，不受机构、人事变动而影响。

说明：本《合同书》中，凡是三方约定无需填写的条款，在该条款的空白处划（\）。

附件：承诺书

承诺书

本人作为本项目参与成员，知悉项目研究研究内容，明确项目任务分工，将严格遵守广州市科学技术局科技计划项目相关管理规定，切实保障工作时间，认真开展工作。

序号	姓名	证件类型	证件号码	分工	所在单位	签名
1	龙健梅	身份证	452123198908283146	项目负责人	华南农业大学	龙健梅
2	张建霞	身份证	422425197805064126	组织定位与亚细胞定位分析	华南农业大学	张建霞
3	高佳钰	身份证	372328199310081547	载体构建与遗传转化	华南农业大学	高佳钰
4	陈鑫	身份证	411327199605160029	上游调控因子与互作蛋白挖掘	华南农业大学	陈鑫

合同书各方签章

广州市科学技术局（甲方）：广州市科学技术局

项目经办人 ：李磊　　联系电话：020-83124052

责任处室负责人：莫雪华

（科学技术局公章）

2021年04月20日

项目承担单位（乙方）：华南农业大学

二级部门：华南农业大学林学与风景园林学院

项目负责人：龙健梅

项目经费汇入账号

帐户名：华南农业大学　　帐号：3602002609000310520

开户银行：广东广州工行五山支行

财务负责人：曾亮珍　　财务负责人联系电话：02085287402

（承担单位公章）

2021年04月13日

组织单位（丙方）：华南农业大学

项目经办人：倪慧群

（组织单位公章）

2021年04月13日

项目编号: 2017KQNCX017

广东省教育厅2017年重点平台及科研项目（自然科学类）

合同书

签约各方共同遵守《关于印发“广东省高等教育‘创新强校工程’专项资金管理办法”的通知》（粤财教〔2014〕130号）和《广东省教育厅关于做好“创新强校工程”科研项目管理工作的通知》（粤科教函〔2017〕22号）。

为顺利完成广东省普通高校省级重大科研项目（青年创新人才类、特色创新类）“NcSUT4在黄梁木蔗糖转运中的功能鉴定与调控机制解析”遵守条款如下：

1. 管理单位（甲方）为华南农业大学；承担单位（乙方）是指该项目具体实施的依托学院（单位）。

2. 合同书中的主要研究内容、项目成员、经费预算、进度和阶段性目标及预期成果等参照申请书执行。

3. 乙方必须按要求于次年年初向甲方报送上一年度项目进展报告。逾期不报，甲方有权暂停拨款。

4. 合同执行过程中，乙方如需调整任务或修改合同中的部分条款，应按《管理办法》向甲方提出变更内容及其理由的申请报告，经甲方审定后实施。甲方提出变更合同，要与乙方达成书面协议。未经正式批准或达成协议前，双方须按原合同履行。

5. 乙方因某种原因致使任务无法执行，而要求终止合同，应视不同情况，部分或全部退还所拨经费并追究相关人员责任；如乙方没有提出终止合同的要求，甲方有权根据实际情况提出终止合同的处理建议。

6. 经费必须按《关于印发“广东省高等教育‘创新强校工程’专项资金管理办法”的通知》（粤财教〔2014〕130号）使用。

7. 合同正式文本一式贰份，存甲方壹份，乙方壹份。

本合同签约各方

甲方：华南农业大学（公章）

代表人（签名）：

2018年5月11日

乙方：所在学院（公章）

负责人（签名）：

2018年5月3日

同意按照合同规定执行。

项目负责人（签名）：龙德梅

2018年5月3日

项目批准号	31870653
申请代码	C161002
归口管理部门	
依托单位代码	51064208A0499-0932

国家自然科学基金委员会

资助项目计划书

资助类别：面上项目

亚类说明：

附注说明：

项目名称：受乙烯诱导的ERF第七亚家族转录因子调控木质素合成的分子机理

直接费用：60万元　　执行年限：2019.01-2022.12

负 责 人：吴蔼民

通讯地址：广州市天河区五山路483号

邮政编码：510642　　电　　话：020-85280259

电子邮件：wuaimin@scau.edu.cn

依托单位：华南农业大学

联 系 人：唐家林　　电　　话：020-85280070

填表日期：2018年08月17日

国家自然科学基金委员会制

Version：1.004.943

国家自然科学基金委员会资助项目计划书填报说明

一、项目负责人收到《关于国家自然科学基金资助项目批准及有关事项的通知》（以下简称《批准通知》）后，请认真阅读本填报说明，参照国家自然科学基金相关项目管理办法及《国家自然科学基金资助项目资金管理办法》（请查阅国家自然科学基金委员会官方网站首页“政策法规”栏目），按《批准通知》的要求认真填写和提交《国家自然科学基金委员会资助项目计划书》（以下简称《计划书》）。

二、填写《计划书》时要求科学严谨、实事求是、表述清晰、准确。《计划书》经国家自然科学基金委员会相关项目管理部门审核批准后，将作为项目研究计划执行和检查、验收的依据。

三、《计划书》各部分填写要求如下：

（一）简表：由系统自动生成。

（二）摘要及关键词：各类获资助项目都必须填写中、英文摘要及关键词。

（三）项目组主要成员：计划书中列出姓名的项目组主要成员由系统自动生成，与申请书原成员保持一致，不可随意调整。如果批准通知中“项目评审意见及修改意见表”中“对研究方案的修改意见”栏目有调整项目组成员相关要求的，待项目开始执行后，按照项目成员变更程序另行办理。

（四）资金预算表：根据批准资助的直接费用，按照《国家自然科学基金项目预算表编制说明》填报资金预算表和预算说明书。国家重大科研仪器研制项目、重大项目还应按照预算评审后批复的直接费用各科目金额填报资金预算表、预算说明书及相应的预算明细表。

（五）正文：

1. 面上项目、青年科学基金项目、地区科学基金项目：如果《批准通知》中没有修改要求的，只需选择“研究内容和研究目标按照申请书执行”即可；如果《批准通知》中“项目评审意见及修改意见表”中“对研究方案的修改意见”栏目明确要求调整研究期限和研究内容等的，须选择“根据研究方案修改意见更改”并填报相关修改内容。

2. 重点项目、重点国际（地区）合作研究项目、重大项目、国家重大科研仪器研制项目：须选择“根据研究方案修改意见更改”，根据《批准通知》的要求填写研究（研制）内容，不得自行降低、更改研究目标（或仪器研制的技术性能与主要技术指标以及验收技术指标）或缩减研究（研制）内容。此外，还要突出以下几点：

（1）研究的难点和在实施过程中可能遇到的问题（或仪器研制风险），拟采用的研究（研制）方案和技术路线；

（2）项目主要参与者分工，合作研究单位之间的关系与分工，重大项目还需说明课题之间的关联；

（3）详细的年度研究（研制）计划。

3. 国家杰出青年科学基金、优秀青年科学基金和海外及港澳学者合作研究基金项目：须选择“根据研究方案修改意见更改”，按下列提纲撰写：

（1）研究方向；

（2）结合国内外研究现状，说明研究工作的学术思想和科学意义（限两个页面）；

（3）研究内容、研究方案及预期目标（限两个页面）；

（4）年度研究计划；

（5）研究队伍的组成情况。

4. 国家自然科学基金基础科学中心项目：须选择“根据研究方案修改意见更改”，应当根据评审委员会和现场考察专家组的意见和建议，进一步完善并细化研究计划，作为评估和验收的依据。按下列提纲撰写：

（1）五年拟开展的研究工作（包括主要研究方向、关键科学问题与研究内容）；

（2）研究方案（包括骨干成员之间的分工及合作方式、学科交叉融合研究计划等）；

（3）年度研究计划；

（4）五年预期目标和可能取得的重大突破等；

（5）研究队伍的组成情况。

5. 对于其他类型项目，参照面上项目的方式进行选择和填写。

简表

<table>
<tr><td rowspan="6">申请者信息</td><td>姓　　名</td><td>吴蔼民</td><td>性 别</td><td>男</td><td>出生年月</td><td>1969年02月</td><td>民 族</td><td>汉族</td></tr>
<tr><td>学　　位</td><td colspan="3">博士</td><td>职称</td><td colspan="3">教授</td></tr>
<tr><td>是否在站博士后</td><td colspan="2">否</td><td>电子邮件</td><td colspan="4">wuaimin@scau.edu.cn</td></tr>
<tr><td>电　　话</td><td colspan="2">020-85280259</td><td>个人网页</td><td colspan="4"></td></tr>
<tr><td>工 作 单 位</td><td colspan="7">华南农业大学</td></tr>
<tr><td>所 在 院 系 所</td><td colspan="7">林学与风景园林学院</td></tr>
<tr><td rowspan="3">依托单位信息</td><td>名　　称</td><td colspan="5">华南农业大学</td><td>代码</td><td>51064208A0499</td></tr>
<tr><td>联 系 人</td><td colspan="2">唐家林</td><td>电子邮件</td><td colspan="4">kycjhk@scau.edu.cn</td></tr>
<tr><td>电　　话</td><td colspan="2">020-85280070</td><td>网站地址</td><td colspan="4">http://web.scau.edu.cn/kjc/</td></tr>
<tr><td rowspan="2">合作单位信息</td><td colspan="8">单 位 名 称</td></tr>
<tr><td colspan="8"></td></tr>
<tr><td rowspan="8">项目基本信息</td><td>项 目 名 称</td><td colspan="7">受乙烯诱导的ERF第七亚家族转录因子调控木质素合成的分子机理</td></tr>
<tr><td>资 助 类 别</td><td colspan="3">面上项目</td><td>亚 类 说 明</td><td colspan="3"></td></tr>
<tr><td>附 注 说 明</td><td colspan="7"></td></tr>
<tr><td>申 请 代 码</td><td colspan="3">C161002:林木遗传改良</td><td colspan="4"></td></tr>
<tr><td>基 地 类 别</td><td colspan="7"></td></tr>
<tr><td>执 行 年 限</td><td colspan="7">2019.01-2022.12</td></tr>
<tr><td>直 接 费 用</td><td colspan="7">60万元</td></tr>
</table>

项目摘要

中文摘要：

木质素在林木生长发育中起到不可或缺的作用，但同时也给制浆造纸、生物质能源利用等带来不少负面影响。因此，合理调节植物体内木质素的生物合成是目前的研究热点。木质素合成关键酶基因的转录调控研究主要集中在MYB家族转录因子，而其它类转录因子报道很少。乙烯能够促进木材的形成，但乙烯信号转导怎样调控木质素的合成还没有报道。本项目将分析受乙烯诱导的ERF第七亚家族转录因子，通过生物信息学分析、组织器官表达、胁迫表达、基因定位等研究ERF-VII成员的生物学特性，再通过过量表达和转录因子抑制型技术对ERF-VII基因的进行转基因研究，通过FT-IR、GC-MS、二维核磁等分析转基因杨树木质素等细胞壁成分的变化，同时通过转录组测序、反式激活和凝胶滞留分析ERF-VII对木质素合成关键酶的调控。这些研究不仅可以丰富木质素合成的调控途径，还可以为我们从上游进行基因工程改良木质素材料提供理论支持。

Abstract：

Lignin, one of the most abundant terrestrial biopolymers, is indispensable for plant structure and defense. However, it also has a negative effect on pulp and paper industry, biomass utilization. Therefore, the suitable modifying lignin biosynthesis is one of the hotest topic in plant. At present, The regulation of lignin biosynthesis mainly focused on MYB family of transcription factors, and less reported on other transcription factors. Ethylene can stimulate wood formation by cambium cells, but how ethylene signal transduction regulate lignin

synthesis has not yet been reported. This project will focus on seventh Ethylene Response Factors (ERF-VII) family which induced by ethylene treatment in poplar.

The members of ERF-VII family from poplar will be studied by bioimformatic analysis, expression levels in poplar, localization, and expression in stress condition. then we will overexpress the target genes or/and inhabit by Chimeric expressor Gene-Silencing technology to analyze lignin component changes in transgenic poplar plants by FT-IR, GC-MS, and two-dimensional NMR. Furthermore, how ERF-VII regulating lignin biosynthesis will be analyzed through RNA-Seq, trans-activation analysis and Electrophoretic Mobile Shift Assay (EMSA). These studies will not only rich the regulatory of lignin biosynthesis pathways, but also provide the genetically engineering method to modify lignin material from upstream regulatory genes

关键词(用分号分开)：次生代谢；代谢调控；ERF 转录因子；木质素；乙烯诱导

Keywords(用分号分开)： secondary metabolism; the regulation of metabolism; ethylene response transcription factors; lignin; ethylene induced

项目组主要成员

编号	姓名	出生年月	性别	职称	学位	单位名称	电话	证件号码	项目分工	每年工作时间（月）
1	吴蔼民	1969.02	男	教授	博士	华南农业大学	020-85280259	320113196902234973	项目负责人	5
2	龙健梅	1989.08	女	讲师	博士	华南农业大学	020-85280259	452123198908283146	转录调控网络研究	8
3	李青粉	1987.02	女	博士后	博士	华南农业大学	18922210205	410901198702052023	基因表达、定位及调控研究	8
4	王凯利	1990.12	女	博士生	硕士	华南农业大学	13610203509	370983199012053244	基因表达及异质性分析	10
5	李倩	1993.01	女	硕士生	学士	华南农业大学	18320728073	370782199301293060	基因、蛋白表达分析	10
6	尚娜	1991.06	女	硕士生	学士	华南农业大学	18320728039	410221199106240222	关键基因调控研究	10
7	陈辰	1995.11	男	硕士生	学士	华南农业大学	14755598988	342502199511072016	合成代谢网络影响研究	10
8	朱忆魁	1994.11	男	硕士生	学士	华南农业大学	15862146801	320311199411267633	成分分析	10

总人数	高级	中级	初级	博士后	博士生	硕士生
8	1	1	0	1	1	4

国家自然科学基金项目直接费用预算表 （定额补助）

项目批准号：31870653　　项目负责人：吴蔼民　　金额单位：万元

序号	科目名称	金额
1	项目直接费用合计	60.0000
2	1、 设备费	0.0000
3	(1)设备购置费	0.00
4	(2)设备试制费	0.00
5	(3)设备升级改造与租赁费	0.00
6	2、 材料费	24.0000
7	3、 测试化验加工费	14.5000
8	4、 燃料动力费	0.00
9	5、 差旅/会议/国际合作与交流费	6.0000
10	6、 出版/文献/信息传播/知识产权事务费	4.5000
11	7、 劳务费	11.0000
12	8、 专家咨询费	0.00
13	9、 其他支出	0.00

预算说明书（定额补助）

（请按照《国家自然科学基金项目预算表编制说明》的有关要求，对各项支出的主要用途和测算理由，以及合作研究外拨资金、单价≥10万元的设备费等内容进行必要说明。）

1、 设备费：无

2、 材料费 24.0 万：

（1）原材料、试剂、药品等消耗品购置费（22.0 万元）

引物合成 2.00 万元，PCR 相关试剂 3.00 万，工具酶类 3.00 万元，感受态细胞、质粒提取试剂盒和胶回收试剂盒 1.50 万元，RNA 提取试剂盒、DNA 提取试剂盒和 cDNA 反转录试剂盒 2.00 万元，蛋白纯化试剂 1.50 万元，抗体 1.00 万元，普通生化试剂 5.00 万元，其它常规耗材 3.00 万元，

（2）其他 （2.0 万元）

主要用于种植实验材料，共计 2.00 万元。

3、 测试化验加工费 14.5 万：

转录组测序 7.00 万元，扫描电镜 1.00 万元、透射电镜 1.00 万元；CHIP sequence 2.00 万元；细胞壁成分分析所要的 PROLYSIS 测定 1.00 万元、GC-MS 1.00 万元、FT-IR 0.50 万元、二维核磁 1.00 万元等仪器使用分析费。

4、 燃料动力费：无

5、 差旅/会议/国际合作与交流费：6.0 万：

市内交通费（广州化学所实验中心、中山大学测试中心、热林所）0.60 万元

参加国内相关学术会议及开展相关学术研究交流（ 0.30 万元/次×8 人次=2.40 万元）。

项目组成员赴国外交流交通及住宿费：2020 年参加世界林木生物技术大会或植物细胞壁大会 2 人 / 次。拟 2018 年赴瑞典农业大学与 Bjorn Sundberg 教授或他们组的 Totte Niittylä 副教授交流杨树细胞壁测定及木质素下降对纤维素丝的角度的影响，交流 1 人次，合计：3.00 万元。

6、 出版/文献/信息传播/知识产权事务费：4.5 万元

按照平均每个专利申报费为 0.3 万元，本项目申请专利 2 个，共计支出 0.60 万元；国内核心期刊论文的发表版面费大约为 0.25 万元/篇×2 篇=0.50 万元，国际论文的发表版面费大约 0.80 万元/篇×3 篇=2.40 万元；入网、信息查询、邮寄等支出 1.00 万元。合计 4.50 万元。

7、 劳务费 11.0 万：

主要用于支付博士、硕士研究生劳务费。平均每年支付 5 名研究生费用，每人每年 10 个月参与工作，4 年×5 人×10 月×550 元/月=11.0 万元。

8、 专家咨询费：无

9、 其他支出：无

项目负责人签字： 科研部门公章： 财务部门公章：

报告正文

研究内容和研究目标按照申请书执行。

国家自然科学基金资助项目签批审核表

<table>
<tr>
<td colspan="2">我接受国家自然科学基金的资助，将按照申请书、项目批准意见和计划书负责实施本项目（批准号：31870653），严格遵守国家自然科学基金委员会关于资助项目管理、财务等各项规定，切实保证研究工作时间，认真开展研究工作，按时报送有关材料，及时报告重大情况变动，对资助项目发表的论著和取得的研究成果按规定进行标注。

项目负责人（签章）：
年　　月　　日</td>
<td>我单位同意承担上述国家自然科学基金项目，将保证项目负责人及其研究队伍的稳定和研究项目实施所需的条件，严格遵守国家自然科学基金委员会有关资助项目管理、财务等各项规定，并督促实施。

依托单位（公章）
年　　月　　日</td>
</tr>
<tr>
<td>本栏目由基金委填写</td>
<td colspan="2">科学处审查意见：

建议年度拨款计划（本栏目为自动生成，单位：万元）：
<table>
<tr><td>年度</td><td>总额</td><td>第一年</td><td>第二年</td><td>第三年</td><td>第四年</td><td>第五年</td></tr>
<tr><td>金额</td><td></td><td></td><td></td><td></td><td></td><td></td></tr>
</table>
负责人（签章）：
年　　月　　日</td>
</tr>
<tr>
<td></td>
<td colspan="2">科学部审查意见：

负责人（签章）：
年　　月　　日</td>
</tr>
<tr>
<td>本栏目主要用于重大项目等</td>
<td colspan="2">相关局室审核意见：

负责人（签章）：
年　　月　　日</td>
</tr>
<tr>
<td></td>
<td colspan="2">委领导审批意见：

委领导（签章）：
年　　月　　日</td>
</tr>
</table>

项目批准号	31971702
申请代码	C161201
归口管理部门	
依托单位代码	51064208A0499-0932

国家自然科学基金委员会

资助项目计划书

资助类别：面上项目

亚类说明：

附注说明：

项目名称：B类MADS-box基因调控墨兰萼片形态变异的功能及机制研究

直接费用：58万元　　执行年限：2020.01-2023.12

负 责 人：张建霞

通讯地址：广东省广州市天河区五山街道华南农业大学林学与风景园林学院712室

邮政编码：510510　　电　　话：020-85280256

电子邮件：zhangjianxia@scau.edu.cn

依托单位：华南农业大学

联 系 人：倪慧群　　电　　话：020-85280070

填表日期：2019年08月20日

国家自然科学基金委员会制

国家自然科学基金委员会资助项目计划书填报说明

一、项目负责人收到《关于国家自然科学基金资助项目批准及有关事项的通知》（以下简称《批准通知》）后，请认真阅读本填报说明，参照国家自然科学基金相关项目管理办法及《国家自然科学基金资助项目资金管理办法》（请查阅国家自然科学基金委员会官方网站首页“政策法规”栏目），按《批准通知》的要求认真填写和提交《国家自然科学基金委员会资助项目计划书》（以下简称《计划书》）。

二、填写《计划书》时要求科学严谨、实事求是、表述清晰、准确。《计划书》经国家自然科学基金委员会相关项目管理部门审核批准后，将作为项目研究计划执行和检查、验收的依据。

三、《计划书》各部分填写要求如下：

（一）简表：由系统自动生成。

（二）摘要及关键词：各类获资助项目都必须填写中、英文摘要及关键词。

（三）项目组主要成员：计划书中列出姓名的项目组主要成员由系统自动生成，与申请书原成员保持一致，不可随意调整。如果批准通知中“项目评审意见及修改意见表”中“对研究方案的修改意见”栏目有调整项目组成员相关要求的，待项目开始执行后，按照项目成员变更程序另行办理。

（四）资金预算表：根据批准资助的直接费用，按照《国家自然科学基金项目预算表编制说明》填报资金预算表和预算说明书。国家重大科研仪器研制项目、重大项目还应按照预算评审后批复的直接费用各科目金额填报资金预算表、预算说明书及相应的预算明细表。

（五）正文：

1. 面上项目、青年科学基金项目、地区科学基金项目：如果《批准通知》中没有修改要求的，只需选择“研究内容和研究目标按照申请书执行”即可；如果《批准通知》中“项目评审意见及修改意见表”中“对研究方案的修改意见”栏目明确要求调整研究期限和研究内容等的，须选择“根据研究方案修改意见更改”并填报相关修改内容。

2. 重点项目、重点国际（地区）合作研究项目、重大项目、国家重大科研仪器研制项目：须选择“根据研究方案修改意见更改”，根据《批准通知》的要求填写研究（研制）内容，不得自行降低、更改研究目标（或仪器研制的技术性能与主要技术指标以及验收技术指标）或缩减研究（研制）内容。此外，还要突出以下几点：

（1）研究的难点和在实施过程中可能遇到的问题（或仪器研制风险），拟采用的研究（研制）方案和技术路线；

（2）项目主要参与者分工，合作研究单位之间的关系与分工，重大项目还需说明课题之间的关联；

（3）详细的年度研究（研制）计划。

3. 国家杰出青年科学基金、优秀青年科学基金和海外及港澳学者合作研究基金项目：须选择“根据研究方案修改意见更改”，按下列提纲撰写：

（1）研究方向；

（2）结合国内外研究现状，说明研究工作的学术思想和科学意义（限两个页面）；

（3）研究内容、研究方案及预期目标（限两个页面）；

（4）年度研究计划；

（5）研究队伍的组成情况。

4. 国家自然科学基金基础科学中心项目：须选择“根据研究方案修改意见更改”，应当根据评审委员会和现场考察专家组的意见和建议，进一步完善并细化研究计划，作为评估和验收的依据。按下列提纲撰写：

（1）五年拟开展的研究工作（包括主要研究方向、关键科学问题与研究内容）；

（2）研究方案（包括骨干成员之间的分工及合作方式、学科交叉融合研究计划等）；

（3）年度研究计划；

（4）五年预期目标和可能取得的重大突破等；

（5）研究队伍的组成情况。

5. 对于其他类型项目，参照面上项目的方式进行选择和填写。

简表

申请者信息	姓　　名	张建霞	性 别	女	出生年月	1978年05月	民 族	汉族
	学　　位	博士			职称	副研究员		
	是否在站博士后	否		电子邮件		zhangjianxia@scau.edu.cn		
	电　　话	020-85280256		个人网页				
	工 作 单 位	华南农业大学						
	所 在 院 系 所	林学与风景园林学院						
依托单位信息	名　　称	华南农业大学					代码	51064208A0499
	联 系 人	倪慧群		电子邮件		kycjhk@scau.edu.cn		
	电　　话	020-85280070		网站地址		http://kjc.scau.edu.cn/		
合作单位信息	单 位 名 称							
	中国科学院华南植物园							
项目基本信息	项 目 名 称	B类MADS-box基因调控墨兰萼片形态变异的功能及机制研究						
	资 助 类 别	面上项目			亚 类 说 明			
	附 注 说 明							
	申 请 代 码	C161201:园林植物种质资源与遗传育种			C150302:观赏植物种质资源与遗传育种学			
	基 地 类 别							
	执 行 年 限	2020.01-2023.12						
	直 接 费 用	58万元						

项目摘要

中文摘要：

墨兰是我国传统名花，花型是决定其经济价值的最重要品质之一，而萼片形态直接决定墨兰花型。前人推测兰科植物萼片花瓣化是由于B类MADS-box基因在萼片中的表达导致，我们前期实验发现墨兰的两个B类基因在不同形态的萼片中表达量存在明显差异，但B类基因如何参与调控萼片的形态变异尚不清楚。本项目将开展如下研究：（1）转录组比较测序不同花型的墨兰，筛选克隆其它差异表达的B类基因；（2）观察不同花型萼片的形态特征和细胞超微结构，检测不同生长发育时期、不同器官、不同生理条件及非生物逆境条件下墨兰B类基因的表达模式，分析萼片形态变异的因素和规律；（3）利用转基因和VIGS技术明确关键B类基因的功能，分析受其调控的与萼片发育相关的靶基因；筛选上述B类基因的互作蛋白，分析其互作机制；最终明确B类基因调控墨兰萼片形态变异的分子机制。研究结果将完善兰科植物花器官发育理论，为墨兰花型定向改良提供理论依据和基因资源。

Abstract：

Cymbidium sinense is high-grade traditional potted flower in China. The flower shape is one of the most important character of its economic value, while sepal directly determines the flower shape of C.sinense. Previous studies suggested that the expression of B-box genes in sepal resulted in the petaling sepals in orchid. We also found that there was a significant difference in the expression of two B genes in sepals of different flower shape. But it is not clear on how B-box genes are involved in the regulation of sepal morphological development and variation. The project will perform the following study: (1) Transcriptome comparision sequence on C.sinense with different flower shape, screen and clone other differentially expressed B-box genes. (2) Observe the morphological characteristics and cellular ultrastructure of sepal in different flower shape varieties, investigate the expression pattern of B-box genes in different growth and development period, different organs, different physiological and abiotic stress conditions. Analyze the factor and rule of sepals morphological variation. (3) Clarify the function of B-box genes by transgenic and VIGS techniques, analyze their target genes related to sepals development. Screen the interaction proteins of key B-box genes and analyze the interaction mechanism. Above research could help clarify the mechanism of B-box genes regulation sepal morphological development and variation of C.sinense. The results will improve the floral organ development theory of orchid, and provide the theoretical basis and gene resources for floral directional improvement of C.sinense.

关键词(用分号分开)：种质创新；基因资源；墨兰；萼片；B-box基因

Keywords(用分号分开)： germplasm innovation; genetic resources; Cymbidium sinense; sepal; B-box gene

项目组主要成员

编号	姓名	出生年月	性别	职称	学位	单位名称	电话	证件号码	项目分工	每年工作时间（月）
1	张建霞	1978.05	女	副研究员	博士	华南农业大学	020-85280256	422425197805064126	项目负责人	10
2	吴坤林	1968.08	男	副研究员	博士	中国科学院华南植物园	13719332759	440106196808262090	超微结构观察	5
3	龙健梅	1989.08	女	讲师	博士	华南农业大学	18820760615	452123198908283146	基因功能验证	5
4	张居生	1995.03	男	硕士生	学士	华南农业大学	13610202041	622224199503011511	功能基因的筛选与克隆	10
5	郝星宇	1995.03	男	硕士生	学士	华南农业大学	18826234234	140106199503050014	基因表达分析	10
6	胡欣荃	1997.02	女	硕士生	学士	华南农业大学	17818522365	360403199702090025	基因表达分析	10
7	徐新	1994.11	女	硕士生	学士	中国科学院华南植物园	15074952771	421127199411095223	互作蛋白筛选与鉴定	10
8	刘荷慧雯	1997.07	女	硕士生	学士	中国科学院华南植物园	15872848218	421281199707130028	基因功能验证	10

总人数	高级	中级	初级	博士后	博士生	硕士生
8	2	1				5

国家自然科学基金项目直接费用预算表 （定额补助）

项目批准号：31971702　　项目负责人：张建霞　　金额单位：万元

序号	科目名称	金额
1	项目直接费用合计	58.0000
2	1、 设备费	2.0000
3	(1)设备购置费	2.00
4	(2)设备试制费	0.0000
5	(3)设备升级改造与租赁费	0.0000
6	2、 材料费	21.8000
7	3、 测试化验加工费	11.0000
8	4、 燃料动力费	0.00
9	5、 差旅/会议/国际合作与交流费	5.20
10	6、 出版/文献/信息传播/知识产权事务费	5.00
11	7、 劳务费	12.00
12	8、 专家咨询费	1.00
13	9、 其他支出	0.00

预算说明书（定额补助）

请按照《国家自然科学基金项目预算表编制说明》的有关要求，对各项支出的主要用途和测算理由，以及合作研究外拨资金、单价≥10万元的设备费等内容进行必要说明。）

本项目资助直接费用58.00万元,本项目合作研究单位是中国科学院华南植物园,主要负责花器官形态发育及超微结构比较分析等研究工作，项目将按照直接经费的30%（17.4万元）拨给合作单位，双方已签订合作协议交由单位存档。具体预算如下:

一、项目直接费用：58.00万元

1、 设备费： 2.00万元

大型仪器配件购置费用1.50万元，仪器修理维护费用0.50万元。

2、 材料费： 21.80万元

（1）植物生理学和细胞生物学试剂3.00万元，购置各种生理生化试剂，抗体，染料等，用于各种生理实验、组织切片制备、细胞超微结构观察、原位杂交等实验。

（2）分子生物学试剂12.80万元，购置各种酶和试剂盒、各种分子试剂等，用于DNA和RNA提取、PCR、酵母双杂交、BiFC、VIGS、转基因、Southern Blot及其它分子实验

（3）实验室常规耗材4.00万元，购置实验所需各种玻璃器皿、塑料器皿、实验防护装备和一次性实验消耗品等

（4）其它2.00万元：购置实验材料种植所需的栽培基质、肥料和农药等耗材。

3、 测试化验加工费： 11.00万元

（1） 转录组测序服务5.50万元：PacBio SMAT测序一个混合样品约2.50万元；RNA-seq测序总共10个样品，3次重复，每次测序约1000元，共计3.00万元。

（2） 信息分析费3.00万元。

（3） 核酸序列合成费及DNA测序费2.50万元，用于基因扩增引物合成和常规DNA片段测序

4、 燃油动力费： 无

5、 差旅/会议/国际合作与交流费： 5.20万元：

参加8人次国内外学术研讨会差旅费，每人次约需费用0.40万元，合计3.20万元；计划邀请新加坡专家来华合作交流2人次，共2.00万元，每人次费用1.00万元，包括国际旅费0.60万元，每人次国内费用0.40万元（每人次国内停留4天，包括住宿费、接待费及交通补助）

6、 出版文献，信息传播，知识产权事务费：5.00万元

拟发表学术论文3-5篇，版面费约0.60万元/篇，5篇共3.00万元；申请1-2个国家发明专利，需1.00万元；文献查新检索费、专用网络费等约1.00万元。

7、 劳务费：12.00万元

直接参加该研究的研究生和临时聘用人员的劳务费用。研究生每人每年补贴0.50万元，5人四年合计10.00万元。项目临时聘用人员费2.00万元。

8、 专家咨询费：1.00万元

聘请专家对研究生进行学术指导交流，研究生毕业论文评审答辩费。

9、 其他支出：无

二、自筹资金

无。

本项目合作研究单位是中国科学院华南植物园,主要负责花器官形态发育及超微结构比较分析研究工作，研究外拨经费17.40万元，各支出预算如下：

一、 项目直接费用：17.40万元

1、设备费：1.00万元

大型仪器配件购置费和设备维护费1.00万元。

2、 材料费： 5.40万元

（1）原材料/试剂/药品购置费4.40万元：购置各种酶、试剂盒及其它普通生化试剂，以及一次性实验消耗品等

（2）其它1.00万元：购置实验材料种植所需的栽培基质、肥料和农药等耗材。

3、 测试化验加工费： 4.00万元

信息分析费3.00万元，核酸序列合成费和DNA测序费1.00万元。

4、 燃油动力费： 无

5、 差旅/会议/国际合作与交流费 2.00万元：

参加3人次国内外学术会议，每人次约需费用0.40万元，合计1.20万元；采集样品出差及学术交流费用约0.8万元。

6、 出版文献，信息传播，知识产权事务费：1.00万元

拟发表学术论文1篇，版面费约0.60万元；文献检索费、网络费等约0.40万元。

7、 劳务费：4.00万元

直接参加该研究的研究生和临时聘用人员的劳务费用。研究生每人每年补贴0.50万元，2人四年合计4.00万元。

8、 专家咨询费：无

9、 其他支出：无

项目负责人签字：　　科研部门公章：　　财务部门公章：

报告正文

研究内容和研究目标按照申请书执行。

国家自然科学基金资助项目签批审核表

<table>
<tr>
<td colspan="2">我接受国家自然科学基金的资助，将按照申请书、项目批准意见和计划书负责实施本项目（批准号：31971702），严格遵守国家自然科学基金委员会关于资助项目管理、财务等各项规定，切实保证研究工作时间，认真开展研究工作，按时报送有关材料，及时报告重大情况变动，对资助项目发表的论著和取得的研究成果按规定进行标注。

项目负责人（签章）：
年　月　日</td>
<td>我单位同意承担上述国家自然科学基金项目，将保证项目负责人及其研究队伍的稳定和研究项目实施所需的条件，严格遵守国家自然科学基金委员会有关资助项目管理、财务等各项规定，并督促实施。

依托单位（公章）
年　月　日</td>
</tr>
<tr>
<td rowspan="3">本栏目由基金委填写</td>
<td colspan="2">科学处审查意见：

建议年度拨款计划（本栏目为自动生成，单位：万元）：
<table>
<tr><td>年度</td><td>总额</td><td>第一年</td><td>第二年</td><td>第三年</td><td>第四年</td><td>第五年</td></tr>
<tr><td>金额</td><td></td><td></td><td></td><td></td><td></td><td></td></tr>
</table>
负责人（签章）：
年　月　日</td>
</tr>
<tr>
<td colspan="2">科学部审查意见：

负责人（签章）：
年　月　日</td>
</tr>
<tr>
<td rowspan="2">本栏目主要用于重大项目等</td>
<td colspan="2">相关局室审核意见：

负责人（签章）：
年　月　日</td>
</tr>
<tr>
<td colspan="2">委领导审批意见：

委领导（签章）：
年　月　日</td>
</tr>
</table>

项目批准号	32271908
申请代码	C1610
归口管理部门	
依托单位代码	51064208A0499-0932

国家自然科学基金

资助项目计划书

（预算制项目）

资助类别：面上项目

亚类说明：

附注说明：

项目名称：黄梁木（Neolamarckia cadamba）卡丹宾生物合成途径中NcSQE和NcOSC的功能解析

直接费用：54万元　　执行年限：2023.01-2026.12

负 责 人：彭昌操

通讯地址：广州市天河区五山路483号

邮政编码：510642　　电　　话：020-85280962

电子邮件：ccpeng@scau.edu.cn

依托单位：华南农业大学

联 系 人：唐家林　　电　　话：020-85280070

填表日期：2022年09月16日

国家自然科学基金委员会制

Version：1.004.409

国家自然科学基金资助项目计划书填报说明

（预算制项目）

一、项目负责人收到《国家自然科学基金资助项目批准通知》（以下简称《批准通知》）后，请认真阅读本填报说明，参照国家自然科学基金相关项目管理办法和新修订的《国家自然科学基金资助项目资金管理办法》（以下简称《资金管理办法》，请查阅国家自然科学基金委员会官方网站首页“政策法规”栏目），按《批准通知》的要求认真填写和提交《国家自然科学基金资助项目计划书》（以下简称《计划书》）。

二、填写《计划书》时要科学严谨、实事求是、表述清晰、准确。《计划书》经国家自然科学基金委员会相关项目管理部门审核批准后，将作为项目研究计划执行、检查和验收的依据。

三、《计划书》各部分填写要求如下：

（一）简表：由系统自动生成。

（二）摘要及关键词：各类获资助项目都应当填写中、英文摘要及关键词。

（三）项目组主要成员：计划书中列出姓名的项目组主要成员由系统自动生成，与申请书原成员保持一致，不可随意调整。如果《批准通知》所附“项目评审意见及修改意见表”中“修改意见”栏目有调整项目组成员相关要求的，待项目开始执行后，按照项目成员变更程序另行办理。

（四）资金预算表：根据批准的项目资助额度，按规定调整项目预算，并按照《国家自然科学基金项目计划书预算表编制说明》填报资金预算表和预算说明书。

（五）正文：

1. 面上项目、地区科学基金项目：如果《批准通知》所附“项目评审意见及修改意见表”中“修改意见”栏目没有修改要求的，只需选择“研究内容和研究目标按照申请书执行”即可；如果《批准通知》中上述栏目明确要求调整研究期限或研究内容等的，须选择“根据研究方案修改意见更改”并填报相关修改内容。

2. 重点项目、重点国际（地区）合作研究项目、重大项目、国家重大科研仪器研制项目、原创探索计划项目：须选择“根据研究方案修改意见更改”，根据《批准通知》的要求填写研究（研制）内容，不得自行降低、更改研究目标（或仪器研制的技术性能与主要技术指标、验收技术指标等）或缩减研究（研制）内容。此外，还要突出以下几点：

（1）研究的难点和在实施过程中可能遇到的问题（或仪器研制风险），拟采用的研究（研制）方案和技术路线；

（2）项目主要参与者分工，合作研究单位（如有）之间的关系与分工，重大项目还需说明课题之间的关联；

（3）详细的年度研究（研制）计划。

3. 创新研究群体项目：须选择“根据研究方案修改意见更改”，按下列提纲撰写：

（1）研究方向；

（2）结合国内外研究现状，说明研究工作的学术思想和科学意义（限两个页面）；

（3）研究内容、研究方案及预期目标（限两个页面）；

（4）年度研究计划；

（5）研究队伍的组成情况。

4. 基础科学中心项目：须选择“根据研究方案修改意见更改”，根据《批准通知》的要求和现场考察专家组的意见和建议，进一步完善并细化研究计划，按下列提纲撰写：

（1）五年拟开展的研究工作（包括主要研究方向、关键科学问题与研究内容）；

（2）研究方案（包括骨干成员之间的分工及合作方式、学科交叉融合研究计划等）；

（3）年度研究计划；

（4）五年预期目标和可能取得的重大突破等；

（5）研究队伍的组成情况。

5. 对于其他类型项目，参照面上项目的方式进行选择和填写。

简表

项目负责人信息	姓　　名	彭昌操	性 别	男	出生年月	1966年10月	民 族	土家族
	学　　位	博士			职称	教授		
	是否在站博士后	否		电子邮件		ccpeng@scau.edu.cn		
	电　　话	020-85280962		个人网页				
	工 作 单 位	华南农业大学						
	所 在 院 系 所	林学与风景园林学院						
依托单位信息	名　　称	华南农业大学					代码	51064208A0499
	联 系 人	唐家林		电子邮件		kycjhk@scau.edu.cn		
	电　　话	020-85280070		网站地址		http://kjc.scau.edu.cn/		
合作单位信息	单 位 名 称							
项目基本信息	项 目 名 称	黄梁木（Neolamarckia cadamba）卡丹宾生物合成途径中NcSQE和NcOSC的功能解析						
	资 助 类 别	面上项目			亚 类 说 明			
	附 注 说 明							
	申 请 代 码	C1610:林木遗传育种						
	基 地 类 别	亚热带农业生物资源保护与利用国家重点实验室						
	执 行 年 限	2023.01-2026.12						
	直 接 费 用	54万元						

项目摘要

中文摘要：

解析单萜类吲哚生物碱生物合成途径及其调控机制一直是药用植物天然产物生物合成领域研究的前沿和难点。卡丹宾作为具有重要药用价值的单萜类吲哚生物碱，其生物合成调控机制的阐明对于利用关键调节因子开展合成底盘构建及异源宿主合成意义重大。我们前期证明了卡丹宾上游合成途径并提出下游合成途径的模型。本项目拟继续以唯一富含卡丹宾的黄梁木为试材，以下游合成途径关键催化酶NcSQE和NcOSC的功能研究为切入点，综合运用现代生物化学、反向遗传学和分子生物学理论和方法从体内和体外催化功能验证、细胞学定位和转录表达与调控等方面开展研究；旨在解析关键催化酶的催化功能；厘清卡丹宾下游合成途径及其关键步骤；阐明关键催化酶转录表达及其调控的分子机制；揭示卡丹宾生物合成的科学奥秘。为丰富和发展（单）萜类吲哚生物碱生物合成理论提供依据，引领与开拓卡丹宾研究领域的发展。

Abstract：

Elucidation of the biosynthesis pathway of monoterpenoid indole alkaloids (MIAs) and its regulatory mechanism has always been the forefront and bottleneck in the field of natural product biosynthesis for medicinal plants. Cadambine is a kind of MIA with important medicinal value. The exploration of cadambine biosynthetic pathway is of great scientific significance which will be favorable for applying the key regulatory factors to chassis construction and heterologous synthesis. We have previously demonstrated the upstream biosynthetic pathway of cadambine, and proposed a model of the downstream pathway. As Neolamarckia cadamba is the only species reported so far that accumulates a high content of cadambine, using N. cadamba as material, this project intends to demonstrate the function of two key enzymes NcSQE and NcOSC in the downstream pathway of cadambine synthesis through analyzing the in vivo and in vitro catalytic activity, cellular localization and the transcriptional profiles and regulation pattern based on theories and techniques of modern biochemistry, reverse genetics and molecular biology. This project aims to identify the catalytic functions of NcSQE and NcOSC, clarify the downstream synthetic pathway and the involved key steps, elucidate the transcriptional expression and regulation pattern of NcSQE and NcOSC, and thus, uncover the mystery of cadambine biosynthesis which has been explored for nearly 40 years. This research will greatly enrich the MIAs biosynthetic theory and further develop and expand the cadambine related research field.

关键词(用分号分开)：萜类；生物合成；黄梁木；卡丹宾；基因功能

Keywords(用分号分开)： terpenoid; biosynthesis; Neolamarckia cadamba; cadambine; gene function

项目组主要成员

编号	姓名	出生年月	性别	职称	学位	单位名称	电话	证件号码	项目分工	每年工作时间（月）
1	彭昌操	1966.10	男	教授	博士	华南农业大学	020-85280962	420106196610035833	项目负责人	10
2	欧阳昆唏	1983.02	男	副教授	博士	华南农业大学	020-85280259	330327198302255375	基因表达、基因编辑	8
3	龙健梅	1989.08	女	讲师	博士	华南农业大学	18820760615	452123198908283146	LCM、免疫沉淀	8
4	张俊杰	1989.09	女	讲师	博士	华南农业大学	13560374816	420683198909223168	遗传转化及质谱分析	8
5	阙青敏	1990.08	男	实验师	硕士	华南农业大学	15820245143	422801199008273670	载体构建、CLSM	8

总人数	高级	中级	初级	博士后	博士生	硕士生
11	2	3	0	1	2	3

国家自然科学基金预算制项目预算表

项目批准号：32271908　　项目负责人：彭昌操　　金额单位：万元

序号	科目名称	金额
1	一、基金资助项目直接费用合计	54.0000
2	1、 设备费	0.0000
3	其中：设备购置费	0.0000
4	2、 业务费	35.6400
5	3、 劳务费	18.3600
6	二、 其他来源资金	0.0000
7	三、 合计	54.0000

注：请按照项目研究实际需要合理填写各科目预算金额。

预算说明书

（请按照《国家自然科学基金项目申请书预算表编制说明》等的有关要求，按照政策相符性、目标相关性和经济合理性原则，实事求是编制项目预算。填报时，直接费用应按设备费、业务费、劳务费三个类别填报，每个类别结合科研任务按支出用途进行说明。对单价≥50万元的设备详细说明,对单价＜50万元的设备费用分类说明，**对合作研究单位资质及资金外拨情况、自筹资金进行必要说明。**）

合计：54.00万元

1. 设备费（0.00万元）

无需购买设备。

2. 业务费（35.64 万元）

（1） 材料费（15.04万元）

分子生物学试剂（**6.00万元**）：酵母单杂交载体、GFP载体、T-载体等各种分子生物学载体购置费1.00万元；核酸内切酶1.00万元；Taq酶、DNA酶等2.00万元；RNA提取、cDNA反转录、质粒提取试剂盒等2.00万元。

生化试剂（**6.00万元**）：荧光底物1.00万元；制备抗体3.00万元；抗生素1.00万元；植物凝胶、琼脂糖等试剂1.00万元。

实验耗材及容器（**3.04万元**）：分子生物学及生化实验常用耗材（2.04万元）； 组培容器及种植基质等（1.00万元）。

（2） 测试化验加工费（13.60万元）

DNA测序（**2.10万元**）: DNA测序费700个×30元/个=2.10万元。

引物合成（**1.50万元**）：引物合成费500个×30元/个=1.50万元。

激光共聚焦显微镜（**3.00万元**）：200小时×150元/小时=3.00万元。

UPLC-Q-TOF/MS测试费（**3.00万元**）：60小时×500元/小时=3.00万元

显微激光切割系统（**4.00万元**）：80小时×500元/小时=4.00万元。

（3） 差旅费/会议费/国际合作（4.00万元）

国内、国际学术会议差旅费：8人次×0.5万元/人次=4.00万元；

（4） 出版/文献/信息传播/知识产权事务费（3.00万元）

论文版面费（**3.00万元**）：3篇×10000元/篇=3.00（万元）。

3. 劳务费（18.36 万元）

博士后劳务费：1人×24个月/人×1500元/月=3.60（万元）；

博士生劳务费：2人×36个月/人×1000元/月=7.20（万元）；

硕士生劳务费：3人×36个月/人×700元/月=7.56（万元）。

报告正文

研究内容和研究目标按照申请书执行。

国家自然科学基金项目负责人、依托单位承诺书

国家自然科学基金项目负责人承诺书

本人郑重承诺：我接受国家自然科学基金的资助，严格遵守中共中央办公厅、国务院办公厅《关于进一步加强科研诚信建设的若干意见》《关于进一步弘扬科学家精神加强作风和学风建设的意见》《关于加强科技伦理治理的意见》等规定，及国家自然科学基金委员会关于资助项目管理、项目资金管理等各项规章，在《计划书》填写及项目执行过程中：

（一）按照《批准通知》《国家自然科学基金资助项目计划书填报说明》的要求填写《计划书》，未自行降低、更改目标任务或约定要求，或缩减研究（研制）内容；

（二）树立“红线”意识，严格履行科研合同义务，按照《计划书》负责实施本项目（批准号：32271908），切实保证研究工作时间，按时报送有关材料，及时报告重大情况变动，不违规将科研任务转包、分包他人，不以项目实施周期外或不相关成果充抵交差；

（三）遵守科研诚信、科技伦理规范和学术道德，认真开展研究工作，对资助项目发表的论著和取得的研究成果按规定进行标注，不在非本项目资助的成果或其他无关成果上标注本项目批准号，反对无实质学术贡献者“挂名”，不在成果署名、知识产权归属等方面侵占他人合法权益，并如实报告本人及项目组成员发生的违背科研诚信要求的任何行为；

（四）尊重科研规律，弘扬科学家精神，严谨求实，追求卓越，反对浮夸浮躁、投机取巧，不人为夸大学术或技术价值，不传播未经科学验证的现象和观点；

（五）将项目资金全部用于与本项目研究工作相关的支出，并结合科研活动需要，科学合理安排项目资金支出进度；

（六）做好项目组成员的教育和管理，确保遵守以上相关要求。

如违背上述承诺，本人愿接受国家自然科学基金委员会和相关部门做出的各项处理决定。

项目负责人（签字）：

年　　月　　日

依托单位科研管理部门：	依托单位财务管理部门：
负责人（签章）： 年　　月　　日	负责人（签章）： 年　　月　　日

国家自然科学基金项目依托单位承诺书

我单位同意承担上述国家自然科学基金项目，将保证项目负责人及其研究队伍的稳定和研究项目实施所需的条件，严格遵守国家自然科学基金委员会有关资助项目管理、项目资金管理、科研诚信管理和科技伦理管理等各项规定，并督促实施。

依托单位（公章）

年　　月　　日

国家自然科学基金资助项目签批审核表

本栏目由自然科学基金委填写	科学处审查意见： 负责人（签章）： 年　　月　　日
	科学部审查意见： 负责人（签章）： 年　　月　　日

项目编号: 2017KQNCX020

广东省教育厅2017年重点平台及科研项目（自然科学类）

合同书

签约各方共同遵守《关于印发“广东省高等教育‘创新强校工程’专项资金管理办法”的通知》（粤财教〔2014〕130号）和《广东省教育厅关于做好“创新强校工程”科研项目管理工作的通知》（粤科教函〔2017〕22号）。

为顺利完成广东省普通高校省级重大科研项目（青年创新人才类、特色创新类）“菠萝抗寒体细胞突变体抗寒分子机制解析及候选基因的功能鉴定 ”遵守条款如下：

1．管理单位（甲方）为华南农业大学；承担单位（乙方）是指该项目具体实施的依托学院（单位）。

2．合同书中的主要研究内容、项目成员、经费预算、进度和阶段性目标及预期成果等参照申请书执行。

3．乙方必须按要求于次年年初向甲方报送上一年度项目进展报告。逾期不报，甲方有权暂停拨款。

4．合同执行过程中，乙方如需调整任务或修改合同中的部分条款，应按《管理办法》向甲方提出变更内容及其理由的申请报告，经甲方审定后实施。甲方提出变更合同，要与乙方达成书面协议。未经正式批准或达成协议前，双方须按原合同履行。

5．乙方因某种原因致使任务无法执行，而要求终止合同，应视不同情况，部分或全部退还所拨经费并追究相关人员责任；如乙方没有提出终止合同的要求，甲方有权根据实际情况提出终止合同的处理建议。

6．经费必须按《关于印发“广东省高等教育‘创新强校工程’专项资金管理办法”的通知》（粤财教〔2014〕130号）使用。

7．合同正式文本一式贰份，存甲方壹份，乙方壹份。

本合同签约各方

甲方：华南农业大学（公章）

代表人（签名）：

2018年5月11日

乙方：所在学院（公章）

负责人（签名）：

2018年5月6日

同意按照合同规定执行。

项目负责人（签名）：刘朝阳

2018年5月6日

学科领域分组： 10．农林与食品科学领域 版本号： 002

所属领域编号： 10

广东省普通高校青年创新人才项目

申请书(自然科学)

项 目 类 别：青年创新人才项目

项 目 名 称：菠萝抗寒体细胞突变体抗寒分子机制解析及候选基因的功能鉴定

学 科 分 类：农学

项目负责人：刘朝阳

负责人手机：18802030615

所 在 学 校：华南农业大学(盖章)

广东省教育厅制

二〇一六年十一月

基本信息

项目信息	项目名称	菠萝抗寒体细胞突变体抗寒分子机制解析及候选基因的功能鉴定		
	项目类别	青年创新人才项目		
	研究类型	基础研究	申请金额	8(万元)
	学科一	农学 - 园艺学		
	学科二			
	学科三			
	计划开始日期	2018.1	计划完成日期	2020.12
	所属学校	华南农业大学	学校类型	博士授权高校
	预期成果形式	论文		

合作单位	合作单位名称	联系人	联系电话	通讯地址

负责人信息	姓　　名	刘朝阳	性　　别	男	民　　族	汉族
	出生年月	1987.6	学　　历	研究生	学　　位	博士
	职　　称	中级		职　　务	无	
	办公电话	02085288262		手　　机	18802030615	
	一级学科	农学		二级学科	园艺学	
	电子邮件	liuchaoyang@scau.edu.cn		身份证号	410182198706153352	
	人才层次					
	研究专长	基因的功能鉴定及调控机制研究				

摘要	低温寒害是影响我国菠萝产业发展的重要因素，解析菠萝低温应答机制及抗寒相关内在分子机理，选育抗寒能力强的优良品种已成为当前亟需解决的问题。细胞培养结合极端低温选择压筛选是获得菠萝抗寒种质的有效手段。本项目拟利用前期经细胞培养获得的菠萝抗寒体细胞突变体材料，借助转录组学和代谢组等组学手段研究突变体与对照材料在低温胁迫下应答机制的差异，从中挖掘出关键的候选抗寒基因并通过遗传转化验证基因的功能。本项目的实施将初步探明菠萝抗寒的相关内在分子机理，为菠萝抗寒性状的遗传改良奠定重要的基础。
关键字	菠萝；低温；抗寒；　功能验证；遗传改良

项目组成员

总数（含负责人）		高级		中级	初级	博士	硕士	学士
5		0		3	2	2	1	2
姓名	性别	出生年月	学位	职称	项目分工	工作单位		研究领域
龙健梅	女	1989.9	博士	中级	转录组分析	华南农业大学		园艺植物生物技术
夏靖娴	女	1985.9	硕士	中级	代谢组分析	华南农业大学		园艺植物生物技术
谢桃	女	1990.6	学士	初级及以下	基因的筛选和验证	华南农业大学		园艺植物生物技术
李楚豪	女	1994.6	学士	初级及以下	基因的遗传转化	华南农业大学		园艺植物生物技术

经费申请表

（金额单位：万元）

预算科目	创新强校工程经费	备注（计算依据与说明）
一、科研业务费	3.0000 万元	
1、测试、计算、分析	2.0000 万元	转录组和代谢组测试费用
2、会议费、差旅费	1.0000 万元	参加学术会议的注册费和交通住宿费用等
3、出版物、文献、信息传播	0.0000 万元	
4、其他	0.0000 万元	
二、试验材料费	4.0000 万元	
1、原材料、试剂、药品购置费	4.0000 万元	实验所需的试剂耗材及常用化学药品等
2、其他	0.0000 万元	
三、仪器设备费	0.0000 万元	
1、购置	0.0000 万元	
2、试制	0.0000 万元	
四、劳务费	1.0000 万元	用于开支研究生的劳务费
五、其他费用	0.0000 万元	
1、	万元	
2、	万元	
3、	万元	
4、	万元	
合计	8.0000	
与本项目有关的其他经费来源	其他计划资助经费	0.0000 万元
	其他经费资助	0 万元
	其他经费合计	0.0000 万元

进度计划

序号	起止时间	阶段性研究工作进展	阶段性目标
1	2018.1-2018.12	实验材料的低温胁迫处理,转录组合代谢组的测定及数据分析	获得组学分析数据,初步分析测序结果
2	2019.1-2019.12	关键基因的筛选挖掘,载体的构建和遗传转化	筛选得到关键的差异基因,开展进行遗传转化工作
3	2020.1-2020.12	转基因材料的获得及表型分析	得到阳性转基因材料并测定表型,撰写和整理文章
4	-		

预期成果

论文（篇）	总数	1	
	其中：CSCD 核心期刊		
	三大索引收录	1	
专著（部）			
研究报告（篇）			
专利（件）	数量（件）	申请	
		授权	
	其中发明专利	申请	
		授权	
鉴定成果（项）			
软件登记（项）			
新产品（种）（或新装备、新药等）			
新技术（项）（或新工艺等）			
其他			

申请书正文

一、立项依据

1．研究意义

菠萝又名凤梨，为多年生常绿草本果树，是世界三大热带水果之一。菠萝原产南美洲热带地区，对低温敏感，抗寒能力较差，7℃时便出现叶片枯黄等寒害现象，3℃持续 24h 以上，绝大多数品种都会出现不同程度的茎尖分生组织坏死和茎叶腐烂等现象(Bartholomew et al. 2002)。中国是世界菠萝生产大国之一，中国的菠萝栽培区是菠萝的北缘产区，尤其是栽培面积占 80%以上的大陆产区，冬季多处于霜冻和寒害威胁之下，会受到不同程度的低温危害。低温会影响植物的生长代谢，引起植物相关生理指标变化，导致植物各种生理机能遭到破坏，严重时会导致植物死亡(Yadav 2010)。低温寒害已成为限制我国菠萝产业发展的一个重要因素，选育抗寒能力强的菠萝新品种，可以减轻低温对植株的伤害，减少寒害损失，扩大菠萝栽培区域，是抵御菠萝生产中低温寒害的有效手段。

常规的育种方法如系统选育、杂交育种等手段，由于育种材料自身变异的限制，针对抗寒性状的改良幅度相对有限。而组织培养诱导再生植株的过程中会产生大量的体细胞无性系变异，为相关细胞突变体的筛选提供了丰富的变异来源。菠萝由于自交不亲和及长期的无性繁殖的特点，杂合性高，细胞异质性显著，这也为通过细胞培养的方法筛选得到优良的抗寒细胞株系提供了便利。目前关于菠萝抗寒性相关的研究主要是针对菠萝受低温寒害后的形态特征的调查及个别生理指标的测定，关于菠萝抗寒分子机理的深入研究相对较少。**本项目旨在利用细胞培养筛选得到的菠萝抗寒体细胞突变体材料，借助转录组学、代谢组学等组学手段分析突变体的抗寒相关内在分子机制，挖掘影响菠萝抗寒能力的关键调控因子并验证其功能，以期为揭示菠萝抗寒分子调控机理及抗寒新品种的培育提供重要的理论基础。**

2、国内外研究现状、水平发展趋势分析

2.1 体细胞突变体的筛选与利用

体细胞无性系变异是植物组织培养过程中出现的普遍现象，变异的产生没有种属特异性，出现的频率较自然突变高，所涉及的性状也相当广泛。外植体来源、基

因型差异、培养基构成、培养条件及时间等诸多因素都会影响体细胞变异的发生频率(Krishna et al. 2016)。体细胞无性系变异具有变异频率高、幅度大、遗传稳定快等优点，能够为相关性状分子机理的研究及品种的选育提供丰富的遗传资源。

在组织培养过程中结合施加相应的选择压，可以针对特定的性状对突变的细胞进行定向选择，有利于获得期望表型的体细胞突变体。相较传统的育种方式，体细胞突变体的定向选择可以在有限的空间、可控的环境及较短的时间内，完成大量细胞的再生、变异、筛选和增殖扩繁的全部过程。利用体细胞变异结合特定的逆境胁迫筛选压，一系列抗盐、抗旱、抗病、抗寒等抗逆突变体材料，如香蕉的抗枯萎病突变体、桃的抗火疫病突变体、猕猴桃的耐盐突变体、柑橘及野牛草的抗寒细胞变异体等，先后被筛选鉴定出来 (林定波等，1999；Caboni et al. 2003; Li et al. 2010; Li et al. 2012; Nacheva LR 2014; Krishna et al. 2016)。其中一些抗逆性状稳定、农艺性状优良的突变体材料已应用到了育种和实际生产当中。抗逆突变体材料的获得，同时也为植物抗逆性状相关的分子机理研究提供了理想的遗传材料，针对突变体材料的遗传差异分析、组学分析及抗逆基因的挖掘和鉴定等工作已在多种植物中相继展开。例如，转录组数据分析表明，香蕉抗枯萎病体细胞突变体在接种枯萎病菌后，一系列防御相关基因相较野生型材料的显著上调表达，是影响突变体抗病性状的重要因素(Li et al. 2012)。深入研究突变体产生的内在机理，有望寻找到与抗逆性状密切相关的一些关键基因位点或基因簇等信息，对研究植物在逆境胁迫条件下的应答与防御机制具有重要意义。

2.2 植物抗寒机理的研究进展

低温是限制植物生长发育及地理分布的主要环境因子之一。低温胁迫导致植物的生物膜膜相和膜透性改变，破坏生物的酶系统，抑制植物的光合作用，引起代谢紊乱，打破植物原有的平衡状态，促进有毒物质积累，进而影响植物的正常生长发育(Yadav 2010)。植物在长期的进化过程中获得了相应的应对低温胁迫的内在机制，可以感知外界低温信号，通过积累或分解诸如可溶性糖、脯氨酸、可溶性蛋白、肌醇等渗透调节类物质，从而缓解低温胁迫对植物所造成的伤害。胁迫条件下代谢物质含量的改变受到相关基因的调节与影响，而低温条件下植物的抗寒性能的强弱很大程度上依赖于对低温应答基因的调控。CBF 低温应答调控途径在多种植物的冷驯化过程中起到了重要的作用，目前研究的也最为清楚。CBF 转录因子可以直接调控一系列低温应答基因的表达，在植物抗寒过程中起着分子开关的作用(Zhao et al. 2016)。

植物中同时存在一些转录因子，如拟南芥中 ZAT10、水稻中的 MYBS3 等，通过不依赖 CBF 的调控途径来调控植物的低温应答(Su et al. 2010; Nguyen et al. 2016)。不同的调控途径间存在着相互交叉及协同调控的调节机制，这也反映了植物低温应答调控网络的高度复杂性(Zhao et al. 2015)。

植物的抗寒性是由多基因控制的数量性状，抗寒相关的关键数量性状位点（QTLs）的定位与克隆相对困难。组学技术的兴起，为植物抗寒性的研究提供了新的有效手段。以转录组、代谢组为代表的组学分析策略，已成功应用于解析多种植物在低温胁迫下的分子应答机制(An et al. 2012; Wang et al. 2015; Shiratake and Suzuki 2016)。转录组技术的应用，能够较全面的揭示低温胁迫下整个基因组水平的表达变化，极大丰富了人们对低温胁迫下植物基因表达调控机理的认识(Sinha et al. 2015)。基于各类抗寒种质及变异材料的转录组学比较分析，有助于挖掘抗寒材料特异的低温相关代谢通路，进而可以更为深入的理解其抗寒的分子调控机理，相关的研究工作近年来已在水稻、番茄、葡萄、香蕉、豇豆、洋葱等多种植物中有大量的报道(Zhang et al. 2012; Xin et al. 2013; Chen et al. 2015; Yang et al. 2015; Yang et al. 2015;Han et al. 2016; Tan et al. 2016)。例如，Zhang 等(2012)通过转录组分析发现，低温胁迫下更多的基因在水稻抗寒材料中上调表达，而更多基因的表达在冷敏感材料中被抑制。低温胁迫下抗寒的野生葡萄与普通栽培葡萄的转录组分析发现，两份材料间存在着一系列显著差异表达的低温应答基因，表明低温胁迫可能特异性的诱导了野生葡萄中的一些代谢通路(Xin et al. 2013)。一些与抗寒性状紧密相关的关键基因，如番茄中的脱水素基因 *ShDHN*，野生葡萄中的 GRAS 类转录因子 *PAT1* 基因等，相继在多种植物中被挖掘筛选出来，其基因功能也得以进一步验证(Liu et al. 2015; Yuan et al. 2016)。

代谢物是基因表达的最终产物，其种类与数量的变化与植物的抗逆性状紧密相关。基于 GC-MS 的代谢组学技术，可以全面的解析植物在低温胁迫下糖、酸、氨基酸、脂肪酸等小分子代谢物质的含量变化，有助于高通量发掘与植物低温胁迫密切相关的代谢物质，找出受到显著影响的代谢通路，在此基础上整合基因的表达数据，能够全方位的解析植物抗寒相关的相关分子机制（Obata et al. 2012）。

2.3 菠萝抗寒研究进展

菠萝中与低温相关的研究多集中在成花诱导和采后果实低温贮藏等方面，菠萝生长过程中的低温胁迫的研究，大多是针对寒害后菠萝形态特征的调查及生理指标的

测定(Maruthasalam et al. 2009; Raimbault et al. 2013)。目前关于菠萝抗寒育种及相关分子机制的研究报道非常之少，一定程度上是受限于抗寒种质资源的相对缺乏。菠萝长期采用无性繁殖，杂合程度高，细胞异质性显著(Ming et al. 2015)。大量观察试验表明菠萝体细胞胚都是单细胞起源，具有遗传上相对稳定和发生量大等特点（何业华等，2010），从而为利用细胞培养筛选得到能够稳定遗传的体细胞突变体材料提供了可能。Pe ŕez 等（2012）通过细胞培养的方法，获得了两个（‘P3R5’和‘Dwarf’）在果实形态、生长习性等诸多方面存在显著变异，且能长期稳定遗传的菠萝体细胞无性系突变体株系。目前在菠萝中尚未有通过细胞培养的方法进行抗寒性状改良的相关报道。

3. 本项目研究思路

综上所述，一系列抗逆体细胞突变体通过细胞培养的手段被筛选鉴定出来，在突变体材料基础上开展的逆境胁迫相关分子机理研究，为植物抗逆性状的遗传改良提供了重要的理论基础。申请人所在课题组前期在田间收集到一批自然低温寒害发生后，仍能正常生长的耐寒菠萝变异植株，借助课题组成熟的高效菠萝体细胞胚再生体系，通过细胞培养结合极端低温筛选压的方法，成功筛选出一批在 0℃+72h 极端低温筛选后，仍能正常生长的抗寒体细胞变异材料。抗寒相关生理生化指标的测定表明变异材料的抗寒性能大幅提升，分子标记检测发现其在分子水平存在稳定的遗传变异。本项目拟在已有抗寒体细胞突变体材料的基础上，综合利用转录组及代谢组学等多种组学技术手段，全方位的挖掘低温胁迫下抗寒突变体/对照间的分子应答机制差异，**解析抗寒体细胞突变体发生的内在机理，从中挖掘关键的候选抗寒基因，并进一步通过遗传转化验证基因功能，以期为菠萝抗寒分子调控机理研究及抗寒性状的遗传改良奠定坚实的理论基础。**

主要参考文献及出处：

1 .林定波，颜秋生，沈德旭. 柑橘抗寒细胞变异体的获得及其抗性遗传稳定性的研究. 植物学报, 1999, 41(2):136-141

2. 何业华, 方少秋, 马均, 等. 菠萝愈伤组织中体细胞胚起源过程的组织细胞学观察. 园艺学报，2010, 37(5): 690-696

3. An D, Yang J, Zhang P (2012) Transcriptome profiling of low temperature-treated cassava apical shoots showed dynamic responses of tropical plant to cold stress. BMC Genomics 13 (1):1

4. Bairu MW, Aremu AO, Van Staden J (2010) Somaclonal variation in plants: causes and detection methods.

Plant Growth Regul 63 (2):147-173.
5. Bartholomew DP, Paull RE, Rohrbach KG (2002) The pineapple: botany, production, and uses. CABI
6. Caboni E, Anselmi S, Donato E, Manes F (2003) In vitro selection of *Actinidia deliciosa* clones tolerant to NaCl and their molecular and in vivo ecophysiological characterisation. Acta Hortic 618：77-83
7. Chen H, Chen X, Chen D, Li J, Zhang Y, Wang A (2015) A comparison of the low temperature transcriptomes of two tomato genotypes that differ in freezing tolerance: *Solanum lycopersicum* and *Solanum habrochaites*. BMC Plant Biol 15:132.
8. Han J, Thamilarasan SK, Natarajan S, Park JI, Chung MY, Nou IS (2016) De Novo Assembly and Transcriptome Analysis of Bulb Onion (*Allium cepa* L.) during Cold Acclimation Using Contrasting Genotypes. PloS One 11 (9):e0161987.
9. Krishna H, Alizadeh M, Singh D, Singh U, Chauhan N, Eftekhari M, Sadh RK (2016) Somaclonal variations and their applications in horticultural crops improvement. 3 Biotech 6 (1).
10. Li C-y, Deng G-m, Yang J, Viljoen A, Jin Y, Kuang R-b, Zuo C-w, Lv Z-c, Yang Q-s, Sheng O (2012) Transcriptome profiling of resistant and susceptible Cavendish banana roots following inoculation with *Fusarium oxysporum* f. sp. *cubense* tropical race 4. BMC Genomics 13 (1):1
11. Li R, Qu R, Bruneau AH, Livingston DP (2010) Selection for freezing tolerance in St. Augustine- grass through somaclonal variation and germplasm evaluation. Plant Breeding 129(4):417-421
12. Liu H, Yu C, Li H, Ouyang B, Wang T, Zhang J, Wang X, Ye Z (2015) Overexpression of *ShDHN*, a dehydrin gene from *Solanum habrochaites* enhances tolerance to multiple abiotic stresses in tomato. Plant Sci 231:198-211
13. Maruthasalam S, Shiu LY, Loganathan M, Lien WC, Liu YL, Sun CM, Yu CW, Hung SH, Ko Y, Lin CH (2009) Forced flowering of pineapple (*Ananas comosus* cv. Tainon 17) in response to cold stress, ethephon and calcium carbide with or without activated charcoal. Plant Growth Regul 60 (2):83-90.
14. Ming R, VanBuren R, Wai CM, Tang H, Schatz MC, Bowers JE, Lyons E, Wang ML, Chen J, Biggers E, et al. (2015) The pineapple genome and the evolution of CAM photosynthesis. Nat Genet 47 (12):1435-1442.
15. Miyao A, Nakagome M, Ohnuma T, Yamagata H, Kanamori H, Katayose Y, Takahashi A, Matsumoto T, Hirochika H (2012) Molecular spectrum of somaclonal variation in regenerated rice revealed by whole-genome sequencing. Plant Cell Physiol 53 (1):256-264.
16. Nacheva LR, Gercheva PS, Andonova MY, Panayotova DV, Dzhuvinov VT (2014) Somaclonal variation: a useful tool to improve disease resistance of pear rootstock 'Old Home 9 Farmingdale' (OHF 333) (*Pyrus communis* L.). Acta Hortic 1056:253–258
17. Nguyen XC, Kim SH, Hussain S, An J, Yoo Y, Han HJ, Yoo JS, Lim CO, Yun D-J, Chung WS (2016) A positive transcription factor in osmotic stress tolerance, ZAT10, is regulated by MAP kinases in Arabidopsis. J Plant Biol 59 (1):55-61
18. Obata T, Fernie AR (2012) The use of metabolomics to dissect plant responses to abiotic stresses. Cell Mol Life Sci 69 (19):3225-3243.
19. Pérez G, Yanez E, Mbogholi A, Valle B, Sagarra F, Yabor L, Aragón C, González J, Isidrón M, Lorenzo JC (2012) New Pineapple Somaclonal Variants: P3R5 and Dwarf. American Journal of Plant Sciences 03 (01):1-11.
20. Raimbault AK, Zuily-Fodil Y, Soler A, Mora P, Cruz de Carvalho MH (2013) The expression patterns of bromelain and AcCYS1 correlate with blackheart resistance in pineapple fruits submitted to postharvest chilling stress. J Plant Physiol 170 (16):1442-1446.
21. Shiratake K, Suzuki M (2016) Omics studies of citrus, grape and rosaceae fruit trees. Breeding Sci 66 (1):122-138.
22. Sinha S, Kukreja B, Arora P, Sharma M, Pandey GK, Agarwal M, Chinnusamy V (2015) The Omics of Cold Stress Responses in Plants. In: Elucidation of Abiotic Stress Signaling in Plants. Springer, pp 143-194
23. Su C-F, Wang Y-C, Hsieh T-H, Lu C-A, Tseng T-H, Yu S-M (2010) A novel MYBS3-dependent pathway confers cold tolerance in rice. Plant Physiol 153 (1):145-158
24. Tan H, Huang H, Tie M, Tang Y, Lai Y, Li H (2016) Transcriptome Profiling of Two Asparagus Bean (*Vigna unguiculata* subsp. sesquipedalis) Cultivars Differing in Chilling Tolerance under Cold Stress.

PloS One 11 (3):e0151105.
25. Wang M, Zhang X, Liu JH (2015) Deep sequencing-based characterization of transcriptome of trifoliate orange (*Poncirus trifoliata* (L.) Raf.) in response to cold stress. BMC Genomics 16:555.
26. Xin H, Zhu W, Wang L, Xiang Y, Fang L, Li J, Sun X, Wang N, Londo JP, Li S (2013) Genome wide transcriptional profile analysis of *Vitis amurensis* and *Vitis vinifera* in response to cold stress. PloS One 8 (3):e58740
27. Yadav SK (2010) Cold stress tolerance mechanisms in plants. Agron Sustain Dev 30 (3):515-527.
28. Yang Q-S, Gao J, He W-D, Dou T-X, Ding L-J, Wu J-H, Li C-Y, Peng X-X, Zhang S, Yi G-J (2015) Comparative transcriptomics analysis reveals difference of key gene expression between banana and plantain in response to cold stress. BMC Genomics 16:446
29. Yang YW, Chen HC, Jen WF, Liu LY, Chang MC (2015) Comparative Transcriptome Analysis of Shoots and Roots of TNG67 and TCN1 Rice Seedlings under Cold Stress and Following Subsequent Recovery: Insights into Metabolic Pathways, Phytohormones, and Transcription Factors. PloS One 10 (7):e0131391.
30. Yuan Y, Fang L, Karungo SK, Zhang L, Gao Y, Li S, Xin H (2016) Overexpression of *VaPAT1*, a GRAS transcription factor from *Vitis amurensis*, confers abiotic stress tolerance in Arabidopsis. Plant Cell Rep 35 (3):655-666.
31. Zhang T, Zhao X, Wang W, Pan Y, Huang L, Liu X, Zong Y, Zhu L, Yang D, Fu B (2012) Comparative transcriptome profiling of chilling stress responsiveness in two contrasting rice genotypes. PloS One 7 (8):e43274
32. Zhao C, Lang Z, Zhu JK (2015) Cold responsive gene transcription becomes more complex. Trends Plant Sci 20 (8):466-468.
33. Zhao C, Zhang Z, Xie S, Si T, Li Y, Zhu J-K (2016) Mutational Evidence for the Critical Role of CBF Genes in Cold Acclimation in Arabidopsis. Plant Physiol pp-00533

二、研究方案

1、主要研究目标与研究内容和拟解决的关键问题

1.1 研究目标

- 以抗寒突变体为研究材料，解析菠萝低温应答的分子基础和代谢基础，初步明晰菠萝抗寒相关的调控机理及作用网络；
- 筛选并验证候选关键抗寒基因的功能，为抗寒性状遗传改良提供重要的基因资源。

1.2 研究内容

（1）低温胁迫下的转录组分析

选取低温处理不同时间段的突变体/对照植株盆栽材料，提取 RNA 进行转录组分析。发掘低温胁迫下的分子应答机理及相关调控网络，比较不同材料间低温胁迫下的基因表达差异。

（2）低温胁迫下的代谢组分析

选取低温处理不同时间段的突变体/对照植株盆栽材料，基于 GC-MS 的方法，

全面检测材料中小分子代谢产物的含量变化，找出与菠萝抗寒性状密切相关的代谢产物，挖掘不同材料间存在显著差异的代谢通路。

（3）关键候选基因的挖掘

综合转录组和代谢组的数据，发掘不同材料间代谢通路相关基因，选取低温胁迫下突变体材料中基因表达变化显著不同于野生型材料的关键差异基因，结合基因功能注释、定量 PCR 验证、启动子元件分析等手段，进一步筛选确定候选关键抗寒基因。

（4）候选基因的功能验证

构建候选基因的超量表达载体，利用根癌农杆菌介导的方法转化菠萝。鉴定转基因阳性植株，综合各类抗寒指标评价鉴定阳性株系的抗寒性能，验证候选基因的功能。

1.3 拟解决的关键问题

目前针对菠萝低温应答机制的研究相对较少，对于抗寒相关的分子调控机理及关键基因功能作用等方面的认识较为缺乏。本项目将以菠萝抗寒体细胞突变体为基础和出发点，**重点解析突变体材料中抗寒相关变异发生的内在机理，发掘关键的差异表达基因并验证其功能，以期为菠萝抗寒性状的遗传改良奠定重要的材料和理论基础。**

2.拟采取的研究方法、技术路线、试验方案和可行性分析

2.1. 实验方案

(1) 研究材料

从受寒害严重的地区收集能正常生长的神湾菠萝田间材料，经细胞培养获得胚性细胞系。以受冷致死的临界条件低温胁迫处理细胞培养材料，获得经过连续 3 轮临界致死温度（0℃+72h）低温筛选后，仍能生长正常的抗寒体细胞突变体材料。抗寒相关生理指标的测定结果显示突变体材料抗寒性能大幅提升，分子标记结果表明突变体材料确实在分子水平上发生了遗传变异。离体材料均保存于园艺学院菠萝课题组的培养室内，利用课题组成熟的组织培养手段对各株系进行继代培养及增殖扩繁，待得到足够数量的植株后移栽至营养钵中以用于后续的一系列分析及筛选。

(2) 转录组测序及数据分析验证

选择抗寒能力强且分子检测遗传变异小的突变体株系进行后续转录组分析。低温处理 0h、4h、24h、72h 分别取样，每个时间段样品取三个生物学重复。采用 Trizol 法提取菠萝样品的 RNA，构建普通转录组文库，使用高通量 Illumina HiSeq 测序平台测序，文库的构建及测序工作交由北京安诺优达基因科技有限公司完成（前期有合作基础）。转录本的组装使用 Trinity 软件（Grabherr et al. Nature Biotech, 2011, 29:644-652），使用 Blast2GO 进行 GO 功能注释，采用 KAAS 进行 KEGG 代谢途径注释。基因差异表达分析采用 edgeR 软件(Robinson et al. Bioinformatics, 2010, 26, 139-140)，筛选阈值为 padj<0.05；GO 和 KEGG Pathway 富集分析使用 TBtool 自制软件（http://cj-chen.github.io/tbtools/）。转录组分析结果中基因表达差异采用 qRT-PCR 的方法进一步验证。RNA 的反转录参照 Titanium® One-Step RT-PCR Kit 试剂盒（Takara）步骤说明进行，定量 PCR 使用 LightCycler® 480(Roche)实时荧光定量 PCR 仪进行。

（3）GC-MS 检测初生代谢物含量

测定方法参照前人报道（Zhang et al. J Exp Bot 2011,62:1103-1118）。低温处理后的菠萝幼苗材料经研磨后加入甲醇，经超声处理、水浴、冷凝，上清液真空浓缩后衍生化、过滤后上样进行 GC-MS（QP2010 Ultra），选用 DB-5MS 毛细管柱测定。实验结果质谱图与 NIST2008 和 WIELY 数据库中的标准谱图进行比对，分析成分。

(4) 候选关键抗寒基因的筛选

结合转录组和代谢组分析结果，找出两份材料间代谢通路存在显著差异的相关基因，参照以下条件进一步从中筛选候选关键抗寒基因：候选基因的表达受低温胁迫的诱导；突变体材料中候选基因表达变化显著不同于对照材料；候选基因的启动子区域经生物信息分析预测存在低温响应相关顺式元件；候选基因在水稻中的直系同源基因定位于水稻抗寒相关的 QTL 区域；低温胁迫下候选基因在菠萝各品种中的表达量高低与品种抗寒性能强弱存在相关性。

(5) 候选基因的克隆及超量表达载体构建

基于菠萝基因组数据库信息(https://phytozome.jgi.doe.gov/pz/portal.html)设计引物，以神湾菠萝材料为模板，经过 PCR 扩增获得候选基因 cDNA 全长，利用双酶切的方法，将目的基因片段连入由 35S 组成型启动子驱动的超量表达载体 pBI121 中（载体为本实验保存），构建目的基因的超量表达载体。

(6) 候选基因的遗传转化

将构建好的质粒载体及空的质粒载体分别转入根癌农杆菌菌株 LBA4404，获得含有目的载体的农杆菌菌液。将切碎后的菠萝愈伤组织预培养 2d 后，用农杆菌菌液侵染愈伤组织，黑暗条件下培养 3d 后，将愈伤转移到含有筛选抗生素的筛选培养基上进行筛选分化培养；培养约 28d 后，将抗性的绿色不定芽切下，继续筛选培养 2 代后转移至生根培养基诱导生根成苗。利用 *Npt II* 基因引物对抗性植株的 DNA 进行 PCR 扩增，qRT-PCR 检测转基因系中目的基因的表达量，以筛选鉴定目的基因超量表达的阳性株系。

（7）转基因阳性株系抗寒相关指标的测定

半致死温度的计算：将菠萝植株置于不同温度梯度（4、2、0、-2、-4℃）条件下，处理 4h 后取样，样品经去离子水浸入，抽气、渗透等步骤后用电导仪测定电导率，利用 Logistic 回归方程计算半致死温度。**丙二醛含量的测定**：将叶片加入 0.5% TCA 三氯乙酸后研磨，离心，上清液加入 0.6%硫代巴比妥酸，煮沸，待冷却后离心，分光光度计测定上清液在 450 nm、 532 nm 和 600 nm 波长处的吸光值。**脯氨酸含量的测定**：将叶片加入 3%的磺基水杨酸溶液研磨，沸水浴中提取，冷却后离心；上清液加入冰醋酸和酸性茚三酮，沸水浴后加入甲苯试剂，离心，测定上清液在 520nm 波长处的吸光值。**可溶性糖含量的测定**：研磨好的新鲜样品加入蒸馏水，煮沸，冷却后过滤冲洗并定容，加入蒽酮试剂测定 620nm 波长处的吸光度。**SOD 酶活性的测定**：使用改进的氮蓝四唑光化还原法测定，参照（Ginnopolitis et al. Plant Physiol 1997, 59:309-314）的方法。**CAT 酶活性的测定**：样品经预冷的磷酸缓冲液研磨后定容，取上清液并加入磷酸缓冲液及 0.1mol/L H_2O_2，测定 240nm 波长下的吸光度。

2.2 技术路线

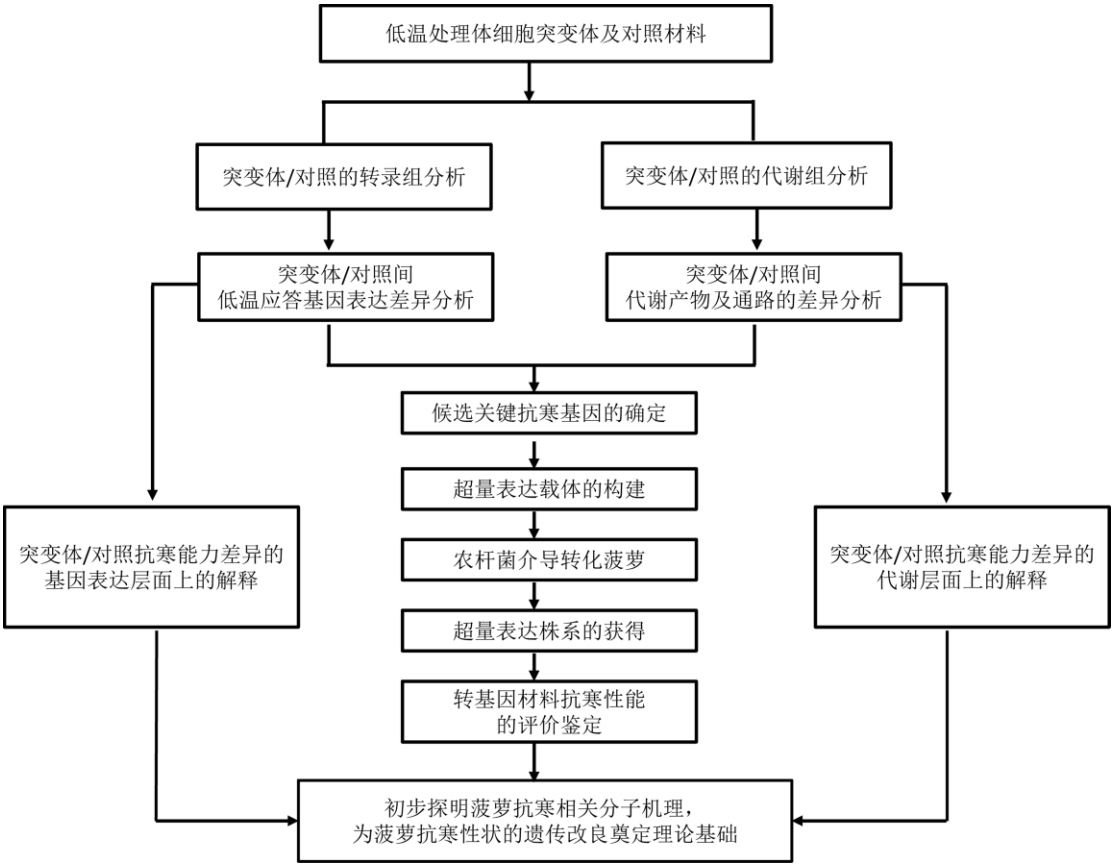

2.3 可行性分析

（1）研究材料可靠

本研究所使用的细胞培养材料来自于极端自然低温寒害下，在田间仍生长正常的耐寒神湾菠萝植株。经移栽后的性状观察，发现耐寒神湾材料能忍受在 4 ℃下生长 7 天而未出现寒害，而普通神湾在 5 ℃时超过 3 天即会受害致死。极端的低温灾害会诱导菠萝植株产生各种类型的自然变异，同时也是选取抗寒变异的有利时机，前期所选取的耐寒菠萝外植体本身很可能已经存在抗寒相关的自然变异，利用组织培养的方法可以增殖原有材料，保证抗寒相关变异不易丢失，同时培养过程也可以扩大变异的发生，经过极端低温连续筛选出的变异株系，其抗寒能力有望会有大幅的提升。

本研究所使用的抗寒体细胞变异材料经过连续 3 轮临界致死温度的极端低温筛选，在 0℃处理 72h 后仍能正常生长，而普通对照材料则逐步萎蔫死亡；抗寒相关生理指标的测定也表明其抗寒性能有显著的提升，分子标记结果证实突变体材料在分子水平上存在遗传变异。本项目所使用的抗寒体细胞突变体，相比普通神湾菠萝对照材料间，遗传背景差异小，使得研究的复杂性大大降低。基于突变体材料的组学

分析所筛选出的差异表达基因，与抗寒目标性状的相关性更加紧密。针对突变体材料抗寒性能显著提升的内在变异机制的研究，将极大促进我们对菠萝抗寒相关分子机理的理解与认识。因此，本研究采用的田间变异材料来源可靠，随后经细胞培养筛选得到的抗寒突变体，为后续分子机理相关研究工作的开展提供了重要的保障。

（2）研究思路清晰，理论依据可靠

本研究以获得抗寒能力强且遗传变异小的菠萝抗寒突变体，作为重要的阶段目标和后期工作开展的基础。利用细胞培养筛选体细胞抗寒突变体已在多种物种中已有相关的报道，本项目前期已成功获得了抗寒能力显著提高，分子水平存在遗传变异的菠萝抗寒体细胞突变体材料，为本项目的顺利开展提供了可靠的保障。基于突变体和对照材料的转录组及代谢组分析，可以在分子水平及代谢水平上为突变体变异性状的发生机理提供诸多可靠的线索，相关的研究已在多种植物中有大量的报道（An et al. BMC Genomics, 2012, 13:1; Wu et al. J Exp Bot, 2014,11(4): e0154330）。本项目中低温胁迫下的转录组分析，除了挖掘到大量的菠萝中低温响应的应答基因之外，更可以通过比较胁迫下差异表达基因在突变体和对照材料中响应模式等方面的差别，从而更有针对性的找出显著影响乃至决定突变体抗寒性状的关键基因。在此基础上挑选出来的关键候选抗寒基因相对较为可靠，转基因功能验证的结果可以预期，可以保障项目的顺利开展并得到预期的结果。

（3）技术体系成熟

申请人所在课题组多年来一直从事菠萝细胞培养方面的研究，重点关注体细胞胚发生的分子调控机制，已成功建立起了稳定的菠萝胚性细胞悬浮系和体细胞胚发生体系（Ma et al. Plant Mol Biol Rep, 2012, 30:195-203; Ma et al. Gene, 2012, 500:115-123），相关基础为本项目利用细胞培养筛选得到再生突变体株系提供了重要的技术支持。课题组拥有成熟的转录组数据分析相关技术，完善了高通量数据分析流程，使用本套流程分析并发表了国内首个菠萝全转录组测序结果（陈程杰等, 2014），独立开发了囊括转录组数据分析所需各项流程的生物信息分析软件 TBtool（http://cj-chen.github.io/tbtools/），为本项目中转录组数据的分析及关键信息的挖掘提供了强有力的保障。课题组拥有完善的基因克隆、载体构建、分子标记检测及定量 PCR 等分子生物学相关实验技术体系。课题组成功建立了高效的农杆菌介导的菠萝遗传转化体系，缩短了转化周期，提高了转化效率，为本项目候选基因功能验证部分获得转基因阳性株系提供了可靠的保障。

（4）实验条件、研究人员满足项目执行要求

本研究项目依托于华南农业大学果树学国家重点学科和农业部华南园艺作物生物学与种质创制重点实验室，具备开展本项目的仪器设备和技术经验。申请人所在课题组有较好的前期研究基础，对本研究将有很好的推动作用。申请人从本科到博士阶段一直从事果树学专业的学习和研 究，专业背景知识扎实。研究生期间从事柑橘次生代谢相关的转录因子的功能验证和调控机制的研究，在读期间参与了国家自然科学基金重点项目、优秀青年科 学基金项目及国家重点基础研究发展计划（ 973 计划）项目等课题的具体实施工作，在组学数据的分析、园艺植物的遗传转化、生理数据的测定、基因的功能验证及调控机制研究等诸多方面积攒了丰富的经验。目前申请人以第一作者发表 SCI 论文 3 篇，其中二区高水平 SCI 论文 2 篇，具备较强的科研能力。项目组成员都从事菠萝相关分子生物学研究，掌握了相关实验技术，能够保障本项目的顺利开展。

3.本项目的特色与创新之处

3.1 选题紧密结合菠萝育种中的实际问题

本项目针对菠萝育种中对培育抗寒新品种的迫切需求以及抗寒内在机理研究基础薄弱的问题，通过筛选抗寒体细胞突变体，研究菠萝抗寒相关分子机理，有望获得菠萝抗寒新种质，挖掘到关键的抗寒基因，为菠萝抗寒性状的遗传改良奠定重要的材料和理论基础。

3.2 研究材料有特色，研究内容新颖

本项目使用的初始外植体材料很可能已发生了抗寒相关的自然变异，经细胞培养获得的抗寒株系能在 0℃+72h 极端低温处理后正常生长，在此基础上筛选出的抗寒能力提高且遗传背景与对照接近的抗寒体细胞突变体，将为后续组学分析等研究工作提供极大的便利。本项目将传统的细胞培养技术与新兴的组学分析技术相结合，是对菠萝抗寒相关的分子调控机理的创新性探索。

4.计划进度

2018 年度：

1） 突变体与对照材料低温胁迫不同时间段处理；

2） 突变体/对照材料的转录组测序；

3） GC-MS 测定突变体/对照材料中代谢产物的种类及含量；

4） 组学数据的分析及相关结果的验证；

2019 年度：

1） 差异基因的挖掘筛选，明确候选基因；

2） 超量表达载体的构建；

3） 遗传转化菠萝。

2020 年度：

1） 成功获得转基因再生株系；

2） 目的基因超量表达株系的筛选鉴定；

3） 转基因材料抗寒相关指标的测定，明确目的基因的功能。

4） 总结实验结果，文章整理及投稿。

三、研究基础

1. 材料基础

申请人所在课题组多年来开展菠萝育种研究，收集、诱导了多种不同菠萝类型的离体培养材料。菠萝各类型及品种间抗寒能力存在不同程度的差异，为本研究中通过检测基因在各材料中的表达情况筛选关键抗寒基因提供了丰富的材料。本研究前期经细胞培养得到的抗寒体细胞突变体材料，抗寒性能提高且分子水平存在变异，为本项目后续的深入分析奠定了重要的材料基础。

2. 技术基础

申请人所在课题组已建立起了完善的分子生物学及组织培养研究平台，具备与本研究直接相关的技术体系如基因克隆、载体构建、分子标记分析等。课题组针对菠萝的体细胞胚胎发生开展了系统深入的研究，建立起了稳定的菠萝胚性细胞悬浮系和体细胞胚发生体系及高效的遗传转化技术体系。已建立了完善的转录组数据分析平台，掌握了转录组数据分析的各项流程及关键信息的挖掘和鉴定等技术。

3. 前期工作基础

申请人所在课题组针对本项目前期已做了大量相关的基础性工作。利用低温致死法对普通神湾的离体培养材料进行耐寒性测定，摸清了培养材料的临界致死条件，

确定了从耐寒神湾的离体培养物筛选更加抗寒的细胞株系的低温筛选条件为 0℃+72h。对田间耐寒植株的离体培养物共进行三轮低温筛选，获得多个抗寒变异株系（图 1-A），逆境处理后每轮筛选离体材料的成活率显著提高（从 5.58×10^{-6} 到 3.46%）。抗寒变异株系经低温处理(0℃+72h)移栽后长势正常，而对照材料则逐步萎蔫死亡（图 1-B），表明所得体细胞突变体株系抗寒性能有显著提高。低温处理后抗寒体细胞突变体材料中脯氨酸含量的测定也表明，各株系抗寒能力显著增强（图 1-C）。ISSR 分子标记检测结果表明，抗寒材料相比对照在分子水平确实存在着遗传变异（图 1-D）。以上课题组前期坚实的工作基础，为本项目利用体细胞突变体材料开展进一步的组学分析及候选基因的功能验证工作提供了可靠的保障。

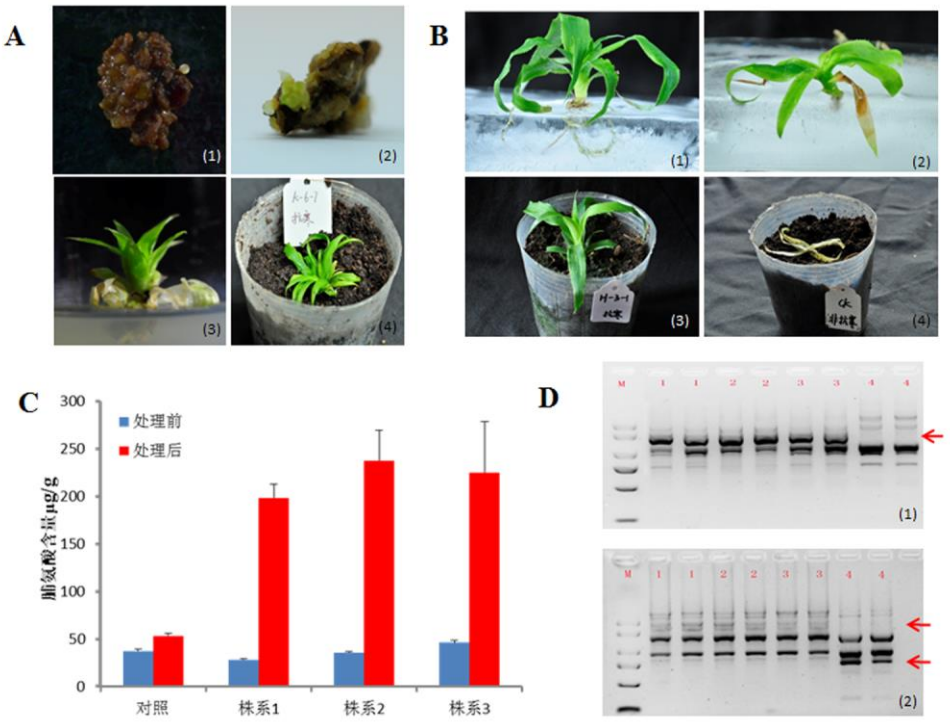

图 1. 与本项目相关的前期研究基础。

A. 抗寒株系从体细胞胚发生到移栽的过程。（1）体细胞胚的发生（体式镜下）；（2）胚性细胞的形成；（3）抗寒植株幼苗的发生；（4）抗寒植株的移栽。

B.（1）抗寒材料和（2）对照在低温胁迫（0 ℃ + 72 h）处理后的生长情况。（3）抗寒材料和（4）对照在冷胁迫处理结束移栽 10d 后的生长情况。

C. 冷胁迫（0 ℃ + 72 h）处理前后各株系及对照材料中脯氨酸含量的测定。

D. 抗寒材料与对照的 ISSR 分子标记结果。（1）和（2）分别代表不同引物的结果，其中 1-3 为抗寒材料，4 为对照。

4. 工作条件

申请人所在单位具备开展本项目的仪器设备和技术平台。拥有用于基因克隆所

需要的 PCR 仪、核酸电泳仪、BIO-RAD 凝胶成像分析系统；用于定量 PCR 分析的 LightCycler®480（Roche）实时荧光定量 PCR 仪，用于初生代谢物测定的 GC-MS（QP2010 Ultra）；生理数据测定所需的 UV-2401PC/2450 紫外可见光分光光度计；组织培养及遗传转化所需的超净工作台、智能培养箱、恒温摇床、光照培养室等基础设施；室外建有菠萝种植用田间科研基地，以供突变体株系及转基因材料的后续移栽。以上这些仪器设备和科研平台能够确保本项目的顺利实施和完成。

四、申请者简介

◆ 申请者学历：

申请者于 2017 年 6 月毕业于华中农业大学果树学专业，获农学博士学位。博士学位论文题目为：“甜橙 *CsMYBF1* 基因的功能鉴定和调控机理研究”。论文指导老师为邓秀新院士，工作单位为华中农业大学。该篇博士学位论文被评为 2015-2016 学年华中农业大学校级优秀博士学位论文。

◆ 申请者研究工作经历：

申请者于 2016 年 7 月入职华南农业大学园艺学院果树系，加入学院热带亚热带果树遗传育种科研团队，主要从事菠萝种质资源的收集及抗逆性状的遗传改良方面的研究工作。主持了 2017 年度华南农业大学青年科技人才培育项目，主要参与了广东省优稀水果种质资源评价与特色品种选育现代农业产业技术体系项目。

◆ 发表论文情况：

1. **Liu Chaoyang**, Xie Tao, Chen Chengjie, Luan Aiping, Long Jianmei, Li Chuhao, Ding Yaqi, He Yehua (2017). Genome-wide organization and expression profiling of the R2R3-MYB transcription factor family in pineapple (*Ananas comosus*). **BMC Genomics**, 18(1), 503.

2. Zhu Feng, Luo Tao, **Liu Chaoyang**, Wang Yang, ..., Deng Xiuxin, Cheng Yunjiang (2017). An R2R3-MYB transcription factor represses the transformation of *α*- and *β*-branch carotenoids by negatively regulating expression of *CrBCH2* and *CrNCED5* in flavedo of *Citrus reticulate*. **New Phytologist.** 216:178-192

3. **Liu Chaoyang**, Long Jianmei, Zhu Kaijie, Liu Linlin, Yang Wei, Zhang Hongyan, Li Li, Xu Qiang, Deng Xiuxin (2016). Characterization of a citrus R2R3-MYB transcription

factor that regulates the flavonol and hydroxycinnamic acid biosynthesis. **Scientific reports**, 6, 25352.

4. **Liu Chaoyang**, Wang Xia, Xu Yuantao, Deng Xiuxin, Xu Qiang (2014). Genome-wide analysis of the R2R3-MYB transcription factor gene family in sweet orange (*Citrus sinensis*). **Molecular Biology Reports**, 41(10), 6769-6785.

5. Xu Qiang, **Liu Chaoyang**, BISWAS Manosh Kumar, Pan Zhiyong, Deng Xiuxin (2014). Recent advances in fruit crop genomics. **Frontiers of Agricultural Science and Engineering**, 1(1), 21-27.

6. Xu Qiang, BISWAS Manosh Kumar, Lan Hong, Zeng Wenfang, **Liu Chaoyang**, Xu Jidi, Deng Xiuxin (2011). Phylogenetic and evolutionary analysis of NBS-encoding genes in Rutaceae fruit crops. **Molecular Genetics and Genomics**, 285(2), 151-161.

签字和盖章页(此页自动生成，打印后签字盖章)

申请者：　　刘朝阳　　依托单位：　　华南农业大学

项目名称：　　菠萝抗寒体细胞突变体抗寒分子机制解析及候选基因的功能鉴定

申请者承诺：

本人符合各项申报条件。本表各项内容真实、数据准确，不涉密，没有知识产权争议。如果获准立项，承诺以本表为有约束力协议，遵守有关规定，按计划认真开展研究工作，取得预期研究成果，并按时报送有关材料。若填报失实和违反规定，本人将承担全部责任。

签字：

项目组主要成员承诺：

本人保证有关申报内容的真实性。本人将严格遵守广东省教育厅的有关规定，切实保证研究工作时间，加强合作、信息资源共享，认真开展工作，及时向负责人报送有关材料。若个人信息失实、执行项目中违反规定，本人将承担相关责任。

编号	姓名	工作单位	分工	签名
1	龙健梅	华南农业大学	转录组分析	
2	夏靖娴	华南农业大学	代谢组分析	
3	谢桃	华南农业大学	基因的筛选和验证	
4	李楚豪	华南农业大学	基因的遗传转化	

依托单位和合作单位承诺

已按填报说明对申请人的资格和申请书内容进行了审核。本单位保证对研究计划实施所需要的人力、物力和工作时间等条件给予保障，严格遵守广东省教育厅有关规定，督促负责人和主要成员以及本单位科研管理部门按照广东省教育厅的规定及时报送有关材料。

	依托单位	合作单位 1	合作单位 2
单位名称	华南农业大学(公章)	(公章)	(公章)
承诺经费	8(万元)	(万元)	(万元)
日期：	年　月　日	年　月　日	年　月　日


科研空间
欢迎您，刘朝阳老师
科研动态
我的办公
我的项目
我的经费
我的成果
我的学术交流
我的考核
我的主页
常用下载
项目立项
项目申报（1）
所有项目
职称评定
主持的项目
参与的项目
博硕导评定
主持的项目
参与的项目
项目性质
纵向(21项)
横向(2项)
项目分类
省重点领域研发计划(3项)
科技特派员扶贫专项(3项)
面上项目(2项)
国家自然科学基金项目(2项)
广东省教育厅人才类项目（自然科学类）(2项)
总数:2项 (表中经费单位：万元)
项目名称
查询
新增
删除
打印
导出
全选
项目名称
所属单位
负责人
立项日期
合同经费
起止时间
项目来源
项目成员
署名顺序
审核状态
操作
NcSUT4在黄梁木蔗糖转运中的功能鉴定与调控机制解析
林学与风景园林学院
龙健梅
2018-04-04
8.0
2018-01-01到2019-12-31
广东省教育厅
龙健梅,刘朝阳,杨静,刘思雯（学）,董甜甜（学）
2
学校通过
菠萝抗寒体细胞突变体抗寒分子机制解析及候选基因的功能鉴定
园艺学院
刘朝阳
2018-01-01
8.0
2018-01-01到2019-12-31
广东省教育厅
刘朝阳,龙健梅,李楚豪（学）,路鑫鑫（学）
1
学校通过
编辑
项目变更
项目结项
1/1 共2条
1


项目查看
项目类型：
独立课题
批准号：
2017KQNCX020
经费来源单位：
广东省教育厅
费用类型：
财政资金项目支出类（科研）
承担方式：
主持
项目状态：
完成
立项日期：
2018-01-01
开始时间：
2018-01-01
计划完成日期：
2019-12-31
结项日期：
2019-12-31
合同经费：
8 万元
间接经费：
0 万元
直接经费：
8 万元
财务账号：
外拨经费：
0 万元
【项目成员】
署名顺序
人员来源
成员姓名
学科方向
成员性别
职称
学历
工作单位
1
本校老师
刘朝阳
农学
男
助理研究员
博士研究生
园艺学院
2
本校老师
龙健梅
林学
女
讲师
博士研究生
林学与风景园林学院
3
本校学生
李楚豪（学）
农学
关闭

SCAULIB202518798

检索证明

根据委托人提供的论文材料，委托人**华南农业大学林学与风景园林学院 龙健梅** 8 篇论文收录情况如下表。

序号	论文名称	发表刊物及发表的年月卷期/页码等	作者排名	论文等级	作者文中单位	收录情况	影响因子	中科院大类分区
1	The high-affinity pineapple sucrose transporter AcSUT1B, regulated by AcCBF1, exhibited enhanced cold tolerance in transgenic Arabidopsis	International Journal of Biological Macromolecules 出版年：2024 卷期： 28310.1016/j.ijbiomac.2024.137952 137952 页码： - 文献号：137952 文献类型：Article	第一作者	A 类	South China Agricultural University	SCI	IF2-year=8.5 IF5-year=8.7 （2024）	生物学 2 区 Top 期刊：是 （2025）
2	Arabidopsis sucrose transporter 4 (AtSUC4) is involved in high sucrose-mediated inhibition of root elongation	Biotechnology & Biotechnological Equipment 出版年：2022 出版日期：2022-09-08 卷期：36 1 页码：561-574 文献号： 文献类型：Article	并列第一作者	B 类	South China Agricultural University	SCI	IF2-year=1.4 IF5-year=1.8 （2022）	工程技术 4 区 Top 期刊：否 （2022）

3	Selection and Validation of Reference Genes for mRNA Expression by Quantitative Real-Time PCR Analysis in Neolamarckia cadamba	Scientific Reports 出版年：2018 卷期：8 9311 页码：- 文献号： 文献类型：	并列第一作者	B 类	South China Agricultural University	SCI	IF2-year=4.011 IF5-year=4.525 （2018）	综合性期刊 3 区 Top 期刊：否 （2018）
4	新农科建设背景下“林木遗传育种学”双语教学探索	科教导刊 出版年：2022 卷期： 页码：- 文献号： 文献类型：	第一作者	普刊类	华南农业大学林学与风景园林学院	CNKI	无	无
5	Genome-Wide Identification and Expression Analysis of WRKY Gene Family in Neolamarckia cadamba	International Journal of Molecular Sciences 出版年：2023 卷期：24 8 页码：- 文献号：7537 文献类型：	共同通讯作者（倒数第一）	A 类	South China Agricultural University	SCI	IF2-year=4.9 IF5-year=5.6 （2023）	生物学 2 区 Top 期刊：否 （2023）
6	黄梁木蔗糖转运蛋白 NcSUT4 和 NcSUT5 的表达与功能分析	分子植物育种 出版年：2024 出版日期：（录用定稿）网络首发时间：2024-07-22 10:08:26 卷期： 页码：- 文献号：	通讯作者	C 类	华南农业大学林学与风景园林学院	北大核心	无	无

		文献类型：						
7	激光显微切割分离黄梁木不定根原基的技术体系建立	植物生理学报 出版年：2019 卷期：55 5 页码：- 文献号： 文献类型：	共同通讯作者	C 类	华南农业大学林学与风景园林学院	北大核心	无	无
8	黄梁木 WOX 基因家族的鉴定与表达分析	基因组学与应用生物学 出版年：2022 卷期： 页码：- 文献号： 文献类型：	共同通讯作者	C 类	华南农业大学林学与风景园林学院	北大核心	无	无

说明：论文等级和中科院大类分区按《华南农业大学学术论文评价方案（试行）》划分。

报告免责声明:如未盖章,报告无效

检索员：尹银怀

华南农业大学图书馆

2025-07-14

新农科建设背景下“林木遗传育种学”双语教学探索

龙健梅*，林元震

（华南农业大学林学与风景园林学院　广东　广州　510642）

摘　要　在新农科建设背景下，双语教学是专业课程改革的重要方向之一。“林木遗传育种学”是培养现代化林木良种选育和繁殖相关人才的专业核心课程，是以遗传学为理论指导研究选育和繁殖林木良种的原理和技术的学科。实施“林木遗传育种学”双语教学，为培养具有国际化视野的新型林木育种人才奠定基础。本文主要探讨“林木遗传育种学”双语课程建设过程中出现的问题，并提出相应的改革措施，以期为林木遗传育种学及其他相似课程的双语教学改革提供参考。

关键词　新农科；林木遗传育种学；双语教学

中图分类号：G424　　文献标识码：A　　DOI:10.16400/j.cnki.kjdk.2022.33.035

Bilingual Teaching Exploration of "Forest Tree Genetics and Breeding" under the New Agricultural Project

LONG Jianmei, LIN Yuanzhen

(College of Forestry and Landscape Architecture, South China Agricultural University, Guangzhou, Guangdong 510642)

Abstract　Bilingual teaching is one of important directions for professional courses reform under the background of the New Agricultural Project. "Forest Tree Genetics and Breeding" is a professional core course for cultivating talents in the selection, breeding and reproduction of forest tree. The implementation of bilingual teaching of "Forest Tree Genetics and Breeding" lays the foundation for cultivating new-type talents in forest tree breeding with an international perspective. This paper mainly discussed the problems in the bilingual course construction of "Forest Genetics and Breeding", and the corresponding improvement measures were proposed. This study would provide reference for the bilingual teaching reform of "Forest Tree Genetics and Breeding" and other similar courses.

Keywords　New Agricultural Project; Forest Tree Genetics and Breeding; bilingual teaching

“林木遗传育种学”是研究森林和树木遗传变异的现象与规律，探索林木遗传改良的理论与技术的一门学科[1]。该课程是林学专业的核心课程之一，主要分为林木遗传学与林木育种学两部分内容。其中，遗传学是基础，育种学则是建立在遗传学的基础上，以遗传进化理论为指导，研究林木选育和良种繁育原理和技术。通过该课程的学习，学生能够掌握遗传学的基本理论，理解林木主要性状的遗传变异特点，熟悉林木育种的主要程序。现代生物技术的迅速发展，为传统的林木遗传育种学科的发展注入新的生命力，拓宽了林木遗传育种研究的广度和深度，为林木遗传育种的高效可持续发展奠定坚实的基础。生命科学的发展也使林木遗传育种学课程的内容不断增多，难度逐渐增大，目前本学科大多数前沿知识以及关键生物技术成果的一般用英语发布，供世界不同语言背景的相关科研工作者学习，因此急需培养既精通本专业知识又能熟练应用外语的高素质人才，跟踪学术前沿，充分利用我国丰富的林木植物资源优势，使我国林木育种理论和应用研究方面获得快速发展。

2021 年教育部指出要深化高等教育内涵式发展，推进新工科、新医科、新农科和新文科（简称“四新”）建设[2]，以提高高校服务经济社会发展能力。在该背景下，对林学专业人才培养模式提出了更高的要求，要从课程体系设置和课程教学模式上进行改革才能达到新农科的标准。双语教学是指除汉语外，用一门外语作为课堂主要用语进行学科教学，绝大部分是用英语，即“汉语+英语”的授课方式[3]。林木遗传育种学作为林学专业的核心课程，探索其双语教学教学模式不仅适应国际化发展，也为新农科建设背景下林学学科的发展奠定一定的基础。

林木遗传育种学课程开设双语教学，一方面使学生可以掌握基本的遗传与育种的基本理论和方法，另一方面可

以提高学生本专业的英语听说与阅读能力，能够有效快速获取本学科的最新科研成果信息。目前已在许多高校开设育种学相关课程的双语教学，如南京农业大学大学开设园艺作物育种学，北京林业大学开设草地植物遗传育种学[4]；甚至有的学校开设全英文林木遗传育种学课程，如南京林业大学[1]。这些高校在双语教学已取得了初步成效，但仍然存在诸多问题。因此，本文就林木遗传育种学实施双语教学过程中出现的问题进行分析，并提出相应的改革措施。

1“林木遗传育种学”双语教学存在的主要问题

1.1 教材可选余地较小

教材是知识传递的载体，优质的教学材料资源是进行双语教学的保障。目前来看，大多数进行双语教学的课程以单一的全英教材为主。“林木遗传育种学”一般仅面向林学专业学生开设，课程比较小众，原版的全英教材较少，可选择的主要有两本：《Forest Genetics》[5]和《Applied Forest Tree Improvement》[6]，两本教材编者均来自美国，其中前者已有中文翻译版本《森林遗传学》。林木遗传育种学作为专业必修课，包含遗传学和育种学两个部分，遗传学部分理论性强，知识点多，内容抽象枯燥；而育种部分则注重生产实践，以遗传测定为主线，讲授不同育种方法的实施过程。全英教材虽然可以提供正宗地道的英文表达，但由于遗传学的知识抽象，以及原版教材的内容与国内林木遗传育种课程教学目标要求不完全一致，导致学生在选用全英教材上受到一定的限制。

1.2 双语教学教师缺乏

双语教师是推行双语教学的关键因素。“林木遗传育种学”课程实施双语教学，要求教师既能够熟练应用英语进行课堂教学，又具备扎实的专业知识和丰富的林木育种实践经验，这就对课程教师提出了更高的要求。很多专业词汇一般比较生僻且难读，虽然很多教师具备留学经历，英语写作水平比较高，但能够使用英语进行自如交流的教师并不多，能达到这种英语程度的大多是青年教师。然而青年教师往往缺乏林木育种生产实践经验，因此对“林木遗传育种学”双语教学提出来极大挑战。

1.3 学生英语基础薄弱

学生是教学活动的中心，也是检验双语教学效果的主体。随着我国国际地位提高以及对英语教育的重视，大学生的英语水平不断提升。林木遗传育种学作为专业必修课，一般设置在大三的第一学期，学生基本完成基础英语学习，但对专业英语学习投入较少，缺乏专业英语词汇的积累；并且由于我国的英语教育过多强调语法结构和阅读能力，口语和听力水平总体上较差，导致学生在课堂上流利使用英语表达观点的能力较弱，影响双语教学的效果，同时也会打击部分学生学习的主动性和积极性，最终适得其反。

1.4 教学模式单一

为保证双语教学活动顺利进行，多数教师都能够做好充分的准备工作。在课堂上，双语教学目前还是以班级为单位进行集中授课，教师多采用传统的讲课方式传递知识，通常借助多媒体与板书结合的模式。由于授课教师口语能力有限，不能即兴自由发挥，难以将知识进行扩充，这种情况会将课堂局限在准备的教案中，从而导致课堂枯燥无味，学生自然也会失去兴趣，难以达到预期的学习效果。

2 新农科背景下“林木遗传育种学”双语教学探索

2.1 培养高质量的双语教师团队

高质量的双语教师团队是保证林木遗传育种学双语教学的决定性因素之一，因此，要注重培养高水平的教师团队。可以从以下几方面入手。第一，比较资深且有丰富的林木育种实践经验的教师往往对林木遗传育种学的课程内容、重难点知识等了如指掌，这部分教师需加强专业英语使用能力，跟踪学科前沿发展动态，通过英文文献、刊物等，不断积累教学素材。第二，对于青年教师而言，大多数都具有留学经历，英语听说读写能力较强，这部分教师需要多与资深教师交流，积累授课经验，同时也要多参与林业育种生产实践工作，增加对育种部分知识点的理解。第三，学校学院应该创造机会给教师提供双语教学学习的机会，如定期开展讲座或派教师到国外访学，学习国外教学模式，还可聘用外籍教师进行授课，从多方面途径提升教师的双语教学能力。

2.2 提升学生英语水平

作为教学活动的主体对象，学生是检验双语教学成效的关键因素[7]。经过前期对本校林学专业学生英语水平的调研，发现学生之间差异比较明显。在“林木遗传育种学”课程开课前，部分学生已通过英语四级或者英语六级考试，但仍有部分学生出现英语考试不及格现象，因此，需要提供有效的引导提升学生的英语水平。首先，在新生入学专业教育时，要跟学生强调林学专业中全英或者双语课程的重要性，引导学生在思想上重视英语学习；其次，教师应向学生介绍英语在未来的升学和就业中的作用，让他们感受英语学习的重要性，从而提高对英语学习的紧迫感。最后，学校为学生营造英语学习的氛围或提供练习英语口语的场所，比如英语角或者定期开展英语学习讲座，在英语学

过程中也要注重口语和听力，提升学生的英语听说能力。

2.3 转变教学模式与考评体系

传统的教授式教学已经不能满足双语教学的需求，需要改变原来单一的教学模式。在互联网日益发达的大环境下，我们需要充分利用线上的英文教学资源，如图片、视频等，帮助学生理解重要知识点，同时也增加学生英语学习的兴趣。此外，鼓励学生多参与英文学术报告，或聘请外籍教师给学生上 1—2 次林木遗传育种学的全英课程，了解国外林木育种的方法与侧重点。要将学生作为课堂的主人，增加学生在课堂的参与度，可设置英文文献汇报，鼓励学生通过阅读文献理解知识点；同时也要注意了解他们的学习目标需求，及时跟进学生学习的效果，根据学生课堂学习的反馈调整教学方法。

考评体系是检验双语教学成效的重要方法。对目前大多数双语课程来讲，传统的理论闭卷考试是考评体系的主流方式，中英文试题各占一半，但这种考评方式存在一定的弊端，忽视了平时的学习过程。因此，除了期末的理论考试之外，考虑在平时课堂上增加英文 PPT 汇报或通过小组合作写一篇小型的英文科技论文等方式。英文 PPT 汇报可以是与林木遗传育种相关的一篇英文文献分享，抑或是根据课程的某一个内容，通过查找文献或者网上素材，以 PPT 的形式进行讲解，师生角色互换，充分发挥学生的主人翁地位，提高学生在课堂的参与度，激发学生的学习兴趣，调动学生课外学习的积极性。在计算学生的期末成绩时，可将平时成绩和期末考试成绩按各 50%分配，这样可以督促学生加强平时学习，全方面提高学生的专业知识及英语水平，同时也锻炼了学生的文献查阅能力、团队合作能力以及口头表达和写作能力，促使他们将专业知识学习与英语应用结合起来，从而达到双语教学的效果。

2.4《林木遗传育种学》双语教材选用

只选用国外全英教材在双语教学过程中并不适宜，而单纯使用中文教材也达不到双语教学的目的，因此可以以全英教材为参考，选用其中一些章节，组织教师进行翻译，同时配备一本中文的《林木遗传育种学》教材，以帮助学生理解专业词汇。此外，本课程增加案例教学部分，以相关文献的研究成果为例子，对其中所涉及的原理、概念等进行教学。重点关注林木遗传育种相关的 SCI 期刊，如《Tree Genetics & Genomes》等，从中选择一些典型的研究成果作为上课的素材，进行案例分析。教师在制作 PPT 课件时，以英文为主，在关键的知识点或者专业名词地方可增加中文翻译或解释，使学生更易于接受与理解。

3 结语

林木遗传育种学是林学专业的核心课程，在新农科建设背景下，开展该课程的改革势在必行。新农科的建设极大推动了林木遗传育种学课程创新的教学改革，我们从教材选用、师资培养、教学模式等方面探索了一套有特色的双语教学模式。然而，“林木遗传育种学”双语教学仍存在许多问题，如学生参与度不够，师资力量欠缺、教学能力不足等，我们将在今后的双语教学工作中不断优化，以期能使“林木遗传育种学”双语教学体系更加完善。

*通讯作者 龙健梅

★基金项目：华南农业大学 2020 年度教育教学改革与研究项目（JG20175）。

参考文献

[1] 边黎明,尹佟明,施季森.“林木遗传育种学”课程全英文授课的实践与探索[J].中国林业教育, 2016,34 (6): 62-64.

[2] 庞阔,陈诚,计宏伟.“四新”建设背景下工商融合课程体系构建探索[J]. 黑龙江教育(高教研究与评估), 2022(7): 42-44.

[3] 崔建国,吴月亮,张丽杰,等. 硕士研究生《林木遗传改良》课程双语教学实践与思考[J]. 安徽农业科学, 2020,48 (10) : 249-251.

[4] 许立新,曾会明,梁小红,等.《草地植物遗传育种学》双语教学实践与探讨[J]. 草业科学, 2012, 29 (12): 1930-1935.

[5] WHITE T T, ADAMS W L, NEALE D B. Forest genetics [M]. Wallingford，Oxfordshire, UK: CABI Publishing, 2007.

[6] ZOBEL B J, TALBERT J T. Applied Forest tree improvement [M]. New York: Wiley, 1984.

[7] 杨贵利,谭艾娟.“双一流”背景下生物化学双语教学的现状与创新模式探究[J]. 中国多媒体与网络教学学报（上旬刊）, 2021(2): 96-98.

主管单位：长江出版传媒股份有限公司
主办单位：湖北长江报刊传媒（集团）有限公司
ISSN 1674-6813
CN 42-1795/N

科教导刊

THE GUIDE OF SCIENCE & EDUCATION

国家新闻出版署认定的学术期刊
中国知网（CNKI）全文收录期刊
万方数据-数字化期刊群收录期刊

2022年11月
第33期（总第501期）

科教导刊 2022年第33期（11月）（总第501期）

目录

科教导刊 旬刊
KE JIAO DAO KAN

2022年第33期(总第501期)
2022年11月25日出版

主管单位:长江出版传媒股份有限公司
主办单位:湖北长江报刊传媒(集团)有限公司
出版单位:《科教导刊》编辑部
总 经 理:周发秋

国内统一连续出版物号:CN 42-1795/N
国际标准连续出版物号:ISSN 1674-6813
社长/主编:谢成宇
副社长/副主编:张永平
执行主编:朱泽玲
电 话:027-87826797 027-87348017
网 址:www.kjdkzzs.com
邮 箱:kjdk@kjdkzzs.com
地 址:武汉市洪山区珞喻路78号
邮 编:430079
印 刷:武汉贝思印务设计有限公司
发行单位:武汉广渊广告有限公司
电 话:027-87058489
定 价:24.00元

前沿视角

高教论坛

学科探索

师资建设

课程教学

学生工作

场馆管理

实证调研

出版单位：《科教导刊》编辑部
总 经 理：周发秋
社长/主编：谢成宇
国内统一连续出版物号：CN 42-1795/N
国际标准连续出版物号：ISSN 1674-6813
地　　址：武汉市洪山区珞喻路78号
电　　话：027-87826797　87348017
邮　　箱：kjdk@kjdkzzs.com
网　　址：www.kjdkzzs.com
发行单位：武汉广渊广告有限公司
印　　刷：武汉贝思印务设计有限公司
发行范围：公开

ISSN 1674-6813
9 771674 681222 33>
定价：24.00元

International Journal of Biological Macromolecules 283 (2024) 137952

Contents lists available at ScienceDirect

International Journal of Biological Macromolecules

journal homepage: www.elsevier.com/locate/ijbiomac

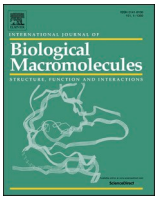

The high-affinity pineapple sucrose transporter *AcSUT1B*, regulated by AcCBF1, exhibited enhanced cold tolerance in transgenic *Arabidopsis*

Jianmei Long [a], Huimin Zhou [a], Haixin Huang [a], Yufei Xiao [a], Jiandong Luo [a], Yue Pu [a,b], Zihong Liu [a,b], Mengqing Qiu [a], Xinxin Lu [a], Yehua He [a], Chaoyang Liu [a,*]

[a] *State Key Laboratory for Conservation and Utilization of Subtropical Agro-Bioresources, Guangdong Key Laboratory for Innovative Development and Utilization of Forest Plant Germplasm, Key Laboratory of Biology and Germplasm Enhancement of Horticultural Crops, Ministry of Agriculture and Rural Affairs, South China Agricultural University, Guangzhou 510642, China*

[b] *Institute of South Subtropical Crops, Chinese Academy of Tropical Agricultural Sciences, Zhanjiang 524091, Guangdong, China*

ARTICLE INFO

Keywords:
Pineapple
Sucrose transporter
Cold stress
CBF

ABSTRACT

Sucrose transporter (SUT) plays essential roles in plant growth and development, as well as responses to diverse abiotic stresses. However, limited information about the function of SUT was available in pineapple, an important tropical fruit crop with crassulacean acid metabolism. Here, four *AcSUT* genes were identified in pineapple genome, and divided into three clades according to the phylogenetic analysis. The expression profiles of *AcSUTs* were systemically examined, and they were all localized to plasma membrane. Transport activity assay by two-electrode voltage clamp of *Xenopus* oocytes showed that AcSUT1A and AcSUT1B were capable of transporting a range of glucosides, and they were exhibited high affinity for sucrose with Km value of 0.09 mM and 0.41 mM at pH 5.0, respectively. Overexpression of the cold-induced *AcSUT1B* conferred enhanced cold tolerance in transgenic *Arabidopsis*. DNA-protein interaction analysis further demonstrated that AcCBF1 directly binds the CRT/DRE element of the *AcSUT1B* promoter and activated its expression. Heterologous expression of *AcCBF1* in *Arabidopsis* also increased cold tolerance. In this study, we investigated the transport activities of AcSUTs in pineapple and identified the *AcCBF1-AcSUT1B* module involved in cold stress, which provided new insights into the molecular mechanism of the cold response in pineapple.

1. Introduction

Sucrose is a major translocatable product of photosynthesis produced by green leaves and is transported to sink tissues through the long-distance pathway [1]. It not only served as a source of carbon skeletons and energy to support growth and development of sink organs incapable of performing photosynthesis, but also played a crucial role as signal molecule in plants [2,3]. Transportation and distribution of sucrose from source organs towards sink organs is mainly mediated by sucrose transporters (SUTs), which are transmembrane proteins belonging to the major facilitator superfamily (MFS). Typically, SUTs have twelve transmembrane spanning domains with N- and C- termini and seven-numbered loops in the cytoplasm [4,5]. Members in SUT family were functionally characterized to modulate the flux of sucrose over cellular membranes, with acting as proton-coupled sucrose symporters in a pH- and energy-independent manner [6,7].

According to the homology of sequence evolution of sucrose transporters, the SUT family has been divided into five clades: SUT1～SUT5 [8]. The SUT1 clade was specifically found in dicotyledons, whereas SUT3 and SUT5 is monocotyledon-specific. SUT2 and SUT4 were shared in both dicotyledons and monocotyledons. Since the first plant *SUT* gene (*SoSUT1*) was isolated in spinach [9], a growing number of *SUT* genes have been identified in numerous species including herbaceous annual plants such as *Arabidopsis* [10], rice [11], tobacco [12], cotton [5], sugar beet [13], and woody perennial species such as poplar [14], cacao [15] and citrus [16]. For most plant species, it has been indicated that SUTs was a small size gene family usually with less than ten members. For example, there were nine and five SUT genes that have been identified in *Arabidopsis* and rice, whereas five were found in the model tree genus *Populus* [14].

Transport activity plays a crucial role in elucidating the functions of the SUT in plants. The combination of the two-electrode voltage clamp (TEVC) technique with the heterologous expression system in *Xenopus laevis* oocytes represents a robust electrophysiological method

* Corresponding author.
E-mail address: liuchaoyang@scau.edu.cn (C. Liu).

https://doi.org/10.1016/j.ijbiomac.2024.137952
Received 29 August 2024; Received in revised form 5 November 2024; Accepted 20 November 2024
Available online 22 November 2024

extensively utilized for the investigation of SUT transport properties, including transport kinetics, substrate specificity and pH dependence [17,18]. By this powerful method, transport activity of many SUTs from both monocots and dicots has been characterized, such as three SUTs (AtSUC1, AtSU2 and AtSUC9) in *Arabidopsis* [19–21], two SUTs (OsSUT1 and OsSUT5) in rice [17] and HvSUT1 from wheat [22]. According to the affinity and transport capacity of SUT for sucrose, they can be divided into two subgroups, including high-affinity/low-capacity (HALC) with a Km of 0.3–2.0 mmol/L and Low-affinity/High-capacity (LAHC) with a Km of 6.0–11.70 mmol/L [10]. It is well known that the transport activity of SUTs is highly correlated with physiological functions in plants. In dicots, *Arabidopsis* AtSUC2 functions as a high-affinity transporter, which was essential for phloem loading in major veins, while AtSUT4 acts as a low-affinity transporter involved in phloem loading in minor veins [23]. In addition to phloem loading, SUTs also function in sucrose unloading into sink tissues, thus participated in plant growth and development. They were found to be essential for pollen and seed development, flowering, and fruit ripening [24–27]. For example, rice OsSUT1 was a LAHC transporter, and disruption of OsSUT1 impaired pollen function but did not influence pollen development, and knockout of rice OsSUT1 by CRISPR-Cas9 resulted in complete infertility [28,29]. AtSUC1 was essential for normal pollen germination and sucrose-induced anthocyanin accumulation [30]. AtSUC9, another SUT1 member in *Arabidopsis*, was also a high affinity similar with AtSUC2, but it showed different functions with participating in early flowering [20]. To our knowledge, the transport activity of SUT has been systematically identified only in several dicots and a few monocots (mainly in cereals), but largely uncharacterized in most of the monocotyledonous plants.

In general, sucrose supply is affected under adverse conditions by repressing photosynthesis. Therefore, sugar partitioning through the whole plant is of great importance in response to stress [31,32]. Increasing evidence has shown that SUTs contributed to regulating multiple stress responses. Modification of SUT expression could alter plant stress tolerance. For instance, *AtSUC2* and *AtSUC4* were induced under salt, osmotic, drought, low temperature and exogenous ABA treatment, and loss-of-function mutation of *AtSUC2* and *AtSUC4* led to hypersensitive responses to the above various stress in seed germination and seedling growth [33]. Overexpression of *IbSUT4* gene in *Arabidopsis* accelerated growth and improved abiotic stress resistance by enhancing the sucrose content of the sink organs [34]. Likewise, MdSUT2.2 overexpressed apple exhibited higher sugar accumulation and drought and salt tolerance [35,36], while PpSUT2 in peach increased cold and drought stress tolerance [37]. Additionally, in monocots, rice OsSUT1 and OsSUT2 were found to participate in salt and drought stress response [38,39]. These findings indicated that SUTs were induced under stress treatment and involved in abiotic stress through modulating sucrose transport and distribution. However, the functions of SUTs in other plant species remain largely unknown in sucrose accumulation under abiotic stress conditions.

Pineapple is one of the most economically significant fruit crops and is found in almost all the tropical and subtropical regions of the world. As a crassulacean acid metabolism (CAM) plant, the pineapple possesses special mechanism that regulate distribution and partitioning of assimilates [40]. Differences in the content and composition of sugars in pineapple fruit were found among different varieties and the same variety that harvested at different seasons, which could be correlated with the synthesis, accumulation, transportation, and utilization of sugars in pineapple [41,42]. To date, the sugar transportation in pineapple has received relatively little attention, the sugar transporters have been recognized previously as key targets for revealing this process [43]. Until now, the sucrose transporter gene family has not yet been systematically studied in pineapple. Thus, there is an urgent need to completely identify and classify the SUTs and to characterize their roles in pineapple. In this study, members of the SUT gene family were identified and cloned in pineapple, the expression patterns and subcellular localization of AcSUTs were investigated. The transport activities of the AcSUTs were tested by expression in *Xenopus* oocytes and TEVC. The gene *AcSUT1B*, which exhibited high-affinity sucrose transport activity and obvious cold-induced gene expression pattern, was selected for further functional analysis by heterologous expression in *Arabidopsis*. Moreover, the CBF transcription factor *AcCBF1*, which also conferred higher cold tolerance, was identified as the upstream regulatory gene of *AcSUT1B*. These results contribute to a further understanding of *AcSUT1B* in response to cold stress and provide candidate genes to enhance cold tolerance in pineapple.

2. Materials and methods

2.1. Identification, cloning and sequence analysis and SUTs in pineapple

Since pineapple is a monocot plant, the amino acid sequences of model monocot rice SUTs obtained from the rice database (http://rice.uga.edu/index.shtml) were employed as queries to search for pineapple genome (https://phytozome-next.jgi.doe.gov/info/Acomosus_v3) using BlastP program with E value of 10^{-5}, and the putative pineapple *SUT* genes were explored. To confirm the presence of MFS domain, the putative SUT sequences were subsequently investigated using Pfam. The transmembrane helices in putative SUT deduced proteins were predicted using TMHMM Server v. 2.0 (http://www.cbs.dtu.dk/services/TMHMM/), and the physicochemical properties of SUT protein were analyzed by the tool of ProtParam at ExPASy (https://web.expasy.org/protparam/).

Total RNA was extracted form leaf tissues of 'Shenwan' pineapple (*Anana comosus*) using and RNAprep Pure Plant Kit (Tiangen, China), and the first-strand cDNA was synthesized using a PrimeScript™ II 1st Strand cDNA Synthesis Kit (Takara, Japan) according to the manufacturers' instructions. Based on the above putative SUT sequences from the pineapple genome database (https://phytozome-next.jgi.doe.gov/info/Acomosus_v3), the specific primers were designed to amplify the ORF of the *SUT* genes in pineapple (Table S1). The multiple alignments of the deduced amino acid sequence were performed using the Clustal W program. Multiple sequence alignments of the MFS domain and 12 transmembrane helices were generated using webserver Clustal Omega with default parameters (https://www.ebi.ac.uk/Tools/msa/clustalo/).

The full-length SUT protein sequences from *A. thaliana*, rice, *populus*, tobacco, potato, tomato, apple, citrus, *Hevea brasiliensis*, *Beta vulgaris* L., *Vitis vinifera*, *Selaginella moellendorffii*, *Physcomitrella patens*, *Hordeum vulgare*, *Spinacia oleracea* L. were downloaded from the National Center for Biotechnology Information (NCBI) database. The phylogenetic tree was subsequently constructed using neighbor-joining (NJ) method of MEGA 7.0 with the parameters of Poisson model, pairwise deletion and 1000 bootstrap iterations. The accession numbers of the SUT proteins were listed in Table S2.

2.2. qRT-PCR analysis

Thirteen different parts of the 'Shenwan' pineapple, including bract, sepal, receptacle, ovary, ovule, stamen, style, core, petal, stem, leaf, root and callus were separately collected. For the cold stress treatment, the tissue cultured pineapple plantlets were kept at 4 °C, the plantlets that were placed at 25 °C were used as control. In the NaCl and ABA treatment, the pineapple callus samples were transferred to the Murashige and Skoog (MS) solution with or without (control) 150 mM NaCl and 100 μM abscisic acid (ABA), respectively. The samples were collected at 0, 2, 4, 8, 12, 24 and 48 h after treatment, respectively. All samples were immediately frozen in liquid nitrogen and store at −80 °C until RNA extraction.

qRT-PCR was performed using BioRad with the SYBR Premix Ex Taq (TaKaRa; RR041A), following the manufacturer's instructions. Primers were designed using the online software Primer3Plus (https://www.

primer3plus.com/). The cycling condition was set as follows: 95 °C for 30 s, followed by 40 cycles of 95 °C /10 s, 60 °C/30 s. The dissolution curve was used for verifying the qPCR amplification specificity under the procedure as follows: 95 °C for 15 s, 60 °C for 60 s, and warming up to 95 °C then 50 °C for 30 s. The *β-Actin* gene was used as an endogenous control. Three biological replicates and at least three technical replicates were performed. Gene-specific primers are shown in Table S1.

2.3. Subcellular localization of AcSUTs

To investigate the subcellular localization of AcSUTs, the CDS of *AcSUTs* were amplified and inserted into the pAN580 vector to generate the pAN580-AcSUTs-GFP constructs. Each construct and the positive control PIP2-mCherry (a plasma membrane marker) were subsequently transiently co-transformed into protoplasts of rice leaves according to the protocol described by Zhang et al. [44]. Images of protoplasts were taken with a confocal laser scanning microscope (Zeiss LSM880). Primers are listed in Table S1.

2.4. Plasmid construction, in vitro cRNA transcription and expression of AcSUTs in oocytes

The coding sequence (CDS) of *AcSUTs* were amplified by PCR using the primers listed in Table S1. The PCR products were purified and inserted into the oocyte expression vector pOO2 linearized with *Bam*H I and *Eco*R I. The pOO2-AtSUC2 was used as positive control (kindly provided by Prof. John Ward, University of Minnesota). Capped cRNA was transcribed in vitro using mMessage mMachine SP6 transcription kit (Ambion, Life Technologies), after linearization of the plasmids with *Pml* I restriction enzyme (New England Biolabs Inc.). The *Xenopus laevis* oocytes at the defolliculated stages V–VI were isolated and separated. Each well-separated oocyte was subsequently injected with 50 nL (~1000 ng/μl) cRNA of *AcSUTs,* and incubated at 17 °C for 2–3 days till electrophysiological recording.

2.5. Two electrode voltage clamping and data analysis

The oocytes expressed with *AcSUTs* or *AtSUC2* were bathed in the recording solution contained 90 mM NaCl, 1 mM KCl, 1.3 mM $MgCl_2$, and 10 mM HEPES [45] at specific pH indicated figure legends. The holding potential was set with −50 mV and the recording pipette was filled with 1 M KCl. Different sugars or different concentrations of sucrose stock solutions were diluted in the recording solution. The current was recorded using a npi Turbo TEC-10CD (npi Electronics, Tamm, Germany) and Digidata 1322 A (Axon Instruments, Union City, CA, USA). For the kinetic analysis of sucrose transport by AcSUTs, currents were normalized to the maximum concentration in each oocyte, and at least 3 oocytes were tested. Curve fitting on normalized current versus sucrose concentration plots was done with Hill equation (Sigmaplot 12.5). For the substrate specificity analysis, six substrates including sucrose, maltose, trehalose, salincin, esculin and glucose were added at a concentration of 30 mM in the recording solution with pH 5.0, except for esculin concentration of 5 mM with limitation of its solubility. The currents for each of the substrates were normalized to the currents for 30 mM sucrose.

2.6. Plasmid construction and plant transformation

The ORF region of *AcSUT1B* and *AcCBF1* were respectively amplified and inserted into binary vector pCMABIA1301 linearized with *BamH* I and *Xba* I under the control of the CaMV35S promoter. The over-expression vectors were introduced into *Agrobacterium tumefaciens* strain GV3101 and then used to transform wild type (WT) *Arabidopsis* Col-0 by the floral dip method. Independent transgenic lines were screened on MS media supplemented with hygromycin (25 mg/L) and further verified by genomic PCR using gene-specific primers. T3 homozygous transgenic lines were used for cold tolerance assessments and physiological index measurements.

2.7. Cold treatment of transgenic plants and analysis of physiological characteristics

To assess the cold tolerance of the transgenic lines, three-week-old T3 homozygous transgenic and WT seedlings were transferred to 4 °C growth chambers with same ambient conditions for 48 h and then were exposed to −4 °C for 6 h, and subsequent thawing at 4 °C for 12 h, after which they were returned to normal conditions for recovery. The plant survival rates and phenotypes were recorded. The chlorophyll fluorescence and multispectral imaging were captured at different time points using PlantExplorer PSII HS (PhenoVation Life Sciences, Wageningen, the Netherlands). The data of quantum efficiency of photosystem II (Fv/Fm), chlorophyll index (ChlIdx) and anthocyanin index (AriIdx) were generated by automated plant phenotyping platform and automatically analyzed by DATM software (PhenoVation B.V., Wageningen, the Netherlands). Images obtained from the phenotyping platform were used for illustration purposes. The rosette leaves were collected for the analysis of physiological indexes. The POD, SOD and CAT activities, soluble sugar and malondialdehyde (MDA) contents were determined as described in the kit manual (Nanjing Jiancheng Bioengineering Institute, China).

2.8. Transcriptome analysis of transgenic and WT Arabidopsis plants

For RNA-seq, four separate cDNA libraries were prepared: three-week-old WT seedlings treated with cold stress (cold, 24 h at 4 °C); untreated WT seedlings (normal); transgenic (*35S::AcSUT1B*) seedlings treated with cold stress (cold, 24 h at 4 °C), and untreated transgenic seedlings (normal). There were three replicates for each library. RNA extraction, library preparation, deep sequencing and data analysis were conducted at the Novogene Biotechnology Co., Ltd. (Beijing, China) using Illumina Hiseq 2000 platform. Differentially expressed genes between transgenic and WT plants were calculated using the cuffdiff program, filtering DEGs of significance (FDR < 0.05 and $|\log_2$ fold change$| > 1$). The RNA-seq raw data was submitted to the NCBI database under the accession number PRINA1175383.

2.9. Promoter isolation and cis-elements prediction

Genomic DNA was extracted from fresh pineapple leaves using the DNeasy plant Mini Kit (Qiagen, Germany). The promoter of *AcSUT1B* was isolated according to the corresponding sequences of the reference pineapple genome database by PCR amplification. The primer used for promoter isolation are listed in Table S1. After sequencing, the cis-elements in the *AcSUT1B* promoter were predicted using the PlantCARE (http://bioinformatics.psb.ugent.be/webtools/plantcare/html/) and PLACE (https://www.dna.affrc.go.jp/) database.

2.10. Identification and phylogenetic analyses of pineapple CBF gene family

Arabidopsis thaliana and *Oryza sativa* CBF proteins were acquired from TAIR (http://www.arabidopsis.org/) and Phytozome (https://phytozome.jgi.doe.gov/pz/portal.html) database, respectively. All *Arabidopsis* and rice *CBF* genes were used as queries to search for the protein database of pineapple using the BLAST method with an *E*-value threshold of $<1E^{-20}$. The CBF Pfam number (PF00847) was queried to search for pineapple CBF protein sequences using HMMER3.0 software. The pineapple CBF sequences were further authenticated based on the conserved domains using SMART (http://smart.emblheidelberg.de). The CBF proteins of *Hordeum vulgare*, *Zea mays* and *Medicago truncatula* were downloaded from NCBI database. The phylogenetic tree of the full-length amino-acid sequences of CBF proteins from pineapple and other

five plant species was constructed using the neighbor-joining (NJ) method of MEGA 7.0, with the following parameters: poisson model; pairwise deletion; and 1000 bootstrap replications. The accession numbers of the CBF proteins were listed in Table S2.

2.11. DAP-seq analysis

The DNA affinity purification sequencing (DAP-seq) was carried out according to the method by Bartlett et al. [46]. 'Shenwan' pineapple leaves were used to extract genomic DNA (gDNA). Yongji Biotechnology Co. Ltd. (Guangzhou, China) handled the purification and sequencing of the DNA samples. Eluted DNA was sequenced on an Illumina Navo-Seq6000 with two technical duplicates. DAP-seq reads were aligned to the reference *Ananas comosus* genome using Bowtie2. The conserved motifs in peaks were identified via MEME-CHIP. The target genes of AcCBF1 were defined as peaks located 2 kb upstream of ATG. The DAP-seq data was submitted to NCBI under the accession number PRJNA1180265.

2.12. Yeast one-hybrid assays

Yeast one-hybrid (Y1H) assays were conducted using a Matchmaker™ Gold Yeast One-Hybrid Library Screening System (Clontech, San Francisco, USA) to examine the interaction of AcCBF1 and the *AcSUT1B* promoter. The 386 bp sequence of the *AcSUT1B* promoter which contains a CRT/DRE cis element, was amplified and inserted into the *Kpn* I and *Sal* I sites of pAbAi vector to construct bait. The full-length coding sequence of *AcCBF1* was fused with the GAL4 activation domain (AD) in the pGADT7-AD vector to produce a prey vector (pGAD-AcCBF1). After the transformants were screened on SD/-Ura plates and the minimal inhibitory concentration of aureobasidin A (AbA) for the positive bait strains was measured, pGAD-AcCBF1 was transferred to yeast cells. A positive yeast strain was selected on SD/−Leu plates that included 300 ng/mL AbA and were cultured at 30 °C for 2–3 days. Positive yeast cells harboring pGADT7–53 and p53-AbAi were used as positive controls.

2.13. Dual-luciferase transient expression system

To verify the interaction between AcCBF1 and *AcSUT1B* promoter, the *AcSUT1B* promoter (1613 bp) was inserted into the *Kpn* I and *Nco* I sites of pGreenII0800-LUC vector as a reporter, while the ORF of *AcCBF1* was ligated into pBI121 to produce effector constructs. The effector and reporter constructs were subsequently transferred into *Agrobacterium tumefaciens* strain GV3101 (pGreenII series holding psoup plasmid), which were then coinfiltrated into tobacco leaves via agroinfiltration. After coculturing in an illuminated chamber for 2 days at 25 °C, a Dual-Luciferase Reporter Assay System (Promega, USA) was used to determine firefly luciferase (LUC) and Renilla luciferase (REN) activities according to the manufacturer's instructions. The analysis was performed using the Luminoskan™ Ascent Microplate Luminometer (Thermo Fisher Scientific, USA) with a 5 s delay and 15 s integration time. The binding activity was measured as a ratio of LUC to REN. At least six replicates were measured for each assay.

2.14. Electromobility shift assay assays

Specific primers were designed to ligate the full-length cDNA of *AcCBF1* into the pET-28a vector using *BamH* I and *Hin*d III sites (Table S1). AcCBF1-His fusion proteins were produced in *Escherichia coli* strain BL21 and purified using His purification columns (Beyotime, Shanghai, China). Probes were designed according to the locations of the CRT/DRE element. Competitor probes (cold probes) were unlabeled probes. The probe sequences can be found in Table S1. The EMSA reaction was carried out using the Light Shift Chemiluminescent EMSA Kit (Thermo Scientific, Waltham, MA, USA). DNA-protein complexes were fractionated on a non-denaturing 6 % polyacrylamide gel, transferred to a positive nylon membrane, and UV crosslinked. Complexes were detected using streptavidin-HRP conjugate with an Enhanced Chemiluminescence (ECL) Kit (Beyotime).

3. Results

3.1. Identification, cloning and protein characterization of the pineapple sucrose transporter genes

In a BlastP search using Rice SUT proteins as queries in the *Ananas comosus* genome database, four members of the SUT gene family were identified in the pineapple genome. Full length coding sequences for all four pineapple sucrose transporter genes were cloned with RT-PCR and named as *AcSUT1A, AcSUT1B, AcSUT2* and *AcSUT4*, according to their homologous genes in rice. These four *AcSUT* genes encoded 508 to 614 amino acids, and their theoretical isoelectric points (PI) ranged from 6.40 to 9.69. The molecular weight (NW) of AcSUT proteins was between 53.87 and 65.85 kD, while Instability Index (II) was between 32.60 and 41.48, among which AcSUT4 was unstable protein due to Instability Index was higher than 40. The aliphatic index in AcSUTs was 94.87–110.65, and Grand average of hydropathicity (GRAVY) was all >0, hence they were all hydrophobic proteins (Table S3). The amino acid sequence analysis revealed that there were 12 transmembrane domains in AcSUTs (Fig. S1), which is the typical feather of MFS family.

3.2. Phylogenetic analysis of the pineapple sucrose transporter genes

The phylogenetic analysis of AcSUTs and the SUT orthologs from perennial and herbaceous species was carried out. Previous studies indicated that the plant SUT proteins can be divided into five clades [8]. SUT3 clade and SUT5 clade represent the monocot-specific branches, while SUT1 clade was dicot-specific branch. In this study, the phylogenetic tree analysis indicated that AcSUT1A and AcSUT1B from the monocot pineapple belonged to the SUT3 clade. AcSUT2 and AcSUT4 fall into SUT2 clade and SUT4 clade, respectively (Fig. 1).

3.3. The gene expression pattern of AcSUTs

The transcript levels of *AcSUT* genes in 13 pineapple tissues, including bract, sepal, receptacle, ovary, ovule, stamen, style, petal, core, stem, leaf, root and callus were investigated by qRT-PCR. The expression level of four *AcSUT* genes could be detected in all tissues examined and different expression patterns among them were observed. The results showed that *AcSUT1A* was predominately expressed in leaf and flower tissues, while *AcSUT1B* was mainly expressed in core, stem, leaf, root and callus. Interestingly, *AcSUT2* was expressed in all the examined sink and source tissues. *AcSUT4* exhibited lower expression levels in style, root and callus tissues in comparison to other tissues (Fig. 2). Moreover, according to the previously published transcriptome data [47], we found that *AcSUT1A* and *AcSUT1B* exhibited diurnal cycling expressions in the leaf tip tissues (Fig. S2).

The expression patterns of *AcSUT* genes in response to different exogenous treatments, including cold, NaCl and ABA treatment, were also examined. For the cold treatment, both *AcSUT1A* and *AcSUT1B* were sharply induced, and the expression of *AcSUT1A* reached highest levels at 4 h after treatment, while the continuous increases of the expression of *AcSUT1B* was observed with the extension of the treatment time. The expressions of *AcSUT1B* were significantly induced while *AcSUT1A* was significantly repressed by the ABA treatments at several different timepoints. All four *AcSUT* genes were significantly upregulated with different expression levels by the NaCl treatment (Fig. S3).

3.4. Subcellular localization of AcSUTs

The subcellular localization of four pineapple sucrose transporter

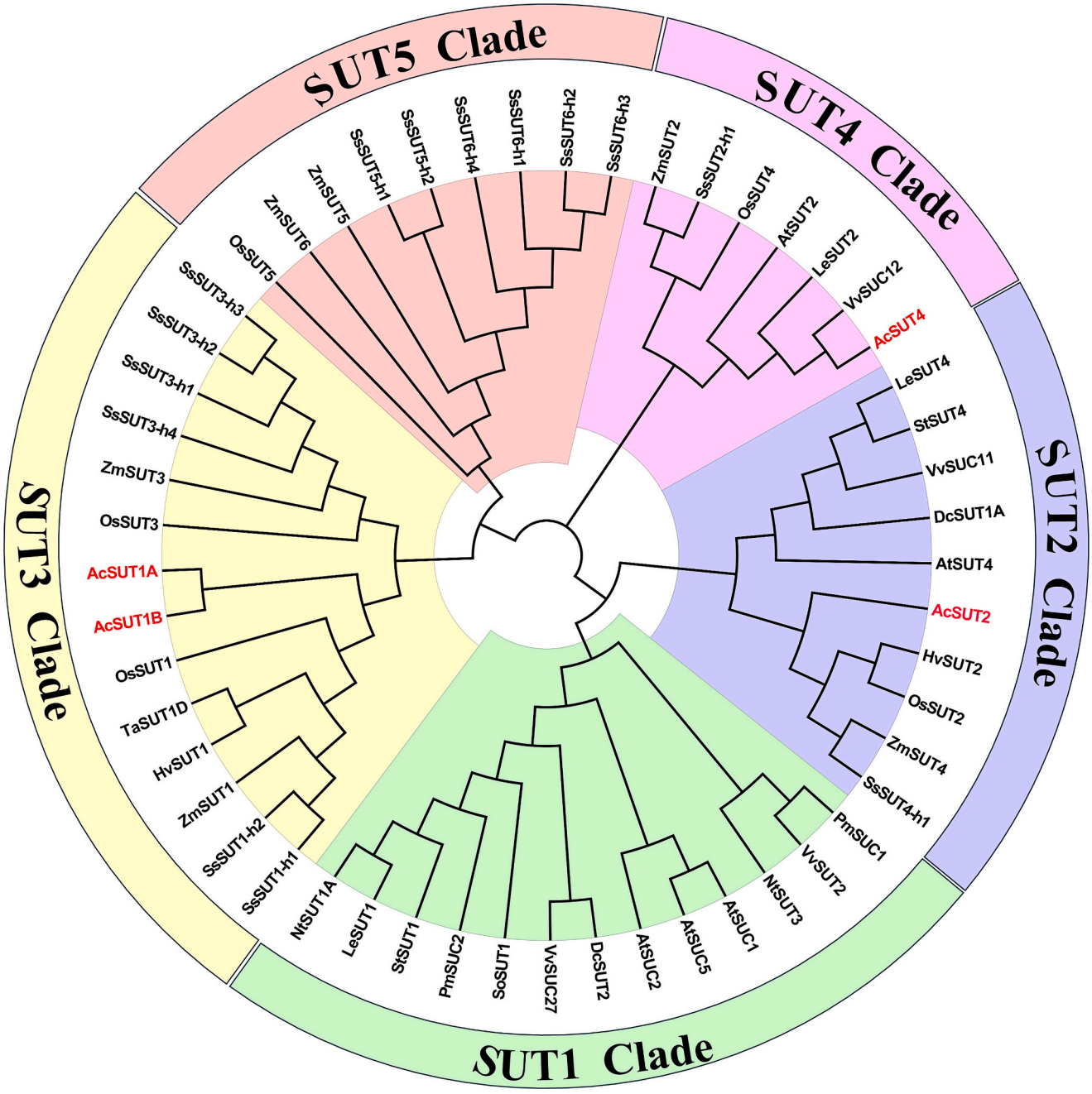

Fig. 1. The phylogenetic analysis of AcSUTs with protein sequences of sucrose transporters from other plant species. The unrooted tree was constructed with the NJ tree with 1000 bootstraps based on protein sequences. The SUT proteins were clustered into five clades named as SUT1-SUT5 clade. The accession numbers of the SUT proteins were listed in Table S3.

proteins were analyzed using transient expression in rice leaf protoplast. The green fluorescence signals generated by four AcSUTs-GFP fusion proteins were all overlapped with the plasma membrane localized marker (PM-mCherry) [48], confirming that four AcSUT proteins were all localized to the plasma membrane (Fig. 3).

3.5. Electrophysiological characterization of the pineapple sucrose transporters

In order to study their transport activity, each of the four pineapple SUTs was expressed in *Xenopus* oocytes and analyzed by TEVC. External application of sucrose induced inward currents in oocytes expressing *AcSUT1A* and *AcSUT1B*, whereas no currents were induced in oocytes expressing *AcSUT2* and *AcSUT4* (Fig. 4).

To examine the substrate affinity of AcSUT1A and AcSUT1B, kinetic analysis was performed using TEVC. At a membrane potential of −50 mV and extracellular pH of 5.0, 5.5 and 6.0, the sucrose-induced currents mediated by AcSUT1A and AcSUT1B were measured. By fitting the Michaelis–Menten equation to these data, the $K_{0.5}$ values for the two pineapple sucrose transporters were determined. The result showed that at three different extracellular pH, AcSUT1A had a lower $K_{0.5}$ value than that of AcSUT1B, indicating a higher affinity of AcSUT1A for sucrose (Fig. 5). AcSUT1A was less affected by the external pH level. The $K_{0.5}$ value of AcSUT1B was more pH dependent, with values of 0.99 mM at pH 5.5 and 3.08 mM at pH 6.0 (Fig. 5).

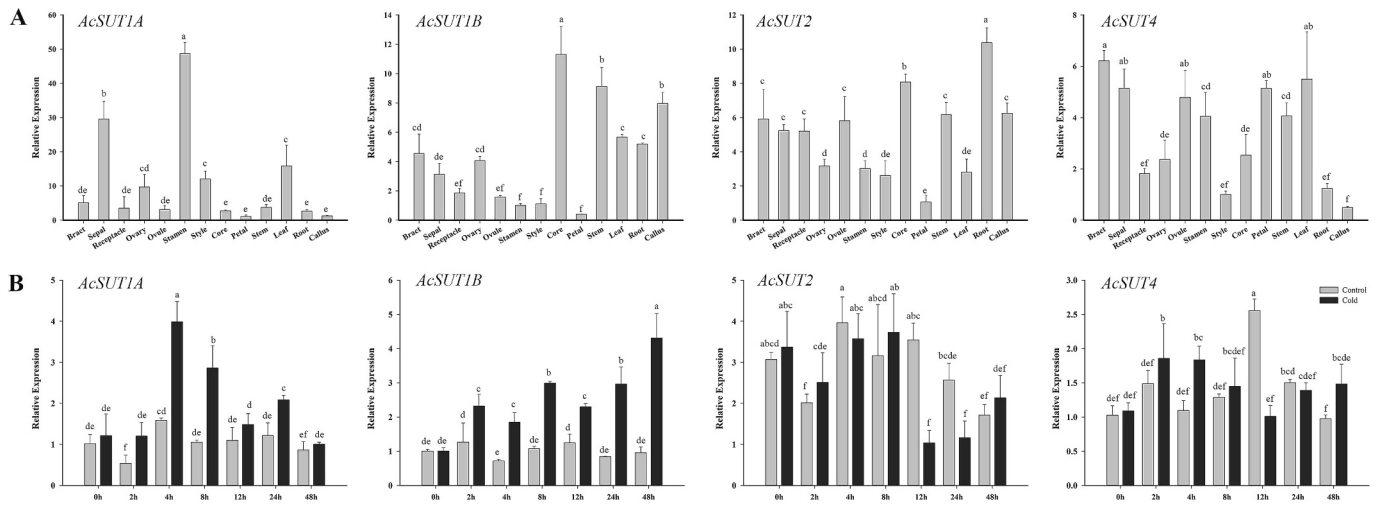

Fig. 2. The gene expression patterns of *AcSUT*s analyzed by qRT -PCR. The relative expression level of AcSUTs in different parts of the pineapple plants, tissue culture seedlings under cold (B), and callus tissues under ABA (C) and NaCl (D) treatment, respectively. Values were mean ± standard deviation of three biological replicates.

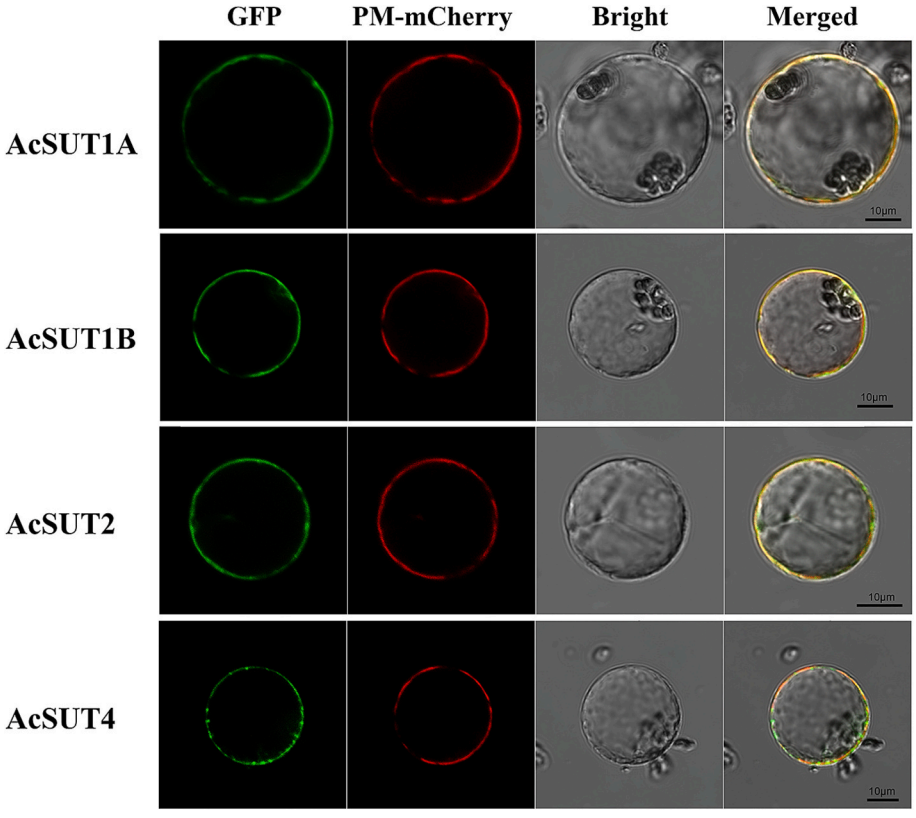

Fig. 3. The subcellular localization of the four AcSUTs in rice protoplasts. GFP and mCherry indicated the fluorescence signals of AcSUT-GFP and the plasma membrane marker PIP2-mCherry, respectively, and the merged images were shown. Bars =10 μm.

3.6. AcSUT1A and AcSUT1B have similar substrate specificity

A series of glucosides were tested as potential substrates for AcSUT1A and AcSUT1B. A range of six potential substrates was applied to *AcSUT1A* and *AcSUT1B*-expressing oocytes and the resulting currents were recorded at a membrane potential of −50 mV (Fig. 6). The data represented the substrate-dependent currents (background subtracted), normalized to the sucrose-dependent currents for each oocyte (at 30 mM sucrose). The two pineapple sucrose transporters exhibited similar substrate specificity patterns, and the significant currents were induced by four different compounds, including sucrose, maltose, salicin and esculin. In addition, they were more selective for sucrose over other substrates since the highest current was induced when feeding sucrose. However, no currents were observed in both *AcSUT1A* and *AcSUT1B*-expressing oocytes with trehalose and glucose. These results indicated that the two pineapple SUTs exhibited similar substrate specificity patterns as OsSUT1 and HvSUT1 [17,22], consistent with their close relationship in the phylogenetic tree.

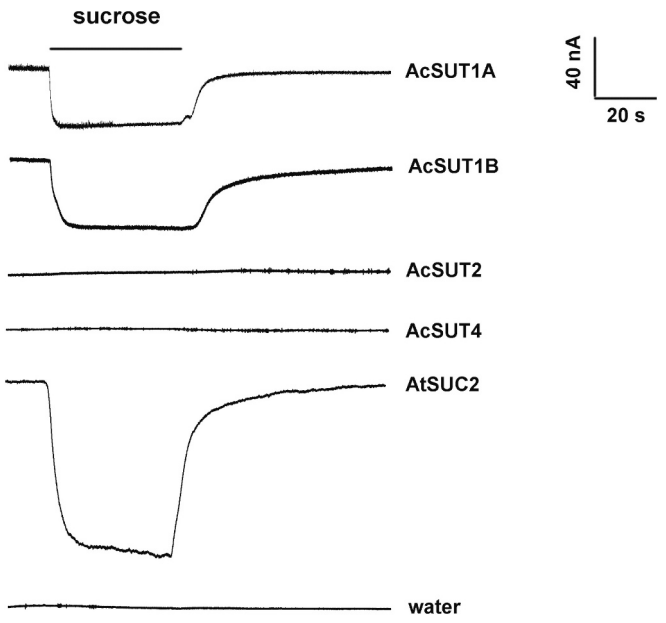

Fig. 4. Sucrose-induced current in the AcSUTs-expressing *Xenopus* oocytes. The oocytes were voltage clamp at −50 mV in the recording solution at pH 5.0 and currents were recorded. Each trace indicated the current induced by 30 mM sucrose. AtSUC2 cRNA injected oocytes were used as positive control, whereas water was used as negative control.

3.7. Overexpression of *AcSUT1B* enhances cold tolerance in Arabidopsis

To further investigate the biological function of *AcSUT1B*, transgenic *Arabidopsis* plants overexpressing *AcSUT1B* under control of the cauliflower mosaic virus (CaMV) 35S promoter were generated. Independent transgenic lines (T1 generation) were obtained based on hygromycin resistance selection and genomic PCR verification. Homozygous T3 lines were obtained on the basis of 3:1 segregation for hygromycin resistance. An increased transcript level of *AcSUT1B* was detected in three T3 homozygous *35S::AcSUT1B* transgenic lines (named 1B-1, 1B-3 and 1B-10) by RT-PCR (Fig. S4).

Under normal conditions, no significant difference in morphology was observed between *AcSUT1B*-overexpressing lines and WT plants. Considering the cold-inducible gene expression of *AcSUT1B*, we speculated that it might be involved in the plant cold tolerance. Under freezing treatment (−4 °C for 6 h) after cold acclimation (48 h at 4 °C) and recovery for 4 days in a normal ambient environment, the transgenic lines presented obviously less severe injury than the WT. Color and pseudo-color images showing the effect of the cold stress on several selected traits (color, Fv/Fm, ChlIdx, and AriIdx) are presented (Fig. 7A). The survival rates of the transgenic lines were significantly higher than those of the WT (Fig. S4). The Fv/Fm values of all tested plants decreased after cold treatment until 1 day after recovery, moreover, the extent of decrease was significantly lower in the transgenic lines. The Fv/Fm values of the transgenic lines were subsequently increased and significantly higher than that of WT plants at 4 days after recovery (Fig. 7B). The ChlIdx and AriIdx values of the WT plants were significantly lower than that in the transgenic lines at the recovery stage (Fig. 7C and D), reflecting the relatively higher chlorophyll and anthocyanin contents in transgenic lines after cold treatment.

Physiological indexes including soluble sugar, MDA contents, the POD and CAT enzyme activities were measured to evaluate the effects of cold stress on Arabidopsis plants. Under normal conditions (22 °C), soluble sugar and the MDA contents in *AcSUT1B*-overexpressing lines were similar to that in the WT plants. After cold treatment, both the soluble sugar and MDA contents were increased in transgenic lines and WT plants. The MDA contents in the transgenic lines were distinctly lower than that in WT plants, whereas the soluble sugar contents in transgenic lines were significantly higher than that in WT plants (Fig. 8A

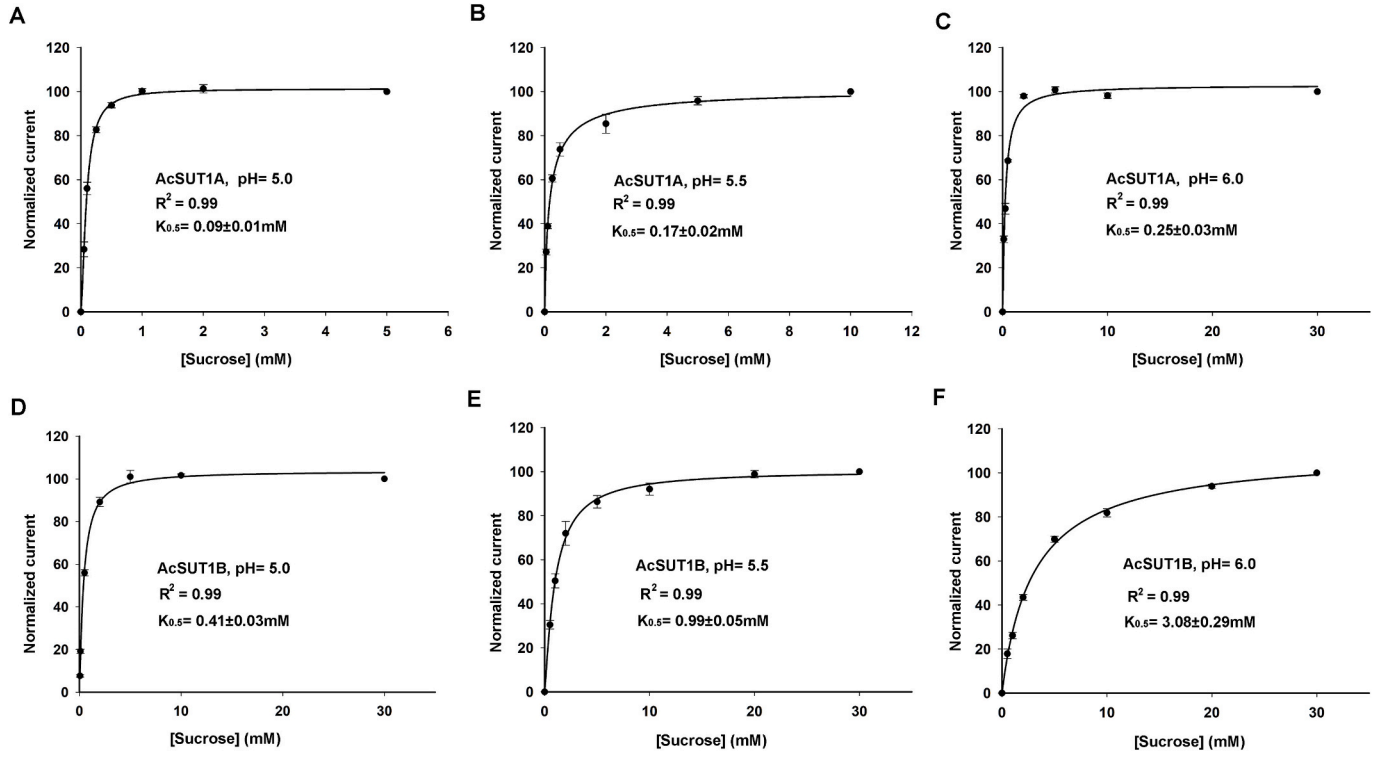

Fig. 5. Kinetic analysis of sucrose transport by AcSUT1A (A-C) and AcSUT1B (D—F). Sucrose-dependent currents were recorded under voltage-clamped conditions at a membrane potential of −50 mV. Currents were normalized to V_{max} and plotted against the substrate concentration. Substrates were applied in recording solution at pH 5.0, pH 5.5 and pH 6.0. Line indicated a fit of the Michaelis-Menten equation to the data, and error bars were SE with $n = 3$ oocytes.

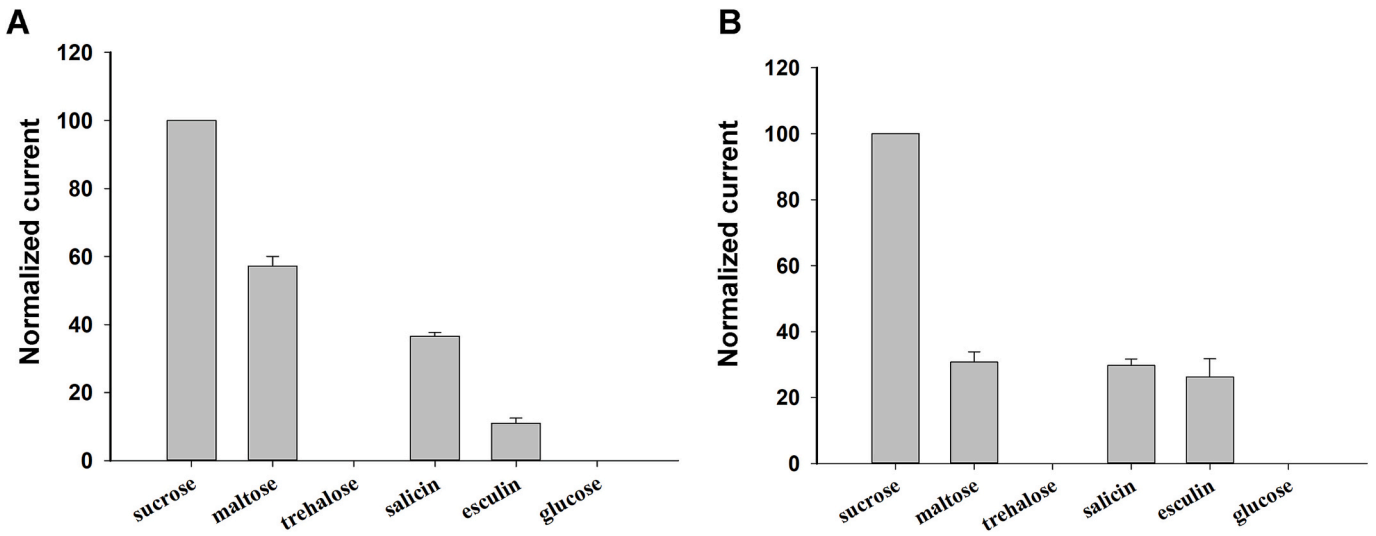

Fig. 6. Substrate specificity of AcSUT1A (A) and AcSUT1B (B). Substrate-dependent currents were at a membrane potential of −50 mV. Substrates were applied at a concentration of 30 mM in recording solution at pH 5.0. Currents were normalized to currents for 30 mM sucrose to eliminate the influence of expression level differences between oocytes.

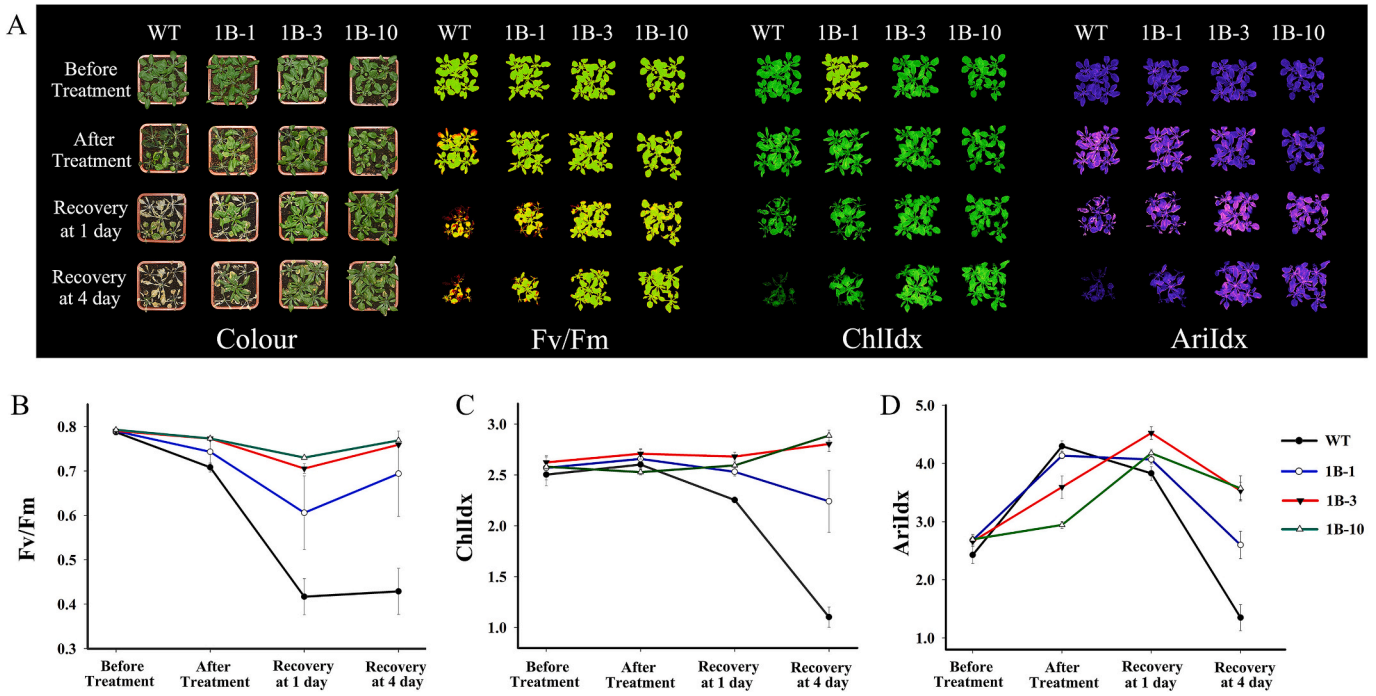

Fig. 7. Effect of *AcSUT1B* overexpression on cold tolerance in transgenic *Arabidopsis* plants. (A) Multispectral images of the transgenic and WT *Arabidopsis* at different stages during the cold stress treatment. The different images represent the *Arabidopsis* measuring the following traits: RGB Color image; Fv/Fm: quantum efficiency of photosystem II; ChlIdx: chlorophyll index; AriIdx: anthocyanin index. Change trends of Fv/Fm (B), ChlIdx(C) and AriIdx (D) in transgenic lines and WT plants under cold stress. The error bars indicate the SDs from three biological replicates.

and B). The POD enzyme activities in transgenic lines were distinctly higher than that in WT plants after cold treatments (Fig. 8C). For the CAT enzyme activities, distinctly higher activity values were continuously observed in transgenic lines than that in WT plants both before and after cold treatment (Fig. 8D).

To further evaluate the possible molecular mechanism of the cold response of the *AcSUT1B-OE* transgenic lines, transcriptome analysis was used to analyze the expression changes of cold-responsive genes in both the transgenic lines and WT plants under low-temperature stress (Table S4). The analysis results showed that 3605 cold-induced differential expressed genes (DEGs) were identified in transgenic plants (Fig. S5). Among them, a total of 224 DEGs, including several well-studied cold-responsive genes like *CBF2*, *ZAT12*, *ERD10*, *RD29A* and *SRC2*, were significantly upregulated in transgenic plants than WT under cold conditions (Table S5). Moreover, several ROS-responsive genes like *glutathione transferase* and *peroxidase*, *sugar transporter* genes, and *late embryogenesis abundant* genes were observed in the above DEGs list, providing a deep insight into the mechanism of the cold response affected by *AcSUT1B*.

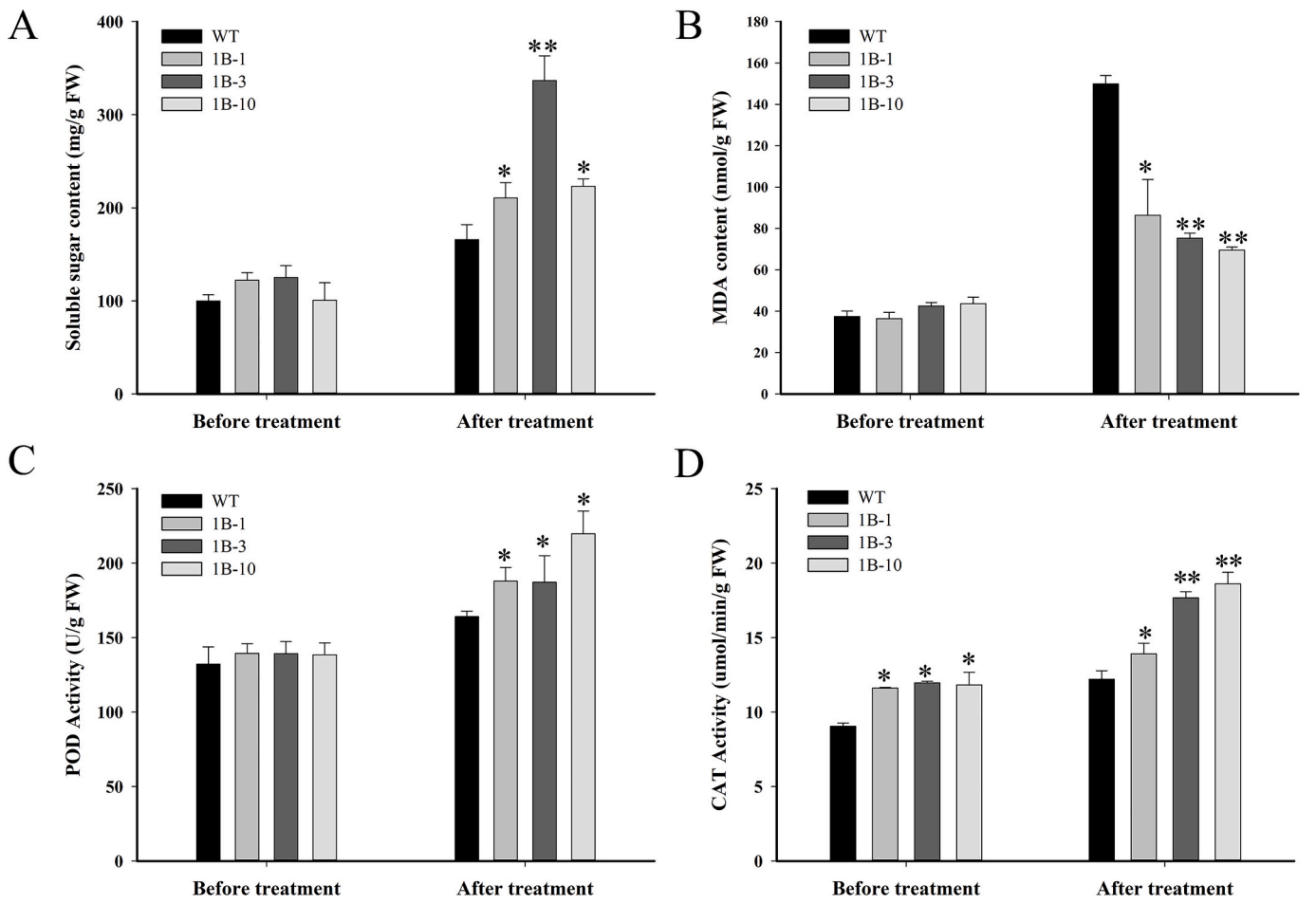

Fig. 8. Change trends of physiological parameters of *AcSUT1B* transgenic lines and WT plants under cold stress. The soluble sugar content (A), MDA content (B), POD (C) and CAT (D) activities were measured in transgenic lines and WT plants under cold stress. The error bars indicate the SDs from three biological replicates. The asterisk (*$P < 0.05$, ** $P < 0.01$, Student' s *t*-test) indicates significant differences compared with the WT plants.

3.8. Identification and functional analysis of AcCBF1 involved in cold tolerance

To better understand the inductivity of *AcSUT1B* expression, a 1.6 kb *AcSUT1B* promoter region lying upstream of the translational start site (ATG) was identified. Sequence analysis of *AcSUT1B* promoter using the PlantCARE and PLACE database revealed a few predicted abiotic stress response elements (Table S6). Among of them, the conserved C-repeat/dehydration-responsive element (CRT/DRE; G/ACCGAC) was found in the promoter regions of *AcSUT1B* genes, which was consistent with its cold-inducible expression pattern.

The interaction between the CRT/DRE elements with the CBF transcription factors has been identified in various plants [49]. The CBF sequences of *Arabidopsis* and rice were used as queries to search for the protein database of pineapple using the BlastP method, and a total of eight pineapple *CBF* genes were identified. Phylogenetic analysis of the *CBF* genes from pineapple and other five plant species revealed their orthologous relationships (Fig. S6A). The expression profiles of the pineapple *CBF* genes were examined according to the previously published transcriptome data [50,51], and only one gene, *Aco022517.1*, was expressed in all examined pineapple tissues and significantly induced by cold stress treatment (Fig. S6). Therefore, this gene was renamed *AcCBF1* and regarded as the candidate upstream regulatory gene of *AcSUT1B*.

The *35S::AcCBF1* lines in *Arabidopsis* were generated to gain further insight into the function of *AcCBF1* involved in cold tolerance. Increased expression levels of *AcCBF1* was detected in three T3 homozygous *35S::AcCBF1* transgenic lines (named OE-AcCBF1–1, OE-AcCBF1–2 and OE-AcCBF1–3). Under freezing treatment after cold acclimation and recovery for 6 days in a normal ambient environment, obviously less severe injuries were observed in the *35S::AcCBF1* transgenic lines compared with that in WT (Fig. 9A), and the transgenic lines exhibited significantly higher survival rates (Fig. 9B).

Physiological indexes including soluble sugar, POD and SOD enzyme activities were further measured. Both under normal and cold stress conditions, the content of soluble sugar and the activities of POD and SOD in transgenic *Arabidopsis* were significantly higher than those in WT. The increases in soluble sugar content and enzyme activities in transgenic *Arabidopsis* were greater than those of WT (Fig. 9). The results showed that the expression of the *AcCBF1* gene increased the cold tolerance of the transgenic *Arabidopsis*.

3.9. AcCBF1 promotes AcSUT1B expression by directly binding to its promoter

DNA affinity purification sequencing was performed to explore the potential target genes of AcCBF1 at the genome-wide level. A total of 34,526 notable peaks were identified in the genomic regions, with the majority located in either intergenic (47.9 %) or promoter (22.8 %) regions (Fig. S7). The highest scoring cis-acting element, CRT/DRE element (G/ACCGAC), was identified (Figs. 10A), and the AcCBF1 binding site were observed in the promoter region of *AcSUT1B* based on DAP-seq analysis.

The yeast one-hybrid assay was performed to verify whether

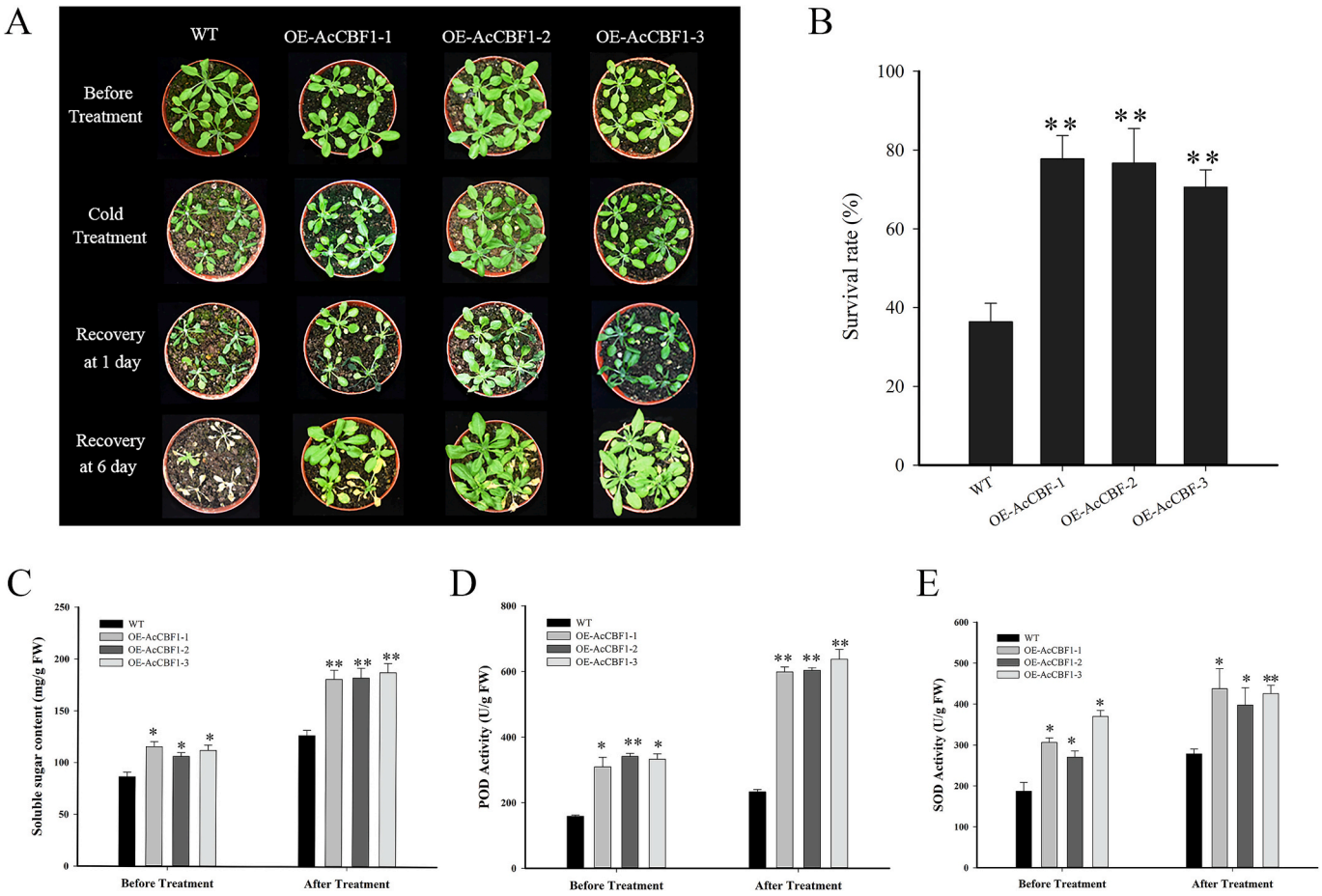

Fig. 9. Overexpression of *AcCBF1* in *Arabidopsis* enhanced the cold tolerance. Phenotype (A) and survival rates (B) of the transgenic lines and WT plants after cold stress treatment. Change trends of physiological parameters including soluble sugar content (C), POD (D) and SOD (E) activities of transgenic lines and WT plants under cold stress. The error bars indicate the SDs from three biological replicates. The asterisk (*$P < 0.05$, ** $P < 0.01$, Student' s *t*-test) indicates significant differences compared with the WT plants.

AcSUT1B promoter could be bound by AcCBF1. For this purpose, the promoter fragment of *AcSUT1B* was used to generate bait pAbAi-proAcSUT1B, while AcCBF1 fused to the GAL4 activation domain (AD) was used as prey (Fig. 10B). The result demonstrated that the cells co-transformed with prey and bait, along with the cells in the positive control group, exhibit normal growth in the SD/−Leu medium with 300 ng/mL AbA added. In contrast, no yeast cells in the negative control group were found to grow normally on the selective media (Fig. 10C).

To further determine whether *AcSUT1B* promoter could be activated by AcCBF1, a dual-luciferase reporter assay was performed on the tobacco leaves. The *AcSUT1B* promoter fragment was inserted into the pGreenII0800-LUC vector to generate a ProAcSUT1B-LUC reporter, and *35S::AcCBF1* and empty vector were used as effectors (Fig. 10D). As expected, co-transformation of the ProAcSUT1B-LUC reporter and the *35S::AcCBF1* effector significantly elevated the LUC/REN ratio as compared to the empty control (transformed with the reporter and the empty vector) (Fig. 10E). Therefore, the expression of *AcSUT1B* could be activated by AcCBF1.

Moreover, the electrophoretic mobility shift assay (EMSA) was conducted using the purified AcCBF1-His protein and labeled ProAcSUT1B probe. As shown in Fig. 10F, as single shifted band was observed in the presence of both AcCBF1-His protein and labeled ProAcSUT1B probe containing the CRT/DRE motif. The intensity of this band decreased with increasing concentrations of a cold competitor. When the CRT/DRE motif (ACCGAC) in the promoter of *AcSUT1B* was mutated (AAAAAA), the binding activity disappeared, indicating that this binding was specific. Therefore, the above results confirmed that AcCBF1 could promote the expression of *AcSUT1B* by directly binding to the CRT/DRE element in its promoter.

4. Discussion

Sucrose serves as the primary photosynthetic product in higher plants and functions as an energy source to support organ growth and environmental stress responses. It is transported from source tissues to storage sink tissues via sucrose transporters (SUTs), which are crucial for plant growth and stress tolerance [27,34]. Although SUTs have been identified in various plant species, research on SUTs in pineapple has been limited. In this study, four *SUT* genes in pineapple were identified, the gene expression pattern, subcellular localization and transport activities were systematically analyzed. Among of them, *AcSUT1B* was functional in *Xenopus* oocyte expression system and significantly induced by cold stresses, and therefore was selected for further analysis. Overexpression of *AcSUT1B* and its upstream regulatory gene *AcCBF1* both conferred enhanced cold tolerance in *Arabidopsis*. Further assays indicated that AcCBF1 could activate the expression of *AcSUT1B* by directly binding to the CRT/DRE cis-element in its promoter region. Based on these findings, the potential functions and regulatory mechanisms of *AcSUT1B* in pineapple under cold stress will be discussed.

4.1. AcSUTs were localized to plasma membrane and functional sucrose transporter

In general, there are two primary pathways for the transport of

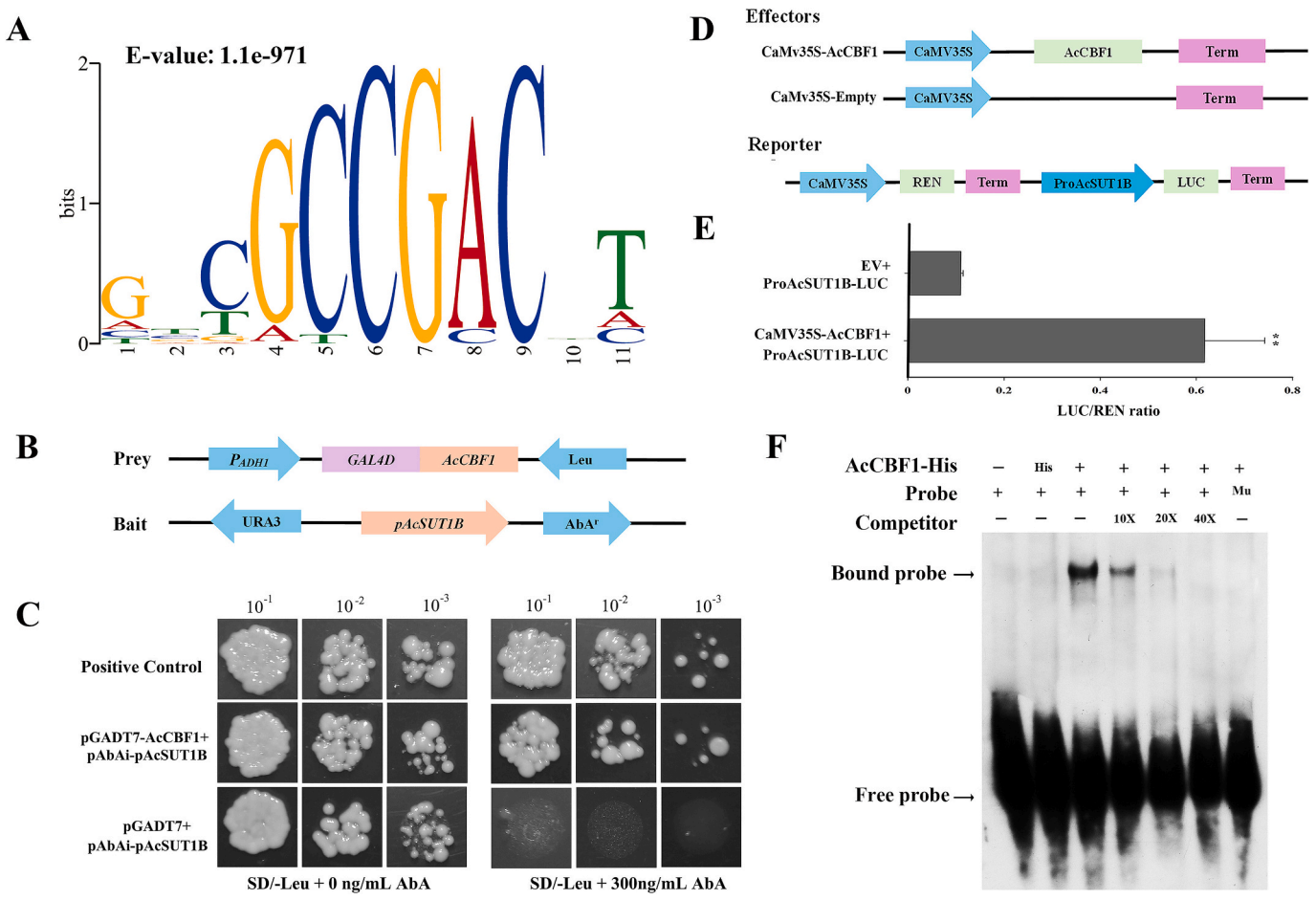

Fig. 10. AcCBF1 binds to the promoter of *AcSUT1B*. (A) The identified DNA-binding motif of AcCBF1 protein by DAP-seq. (B)Schematic structures of the yeast one hybrid prey (pGADT7-AcCBF1) and bait (pABAi-ProAcSUT1B) vector. (C) Growth of yeast cells transformed with the prey and bait plasmid on SD-Leu supplemented with or without 300 ng/mL AbA. (D) Diagrams of effector and reporter constructs in dual luciferase assays. (E) Dual luciferase assays using 35S-AcCBF1 and 35S-empty as the effectors and ProAcSUT1B-LUC as the reporters. Significant differences between means were determined using Student's *t*-tests (**$P < 0.01$). (F) EMSAs showing that AcCBF1 binds to the CRT/DRE motif of the *AcSUT1B* promoter. Unlabeled probes were used as cold competitors, 10×, 20×, and 40× indicate the fold excess of cold competitors relative to that of the labeled probe. The labeled mutant probe (Mu) was used to confirm the binding specificity of the CRT/DRE motif to AcCBF1. '+' and '–' indicate the presence or absence, respectively, of proteins and probes in the loading mixture. His alone was used as negative control of the binding.

sucrose from source tissues to sink organs: one is symplastic loading, in which sucrose moves from cell to cell via plasmodesmata, and the other is apoplastic loading, where sucrose is transported over long distances by sucrose transporters through the phloem, a specific component of the vascular system [52–54]. Consequently, sucrose transporters (SUTs) are predominantly localized to the plasma membrane in the apoplastic pathway. Numerous studies have demonstrated that members of the SUT1 clade were localized on the plasma membrane of sieve elements (SE), companion cells (CC), or the SE-CC complex [55–57]. Likewise, SUT2 members were targeted on SE plasma membrane [58,59]. For the monocot-specific clade, members of the SUT3 clade, including OsSUT1 [29], ZmSUT1 [60], and HvSUT1 [61], have been reported to localize to the plasma membrane. In our investigation, both AcSUT1A and AcSUT1B, which are part of the SUT3 clade, and AcSUT2 from SUT2 clade, were localized to the plasma membrane (Fig. 3), indicating a conserved localization pattern with other members of the SUT2 and SUT3 clades. Accumulating evidence has shown that proteins in SUT4 clade were plasma membrane- or/and tonoplast-localized. Interestingly, SUT4 proteins in several species were found to be dual target to both plasma membrane and tonoplast as demonstrated by fluorescence protein-fusion analyses, such as LjSUT4 from *Lotus japonicas* [62], AtSUC4 from *Arabidopsis* [53,63], and GeSUT4 in *Gastrodia elata* [64]. In our study, AcSUT4 was identified as exclusively localized to the plasma membrane. However, variations in localization may arise due to differences in experimental methodologies. For instance, AtSUC4 was localized to the plasma membrane when analyzed using a stable transformation system with the AtSUC4-GFP construct. In contrast, it was localized to the vacuole when assessed via a protoplast transient expression assay and was even reported to be located in the chloroplast envelope in a proteomic study [53,63,65]. Therefore, additional work will be required to determine whether AcSUT4 localize to the tonoplast or other organelle.

Sucrose transporters play a crucial role in the phloem-mediated long-distance transport of sugars in plants. They were classified into five different clades (SUT1-SUT5), and exhibit diverse substrate affinity, which contributed to their distinct physiological functions in plants. SUT1 is a unique SUT in dicotyledons, functioning as a HALC sucrose carrier. An illustrative example is AtSUC2, which exhibited a Km value of 1.44 mM at pH 5.0 [19]. Members in SUT1 subfamily play a pivotal role in collecting low concentrations of extracellular sucrose from vascular tissues during phloem loading and long-distance transportation [10,66]. In contrast, some members of the SUT2 family exhibited low rates and affinities for sucrose transport (Km = 11.7 mM for AtSUT2), whereas others, such as LeSUT2 and StSUT2, were incapable of transporting sucrose when complemented into the yeast mutant SUSY7/ura3 [58]. SUT2 clade was supposed to serve as sucrose sensors within sieve

elements [67]. For the monocot specific SUT3 clade, HvSUT1 from barley were expressed in yeast and Km values for sucrose transport of 3.8 mM were reported [22], while OsSUT1 showed sucrose-dependent inward currents in oocytes with Km value of 7.5 mM at pH 5.6 [17], suggesting the similar sucrose affinity of these two SUTs. In our study, transport activity of four SUTs from pineapple was analyzed by expression in *Xenopus* oocytes and electrophysiology. The results showed that both AcSUT1A and AcSUT1B, two members in SUT3 clade, exhibited sucrose transport activity with 0.17 mM and 0.99 mM at pH 5.5 (Fig. 5), respectively, suggesting higher sucrose affinity than OsSUT1 and HvSUT1. According to Km value, AcSUT1A and AcSUT1B were defined as HALC protein, which was probably responsible for phloem loading in pineapple, similar with SUT1 in dicots. Expression of *AcSUT2* and *AcSUT4* in *Xenopus* oocytes did not show sucrose transport activity (Fig. 4). In rice, OsSUT3 was to be functional in yeast since it has been previously reported to allow the yeast strain SuSy7 to grow on sucrose [11]. But no inward currents were induced in oocytes expressing OsSUT3 by external application of sucrose [17], indicating the divergence of SUT expression between yeast and oocyte. Perhaps the *AcSUT2* and *AcSUT4* cDNA sequence should be optimized for expression in oocytes in the future experiment.

The substrate specificity of SUT1 members investigated thus far is quite consistent, which a wide range of natural and synthetic sugars could be transported. In SUT3 clade, both OsSUT1 and HvSUT1 transported sucrose, maltose, salicin, helicin, α-phenylglucoside and α-para-nitrophenyl-D-glucoside [17,22], appearing more selective than previous reported SUT1 members AtSUC2 and AtSUC9 [19,20]. In our present study, sucrose, maltose, salicin and esculin could be transported by both AcSUT1A and AcSUT1B, showing similar substrate specificity with OsSUT1 and HvSUT1. These results suggested that similar substrate specificity was found within members in the same SUT clade.

4.2. *AcCBF1-AcSUT1B module regulated cold tolerance*

Sucrose metabolism is crucial for plant development and stress responses, primarily through the production of various sugars that serve as energy sources for growth and as signaling molecules to modulate gene expression in coordination with hormonal pathways [68]. This process involves the generation of key signaling compounds such as sucrose, glucose, and trehalose-6-phosphate, or may involve the metabolic process itself as a signaling mechanism. Consequently, the regulation of sucrose transport, synthesis, and degradation is essential for controlling plant growth and adaptation to environment change. Accumulating studies have suggested that SUT expression pattern is closely related with its physiological functions. A tissue-specific expression analysis demonstrated that *AcSUT1A* was highly expressed in leaf and different parts of flower (Fig. 2). Based on the high affinity for sucrose and high expression in leaf, we speculated that *AcSUT1A* was crucial for phloem loading in leaf of pineapple. *AcSUT1B* was also expressed high in the source leaf and the sink tissues of ovary, stem, root and callus, indicating its important roles in both sucrose loading and unloading. Under different exogenous treatments, including cold, ABA and salt, we found that the four *AcSUTs* exhibited distinct expression features, suggesting their various responses to abiotic conditions. Most notably, *AcSUT1B* were significantly induced by all three treatments, which might play an important role in participating in the abiotic stress responses in pineapple.

Sugar transport via the phloem can be influenced by various environmental factors that modify source-sink relationships. Temperature is recognized as a significant determinant of the phloem-loading mode in plants [31]. Low temperatures can influence phloem sugar transport through different ways, involving distinct cell types such as intermediary cells, parenchyma transfer cells, and sieve elements. Increasing reports showed that SUT expression was induced under low temperature condition [5,33,37]. In this study, the expression of *AcSUT1B* was also significantly increased under cold treatment (Fig. 2). Furthermore, the *AcSUT1B*-overexpressing *Arabidopsis* lines exhibited improved tolerance to cold stress, which was revealed by the significantly reduced MDA levels and higher POD and CAT activities (Fig. 7). Accordingly, these results suggested that the overexpression of *AcSUT1B* contributed to the improved cold tolerance of plants.

It has been found that high levels of soluble sugars, which function as osmoprotectants, enhance plant tolerance to cold stress [69]. The previous studies showed that overexpression of the sugar transporter genes affected the distribution of sugars and improved the cold tolerance of plants. The sucrose level increased in source leaf during chilling treatment in rice [70]. In cucumber (*Cucumis sativus* L.), exposure to cold temperatures resulted in a notable increase in the accumulation of soluble sugar in leaves, and overexpression of a sugar transporter CsSWEET2 improved glucose and fructose contents and showed higher resistance to cold stress [71,72]. Similarly in peach, heterologous expression of *PpSUT2* increased soluble sugar contents and thus enhanced cold stress tolerance [37]. The *Arabidopsis* plastidic sugar transporter (*pSuT*) mutant exhibited impaired cold tolerance that was associated with sugar deficiency [73]. In our present study, *AcSUT1B*-overexpressing plants, whose soluble sugar content was significantly higher than the WT plants, exhibited improved tolerance to cold stress (Fig. 8). The soluble sugars also function as signaling molecules regulating the expression of cold-responsive genes during cold stress [74], the upregulation of the cold-induced DEGs in *AcSUT1B*-overexpressing plants in this study might be associated with their increased soluble sugar contents. It thereby makes a conclusion of positive correlation between soluble sugar accumulation and tolerance to cold stress.

Previous studies have revealed that *CBF* genes played crucial roles in plant responses to cold stress and acted as a hub linking the downstream cold response with upstream signal transmission [75]. The orthologues of *CBF* have been isolated from many different plant species, and heterologous expressions of these *CBF* genes were usually shown to intensify the cold tolerance in transgenic plants [76]. In this study, eight *CBF* orthologous genes were identified in the pineapple genome and the only cold-induced CBF gene, *AcCBF1*, was selected for further heterologous expression and functional identification in *Arabidopsis*. The significantly increased survival rate, soluble sugar content, the POD and SOD activities under cold stress in *AcCBF1*-overexpressing *Arabidopsis* plants further confirmed the roles of *AcCBF1* in regulating cold tolerance.

The *CBF* genes could directly bind CRT/DRE cis-element (G/ACCGAC) in the promoters of cold-responsive (COR) genes that are essential for plant adaptation to low temperatures [49]. Different types of COR genes, including *low temperature induced* (LTI), *responsive to desiccation* (*RD*), *early dehydration-inducible* (*ERD*), and those encoding antioxidant and metabolic enzymes like superoxide dismutase (SOD), peroxidase (POD), and arginine decarboxylase (ADC) have already been reported in previous studies [49]. In this study, a series of potential downstream target genes containing CRT/DRE cis-elements in their promoters were identified by the DAP-seq analysis of AcCBF1, which was helpful for better understanding its regulatory mechanism in response to cold stress in pineapple.

It was found that overexpression of the *CBF* genes is often accompanied by higher levels of sugar content, and the effects of *CBF* genes on sugar levels could be mediated by directly regulating the genes involved in sugar metabolism and transport. The *Sucrose Synthase 1* (*SUS1*) and *Sugar Transporter 1* (*STP1*) genes were detected as targets of *Arabidopsis CBF* genes in ChIP-seq assays [49]. MdCBF1/2 directly activated the expression of the *Tonoplast Sugar Transporter* genes *MdTST1/2* and regulated the sugar accumulation in response to low temperatures [77]. PpCBF6 could bind the promoter of the *vacuolar invertase* gene *PpVIN2* and regulate sucrose metabolism and chilling injury in peach fruit [78]. AaCBF4 directly regulated the expression of *β-amylase* gene *AaBAM3.1* in kiwifruit [79]. *PtrBAM1* is a member of CBF regulon and plays an important role in cold tolerance by modulating the levels of soluble sugars [80].

Several previous studies have shown that the sucrose transporter

genes were directly regulated by different transcription factors. A DNA binding with one finger (DOF) transcription factors, OsDOF11, was capable of binding the promoter regions of OsSUT1, OsSWEET11, and OsSWEET14, which were responsible for sucrose transport in rice growth and development [81]. The ABA-responsive transcription factor MdAREB2 directly activates the expression of the sucrose transporter genes *MdSUT2* to promote soluble sugar accumulation in apple [32]. In this study, the pineapple sucrose transporter gene *AcSUT1B* was identified as target of the cold-induced *AcCBF1* genes. As far as we know, studies about the direct regulatory relationship between *CBF* and *SUT* genes have not been reported before. The CRT/DRE cis-element was found in the *AcSUT1B* promoter, and the interaction between AcCBF1 and *AcSUT1B* promoter was systematically verified by DAP-seq, Y1H, LUC and EMSA assays. Combining with the alteration of soluble sugar accumulation and improved cold tolerance in the transgenic lines of *AcSUT1B* and *AcCBF1*, it is speculated that *AcCBF1-AcSUT1B* module plays a significant role in participating cold response by alteration of soluble sugar accumulation.

Temperature is one of the most important environmental factors determining the distribution and production of pineapple [82]. The low-temperature injury during the winter period could affect the yield and quality of pineapple, especially in cool subtropical cultivation regions [42]. The composition and proportion of sugars in pineapple fruit that harvested in winter were different from that harvested in summer [41,42]. Therefore, we further inferred that the cold-induced *AcCBF1-AcSUT1B* module might be involved in the sugars transport and distribution of pineapple during low temperature conditions.

5. Conclusion

In summary, four sucrose transporters have been identified at genome-wide level in pineapple, and their sequence features, phylogenetic relationship, expression pattern, subcellular localization and transport activity were comprehensively investigated. All four AcSUTs were localized to plasma membrane. Transport activity assay by two-electrode voltage clamp of *Xenopus* oocytes showed that AcSUT1A and AcSUT1B displayed high affinity sucrose transport activity. The cold-induced *AcSUT1B* and *AcCBF1* genes played vital roles in increasing cold tolerance in *Arabidopsis*. The expression of *AcSUT1B* could be activated by AcCBF1 through directly binding to the CRT/DRE cis-element in its promoter region. The identification of the A*cCBF1-AcSUT1B* module in pineapple thus provides new insights into the regulatory mechanism of cold response in plant.

Supplementary data to this article can be found online at https://doi.org/10.1016/j.ijbiomac.2024.137952.

CRediT authorship contribution statement

Jianmei Long: Writing – original draft, Methodology, Investigation, Funding acquisition, Formal analysis, Conceptualization. **Huimin Zhou:** Software, Methodology, Investigation, Formal analysis. **Haixin Huang:** Methodology, Investigation, Formal analysis. **Yufei Xiao:** Software, Methodology, Investigation. **Jiandong Luo:** Validation, Software, Methodology. **Yue Pu:** Investigation, Formal analysis. **Zihong Liu:** Methodology, Investigation. **Mengqing Qiu:** Investigation, Formal analysis. **Xinxin Lu:** Software, Methodology. **Yehua He:** Validation, Supervision. **Chaoyang Liu:** Writing – review & editing, Funding acquisition, Conceptualization.

Declaration of competing interest

The authors declare that they have no known competing financial interests or personal relationships that could have appeared to influence the work reported in this paper.

Acknowledgement

We appreciated Richard Hume from University of Michigan providing the voltage clamp system to detect the transport activity of AcSUTs, and Prof. John M. Ward from University of Minnesota for kindly providing the plasmid pOO2-AtSUC2. This work was financially supported by the Basic and Applied Basic Research Foundation of Guangdong Province (2022A1515010463, 2023A1515030250, 2021A1515010816) and National Natural Science Foundation of China (31800560).

Data availability

Data will be made available on request. The RNA-seq raw data was submitted to the NCBI under the accession number PRINA1175383. The DAP-seq raw data was submitted to NCBI under the accession number PRJNA1180265.

References

[1] G.N. Scofield, N. Aoki, T. Hirose, M. Takano, C.L.D. Jenkins, R.T. Furbank, The role of the sucrose transporter, OsSUT1, in germination and early seedling growth and development of rice plants, J. Exp. Bot. 58 (3) (2007) 483–495.
[2] R. Lemoine, Sucrose transporters in plants: update on function and structure, BBA-Biomembranes 1465 (1–2) (2000) 246–262.
[3] F. Rolland, E. Baena-Gonzalez, J. Sheen, Sugar sensing and signaling in plants: conserved and novel mechanisms, Annu. Rev. Plant Biol. 57 (1) (2006) 675–709.
[4] S. Lalonde, D. Wipf, W.B. Frommer, Transport mechanisms for organic forms of carbon and nitrogen between source and sink, Annu. Rev. Plant Biol. 55 (1) (2004) 341–372.
[5] W. Li, K. Sun, Z. Ren, C. Song, X. Pei, Y. Liu, Z. Wang, K. He, F. Zhang, X. Zhou, X. Ma, D. Yang, Molecular evolution and stress and phytohormone responsiveness of SUT genes in *Gossypium hirsutum*, Front. Genet. 9 (2018).
[6] Y. Zhou, H. Qu, K.E. Dibley, C.E. Offler, J.W. Patrick, A suite of sucrose transporters expressed in coats of developing legume seeds includes novel pH-independent facilitators, Plant J. 49 (4) (2007) 750–764.
[7] K.A. Leach, T.M. Tran, T.L. Slewinski, R.B. Meeley, D.M. Braun, *Sucrose transporter2* contributes to maize growth, development, and crop yield, J. Integr. Plant Biol. 59 (6) (2017) 390–408.
[8] C. Kühn, C.P.L. Grof, Sucrose transporters of higher plants, Curr. Opin. Plant Biol. 13 (3) (2010) 287–297.
[9] J.W. Riesmeier, L. Willmitzer, W.B. Frommer, Isolation and characterization of a sucrose carrier cDNA from spinach by functional expression in yeast, EMBO J. 11 (13) (1992) 4705–4713.
[10] A. Weise, L. Barker, C. Kühn, S. Lalonde, H. Buschmann, W.B. Frommer, J.M. Ward, A new subfamily of sucrose transporters, SUT4, with low affinity/high capacity localized in enucleate sieve elements of plants, Plant Cell 12 (8) (2000) 1345–1355.
[11] N. Aoki, T. Hirose, G.N. Scofield, P.R. Whitfeld, R.T. Furbank, The sucrose transporter gene family in rice, Plant Cell Physiol. 44 (3) (2003) 223–232.
[12] S. Wang, J. Yang, X. Xie, F. Li, M. Wu, F. Lin, Z. Wang, C. Willenborg, Genome-wide identification, phylogeny, and expression profile of the sucrose transporter multigene family in tobacco, Can. J. Plant Sci. 99 (3) (2019) 312–323.
[13] F. Sun, X. Dong, S. Li, H. Sha, W. Gao, X. Bai, L. Zhang, H. Yang, Genome-wide identification and expression analysis of SUT gene family members in sugar beet (*Beta vulgaris* L.), Gene 870 (2023) 147422.
[14] R.S. Payyavula, K.H.C. Tay, C.J. Tsai, S.A. Harding, The sucrose transporter family in Populus: the importance of a tonoplast PtaSUT4 to biomass and carbon partitioning, Plant J. 65 (5) (2011) 757–770.
[15] F. Li, B. Wu, X. Qin, L. Yan, C. Hao, L. Tan, J. Lai, Molecular cloning and expression analysis of the sucrose transporter gene family from *Theobroma cacao* L, Gene 546 (2) (2014) 336–341.
[16] Q.M. Zheng, Z. Tang, Q. Xu, X.X. Deng, Isolation, phylogenetic relationship and expression profiling of sugar transporter genes in sweet orange (*Citrus sinensis*), Plant Cell Tiss. Org. 119 (3) (2014) 609–624.
[17] Y. Sun, A. Reinders, K.R. LaFleur, T. Mori, J.M. Ward, Transport activity of rice sucrose transporters OsSUT1 and OsSUT5, Plant Cell Physiol. 51 (1) (2010) 114–122.
[18] S. Cao, Y. Liu, G. Wang, Protocol to identify ligands of odorant receptors using two-electrode voltage clamp combined with the *Xenopus* oocytes heterologous expression system, STAR Protocols 3 (2) (2022) 101249.
[19] D. Chandran, A. Reinders, J.M. Ward, Substrate specificity of the *Arabidopsis thaliana* sucrose transporter AtSUC2, J. Biol. Chem. 278 (45) (2003) 44320–44325.
[20] A.B. Sivitz, A. Reinders, M.E. Johnson, A.D. Krentz, C.P.L. Grof, J.M. Perroux, J. M. Ward, Arabidopsis sucrose transporter AtSUC9. High-affinity transport activity, intragenic control of expression, and early flowering mutant phenotype, Plant Physiol. 143 (1) (2007) 188–198.
[21] J.J. Zhou, F. Theodoulou, N. Sauer, D. Sanders, A. Miller, A kinetic model with ordered cytoplasmic dissociation for SUC1, an Arabidopsis H^+/sucrose

cotransporter expressed in *Xenopus* oocytes, J. Membrane Biol. 159 (1997) 113–125.
[22] A.B. Sivitz, A. Reinders, J.M. Ward, Analysis of the transport activity of barley sucrose transporter HvSUT1, Plant Cell Physiol. 46 (10) (2005) 1666–1673.
[23] W. Schulze, A. Weise, W.B. Frommer, J.M. Ward, Function of the cytosolic N-terminus of sucrose transporter AtSUT2 in substrate affinity, FEBS Lett. 485 (2–3) (2000) 189–194.
[24] A. Mahboubi, C. Ratke, A. Gorzsas, M. Kumar, E.J. Mellerowicz, T. Niittyla, Aspen SUCROSE TRANSPORTER3 allocates carbon into wood fibers, Plant Physiol. 163 (4) (2013) 1729–1740.
[25] Y. Li, L.L. Li, R.C. Fan, C.C. Peng, H.L. Sun, S.Y. Zhu, X.F. Wang, L.Y. Zhang, D. P. Zhang, Arabidopsis sucrose transporter SUT4 interacts with cytochrome b5-2 to regulate seed germination in response to sucrose and glucose, Mol. Plant 5 (5) (2012) 1029–1041.
[26] I.A. Chincinska, J. Liesche, U. Krügel, J. Michalska, P. Geigenberger, B. Grimm, C. Kühn, Sucrose transporter StSUT4 from potato affects flowering, tuberization, and shade avoidance response, Plant Physiol. 146 (2) (2008) 323–324.
[27] A. Hackel, N. Schauer, F. Carrari, A.R. Fernie, B. Grimm, C. Kühn, Sucrose transporter LeSUT1 and LeSUT2 inhibition affects tomato fruit development in different ways, Plant J. 45 (2) (2006) 180–192.
[28] T. Hirose, Z. Zhang, A. Miyao, H. Hirochika, R. Ohsugi, T. Terao, Disruption of a gene for rice sucrose transporter, OsSUT1, impairs pollen function but pollen maturation is unaffected, J. Exp. Bot. 61 (13) (2010) 3639–3646.
[29] X. Wang, X. Liu, Z. Hu, S. Bao, H. Xia, B. Feng, L. Ma, G. Zhao, D. Zhang, Y. Hu, Essentiality for rice fertility and alternative splicing of OsSUT1, Plant Sci. 314 (2022) 111065.
[30] A.B. Sivitz, A. Reinders, J.M. Ward, Arabidopsis sucrose transporter AtSUC1 is important for pollen germination and sucrose-induced anthocyanin accumulation, Plant Physiol. 147 (1) (2008) 92–100.
[31] R. Lemoine, S.L. Camera, R. Atanassova, F. Dédaldéchamp, T. Allario, N. Pourtau, J.-L. Bonnemain, M. Laloi, P. Coutos-Thévenot, L. Maurousset, M. Faucher, C. Girousse, P. Lemonnier, J. Parrilla, M. Durand, Source-to-sink transport of sugar and regulation by environmental factors, Front. Plant Sci. 4 (2013) 272.
[32] Q.J. Ma, M.H. Sun, J. Lu, Y.J. Liu, D.G. Hu, Y.J. Hao, Transcription factor AREB2 is involved in soluble sugar accumulation by activating sugar transporter and amylase genes, Plant Physiol. 174 (4) (2017) 2348–2362.
[33] X. Gong, M. Liu, L. Zhang, Y. Ruan, R. Ding, Y. Ji, N. Zhang, S. Zhang, J. Farmer, C. Wang, Arabidopsis AtSUC2 and AtSUC4, encoding sucrose transporters, are required for abiotic stress tolerance in an ABA-dependent pathway, Physiol. Plant. 153 (1) (2014) 119–136.
[34] D. Wang, H. Liu, H. Wang, P. Zhang, C. Shi, A novel sucrose transporter gene IbSUT4 involves in plant growth and response to abiotic stress through the ABF-dependent ABA signaling pathway in Sweetpotato, BMC Plant Biol. 20 (157) (2020) 1–15.
[35] Q.J. Ma, M.H. Sun, H. Kang, J. Lu, C.X. You, Y.J. Hao, A CIPK protein kinase targets sucrose transporter MdSUT2.2 at Ser254 for phosphorylation to enhance salt tolerance, Plant Cell Environ. 42 (3) (2018) 918–930.
[36] Q.J. Ma, M.H. Sun, J. Lu, H. Kang, C.X. You, Y.J. Hao, An apple sucrose transporter MdSUT2.2 is a phosphorylation target for protein kinase MdCIPK22 in response to drought, Plant Biotech. J. 17 (3) (2018) 625–637.
[37] W. Zhao, H. Meng, J. Shi, Y. Liu, Y. Yang, L. Li, C. Wu, L. Wang, G. Wu, Heterologous expression of the peach sucrose transporter (PpSUT2) in increased cold and drought stress tolerance in tobacco, J. Hortic Sci. Biotech. 97 (3) (2022) 315–327.
[38] O. Ibraheem, G. Dealtry, S. Roux, G. Bradley, The effect of drought and salinity on the expressional levels of sucrose transporters in rice ('*Oryza sativa*' nipponbare) cultivar plants, Plant Omics 4 (2) (2011) 68–74.
[39] M.R. Siahpoosh, D.H. Sanchez, A. Schlereth, G.N. Scofield, R.T. Furbank, J.T. van Dongen, J. Kopka, Modification of *OsSUT1* gene expression modulates the salt response of rice *Oryza sativa* cv. Taipei 309, Plant Sci. 182 (2012) 101–111.
[40] E. Antony, T. Taybi, M. Courbot, S.T. Mugford, J.A.C. Smith, A.M. Borland, Cloning, localization and expression analysis of vacuolar sugar transporters in the CAM plant *Ananas comosus* (pineapple), J. Exp. Bot. 59 (7) (2008) 1895–1908.
[41] X.M. Zhang, J.G. Li, M.A. Dou, Y.L. Yao, L.Q. Dd, G.M. Sun, Difference in sugar accumulation of pineapple fruit harvested in different seasons, Acta Horticulturae Sinica 37 (11) (2010) 1751–1758.
[42] G.M. Sanewski, D.P. Bartholomew, R.E. Paull, The Pineapple: Botany, Production and Uses, second ed., CAB international, Boston, 2018.
[43] L.E. Williams, R. Lemoine, N. Sauer, Sugar transporters in higher plants-a diversity of roles and complex regulation, Trends Plant Sci. 5 (7) (2000) 283–290.
[44] Y. Zhang, J. Su, S. Duan, Y. Ao, J. Dai, J. Liu, P. Wang, Y. Li, B. Liu, D. Feng, A highly efficient rice green tissue protoplast system for transient gene expression and studying light/chloroplast-related processes, Plant Methods 7 (2011) 1–14.
[45] J.D. Clyne, L.F. Wang, R.I. Hume, Mutational analysis of the conserved cysteines of the rat P2X2 purinoceptor, J. Neurosci. 22 (10) (2002) 3873–3880.
[46] A. Bartlett, R.C. O'Malley, S.C. Huang, M. Galli, J.R. Nery, A. Gallavotti, J.R. Ecker, Mapping genome-wide transcription-factor binding sites using DAP-seq, Nat. Protoc. 12 (2017) 1659–1672.
[47] R. Ming, R. VanBuren, C.M. Wai, H. Tang, M.C. Schatz, J.E. Bowers, E. Lyons, M.-L. Wang, J. Chen, E. Biggers, J. Zhang, L. Huang, L. Zhang, W. Miao, J. Zhang, Z. Ye, C. Miao, Z. Lin, H. Wang, H. Zhou, W.C. Yim, H.D. Priest, C. Zheng, M. Woodhouse, P.P. Edger, R. Guyot, H.-B. Guo, H. Guo, G. Zheng, R. Singh, A. Sharma, X. Min, Y. Zheng, H. Lee, J. Gurtowski, F.J. Sedlazeck, A. Harkess, M. R. McKain, Z. Liao, J. Fang, J. Liu, X. Zhang, Q. Zhang, W. Hu, Y. Qin, K. Wang, L.-Y. Chen, N. Shirley, Y.-R. Lin, L.-Y. Liu, A.G. Hernandez, C.L. Wright, V. Bulone, G. A. Tuskan, K. Heath, F. Zee, P.H. Moore, R. Sunkar, J.H. Leebens-Mack, T. Mockler, J.L. Bennetzen, M. Freeling, D. Sankoff, A.H. Paterson, X. Zhu, X. Yang, J.A. C. Smith, J.C. Cushman, R.E. Paull, Q. Yu, The pineapple genome and the evolution of CAM photosynthesis, Nat. Genet. 47 (12) (2015) 1435–1442.
[48] Y. Heng, C. Wu, Y. Long, S. Luo, J. Ma, J. Chen, J. Liu, H. Zhang, Y. Ren, M. Wang, J. Tan, S. Zhu, J. Wang, C. Lei, X. Zhang, X. Guo, H. Wang, Z. Cheng, J. Wan, OsALMT7 maintains panicle size and grain yield in rice by mediating malate transport, Plant Cell 30 (4) (2018) 889–906.
[49] Y. Song, X. Zhang, M. Li, H. Yang, D. Fu, J. Lv, Y. Ding, Z. Gong, Y. Shi, S. Yang, The direct targets of CBFs: in cold stress response and beyond, J. Integr. Plant Biol. 63 (11) (2021) 1874–1887.
[50] Q. Mao, C. Chen, T. Xie, A. Luan, C. Liu, Y. He, Comprehensive tissue-specific transcriptome profiling of pineapple (*Ananas comosus*) and building an eFP-browser for further study, Peer J 6 (2018) e6028.
[51] C. Chen, Y. Zhang, Z. Xu, A. Luan, Q. Mao, J. Feng, T. Xie, X. Gong, X. Wang, H. Chen, Y. He, Transcriptome profiling of the pineapple under low temperature to facilitate its breeding for cold tolerance, PloS One 11 (9) (2016) e0163315.
[52] Y. Chen, A.J. Miller, B. Qiu, Y. Huang, K. Zhang, G. Fan, X. Liu, The role of sugar transporters in the battle for carbon between plants and pathogens, Plant Biotech. J. 22 (2024) 2844–2858.
[53] S. Liu, J. Long, L. Zhang, J. Gao, T. Dong, Y. Wang, C. Peng, *Arabidopsis* sucrose transporter 4 (AtSUC4) is involved in high sucrose-mediated inhibition of root elongation, Biotechnol. Biotec. Eq. 36 (1) (2022) 561–574.
[54] E. Truernit, Plant physiology: the importance of sucrose transporters, Curr. Biol. 11 (5) (2001) R169–R171.
[55] C. Kühn, V.R. Franceschi, A. Schulz, R. Lemoine, W.B. Frommer, Macromolecular trafficking indicated by localization and turnover of sucrose transporters in enucleate sieve elements, Science 275 (5304) (1997) 1298–1300.
[56] B. Schmitt, R. Stadler, N. Sauer, Immunolocalization of Solanaceous SUT1 proteins in companion cells and xylem parenchyma: new perspectives for phloem loading and transport, Plant Physiol. 148 (1) (2008) 187–199.
[57] S. Öner-Sieben, C. Rappl, N. Sauer, R. Stadler, G. Lohaus, Characterization, localization, and seasonal changes of the sucrose transporter FeSUT1 in the phloem of *Fraxinus excelsior*, J. Exp. Bot. 66 (15) (2015) 4807–4819.
[58] L. Barker, C. Kühn, A. Weise, A. Schulz, C. Gebhardt, B. Hirner, H. Hellmann, W. Schulze, J.M. Ward, W.B. Frommer, SUT2, a putative sucrose sensor in sieve elements, Plant Cell 12 (7) (2000) 1153–1164.
[59] S. Meyer, C. Lauterbach, M. Niedermeier, I. Barth, R.D. Sjolund, N. Sauer, Wounding enhances expression of AtSUC3, a sucrose transporter from Arabidopsis sieve elements and sink tissues, Plant Physiol. 134 (2) (2004) 684–693.
[60] R.F. Baker, K.A. Leach, N.R. Boyer, M.J. Swyers, Y. Benitez-Alfonso, T. Skopelitis, A. Luo, A. Sylvester, D. Jackson, D.M. Braun, Sucrose transporter ZmSut1 expression and localization uncover new insights into sucrose phloem loading, Plant Physiol. 172 (3) (2016) 1876–1898.
[61] V. Radchuk, D. Riewe, M. Peukert, A. Matros, M. Strickert, R. Radchuk, D. Weier, H.-H. Steinbiß, N. Sreenivasulu, W. Weschke, H. Weber, Down-regulation of the sucrose transporters HvSUT1 and HvSUT2 affects sucrose homeostasis along its delivery path in barley grains, J. Exp. Bot. 68 (16) (2017) 4595–4612.
[62] A. Reinders, A.B. Sivitz, C.G. Starker, J.S. Gantt, J.M. Ward, Functional analysis of LjSUT4, a vacuolar sucrose transporter from *Lotus japonicus*, Plant Mol. Biol. 68 (3) (2008) 289–299.
[63] S. Schneider, S. Hulpke, A. Schulz, I. Yaron, J. Höll, A. Imlau, B. Schmitt, S. Batz, S. Wolf, R. Hedrich, N. Sauer, Vacuoles release sucrose via tonoplast-localised SUC4-type transporters, Plant Biol. 14 (2) (2012) 325–336.
[64] L.H. Ho, Y.I. Lee, S.Y. Hsieh, I.S. Lin, Y.C. Wu, H.Y. Ko, P.A. Klemens, H. E. Neuhaus, Y.M. Chen, T.P. Huang, C.H. Yeh, W.J. Guo, GeSUT4 mediates sucrose import at the symbiotic interface for carbon allocation of heterotrophic *Gastrodia elata* (Orchidaceae), Plant Cell Environ. 44 (1) (2020) 20–33.
[65] M. Ferro, D. Salvi, H. Rivière-Rolland, T. Vermat, D. Seigneurin-Berny, D. Grunwald, J. Garin, J. Joyard, N. Rolland, Integral membrane proteins of the chloroplast envelope: identification and subcellular localization of new transporters, Proc. Natl. Acad. Sci. 99 (17) (2002) 11487–11492.
[66] J.S. Eom, J.I. Cho, A. Reinders, S.W. Lee, Y. Yoo, P.Q. Tuan, S.B. Choi, G. Bang, Y. I. Park, M.H. Cho, Impaired function of the tonoplast-localized sucrose transporter in rice, OsSUT2, limits the transport of vacuolar reserve sucrose and affects plant growth, Plant Physiol. 157 (1) (2011) 109–119.
[67] N.A. Eckardt, The function of SUT2/SUC3 sucrose transporters: the debate continues, Plant Cell 15 (6) (2003) 1259–1262.
[68] Y.L. Ruan, Sucrose metabolism: gateway to diverse carbon use and sugar signaling, Annu. Rev. Plant Biol. 65 (1) (2014) 33–67.
[69] M. Janmohammadi, Metabolomic analysis of low temperature responses in plants, Current Opinion in Agriculture 1 (1) (2012) 1.
[70] S. Takahashi, A. Meguro-Maoka, M. Yoshida, Analysis of sugar content and expression of sucrose transporter genes (*OsSUTs*) in rice tissues in response to a chilling temperature, JPN. Agr. Res. Q. 51 (2) (2017) 137–146.
[71] H. Gu, M. Lu, Z. Zhang, J. Xu, W. Cao, M. Miao, Metabolic process of raffinose family oligosaccharides during cold stress and recovery in cucumber leaves, J. Plant Physiol. 224-225 (2018) 112–120.
[72] L. Hu, F. Zhang, S. Song, X. Yu, Y. Ren, X. Zhao, H. Liu, G. Liu, Y. Wang, H. He, CsSWEET2, a hexose transporter from cucumber (*Cucumis sativus* L.), affects sugar metabolism and improves cold tolerance in *Arabidopsis*, Int. J. Mol. Sci. 23 (7) (2022) 3886.
[73] K. Patzke, P. Prananingrum, P.A.W. Klemens, O. Trentmann, C.M. Rodrigues, I. Keller, A.R. Fernie, P. Geigenberger, B. Bölter, M. Lehmann, S. Schmitz-Esser, B. Pommerrenig, I. Haferkamp, H.E. Neuhaus, The plastidic sugar transporter pSuT influences flowering and affects cold responses, Plant Physiol. 179 (2) (2019) 569–587.

[74] S. Gusain, S. Joshi, R. Joshi, Sensing, signalling, and regulatory mechanism of cold-stress tolerance in plants, Plant Physiol. Bioch. 197 (2023) 107646.
[75] Y. Shi, Y. Ding, S. Yang, Molecular regulation of CBF signaling in cold acclimation, Trends Plant Sci. 23 (7) (2018) 623–637.
[76] L.S. Manasa, M. Panigrahy, K.C.S.R. Panigrahi, R. Gyana, Overview of cold stress regulation in plants, Bot. Rev. 88 (3) (2022) 359–387.
[77] B. Li, S. Qu, J. Kang, Y. Peng, N. Yang, B. Ma, Y.L. Ruan, F. Ma, M. Li, L. Zhu, The *MdCBF1/2-MdTST1/2* module regulates sugar accumulation in response to low temperature in apple, Plant J. 118 (3) (2024) 787–801.
[78] K. Cao, Y. Wei, Y. Chen, S. Jiang, X. Chen, X. Wang, X. Shao, PpCBF6 is a low-temperature-sensitive transcription factor that binds the *PpVIN2* promoter in peach fruit and regulates sucrose metabolism and chilling injury, Postharvest Biol. Tec. 181 (2021) 111681.
[79] S. Sun, C. Hu, X. Qi, J. Chen, Y. Zhong, A. Muhammad, M. Lin, J. Fang, The *AaCBF4-AaBAM3.1* module enhances freezing tolerance of kiwifruit (*Actinidia arguta*), Hort. Res. 8 (97) (2021) 1–15.
[80] T. Peng, X. Zhu, N. Duan, J.H. Liu, *PtrBAM1*, a β-amylase-coding gene of *Poncirus trifoliata*, is a CBF regulon member with function in cold tolerance by modulating soluble sugar levels, Plant Cell Environ. 37 (12) (2014) 2754–2767.
[81] Y. Wu, S.K. Lee, Y. Yoo, J. Wei, S.Y. Kwon, S.W. Lee, J.-S. Jeon, G. An, Rice transcription factor OsDOF11 modulates sugar transport by promoting expression of *sucrose transporter* and *SWEET* genes, Mol. Plant 11 (6) (2018) 833–845.
[82] T. Ogata, S. Yamanaka, M. Shoda, N. Urasaki, T. Yamamoto, Current status of tropical fruit breeding and genetics for three tropical fruit species cultivated in Japan: pineapple, mango, and papaya, Breeding Sci. 66 (1) (2016) 69–81.

Volume 318P4, July 2025

ISSN 0141-8130
318P4

ELSEVIER

INTERNATIONAL JOURNAL OF

Biological Macromolecules

STRUCTURE, FUNCTION AND INTERACTIONS

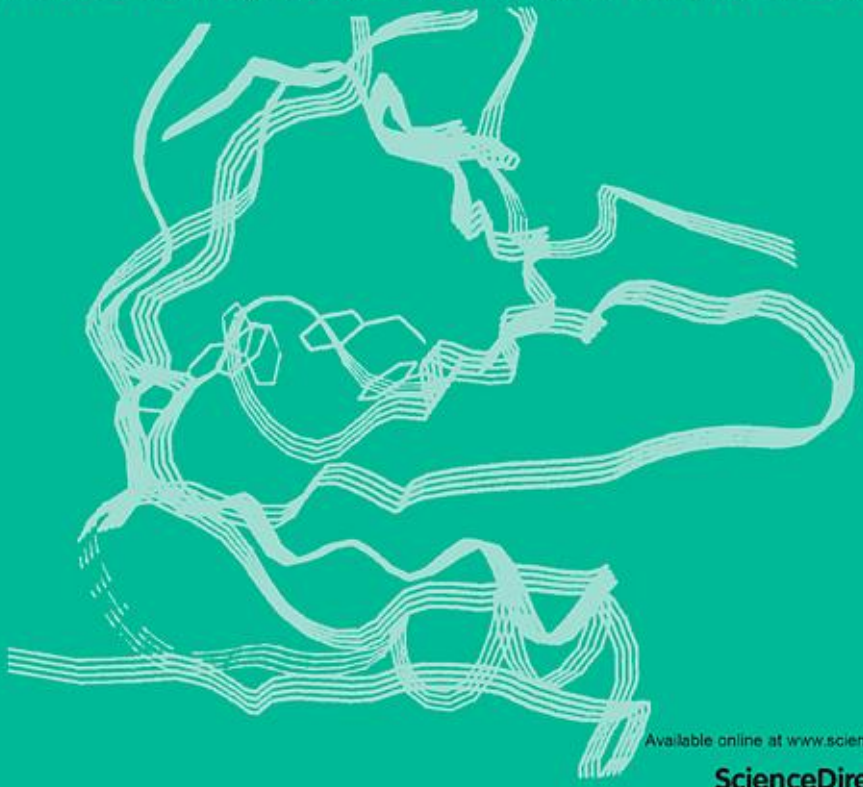

Available online at www.sciencedirect.com

ScienceDirect

Actions for selected articles

Select all / Deselect all

Download PDFs

Export citations

Show all article previews

Contents

Research article • Full text access

Analysis on the involvement of phosphoglycerate mutase 1 in the aerobic glycolysis of melanoma cells

Qiang Wang, Zhongliang Lang, Guangdi Yin, Peng Zheng, ... Liping Zhao

Article 137898

View PDF Article preview

Research article • Full text access

CircITGB5 regulates the proliferation and adipogenic differentiation of chicken intramuscular preadipocytes through the miR-181b-5p/*CPT1A* axis

Hongtai Li, Hongyuan Zhang, Yaqi Dai, Shuaihao Li, ... Guoxi Li

Article 137608

View PDF Article preview

Research article • *Open access*

Enhancing under-urine adhesion and bladder adaptation of silk fibroin hydrogels with tea polyphenols for hemorrhagic cystitis

Yaoqi Chen, Xu Cao, Jie Yao, Zeming Hu, ... Kerong Wu

Article 137487

View PDF Article preview

Research article • Full text access

The high-affinity pineapple sucrose transporter *AcSUT1B*, regulated by AcCBF1, exhibited enhanced cold tolerance in transgenic *Arabidopsis*

Jianmei Long, Huimin Zhou, Haixin Huang, Yufei Xiao, ... Chaoyang Liu

Article 137952

View PDF Article preview

Research article • Full text access

Rapid detection of *Puccinia striiformis* f. sp. *tritici* from wheat stripe rust samples using recombinase polymerase amplification combined with multiple visualization methods

Xuan Lv, Jiarui Jiang, Ziqian Yang, Sishu Lan, ... Zhanhong Ma

Article 137634

View PDF Article preview

Research article • Full text access

Inhalable multi-stimulus sensitive curcumin-alginate nanogels for scavenging reactive oxygen species and anti-inflammatory co-ordination to alleviate acute lung injury

Jinyun Cai, Haiyi Zhong, Jianwei Luo, Xinghai Huang, ... Peiyuan Li

Article 137816

View PDF Article preview

Taylor & Francis
Taylor & Francis Group

Biotechnology & Biotechnological Equipment

ISSN: (Print) (Online) Journal homepage: https://www.tandfonline.com/loi/tbeq20

Arabidopsis sucrose transporter 4 (AtSUC4) is involved in high sucrose-mediated inhibition of root elongation

Siwen Liu, Jianmei Long, Liding Zhang, Jiayu Gao, Tiantian Dong, Ying Wang & Changcao Peng

To cite this article: Siwen Liu, Jianmei Long, Liding Zhang, Jiayu Gao, Tiantian Dong, Ying Wang & Changcao Peng (2022) *Arabidopsis* sucrose transporter 4 (AtSUC4) is involved in high sucrose-mediated inhibition of root elongation, Biotechnology & Biotechnological Equipment, 36:1, 561-574, DOI: 10.1080/13102818.2022.2101942

To link to this article: https://doi.org/10.1080/13102818.2022.2101942

BIOTECHNOLOGY & BIOTECHNOLOGICAL EQUIPMENT
2022, VOL. 36, NO. 1, 561–574
https://doi.org/10.1080/13102818.2022.2101942

Arabidopsis sucrose transporter 4 (AtSUC4) is involved in high sucrose-mediated inhibition of root elongation

Siwen Liu[a,#], Jianmei Long[b,#], Liding Zhang[a], Jiayu Gao[a], Tiantian Dong[a], Ying Wang[b] and Changcao Peng[a,b,#]

[a]State Key Laboratory for Conservation and Utilization of Subtropical Agro-Bioresources, South China Agricultural University, Guangzhou, PR China; [b]Guangdong Key Laboratory for Innovative Development and Utilization of Forest Plant Germplasm, College of Forestry and Landscape Architecture, South China Agricultural University, Guangzhou, PR China

ABSTRACT

Sucrose transporters (SUCs/SUTs) play crucial roles in apoplast transport and long-distance distribution of sucrose throughout the whole plant. However, whether and how the *Arabidopsis* AtSUC4 modulates sucrose import from apoplast to cytosol remains unclear. In the present study, we found that AtSUC4 protein was localized to the plasma membrane in the root. Expression of *AtSUC4* in roots was gradually induced with the increasing sucrose concentrations (0%, 2%, 4% and 6%). When feeding high concentrations (4% and 6%) of sucrose, the primary root growth of seedling was inhibited. Interestingly, *atsuc4* mutants exhibited longer primary root than the wild type under these conditions, indicating that *atsuc4* mutants were less sensitive to excess sucrose. Moreover, the root of *atsuc4* mutants accumulated less sucrose and abscisic acid (ABA) and more indole-3-acetic acid (IAA) on 4% and 6% sucrose supplementation. Transcriptomic analysis revealed that numerous genes associated with sugar transport and metabolism, as well as ABA signalling were down-regulated, whereas many IAA signaling-related genes were up-regulated in mutant plants relative to the wild type under 6% sucrose treatment. Collectively, our finding demonstrated that the deficiency of *AtSUC4* reduced the inhibition of primary root growth under high sucrose condition, probably through reducing the sucrose transportation and metabolism, and subsequent alteration in IAA and ABA signalling.

ARTICLE HISTORY
Received 14 February 2022
Accepted 12 July 2022

KEYWORDS
AtSUC4; root growth; sucrose; auxin; abscisic acid

Introduction

Sucrose, functioning as a nutritional substance, osmolyte and signal molecule, plays a central role in the response and adaptation to environmental stress in most plants [1]. Most sucrose is derived from the photosynthetic source organ, the leaves, and transported into sink organs, including flowers, stems, roots and seeds. This involves the uptake or release of sucrose from cells or subcellular compartments via transport proteins. Thus, not surprisingly, sucrose transporters (SUCs or SUTs) are critical for plant growth and development [2]. Sucrose is synthesized in the source cells and exported to the apoplasm probably by the SWEET efflux proteins, then imported into the sieve elements and companion cell complexes (SE-CCCs) via sucrose transporters (SUTs or SUCs) in most plants [3]. Studies have detected that the concentration of sucrose could reach 10^{-1} mol L^{-1} to 1 mol L^{-1} in the conducting vascular cells, while extracellular sucrose concentrations are in the 10^{-3} mol L^{-1} range [4,5]. However, the mechanism of how these cells respond to such higher sucrose concentrations to maintain the sucrose equilibrium in extra- and intra-cellular components is still unknown.

SUCs are H^+/sucrose symporters that utilize the proton motive force present across the plasma membrane (PM) of the SE-CCCs to load sucrose against its concentration gradient into the phloem [6]. Multiple SUT genes have been identified and initially classified into three subgroups (SUT1, SUT2 and SUT4 subfamily) but later into four distinct groups (Group I, II, III and IV) according to phylogenetic analysis [7,8]. Among them, most members of Group II are high-affinity/low-capacity sucrose transporters with Km values in the range of 139 µmol L^{-1}–1.5 mmol L^{-1} and described as PM-localized transporters, whereas members of the Group IV (with the exception of OsSUT2 from rice) are

CONTACT Changcao Peng ccpeng@scau.edu.cn State Key Laboratory for Conservation and Utilization of Subtropical Agro-Bioresources, South China Agricultural University, 483 Wushan Road, Tianhe District, Guangzhou, PR China.
[#]These authors contributed equally to this article.

Supplemental data for this article can be accessed online at https://doi.org/10.1080/13102818.2022.2101942.

low-affinity/high-capacity sucrose transporters with Km values ranging from 5 mmol L^{-1} to 6 mmol L^{-1} and suggested as the tonoplast-localized transporters [9]. There are nine SUCs in *Arabidopsis* (*Arabidopsis thaliana*), among which only AtSUC4 belong to Group IV. Numerous studies showed that SUTs in Group IV have distinct functions in different plant species, indicating a versatile role of the members in this group in plant growth and development [10,11]. AtSUC4 can also catalyse the transport of sucrose from the vacuolar lumen into the cytoplasm in the cells [12]. Due to the low expression level of *AtSUC4*, the aerial part of *atsuc4.1* (cs856419) mutant behaved essentially as the wild type (WT) in sucrose content, germination, development and response to cold treatment when cotyledons were fully unfolded. The *AtSUC4*-overexpressing lines showed a 30% reduction in sucrose content in aerial parts compared with WT under 3% sucrose treatment [13], implying that AtSUC4 releases sucrose from the vacuole for cellular metabolism. However, little is known about whether and how AtSUC4 participate in the sucrose import under higher sucrose status.

In *Arabidopsis*, the primary root elongation rate is basically dependent on the sugar concentration in the medium, and a good correlation between the elongation rate and sucrose content (0–2%) in primary roots was found [14]. In addition, sugars transported into the root also transmit as signals. In young developing seedling root of *Arabidopsis*, sucrose transported into the root can act as a necessary and sufficient signal regulating root elongation together with light [15]. The expression patterns of *AtSUC1* and *AtSUC2* displayed contrasting roles during the night, showing increased transcript accumulation of *AtSUC2* (sucrose loading in phloem) in leaves and *AtSUC1* (sucrose unloading) in roots [16,17]. However, the function of *AtSUC4* in root elongation was uncertain, and a clear linking on the interaction between sucrose transport and root growth remains to be elucidated.

Apart from sucrose, multiple plant hormones also regulate root elongation, among which auxin stands out as a key instructive signal [18]. Exogenous sucrose could promote the root growth through sugar-hormone crosstalk in *Arabidopsis* and peach [19,20]. Specifically, exogenous sucrose increased the expression of auxin synthesis- and transport-related genes in roots, resulting in auxin accumulation in the root system [20]. Abscisic acid (ABA) signalling also plays a critical role in regulating root elongation and root system architecture [21]. Yu et al. [22] revealed that *OsERF2* was required for the root architecture and ABA-response by regulating the expression of some genes involved in sugar metabolism and hormone signalling pathways. Additionally, excessive exogenous glucose inhibits primary root growth via *ABI5*, which represses *PIN1* accumulation and auxin activity in *Arabidopsis* [23]. To date, however, the molecular mechanism of crosstalk among sucrose transporters, indole-3-acetic acid (IAA) and ABA regulating root growth remains unclear.

To gain more information about sucrose transport regulation in root with emphasis on AtSUC4 while extracellular sucrose concentration is high, expression patterns and subcellular localization of AtSUC4 were performed first. Several *atsuc4* mutant lines were generated and showed longer root length under high concentrations (4% and 6%) of exogenous sucrose. The contents of sugars and hormones (IAA and ABA) in the roots in WT and mutant lines were analysed. Transcriptome analysis was carried out and indicated that the expression of genes involved in sucrose transport and metabolism, IAA- and ABA signalling were changed in mutant lines. This study confirmed the novel function of AtSUC4 and provided insights into the regulation of AtSUC4 on root elongation under higher sucrose.

Materials and methods

Strains materials and growth conditions

Arabidopsis thaliana (ecotype Col-0) and *atsuc4* mutants were grown in a growth chamber in soil under long-day (LD) conditions (16 h light/8 h dark) at 22 °C and 70% relative humidity, light was present at 100–120 $\mu mol.m^{-2}.s^{-1}$. Before germination, plates were incubated at 4 °C for 2 d in the dark and subsequently transferred to the growth chamber. *Escherichia coli* strain DH5α was used for all cloning steps. Transformation of *Arabidopsis* was performed using *Agrobacterium tumefaciens* strain GV3101 [24].

Genes expression level detection

For gene expression analysis, total RNA was isolated from roots of different plants using the Plant RNA Extraction Kit (Omega, Norcross, GA, USA), and cDNA was synthesized using HiScript II 1st Strand cDNA Synthesis Kit (+gDNA wiper) (Vazyme). Reverse transcription-quantitative real time polymerase chain reaction (RT-qPCR) was conducted using FastStart DNA Master SYBR Green I (Roche) on the Roche LightCycler 480 System (Roche Applied Science), with *ACTIN2* as the internal control [25]. Three independent biological replicates and four technical replicates were performed. The primer sequences are listed in Supplemental Data S1.

Subcellular localization assay of AtSUC4

The subcellular localization of AtSUC4 was detected by three methods. For the method of *Arabidopsis* stable transformation system, the promoter (2000 bp upstream of ATG) and gDNA sequence of *AtSUC4*, named *gAtSUC4*, were amplified and cloned into a pCAMBIA1300 vector. As a result, the construct pCAMBIA1300-p*SUC4::*g*AtSUC4-GFP* was generated and subsequently transformed into WT plants. The localization of AtSUC4 in root was detected. The second method used the transient expression system of *Arabidopsis* protoplast to check the subcellular localization of AtSUC4. Protoplast isolation and transformation of a rosette leaf were performed according to Robert et al. [26]. The 35S promoter and cDNA sequence of *AtSUC4* were amplified and cloned into pEarley101 vector, the vector pEarley101-*35S::*c*AtSUC4-GFP* was generated and used for protoplast transient transformation. All the fluorescence was detected using a Leica TCS SP5 confocal microscope. The excitation wavelength was 488 nm and the emitted fluorescence was recorded from 500 to 550 nm for green fluorescent protein (GFP). The third method was Immunogold labelling of AtSUC4, which was essentially performed as described previously [27] using the mouse anti-AtSUC4 monoclonal antibody (Beijing Protein Innovation, Beijing, China). We selected 'ASLASEAHGQTSGTDEAFL' as the synthesized target peptide. Four SPF Balb/c female mice were immunized for the first time with 'AtSUC4-KLH'. Before fusion, we used 'AtSUC4-KLH' to shock immunize a mouse with the best physiological state. The fused cells were transferred to semi-solid medium for culture. Then, the single clones grown on the semi-solid medium were picked into a 96-well culture plate for cultivation and subsequent screening. Subsequently, the plates were coated with 'AtSUC4-BSA', and the selected clones were screened by enzyme-linked immunosorbent assay (ELISA) for the first time, yielding 24 positive hybridoma cell lines. These positive cell lines were screened for the second time by ELISA, and the positive cell lines were screened for subclass identification. As a result, nine IgG-type positive hybridoma cell lines were obtained and frozen. Finally, the monoclonal antibody was used to detect the total protein of *Arabidopsis* by Western blot.

Verification of expression pattern of AtSUC4 at tissue level

To verify the expression pattern of AtSUC4 during *Arabidopsis* development at the tissue level, we created p*AtSUC4::GUS* transgenic plants under the control of the endogenous *AtSUC4* promoter. A 998-bp fragment before the coding region of *AtSUC4* was amplified from total DNA of leaf, subcloned into the entry vector pDONR207 and inserted upstream of the *GUS* into the destination vector pHGWFS7 [28], yielding construct pHGWFS7-p*AtSUC4::GUS*, which was used for *A. tumefaciens* transformation. Primer pairs used are shown in Supplemental Data S1. Samples including the whole seedlings (grown for 4 d, 14 d and 25 d period), flowers (grown for 35 d period), siliques and seeds (grown for 50 d period) were stained according to a standard protocol [13]. For each sample, we analysed 10–15 independent lines, and representative results are presented. Photographs were captured by a stereomicroscope (Leica MZFL III; Leica Microsystems, Bensheim, Germany).

Generation of Arabidopsis atsuc4 mutant lines

Three types of *atsuc4* mutant lines were used in this study. The *atsuc4* mutant (cs93419) was obtained from the Nottingham Stock Centre (http://arabidopsis.info/) and was screened for the *AtSUC4* point mutation homozygous with no *ERECTA* gene mutation, which was named as *suc4-1*. To generate an *AtSUC4* knockout line *suc4-2*, we adopted the CRISPR/Cas9 genome editing system provided by Ma et al. [29]. Two gene-specific gRNA sequences (TCACAGAGTCACTCGCAACC and CTCGTTGGGCATAGTAGCGA) were designed using the tools at http://skl.scau.edu.cn/. The *AtSUC4* T-DNA insertion line named *suc4-3* (WiscDsLox450E10) was obtained from the Nottingham Stock Centre (http://arabidopsis.info/). The position of the T-DNA insertion was determined by sequencing a PCR product obtained from *suc4-3* genomic DNA [13]. For the *AtSUC4* complement-expressors (marked as *AtSUC4*/*suc4-1*), the *AtSUC4* promoter and gDNA sequence fragments were amplified from the total DNA of leaves, and inserted into the *Bam*H I- and *Eco*R I-digested plant transformation vector pCAMBIA1300 [30] by ClonExpress MultiS One Step Cloning Kit (Vazyme). The resulting plasmid pCAMBIA1300-p*SUC4::*g*SUC4-GFP* was used for *suc4-1* mutant transformation. Primer pairs for vector construction and identification of *atsuc4* mutants are shown in Supplemental Data S1.

Measurement of root length, plant height and the number of rosette leaves

For sugars treatment, the seeds of WT and *atsuc4* mutant lines were sown on Murashige and Skoog (MS) solid media containing different concentrations of sucrose, glucose and mannitol after sterilizing the seeds (0%, 2%, 4% and 6%). Bright-field images of

different plants were captured at 6 d after sowing using a Canon 60 D camera. Root length was measured by Image J software. For the phenotype comparison between WT and mutants, plants were grown in soil under LD condition. The number of rosette leaves was recorded at 25 d, and the plant height was measured at 50 d. Three biological replicates and more than 30 plants for each replicate were used for analysis.

Analysis of carbohydrate content

Preparation of plant materials and determination of carbohydrate content via ion chromatography was performed as previously described [25]. WT, *atsuc4* mutants and *AtSUC4*/*suc4-1* seeds were sown on MS solid media containing different concentrations of sucrose (0%, 2%, 4% and 6%). Roots were collected and quickly grinded in liquid nitrogen. An aliquot of each individual sample was precisely weighed (20 mg) and transferred to an Eppendorf tube. After adding the addition of 500 µL of extract solvent (ethanol–water, 8:1) and including the isotope as internal stand with the fix concentration. The samples were vortexed sonicated. The homogenate and sonicate circle were repeated three times, followed by incubation at 90 °C for 30 min and centrifugation at 18,500 *g* for 15 min. The supernatant was transferred to an auto-sampler vial for ultra-high-performance liquid chromatography-tandem mass spectrometry (UHPLC-MS/MS) analysis to measure glucose and fructose. Another aliquot was further diluted 10 times for UPLC-MS/MS analysis to quantitate the sucrose. When the concentrations of metabolites were beyond the standard curve range, the samples were diluted accordingly to place their concentrations within the range. The final concentration was in µg mg^{-1}. FW equals the calculated concentration multiplied by the dilution factor.

Determination of IAA and ABA content in roots

Roots were collected from WT and *suc4-1* mutant grown on MS solid media with 2% and 6% sucrose supplementation under LD condition at 6 d after sowing, with three biological replicates (approximately 0.5 g fresh weight per sample). And the contents of endogenous IAA and ABA were determined according to a previously reported method with modification [31]. The samples (50 mg) were analysed using Thermo Scientific Ultimate 3000 UHPLC System equipped with a Thermo Scientific TSQ Quantiva-Stage Quandrupole Mass Spectrometer (http://www.greenswordcreation.com).

Analysis of the RNA-seq data

Total RNA was isolated from the 6-d-old seedling roots of WT and *suc4-1* plants grown on MS solid media containing different concentrations of sucrose (2%, 4% and 6%) in three biological replicates. As previously described [32], RNA samples were treated with DNase before being quality checked using an Agilent 2100 Bioanalyzer. Total RNA was prepared for a strand-specific TruSeq™ RNA-seq library, and all 27 samples were sequenced on an Illumina HiSeq 4000, with 150 bp paired end reads. Differential expression analysis was performed using the DEGSeq R package (1.12.0). *P*-values were adjusted using the Benjamini & Hochberg method. A corrected *P*-value of 0.05 and $\log_2$ (Fold Change) of 1 were set as the threshold for significantly differential expression. Gene ontology enrichment analysis of differentially expressed genes (DEGs) was implemented by the GOseq R package, in which gene length bias was corrected. Gene ontology terms with a corrected *P*-value less than 0.05 were considered significantly enriched by DEGs. All sequences generated in this study have been deposited in the National Center for Biotechnology Information Sequence Read Archive (https://www.ncbi.nlm.nih.gov/sra/) with project number PRJNA666009.

Statistical analyses

The overall data were statistically analysed using SPSS 20 software (IBM China Company Ltd., Beijing, China). One-way or two-way analysis of variance with Duncan test at the 5% level was used to test differences between multiple samples. Data were presented as means and SEs or SDs using Microsoft Excel.

Results

Expression pattern and subcellular localization of AtSUC4

To investigate whether the *AtSUC4* expression was induced by sucrose, we generated a construct (p*AtSUC4::GUS*) harbouring the GUS reporter gene driven by the endogenous *AtSUC4* promoter and transformed into Col-0. p*AtSUC4::GUS* seedlings were grown on the medium with different concentrations of sucrose (0%, 2%, 4% and 6%) for 7 d and then stained for *GUS* activity detection. As shown in Figure 1A, with the increase in sucrose concentration in the medium, the activity of *GUS* became gradually higher, suggesting that *AtSUC4* expression was significantly induced by sucrose. This result was further supported by *GUS*

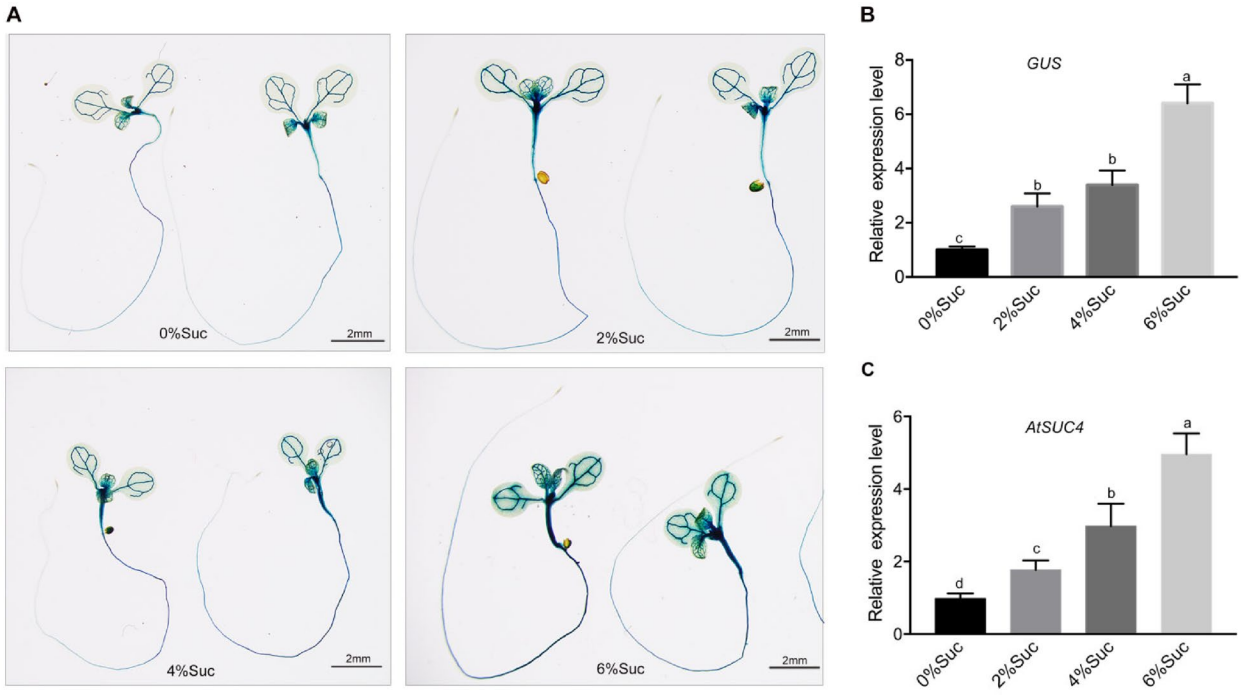

Figure 1. Expression level of *AtSUC4* in response to different concentrations of sucrose. (A) 7 d-old p*AtSUC4::GUS* seedling on MS solid media with different concentrations of sucrose (0%, 2%, 4% and 6%). (B) The relative expression level of GUS in roots of p*AtSUC4::GUS* plants. (C) The relative expression level of *AtSUC4* in roots of 7-d-old WT seedlings under different concentrations of sucrose treatment (0%, 2%, 4% and 6%). Data are mean values ± SE of three biological replicates. Bars with different letters indicate significant differences among treatments for the same stage according to Duncan's test (at $p < 0.05$).

expression analysis using RT-qPCR (Figure 1B). We also detected the expression level of *AtSUC4* in the root of 7-d-old WT seedlings. The result showed that the expression level of *AtSUC4* increased significantly as the concentration of external sucrose increased (Figure 1C). These results indicated that *AtSUC4* expression was induced by sucrose.

We next detected the spatio-temporal expression of AtSUC4 in *Arabidopsis* using p*AtSUC4::GUS* seedlings. As shown in Supplemental Figures S1A and B, AtSUC4 was mainly expressed in vasculature cells of leaves and mature portion of roots in 4-d- and 14-d-old seedlings. In 25-d-old plants, GUS staining covered the entire root and juvenile leaves but not mature leaves (rosette) (Supplemental Figure S1C). The inflorescence, petals, styles and the developing flower buds showed the presence of GUS staining. Specifically, we detected the GUS activity in vasculature of petals and styles in mature flower (Supplemental Figure S1D). In addition, it showed that strong GUS activity was detected in vascular tissues of siliques at 1 DAF (days after flowering) and embryo at 15 DAF (Supplemental Figures S1E and F).

It has been known that the Group IV sucrose transporters are tonoplast- or/and PM-localized. Since the tonoplast localization of AtSUC4 was found only by protoplasts transient system [13], we wanted to re-check whether AtSUC4 localized to the PM using three different approaches. The AtSUC4-GFP fusions protein was stably expressed in the root of *Arabidopsis*, showing clear and strong fluorescence in the PM (Figure 2A). Immune colloidal gold assay was also conducted for subcellular localization detection. The identification of IgG-type positive hybridoma cell lines by Western Blot are shown in Supplemental Figure S2, and a monoclonal antibody of AtSUC4, which belongs to subclass G2b, was successfully obtained. Both immune colloidal gold assay and transient transformation of *Arabidopsis* protoplasts with 35S::*AtSUC4-GFP* vector showed that AtSUC4 was localized to the PM (Supplemental Figures 2B and C). These results indicated that AtSUC4 was mainly located in the PM in root cells.

Analysis of root length in atsuc4 mutants under higher sucrose condition

In order to determine the effect of *AtSUC4* mutation on plant growth, three mutant lines were generated, including *suc4-1* (generated by EMS mutagenesis), *suc4-2* (generated by CRISPR/Cas9 editing) and *suc4-3* (T-DNA insertion) (Supplemental Figure S3A). The

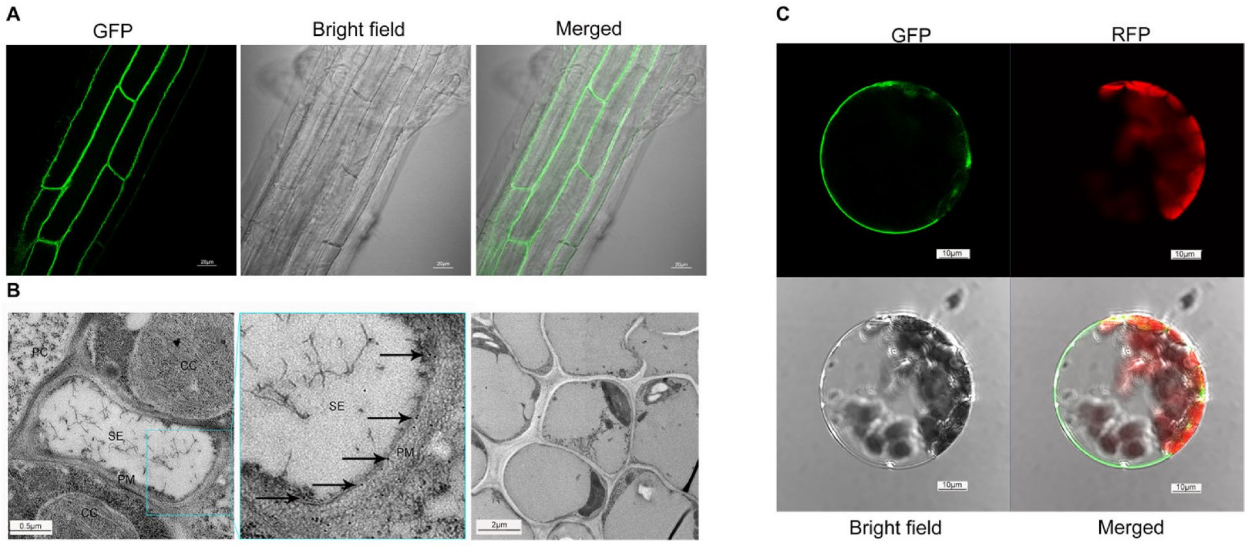

Figure 2. Subcellular localization of AtSUC4. (A) Root image of GFP fusion to the C-terminus of AtSUC4 by stable transformation. (B) Detection of AtSUC4 localization by immune colloidal gold. SE: sieve element, CC: companion cell, PM: plasma membrane. The black arrow represents the gold particles. The right image served as a negative control. (C) The subcellular localization of a GFP fusion to the C-terminus of AtSUC4 by transient transformation of *Arabidopsis* protoplasts. GFP and RFP indicated the fluorescence of AtSUC4-GFP fusion protein and chlorophyll auto-fluorescence, respectively.

suc4-1 point mutation (C502A) and *suc4-2* inserted mutation (A was inserted between nucleotides 29 and 30) introduced stop codon (TAA), resulting an early termination of AtSUC4 protein translation (Supplemental Figure S3B). The *AtSUC4* transcript in all the three mutants was significantly lower than in the WT, whereas it was similar to that of the WT in the *AtSUC4*/*suc4-1* (Supplemental Figures S3C and D). Under the LD conditions, both plant height and leaf number were similar in all genotypes (Supplemental Figures S3E and F, S4A and B). The root length of WT was similar to all the three *atsuc4* mutants on medium supplemented with low sucrose concentration, including 0%, 0.5%, 1%, 1.5% or 2% sucrose (Supplemental Figure S4C). These data demonstrated that there was no difference in phenotype between *atsuc4* mutants and WT plants on the sucrose-free or low concentration of sucrose condition.

To test whether the phenotypes of *atsuc4* mutants were altered in response to high content of sucrose, *atsuc4* mutants, WT and the complementary line *AtSUC4*/*suc4-1* were cultured under different concentrations (0%, 2%, 4% and 6%) of three different sugars. When feeding sucrose to the medium, the root length was the longest in all plants at 2% sucrose concentration. As the sucrose concentration became higher, the root length in all lines gradually decreased (Figure 3A and B), indicating that higher concentration of sucrose would inhibit the root growth. Interestingly, the primary root of the *atsuc4* mutants was significantly longer than that of WT and *AtSUC4*/*suc4-1* plants when the sucrose concentrations in the medium was raised to 4% and 6% (Figure 3A and B). We next explored whether the high concentration of glucose or mannitol (served as osmotic stress) would cause the similar difference of primary root length among WT, *atsuc4* mutants and *AtSUC4*/*suc4-1*. As shown in Figure 3C–F, no differences were found in the root length among these three genotypes of plants under the same treatment. Taken together, these results suggested that disruption of *AtSUC4* in *atsuc4* mutants repressed the inhibition of high concentration sucrose on root growth, which displayed a sucrose-specific response.

Accumulation of sucrose, ABA and IAA in roots of atsuc4 mutants under higher sucrose condition

To investigate whether the difference in root length was caused by the sucrose content, we then compared the sucrose content in roots between mutants and WT. The results revealed that when no exogenous sucrose was added, the sucrose content in all lines showed no significant difference. After adding exogenous sucrose (2%, 4% and 6%), the sucrose content in the roots of all lines increased as the exogenous sucrose concentration became higher. However, an obviously reduced sucrose content in root was shown in *atsuc4* mutants compared with WT and *AtSUC4*/*suc4-1* on medium with 2%, 4% and 6% sucrose supplementation, especially when 6% sucrose was added, the difference of sucrose

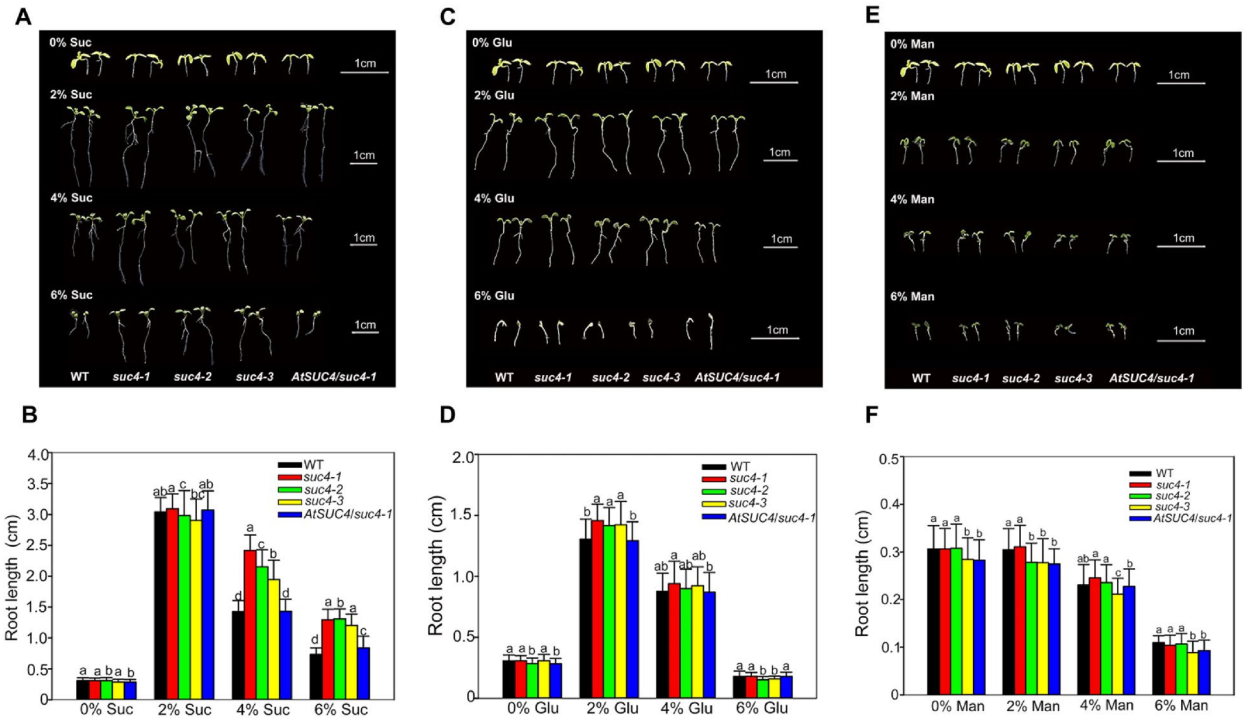

Figure 3. The phenotypic and statistics of primary root length under different concentrations (0%, 2%, 4% and 6%) of sugar treatments: sucrose (A, B); glucose (C, D); mannitol (E, F). The first row plants in (A), (C) and (E) are the shared control group. Data in (B), (D) and (F) are mean values ± SE of three biological replicates. All the plants were grown on MS solid media for 6 days after sowing. Bars with different letters indicate significant differences among genotypes for the same treatment according to Duncan's test (at $p < 0.05$), $n > 50$.

Table 1. Sucrose content in roots of different types of plants.

Treatment	WT	*suc4-1*	*suc4-2*	*suc4-3*	*AtSUC4/suc4-1*
0% Suc	0.27 ± 0.03	0.31 ± 0.04	0.26 ± 0.04	0.26 ± 0.03	0.30 ± 0.05
2% Suc	1.45 ± 0.11	0.58 ± 0.17**	0.98 ± 0.11**	0.95 ± 0.13**	1.82 ± 0.17*
4% Suc	2.77 ± 0.38	1.89 ± 0.13**	2.18 ± 0.17**	1.90 ± 0.28**	4.17 ± 0.46**
6% Suc	19.40 ± 1.03	5.06 ± 0.61**	8.29 ± 0.50**	4.67 ± 0.37**	17.57 ± 1.81

Values, means ± SD; (unit: μg mg_{FW}^{-1}).

content between *atsuc4* mutants and WT was conspicuous (Table 1). To a lesser extent, the glucose content of *suc4-1* and *suc4-3* roots were decreased compared with WT on medium supplemented with 4% and 6% sucrose, whereas no significant difference between *suc4-2* and WT (Supplemental Figure S5A). The content of fructose in three *atsuc4* mutants was significantly lower than that of WT and *AtSUC4/suc4-1* on medium without sucrose. As the concentration of sucrose increased to 6%, markedly reduced fructose content was detected in *suc4-2* compared with WT, but no significant differences in WT, *suc4-1* and *suc4-3* (Supplemental Figure S5B). These results showed that *atsuc4* mutants accumulated less sucrose under higher sucrose condition, which was probably contributed to longer root length compared with WT.

All the plants were grown on MS solid media with different concentration of sucrose (0%, 2%, 4% and 6%) for 6 days after sowing. Data are mean values ± SD of three biological replicates. '*' and '**' indicate significant differences among genotypes for the same treatments according to Duncan's test (at $p < 0.05$ and $p < 0.01$, respectively), $n > 50$.

In order to verify whether the longer root length of the *atsuc4* mutants crossed with the IAA and ABA signal pathway under high sucrose condition, we detected the IAA and ABA contents in roots of WT and *suc4-1* (Table 2). The result showed that the accumulation of IAA in both *suc4-1* and WT was decreased in the 6% sucrose supplementation compared with 2% sucrose. However, it was significantly higher in *suc4-1* than WT, suggesting that the less reduction of IAA might alleviate the inhibition of root growth under high sucrose. On the contrary, 6% sucrose stimulated the accumulation of ABA in both *suc4-1* and WT, and less ABA was accumulated in the *suc4-1* compared with WT.

Table 2. ABA and IAA content in roots of different plants.

Analyte	IAA	ABA
WT (2% Suc)	10.9 ± 1.2	6.3 ± 0.6
suc4-1 (2% Suc)	9.6 ± 0.7	4.1 ± 0.2*
WT (6% Suc)	3.2 ± 0.3*	9.6 ± 0.7
suc4-1 (6% Suc)	5.3 ± 0.1	7.2 ± 0.4*

Values, means ± SD; (unit: ng g_{FW}^{-1}).

All the plants were grown on MS solid media with different concentration of sucrose (2% and 6%) for 6 days after sowing. Data are mean values ± SD of three biological replicates. '*' indicates significant differences among genotypes for the same treatments according to Duncan's test (at $p < 0.05$), $n > 50$.

Analysis of global gene expression change in atsuc4 mutants under different sucrose condition

To better understand the role of *AtSUC4* at the molecular level under high sucrose, comparative transcriptome analysis was performed between *suc4-1* and WT using roots grown for 6 d under 2%, 4% and 6% sucrose treatments. A total of 1,259 (581 up, 678 down) DEGs were identified in *suc4-1* compared with WT on the medium supplemented with 2% sucrose, respectively. At 4% sucrose condition, 452 (182 up, 270 down) DEGs were found in *suc4-1*. Under high concentration of sucrose condition (6% sucrose), the number of DEGs increased, among which 6,485 (2,837 up, 3,648 down) DEGs were identified in *suc4-1*. Besides, only 26 DEGs overlapped under these three conditions (Supplemental Figure S6). KEGG enrichment analysis among the DEGs revealed that three pathways, including carbon metabolism, glyoxylate and dicarboxylate metabolism and pyruvate metabolism, were enriched under 4% sucrose treatment (Supplemental Figure S7A). Additionally, plant hormone signal transduction, starch and sucrose metabolism and phenylpropanoid biosynthesis were the most enriched pathways in the *suc4-1* plants at 6% sucrose condition (Supplemental Figure S7B).

Atsuc4 mutants response to higher sucrose through sucrose, IAA and ABA signalling pathway

Our study showed that the sucrose accumulation was much lower in *atsuc4* mutants than in WT under 6% sucrose. We therefore checked the expression change of *AtSUCs* and *AtSWEETs*, two main kinds of carriers for sucrose transport, in *suc4-1* in RNA-seq data. As shown in Figure 4A, *AtSUC2, 4* and *5, AtSWEET1, 4, 11, 12, 13* and *15* were significantly down-regulated in *suc4-1* compared with WT at 6% sucrose condition, whereas a reverse expression pattern was found for *AtSWEET2, 14, 16* and *17*, as well as *AtSUC1* and *3*. We further investigated the expression of *AtSUC2, AtSWEET11, 12* and *15* by qRT-PCR, showing consistence with RNA-seq data (Figure 4B). These results revealed that more sucrose transporters tend to be down-regulated in *suc4-1*, which might contribute to lower level of sucrose in the mutants under high sucrose. Except for sucrose transport, sucrose accumulation is also affected by sucrose synthesis and degradation. Hence, we explored the expression of genes related to sucrose synthesis and degradation in *suc4-1* under high sucrose conditions. As shown in Figure 4A, three genes that encode Sucrose Synthase (*SUS1, 4, 5*), which are important for sucrose degradation, were significantly up-regulated in *suc4-1* lines compared with WT under high sucrose. On the contrary, the transcript levels of the genes encoding Sucrose-Phosphate Synthase (*SPS*), which is involved in sucrose synthesis, were reduced significantly.

The content of ABA and IAA were significantly different between *suc4-1* and WT under 6% sucrose treatment (Table 2). Therefore, the expression levels of IAA- and ABA-related genes were investigated by RNA-seq. As shown in Figure 4C, two IAA biosynthesis genes (*YUC2*, *6*), two IAA transporter genes (*PIN1*, *4*) and five IAA signal transduction genes (*PLT1*, *2*, *SHR*, *IAA6* and *19*) were up-regulated in *suc4-1* under 6% sucrose condition. On the contrary, one ABA biosynthesis gene (*NCED3*), seven ABA signal transduction genes (*PYL2*, *8*, *SnRK2.3*, *2.6*, *ABI3*, *4* and *5*) were down-regulated in *suc4-1* (Figure 4E). These results were in agreement with the increased accumulation of IAA and reduction in ABA in *atsuc4* mutant plants under 6% sucrose treatment. To test the reliability of the transcriptome data, five sucrose metabolism genes, five IAA signalling pathway genes and five ABA signalling pathway genes were chosen for RT-qPCR assay. Gene expression as elucidated by RT-qPCR exhibited similar trends with that of the transcriptome data, with some variation in the magnitude (Figures 4B, D and F). Taken together, these results suggested that deficiency of *AtSUC4* had directly or indirectly stimulated the IAA signalling pathway but repressed the ABA signalling pathway under high sucrose.

Discussion

Although various studies have focussed on AtSUCs in *Arabidopsis*, relatively few have been performed on the effect of AtSUC4, a unique high-affinity/low-capacity sucrose transporter in Group IV in *Arabidopsis*, on root development in recent years. Based on our findings

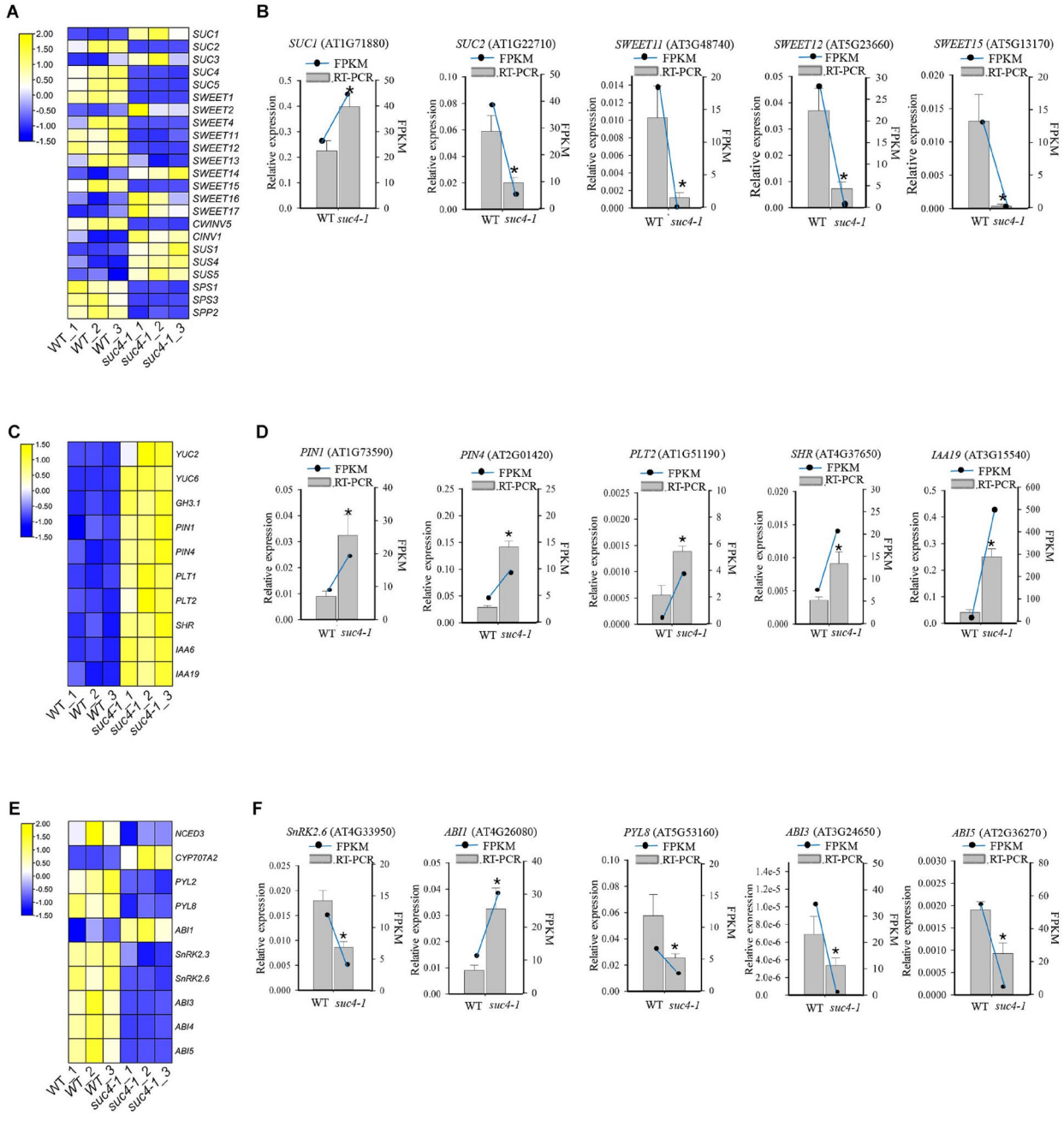

Figure 4. Expression level of genes related to sucrose transport and metabolism, IAA and ABA signalling pathway. (A), (C), (E) Heatmap of representative genes expression related to sucrose, IAA and ABA signalling pathway. (B), (D), (F) Gene expression changes as assessed by RT-qPCR. The relative expression detected by RT-qPCR is represented by a bar graph, and the left ordinate indicates the expression level. FPKM of genes, according to RNA-Seq data, is represented by a line graph, and the right ordinate indicates the FPKM level. Asterisks represent a significant difference compared with WT. The $\log_2$ fold change value of the gene expressions from transcriptome is displayed in different colours. Yellow colour means high expression and blue colour means low expression. Each sample was assayed in three biological replicates. The experimental materials were selected from the roots of different plants which were grown on MS solid media with 6% sucrose for 6 days.

in this study, the possible function and the regulation mechanism of AtSUC4 in the root under high sucrose would be discussed.

Long-distance transport of sucrose from source to sink organs occurs through vascular system, which is mediated mainly by sucrose transporters. In this regard, many SUTs were targeted to PM [33]. It is well known that the members in the SUT4 clade were reported to be either PM- or/and tonoplast-localized [34,35]. To date, dual target to the PM and tonoplast have been characterized in several members, including HvSUT2 (*Hordeum vulgare*), LjSUT4 (*Lotus japonicas*), NtSUT4

(*Nicotiana tabacum*), GeSUT4 and OsSUT2 (*Oryza sativa* L.) [36,37]. In addition, two SUT4 homologs of *Solanaceae*, SlSUT4 from tomato and StSUT4 from potato, were found in the endoplasmic reticulum except for PM and vacuole [36], indicating heterogeneity of SUT4 clade localization in plants. It has been characterized that AtSUC4 localized to vacuole using the protoplast transient expression system and PM by functional characterization in heterogenous yeast [13, 34]. Only one proteomic report indicated that AtSUC4 residue was detectable in the chloroplast envelope [38], but this point of view was fully challenged by lack of more direct evidence [39]. In the present study, using stably transformed plants with an AtSUC4-GFP construct under a native promoter, we demonstrated that AtSUC4 was PM-localized, which was confirmed by two other additional approaches of transient expression and Immunogold label systems (Figure 2). Moreover, the deficiency of *AtSUC4* led to less sucrose accumulation in the root of *atsuc4* mutants under high sucrose concentration (Table 1), implying the sucrose import mediated by AtSUC4 from the extracellular space to the cytoplasm. These observations provided clear evidence that AtSUC4 physiologically functions at the PM in root, the primary site for apoplastic sucrose import. Therefore, the alleviation of sucrose toxicity in root under high sucrose treatment in *atsuc4* mutant was supported by the sucrose import activity of AtSUC4.

Sucrose metabolism plays pivotal roles in development and stress response, mainly by generating a range of sugars as metabolites to fuel growth and as signals to regulate gene expression for crosstalk with hormonal signalling. This is achieved by the generation of sugar signalling molecules such as sucrose itself, glucose and trehalose-6-phosphate or perhaps by the signalling role exerted by the metabolic process itself [40,41]. Therefore, sucrose transport, synthesis and degradation are very important in regulating plant growth. To date, SUCs and SWEETs have been characterized as the two main types of proteins responsible for sucrose transport in plants. *Arabidopsis* genome contains nine *SUC*s, and five of them were found to be differentially expressed between the *atsuc4* mutant and WT under 6% sucrose supplementation, which *AtSUC2*, *4* and *5* were down-regulated, whereas *AtSUC1* and *3* were up-regulated in *suc4-1* (Figure 4A), suggesting that more *AtSUC*s were decreased in *suc4-1*. The clade III member of SWEET family in *Arabidopsis* AtSWEET9-15 and one member of clade V AtSWEET16 have been identified to have sucrose transport activity [3, 42]. As SWEETs facilitate the sugar transport along the sugar gradient, 6% sucrose treatment inhibited the expression of *AtSWEET11, 12* and *15*, but only induced *AtSWEET14* and *16* expression in *suc4-1* (Figure 4A), indicating that a larger number of *AtSWEETs* which was responsible for sucrose transport tend to be repressed in *suc4-1*. Accordingly, we proposed that the notably decreased sucrose accumulation in the *atsuc4* mutants could be a result of the more down-regulated expression of *AtSUC*s and *AtSWEET*s, which are responsible for sucrose transport. It was well known that AtSUC2, functions as a high-affinity, low-capacity transporter, is essential for phloem loading for long-distance sucrose transport from source to sink [43]. The expression of *AtSUC2* was decreased in *atsuc4* mutant (Figure 4A), and was induced by increasing sucrose treatment (Supplemental Figure S8), showing the co-expression pattern of *AtSUC2* and *AtSUC4* under high sucrose condition. Furthermore, the interaction between AtSUC2 and AtSUC4 was found [43], and overexpression of *AtSUC4* and inclusion of *adg1*, *tmt1*, *tmt2* in *atsuc2* mutant could partially rescue the dwarf phenotype [44]. Accordingly, probably *AtSUC2* and *AtSUC4* might be in a complex network to regulate root growth under high sucrose condition. Computational analysis of *cis*-acting regulatory elements in promoters of *AtSUC*s showed that ABA-responsive element (ABRE) was distributed in most of *AtSUC*s, including *AtSUC1* and *AtSUC3* [45]. Furthermore, a bZIP transcriptional factor ABI5, involved in the ABA signalling pathway, was found to bind to ABRE in the context of the *AtSUC1* promoter using yeast-one hybrid assay, and negatively regulating the *AtSUC1* expression level [46]. In the present study, *ABI5* was repressed in the *atsuc4* mutant compared with WT under 6% sucrose treatment (Figure 4C), which thus contributes to the promotion of *AtSUC1* accumulation. Although there is no direct evidence that ABI5 could bind to ABRE in the *AtSUC3* promoter, we speculated that ABI5 might affect the *AtSUC3* expression in a similar way to that in *AtSUC1*.

Sucrose can be degraded by sucrose synthase (SUS; EC 2.4.1.13) into hexose or their derivatives, which are then used in diverse ways. The transcript levels of *AtSUS1, 4* and *5* and *AtCINV1* were increased, whereas sucrose synthesis-related genes, including two *AtSPSs* (*AtSPS1* and *AtSPS3*) and *AtSPP2*, were decreased in the *suc4-1* plants compared with WT (Figure 4A), indicating that the pathway of sucrose degradation was active, but the sucrose synthesis was blocked by the deficiency of *AtSUC4*. Taken together, these data suggest that *AtSUC4* regulates root growth by affecting the expression of many sucrose metabolic enzymes, which reduce sucrose inflow and biosynthesis and increase sucrose degradation in intracellular.

Evidence from some studies highlights the central role of auxin in generation and maintenance of primary root meristems [17, 47,48]. Thus, sucrose and auxin could operate coordinately during root growth. Interestingly, the root length and IAA content of *atsuc4* mutants were higher than that of WT under 6% sucrose treatment (Figure 3A and Table 2). Consistent with this, RNA-seq data showed that the expression of the genes related to IAA biosynthesis (*YUC2*, *6*) and transporters (*PIN1*, *4*) were significantly up-regulated in *suc4-1* under high-sucrose (Figure 4C). Since lower sucrose content was measured in *atsuc4* mutants, and sucrose has been identified as a signal molecule, it is therefore speculated that more sucrose could active expression of genes responsible for IAA biosynthesis and transport. The *PLT, SCR* and *SHR* genes are required to define the root–stem cell niche [49,50]. Meanwhile, *PLT* in turn regulates the auxin accumulation in the quiescent centre both through transport (*PIN4*) and biosynthesis (*YUCs*) [51,52]. According to RNA-seq data, *AtPLT1*, *2* and *AtSHR* were significantly up-regulated in *suc4-1* compared with WT at 6% sucrose application (Figure 4C). Based on the results presented here, we proposed that the higher content of IAA provoked the expression of *AtPLT1*, *2* and *AtSHR* in *suc4-1* compared with WT, which contribute to display the longer primary root under high sucrose. The *aux/iaa* mutants, including *iaa1, 2, 13, 6, 17, 19* and *28,* had reduced multiple auxin responses, with shorter roots than WT [53]. In our study, the expression levels of two *Aux/IAAs* (*IAA6*, *19*) in the *atsuc4* mutant were significantly higher than in the WT in the treatment with 6% sucrose (Figure 4C), contributing to the longer root length in the *atsuc4* mutant accordingly. The interaction between sucrose and IAA has been revealed, in which auxin signalling factor significantly affected the accumulation of sucrose, while sucrose could regulate the auxin signalling [54,55]. Our results indicated that *AtSUC4* influenced the expression of IAA-related genes, and we tested whether IAA has an impact on *AtSUC4* accumulation in turn. However, the result showed that no obvious change occurred in GUS activity under native *AtSUC4* promoter and *AtSUC4* expression under IAA treatment (Figure S9A and B), indicating that *AtSUC4* expression was not affected by IAA during seedling growth. It has been reported that sucrose not only provides the energy for plant growth and development, but also acts as a signal factor to regulate gene expression [56]. Hence, the RNA profiling studies revealed that the deficiency of *AtSUC4* decreased the sucrose content in *atsuc4* mutants root compared with WT under 6% sucrose treatment, with sucrose acting as a signal factor to increase the expression of IAA-related genes, therefore activated the IAA signalling transduction.

Studies have suggested that sucrose and ABA are provital molecular signals that participate in regulating diverse developmental processes in plant [57,58]. It has been reported that manipulation of strawberry FaSUT1 expression is positively correlated with sucrose and ABA content [57]. Similarly, as shown in Table 1 and Supplemental Figure S5, the deficiency of *AtSUC4* led to a strong decrease in sucrose content relative to WT under all the concentrations of exogenous sucrose, but had little effects on the content of glucose and fructose. Moreover, *suc4-1* had significantly lower of ABA content under both low (2%) and high (6%) sucrose concentrations, suggesting positive relationship between AtSUC4 expression and ABA synthesis. In addition, *NCED3*, a key gene that controls the synthesis of ABA, was significantly decreased in *suc4-1* compared with WT (Figure 4E). These results strongly indicated that AtSUC4 probably participates in the sucrose signalling, subsequently regulating the ABA synthesis in the root. ABA signal transduction is highly dependent on its synthesis [59,60]. Consistent with the less ABA in *suc4-1*, we found that the expression levels of seven ABA signal transduction genes (*PYL2*, *8*, *SnRK2.3*, *2.6*, *ABI3*, *4*, *5*) were significantly decreased in *suc4-1* with 6% sucrose supplementation, while *ABI1*, a member of group PP2C which has a negative regulatory effect on ABA signal transduction, was significantly up-regulated (Figure 4E). Similar to IAA, ABA could not affect the expression of *AtSUC4* during seedling growth (Figure S9C and D), suggesting that *AtSUC4* accumulation could not be regulated by ABA. Collectively, our data may indicate that the deficiency of *AtSUC4* reduced the inhibition of root elongation via ABA through repressing the ABA synthesis and signalling mediated by reducing sucrose content.

Conclusions

This study demonstrated a novel role of AtSUC4 involved in high sucrose mediated-inhabitation in root growth. We found that *AtSUC4* was induced by sucrose, and the deficiency of *AtSUC4* resulted in alleviation of sucrose toxicity in root under high sucrose condition, which might be ascribed to reduced sucrose and ABA accumulation and increased IAA levels. The gene expression of sucrose-related, ABA and IAA signalling pathways were altered in *suc4-1* mutant plants under high sucrose. These results provide new insights into the mechanism in which AtSUC4 regulates sucrose translocation when the extracellular sucrose concentration is high. However, how AtSUC4 coordinates with

sucrose, IAA and ABA pathways remains to be elucidated so that we can fully understand the AtSUC4-mediated modulation of root growth under high sucrose condition.

Authors' contributions

Conceptualization, J.L. and C.P.; Formal analysis, S.L., L.Z., J.G. and T.D.; Investigation, S.L., L.Z., J.G. T.D. and Y.W.; Methodology, S.L.; Writing – original draft, S.L. and J.L.; Writing – review & editing, J.L. and C.P.

Disclosure statement

No potential conflict of interest was reported by the authors.

Funding

This research is supported by the [National Natural Science Foundation of China] under grant [nos. 30771759, 31470681 and 31800560]; [National Key Research and Development Program of China] under grant [no. 2016YFD0600104]; [Natural Science Foundation of Guangdong Province of China] under grant [no. 2016A030311032]; [Guangzhou Science and Technology Program] under grant [no. 201607020024] and [Foundation of Young Creative Talents in Higher Education of Guangdong Province] under grant [no. 2017KQNCX017].

Data availability statement

The data that support the findings of this study are openly available in [National Center for Biotechnology Information Sequence Read Archive] at [https://www.ncbi.nlm.nih.gov/sra/], reference number [PRJNA666009].

References

[1] Ruan YL, Jin Y, Yang YJ, et al. Sugar input, metabolism, and signaling mediated by invertase: roles in development, yield potential, and response to drought and heat. Mol Plant. 2010;3(6):942–955.
[2] Wormit A, Trentmann O, Feifer I, et al. Molecular identification and physiological characterization of a novel monosaccharide transporter from *Arabidopsis* involved in vacuolar sugar transport. Plant Cell. 2006;18(12):3476–3490.
[3] Braun DM, Wang L, Ruan YL. Understanding and manipulating sucrose phloem loading, unloading, metabolism, and signalling to enhance crop yield and food security. J Exp Bot. 2014;65(7):1713–1735.
[4] Lohaus G, Hussmann M, Pennewiss K, et al. Solute balance of a maize (*Zea mays L.*) source leaf as affected by salt treatment with special emphasis on phloem retranslocation and ion leaching. J. Exp. Bot. 2000;5:1721–1732.
[5] Geiger D. Plant sucrose transporters from a biophysical point of view. Mol Plant. 2011;4(3):395–406.
[6] Julius BT, Leach KA, Tran TM, et al. Sugar transporters in plants: new insights and discoveries. Plant Cell Physiol. 2017;58(9):1442–1460.
[7] Kühn C. A comparison of the sucrose transporter systems of different plant species. Plant Biol. 2003;5(3):215–232.
[8] Sauer N. Molecular physiology of higher plant sucrose transporters. FEBS Lett. 2007;581(12):2309–2317.
[9] Eom JS, Cho JI, Reinders A, et al. Impaired function of the tonoplast-localized sucrose transporter in rice, OsSUT2, limits the transport of vacuolar reserve sucrose and affects plant growth. Plant Physiol. 2011;157(1):109–119.
[10] Sivitz AB, Reinders A, Ward JM. *Arabidopsis* sucrose transporter *AtSUC1* is important for pollen germination and sucrose-induced anthocyanin accumulation. Plant Physiol. 2008;147(1):92–100.
[11] Gottwald JR, Krysan PJ, Young JC, et al. Genetic evidence for the in planta role of phloem-specific plasma membrane sucrose transporters. Proc Natl Acad Sci U S A. 2000;97(25):13979–13984.
[12] Schulz A, Beyhl D, Marten I, et al. Proton-driven sucrose symport and antiport are provided by the vacuolar transporters SUC4 and TMT1/2. Plant J. 2011;68(1):129–136.
[13] Schneider S, Hulpke S, Schulz A, et al. Vacuoles release sucrose via tonoplast-localised SUC4-type transporters. Plant Biol (Stuttg). 2012;14(2):325–336.
[14] Freixes S, Thibaud M-C, Tardieu F, et al. Root elongation and branching is related to local hexose concentration in *Arabidopsis thaliana* seedlings. Plant Cell Environ. 2002;25(10):1357–1366.
[15] Kircher S, Schopfer P. Photosynthetic sucrose acts as cotyledon-derived long-distance signal to control root growth during early seedling development in *Arabidopsis*. Proc Natl Acad Sci U S A. 2012;109(28):11217–11221.
[16] Durand M, Mainson D, Porcheron B, et al. Carbon source-sink relationship in *Arabidopsis thaliana*: the role of sucrose transporters. Planta. 2018;247(3):587–611.
[17] Hoth S, Niedermeier M, Feuerstein A, et al. An ABA-responsive element in the *AtSUC1* promoter is involved in the regulation of *AtSUC1* expression. Planta. 2010;232(4):911–923.
[18] Chaiwanon J, Wang W, Zhu JY, et al. Information integration and communication in plant growth regulation. Cell. 2016;164(6):1257–1268.
[19] Macgregor DR, Deak KI, Ingram PA, et al. Root system architecture in *Arabidopsis* grown in culture is regulated by sucrose uptake in the aerial tissues. Plant Cell. 2008;20(10):2643–2660.
[20] Zhang S, Peng F, Xiao Y, et al. Peach *PpSnRK1* participates in sucrose-mediated root growth through auxin signaling. Front Plant Sci. 2020;11:409.
[21] Antoni R, Gonzalez-Guzman M, Rodriguez L, et al. PYRABACTIN RESISTANCE1-LIKE8 plays an important role for the regulation of abscisic acid signaling in root. Plant Physiol. 2013;161(2):931–941.
[22] Yu B, Wang Y, Zhou H, et al. Genome-wide binding analysis reveals that ANAC060 directly represses sugar-induced transcription of *ABI5* in *Arabidopsis*. Plant J. 2020;103(3):965–979.

[23] Yuan TT, Xu HH, Zhang KX, et al. Glucose inhibits root meristem growth via *ABA INSENSITIVE 5*, which represses PIN1 accumulation and auxin activity in *Arabidopsis*. Plant Cell Environ. 2014;37(6):1338–1350.
[24] Clough SJ, Bent AF. Floral dip: a simplified method for Agrobacterium-mediated transformation of *Arabidopsis thaliana*. Plant J. 1998;16(6):735–743.
[25] Schneider S, Beyhl D, Hedrich R, et al. Functional and physiological characterization of *Arabidopsis* INOSITOL TRANSPORTER1, a novel tonoplast-localized transporter for myo-inositol. Plant Cell. 2008;20(4):1073–1087.
[26] Robert S, Zouhar J, Carter C, et al. Isolation of intact vacuoles from *Arabidopsis* rosette leaf-derived protoplasts. Nat Protoc. 2007;2(2):259–262.
[27] Fan RC, Peng CC, Xu YH, et al. Apple sucrose transporter SUT1 and sorbitol transporter SOT6 interact with cytochrome b5 to regulate their affinity for substrate sugars. Plant Physiol. 2009;150(4):1880–1901.
[28] Karimi M, Inze D, Depicker A. GATEWAY vectors for Agrobacterium-mediated plant transformation. Trends Plant Sci. 2002;7(5):193–195.
[29] Ma X, Zhang Q, Zhu Q, et al. A robust CRISPR/Cas9 system for convenient, high-efficiency multiplex genome editing in monocot and dicot plants. Mol Plant. 2015;8(8):1274–1284.
[30] Jiang SY, Vanitha J, Bai Y, et al. A novel binary T-vector with the GFP reporter gene for promoter characterization. Plos One. 2014;9(9):e107328.
[31] Chen ML, Fu XM, Liu JQ, et al. Highly sensitive and quantitative profiling of acidic phytohormones using derivatization approach coupled with nano-LC-ESI-Q-TOF-MS analysis. J Chromatogr B Analyt Technol Biomed Life Sci. 2012;905:67–74.
[32] Deng GM, Zhang S, Yang QS, et al. *MaMYB4*, an R2R3-MYB repressor transcription factor, negatively regulates the biosynthesis of anthocyanin in banana. Front Plant Sci. 2021;11:600704.
[33] Kühn C, Grof CP. Sucrose transporters of higher plants. Curr Opin Plant Biol. 2010;13(3):287–297.
[34] Weise A, Barker L, Kühn C, et al. A new subfamily of sucrose transporters, SUT4, with low affinity/high capacity localized in enucleate sieve elements of plants. Plant Cell. 2000;12(8):1345–1355.
[35] Reinders A, Sivitz AB, Starker CG, et al. Functional analysis of LjSUT4, a vascular sucrose transporter from *Lotus japonicas*. Plant Mol Biol. 2008;68(3):289–299.
[36] Chincinska I, Gier K, Krugel U, et al. Photoperiodic regulation of the sucrose transporter StSUT4 affects the expression of circadian-regulated genes and ethylene production. Front Plant Sci. 2013;4:26.
[37] Ho LH, Lee YI, Hsieh SY, et al. *GeSUT4* mediates sucrose import at the symbiotic interface for carbon allocation of heterotrophic *Gastrodia elata* (Orchidaceae). Plant Cell Environ. 2020;44(1):20–33.
[38] Ferro M, Salvi D, Riviere-Rolland H, et al. Integral membrane proteins of the chloroplast envelope: identification and subcellular localization of new transporters. Proc Natl Acad Sci U S A. 2002;99(17):11487–11492.
[39] Doidy J, Grace E, Kühn C, et al. Sugar transporters in plants and in their interactions with fungi. Trends Plant Sci. 2012;17(7):413–422.
[40] O'Hara LE, Paul MJ, Wingler A. How do sugars regulate plant growth and development? New insight into the role of trehalose-6-phosphate. Mol Plant. 2013;6(2):261–274.
[41] Ruan Y, Patrick JW, Bouzayen M, et al. Molecular regulation of seed and fruit set. Trends Plant Sci. 2012;17(11):656–665.
[42] Chen LQ, Cheung LS, Feng L, et al. Transport of sugars. Annu Rev Biochem. 2015;84:865–894.
[43] Srivastava AC, Ganesan S, Ismail IO, et al. Functional characterization of the *Arabidopsis* AtSUC2 sucrose/H + symporter by tissue-specific complementation reveals an essential role in phloem loading but not in long-distance transport. Plant Physiol. 2008;148(1):200–211.
[44] Schulze WX, Reinders A, Ward J, et al. Interactions between co-expressed *Arabidopsis* sucrose transporters in the split-ubiquitin system. BMC Biochem. 2003;4(1):3–10.
[45] Anaokar S, Liu H, Keereetaweep J, et al. Mobilizing vacuolar sugar increases vegetative triacylglycerol accumulation. Front Plant Sci. 2021;12:1664.
[46] Ibraheem O, Botha CE, Bradley G. In silico analysis of cis-acting regulatory elements in 5′ regulatory regions of sucrose transporter gene families in rice (*Oryza sativa* Japonica) and *Arabidopsis thaliana*. Comput Biol Chem. 2010;34(5-6):268–283.
[47] Dello IR, Nakamura K, Moubayidin L, et al. A genetic framework for the control of cell division and differentiation in the root meristem. Science. 2008;322(5906):1380–1384.
[48] Overvoorde P, Fukaki H, Beeckman T. Auxin control of root development. Cold Spring Harb Perspect Biol. 2010;2(6):a1537.
[49] Aida M, Beis D, Heidstra R, et al. The PLETHORA genes mediate patterning of the *Arabidopsis* root stem cell niche. Cell. 2004;119(1):109–120.
[50] Moreno-Risueno MA, Sozzani R, Yardimci GG, et al. Transcriptional control of tissue formation throughout root development. Science. 2015;350(6259):426–430.
[51] Galinha C, Hofhuis H, Luijten M, et al. PLETHORA proteins as dose-dependent master regulators of *arabidopsis* root development. Nature. 2007;449(7165):1053–1057.
[52] Santuari L, Sanchez-Perez GF, Luijten M, et al. The PLETHORA gene regulatory network guides growth and cell differentiation in *Arabidopsis* roots. Plant Cell. 2016;28(12):2937–2951.
[53] Mockaitis K, Estelle M. Auxin receptors and plant development: a new signaling paradigm. Annu Rev Cell Dev Biol. 2008;24:55–80.
[54] Yuan Y, Mei L, Wu M, et al. SlARF10, an auxin response factor, is involved in chlorophyll and sugar accumulation during tomato fruit development. J Exp Bot. 2018;69(22):5507–5518.
[55] Stokes ME, Chattopadhyay A, Wilkins O, et al. Interplay between sucrose and folate modulates auxin signaling in Arabidopsis. Plant Physiol. 2013;162(3):1552–1565.
[56] Ruan YL. Sucrose metabolism: gateway to diverse carbon use and sugar signaling. Annu Rev Plant Biol. 2014;65(4):33–67.
[57] Jia H, Wang Y, Sun M, et al. Sucrose functions as a signal involved in the regulation of strawberry fruit development and ripening. New Phytol. 2013;198(2):453–465.

[58] Yang Z, Zhang L, Diao F, et al. Sucrose regulates elongation of carrot somatic embryo radicles as a signal molecule. Plant Mol Biol. 2004;54(3):441–459.
[59] Zhu GH, Liu YG, Ye NH, et al. Involvement of the abscisic acid catabolic gene CYP707A2 in the glucose-induced delay in seed germination and post-germination growth of *Arabidopsis*. Physiol Plant. 2011;143(4):375–384.
[60] Dong H, Ma XN, Zhang P, et al. Characterization of *Arabidopsis thaliana* root-related mutants reveals ABA regulation of plant development and drought resistance. J Plant Growth Regul. 2020;39(3):1393–1401.

Biotechnology & Biotechnological Equipment

Article

Transcriptome analysis identifies key genes involved in anthocyanin biosynthesis in black and purple fruits (*Lycium ruthenicum* Murr. L) ›

Xuemei Bao, Xiaolong Gan, Guanghui Fan, Guangrui Liu, Xiaolin Ma, Baolong Liu & Yuan Zong

Pages: 553-560

Published online: 08 Sep 2022

Abstract | Full Text | References | PDF (1.5 MB) | EPUB | Supplemental

752 Views
1 CrossRef citations
0 Altmetric
OPEN ACCESS

Article

Arabidopsis sucrose transporter 4 (AtSUC4) is involved in high sucrose-mediated inhibition of root elongation ›

Siwen Liu, Jianmei Long, Liding Zhang, Jiayu Gao, Tiantian Dong, Ying Wang & Changcao Peng

Pages: 561-574

Published online: 08 Sep 2022

Abstract | Full Text | References | PDF (1.6 MB) | EPUB | Supplemental

812 Views
0 CrossRef citations
0 Altmetric

Article

Genome-wide identification, phylogeny and expression analyses of group III WRKY genes in cotton (*Gossypium hirsutum*) ›

Lijun Dong, Meng Wang, Xue Zhang, Jianfeng Liu & Shuling Zhang

Pages: 575-586

Published online: 08 Sep 2022

Abstract | Full Text | References | PDF (1.8 MB) | EPUB | Supplemental

554 Views
0 CrossRef citations
0 Altmetric

Article

Identification and quantification of anthocyanins of 62 blueberry cultivars via UPLC-MS ›

1355 Views

SCIENTIFIC REPORTS

OPEN

Selection and Validation of Reference Genes for mRNA Expression by Quantitative Real-Time PCR Analysis in *Neolamarckia cadamba*

Received: 9 November 2017
Accepted: 7 June 2018
Published online: 18 June 2018

Tian Huang[1,2], Jianmei Long[2], Si-Wen Liu[1,2], Zi-Wei Yang[1,2], Qi-Jin Zhu[1,2], Xiao-Lan Zhao[2] & Changcao Peng[1,2]

Neolamarckia cadamba **is an economically-important fast-growing tree species in South China and Southeast Asia. As a prerequisite first step for future gene expression studies, we have identified and characterized a series of stable reference genes that can be used as controls for quantitative real time PCR (qRT-PCR) expression analysis in this study. The expression stability of 15 candidate reference genes in various tissues and mature leaves under different conditions was evaluated using four different algorithms, i.e., geNorm, NormFinder, BestKeeper and RefFinder. Our results showed that *SAMDC* was the most stable of the selected reference genes across the set of all samples, mature leaves at different photosynthetic cycles and under drought stress, whereas *RPL10A* had the most stable expression in various tissues. *PGK* and *RPS25* were considered the most suitable reference for mature leaves at different developmental stages and under cold treatment, respectively. Additionally, the gene expression profiles of sucrose transporter 4 (NcSUT4), and 9-cis-epoxycarotenoid dioxygenase 3 (NcNCED3) were used to confirm the validity of candidate reference genes. Collectively, our study is the first report to validate the optimal reference genes for normalization under various conditions in *N. cadamba* and will benefit the future discovery of gene function in this species.**

Quantitative real-time polymerase chain reaction (qRT-PCR) is a powerful tool which monitors the entire PCR process in real-time. Currently, northern blot, microarray, qRT-PCR and high-throughput sequencing are the four common methods for gene expression analysis. Among them, qRT-PCR is most widely used for accurate quantification of gene expression because of its high sensitivity, accuracy, specificity and reproducibility and low cost[1–3]. However, the accuracy of gene expression is easily affected by the factors including RNA integrity, reverse transcription reaction efficiency, cDNA quality and genomic DNA contamination[4–7]. Hence, normalization is an essential step in qRT-PCR assay[5]. Among the multiple strategies proposed[8], the use of reference gene is the most popular method for data normalization[9]. Udvardi *et al.*[10] have illustrated eleven golden rules of qRT-PCR, among which a suitable reference gene should be stably expressed in the samples under a range of given experimental conditions, so as to ensure the accuracy and reproducibility of measurement in gene expression[11]. In contrast, inappropriate reference gene selection can lead to discrepancies in interpreting the qRT-PCR data, potentially leading to inappropriate conclusions regarding expression of target genes. Therefore, selection of appropriate reference genes is of great importance for data normalization in qRT-PCR analysis.

Numerous studies have indicated that the housekeeping genes involved in maintaining the basic metabolism of cell, such as *ACT* (*Actin*), *TUA* (*Alpha-tubulin*), *GAPDH* (*Glyceraldehyde 3-phosphate dehydrogenase*) and *18S rRNA*(*18S ribosomal RNA*) have been routinely used as internal controls in qRT-PCR and as the reference genes for standardized analysis in many plants species[12–14]. They were assumed to be stably expressed in various tissues at different developmental stage and under a wide range of conditions[15]. However, several recent reports showed that these traditional reference genes are not always stable in some specific conditions[16,17]. In addition, there is no

[1]State Key Laboratory for Conservation and Utilization of Subtropical Agro-bioresources, South China Agricultural University, Guangzhou, 510642, China. [2]Guangdong Key Laboratory for Innovative Development and Utilization of Forest Plant Germplasm, College of Forestry and Landscape Architecture, South China Agricultural University, Guangzhou, 510642, China. Tian Huang and Jianmei Long contributed equally to this work. Correspondence and requests for materials should be addressed to C.P. (email: ccpeng@scau.edu.cn)

reference gene universally expressed at constant level across all species under wide range of experimental conditions[18]. Thus, it is essential to systematically validate the stability of potential reference genes before their use in qRT-PCR assays in any new experimental organism.

Statistical algorithms such as geNorm[1], NormFinder[19] and Bestkeepeer[20] have been specifically developed for the evaluation of candidate reference genes stability and determination of the best reference in one or several specific experimental conditions. By using these programs, reference gene validation has been successfully carried out in many plant species, including *Arabidopsis*[21], rice[15], maize[22], soybean[23], radish[9], strawberry[24], orchardgrass[7], *Lycoris aurea*[25], banana[5], citrus[26], grape[27], poplar[28], litchi[29] and longan[30]. The reference genes identified in each species have been frequently used in the subsequent studies, which accelerated to explore the mechanisms of key biological processes in plant species.

Neolamarckia cadamba, a member of the Rubiaceae family, is widely distributed in South China and South Asia, and is cultivated due to its inherent economic value in multiple aspects[31]. It has been praised as "a miraculous tree" since the World Forest Congress in 1972 due to its fast growth[32,33], reaching heights of 17 m and trunk diameters of 25 cm within 9 years of growth under normal conditions[34]. Therefore, it is a good choice to use *N. cadamba* for the forest rehabilitation in tropical regions. In addition, *N. cadamba* lumber is also a useful source for raw materials in paper production, furniture, building and biomass utilization. *N. cadamba* has also attracted lots of attention on the medicinal value including application in the treatment of various ailments and extraction of bioactive compounds[35]. Recently, *N. cadamba* was used as model plant to study the xylogenesis during wood formation[31], although these studies were primarily physiological in nature, and did not include molecular details such as transcriptional regulation of these processes. In order to explore the mechanism of wood formation and fast growth in *N. cadamba*, gene expression analysis is one of the most important steps. However, so far there is no report on the identification of reference genes for normalization in gene expression detection in *N. cadamba*.

To identify suitable reference genes for accurate quantification of target genes in *N. cadamba*, fifteen potential reference genes including Actin 1 (ACT1), Actin 7 (ACT7), Actin 11 (ACT11), Tubulin alpha 2 (TUA2), Tubulin alpha 4 (TUA4), Tubulin alpha 5 (TUA5), Elongation factor 1-alpha (EF-1-α), Ribulose bisphosphate carboxylase (Rubisco), Ribosomal protein S25 (RPS25), Ribosomal protein L10A (RPL10A), Malate dehydrogenase (MDH), Glyceraldehyde-3-phosphate dehydrogenase (GAPDH), Phosphoglycerate kinase (PGK), S-adenosylmethionine decarboxylase (SAMDC), F-Box protein (F-BOX) were selected, and their sequences retrieved from our previously generated transcriptome data[31]. The expression stability of the selected candidates was evaluated by qRT-PCR using a set of cDNAs from 22 different samples of *N. cadamba*, which included various tissues, mature leaves at different developmental stages and photosynthetic cycles, and under cold and drought treatments. Optimal reference genes were suggested for each experimental condition by using four different gene expression analysis programs. Furthermore, sucrose transporter 4 (*NcSUT4*), responsible for sucrose transportation, and 9-cis-epoxycarotenoid dioxygenase 3 (*NcNCED3*), a key enzyme involved in the synthesis of ABA, were used to confirm the reliability and effectiveness of the selected reference genes. Our study provided a list of suitable reference genes for normalization of qRT-PCR analyses, which is anticipated to facilitate the gene expression analyses in *N. cadamba*.

Results

Primers specificity, PCR efficiencies and expression profile of the candidate reference genes.

A single PCR product from each primer pair of candidate reference genes was amplified with expected size by agarose gel electrophoresis analysis (see Supplementary Fig. S1). Specific amplifications were also confirmed by melting curves with a single peak in each candidate reference genes (see Supplementary Fig. S2). Standard curves were generated using serial dilution series, and high linear correlations ($R^2 > 0.99$) were detected for in all genes (see Supplementary Table S1). The PCR amplification efficiencies for fifteen genes varied from 94.5% for *ACT1* to 116.3% for *RPS25* (see Supplementary Table S1).

The expression levels of the candidate reference genes were determined by qRT-PCR across 5 subsets of samples including different tissues, developmental stages, photosynthetic cycles, cold and drought treatments. The candidate reference genes displayed wide range of accumulation level across all the tested samples, with threshold cycle (CT) values spanning 19.48–31.79 (Fig. 1). Among them, *Rubisco* exhibited the highest expression abundance, with median CT value of 21.93. Both *GAPDH* and *MDH* showed relative high expression, with median CT values of 22.44 and 23.69, respectively. In contrast, *RPL10A* expressed lowest, with a median CT value of 30.38 (Fig. 1). Additionally, candidate genes showed distinct expression variability, among which *SAMDC* and *RPS25* displayed relative narrower CT range values than others (Fig. 1), showing that these genes expressed more stably. Importantly, however, these results revealed that none of the selected reference genes were expressed constantly in all samples tested from *N. cadamba*. Hence, it was necessary to validate suitable reference genes for normalization under different experimental conditions in *N. cadamba*.

Expression stability of candidate reference genes.

geNorm analysis. In order to rank the candidate reference genes under tested conditions, four commonly used gene expression analysis software programs, i.e., geNorm, NormFinder, BestKeeper, and RefFinder were applied to assess the expression stabilities of fifteen candidate reference genes. In geNorm analysis, the expression stability measure M was calculated for each gene based on the non-normalized expression level Q. A cut-off value of 1.5 was recommended and set for M to evaluate gene stability. For each sample groups in our study, M value in all the candidate genes was lower than 1.5 (Fig. 2a–e). All fifteen candidate genes in each sample group set were ranked by M value. Base on this analysis, a lower M value represents a higher degree of expression stability for the selected reference gene. For tissue group, *RPL10A* and *SAMDC* were the top ranked candidates, followed by *ACT11* and *RPS25* (Fig. 2a). *SAMDC*, *PGK*, *ACT7* and *RPL10A* were the four most stable reference genes in the mature leaves at different developmental stage (Fig. 2b). Among the samples of different photosynthetic cycles in a day, *ACT7*, *SAMDC* and *ACT1* exhibited the three

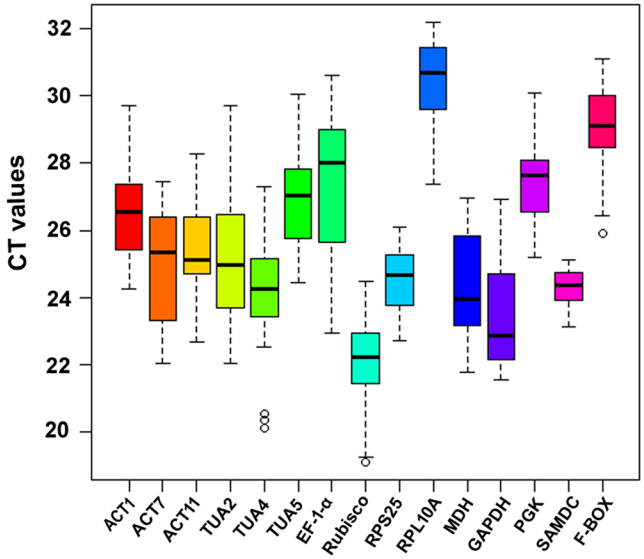

Figure 1. Distribution of threshold cycle (CT) values of 15 candidate reference genes across all 22 samples. The solid line within each box represents the 50th percentile. The lower boundary and upper boundary of each box represents the 25th and 75th percentile, respectively. The circles represent potential outliers.

most stable reference genes (Fig. 2c). *SAMDC* and *RPS25* with M value of about 0.3 ranked as the most stable genes in both groups of drought and cold treatment (Fig. 2d–e). When all samples were mixed and tested, most of the candidate genes had higher M values than their respective calculation in each group, four of which including *EF-1-α*, *TUA2*, *GAPDH* and *ACT7* even excessed the cut-off value of 1.5. *SAMDC* and *RPS25* were the two most stable candidates with M value of 0.78 (Fig. 2f).

In certain conditions, multiple references might be more reliable than a single one for normalization in qRT-PCR assay[1]. To determine the minimum number of reference genes for accurate normalization, GeNorm was applied through calculating the pairwise variation (Vn/n + 1) between two sequential normalization factors to determine whether additional reference gene is necessary. Utilizing this software program, 0.15 was set as a cut-off for V value to determine whether additional reference genes be required[1]. In our study, for each sample group, a pairwise variation value of V2/3 was lower than 0.15 (Fig. 3), suggesting that only two reference genes were sufficient for normalization by qRT-PCR. Specifically, combination of *RPL10A* and *SAMDC* were the optimal reference genes for different tissues, while *PGK* and *SAMDC* were optimal for mature leaves at distinct development stages. Interestingly, combination of *RPS25* and *SAMDC* were the best choice for normalization under both drought and cold stress conditions, whereas *ACT7* and *SAMDC* were the best combination for samples under different photosynthetic cycles. However, when all the samples were analyzed simultaneously, nine reference genes were required since V8/9 was higher than 0.15 whereas V9/10 was below the cut-off value (Fig. 3). This suggested that no reasonable number of reference genes would be suitable for comparing expression levels between large numbers of tissues/growth conditions since the requirement to use nine references to calculate gene expression by qRT-PCR would be unreasonably time consuming. Alternatively, it may have been possible that a pairwise analysis cut-off value of 0.15 was too strict for this case, and this result also suggested that it is hard to find out universal reference genes for samples under different experimental conditions. Despite this limitation, we were able to identify suitable reference genes that exhibited specificity under a certain conditions.

NormFinder analysis. To further confirm the stability of the reference genes obtained by the geNorm software, we applied the NormFinder software for optimal normalization genes identification among the candidates. The statistic algorithm of NormFinder is different from geNorm, the former considers intra- and intergroup variations for the calculation of normalization factors (NF), which were used to estimate the stability values of each reference gene. For the sample group of different tissues, *RPL10A*, *ACT7*, *SAMDC* and *ACT11* were the four top ranked candidates (Fig. 4a). Five stable references including *F-BOX*, *PGK*, *SAMDC*, *RPL10A*, and *ACT7* were top ranked in the sample set of mature leaves at different development stages, which showed good agreement with geNorm analysis but with slight changes in the ranking order (Fig. 4b). For the sample set of different photosynthetic cycle, *ACT7* and *SAMDC* were the most stable candidates (Fig. 4c). *SAMDC* was the most suitable references under drought stress (Fig. 4d), whereas it was ranked second according to geNorm. Consistent with geNorm analysis, *Rubisco* and *RPS25* were the best candidates for normalization under cold condition (Fig. 4e). For all the sample groups, the three top ranked references were *SAMDC*, *F-BOX* and *RPL10A*, of which *SAMDC* was the best single candidate with stability value of 0.548.

BestKeeper analysis. The expression stability of the candidate reference genes were reanalyzed by another program BestKeeper. CT value and efficiencies of each primer were used as input data to calculate the standard deviation (SD), in which lower SD suggested higher stability of reference gene. *ACT7*, which had the lowest SD value

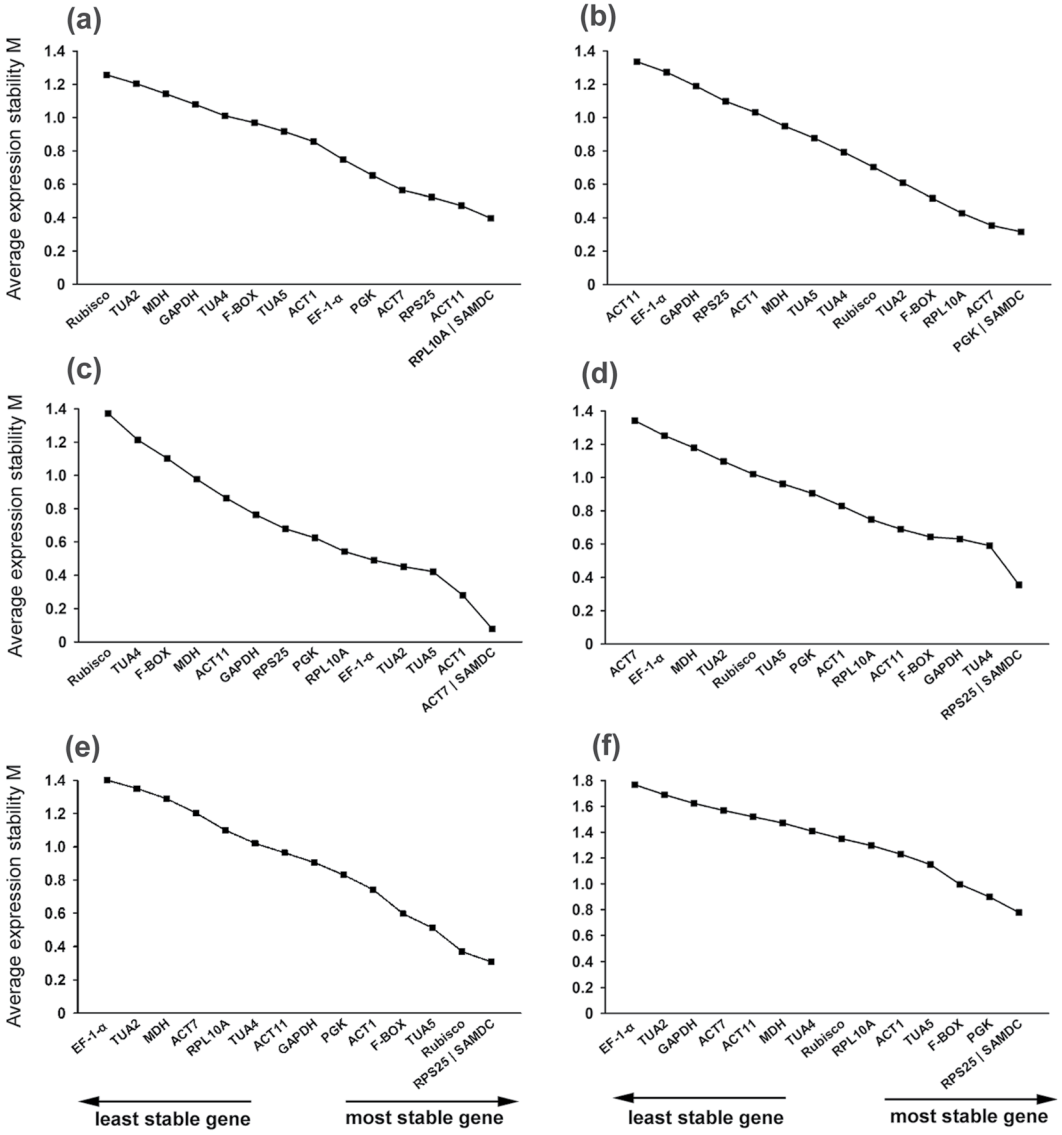

Figure 2. Average expression stability values (M) of 15 candidate reference genes calculated by geNorm. (**a**) Tissue; (**b**) developmental stage; (**c**) photosynthetic cycles; (**d**) drought treatment; (**e**) cold treatment; (**f**) all of the samples in our given conditions.

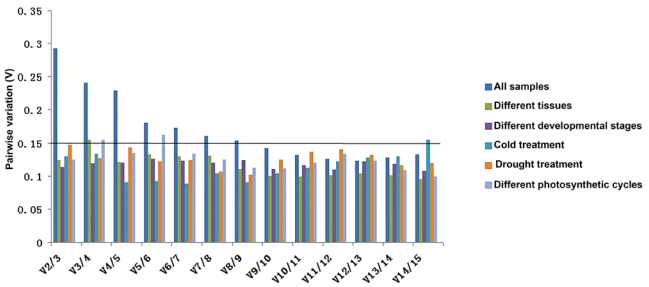

Figure 3. Determination of the optimal number of reference genes for normalization in the tested experimental conditions. geNorm was used to calculate the normalization factor (NF) from at least two genes; the variable V defines the pair-wise variation between two sequential NF values.

of 0.36, was the most stable candidate in the sample group of different tissues, whereas *MDH* was the least stable gene with the highest SD (Table 1). *PGK*, *RPL10A* and *SAMDC* had SD value of less than 0.6, which were the three top ranked references in the sample set of mature leaves at different developmental stage. *SAMDC* were the most

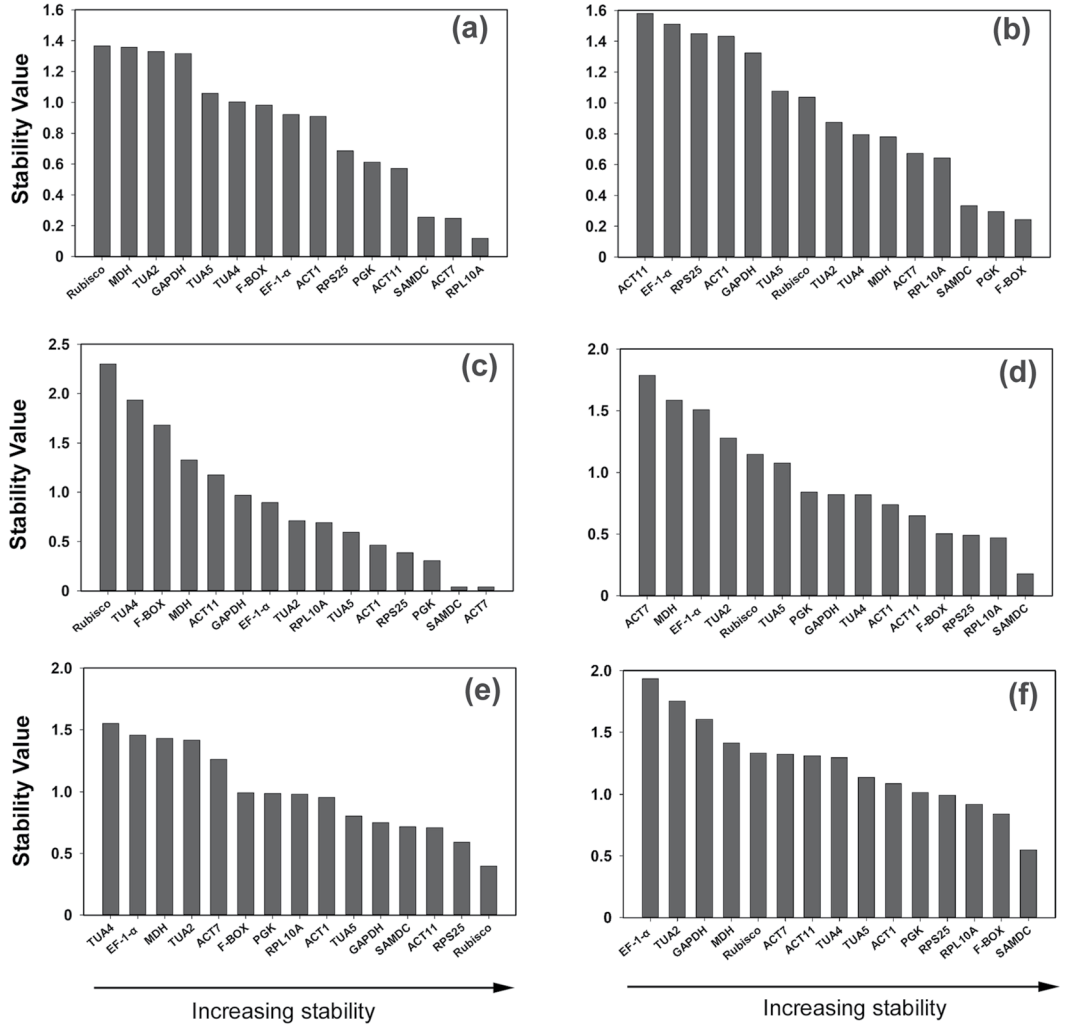

Figure 4. The stability value of 15 candidate reference genes calculated by NormFinder. The lower value indicated the higher stability of gene expression. (**a**) Tissue; (**b**) developmental stage; (**c**) photosynthetic cycles; (**d**) drought treatment; (**e**) cold treatment; (**f**) all of the samples in our given conditions.

stable gene in the sample set of different photosynthetic cycles. Similarly, for the abiotic stress, *SAMDC* was the most suitable reference gene, followed by *RPS25* and *RPL10A* under both cold and drought conditions, respectively. When considering all samples in our study, *F-BOX* and *SAMDC* were the top two ranked reference genes.

RefFinder analysis. The three different programs used for stability analysis showed different ranking orders of candidate reference genes. Therefore, to obtain a consensus result, we used RefFinder program to reorder the selected reference genes comprehensively (Table 2), and the integrated comparison of the evaluation by four programs was shown in Supplementary Table S2. The ranking order by RefFinder showed that the top two ranked reference gene were in agreement with the list yielded by geNorm under all given experimental conditions. *Rubisco* was ranked at the bottom for the group of different tissues and photosynthetic cycle; *EF-1-α* was at the bottom position for cold treatment and all samples tested. *ACT11* and *ACT7* were the least stable genes in the samples of different developmental stage and drought stress, respectively.

Validation of reference genes. In order to verify the stability of reference gene in this study, we analyzed the expression levels of sucrose transporter 4 (*NcSUT4*) and 9-cis-epoxycarotenoid dioxygenase 3 (*NcNCED3*) using the selected reference genes. Sucrose transporters are responsible for phloem loading, transport and unloading of sucrose from source to sink[36]. *NCED* genes encode key enzymes for the synthesis of ABA, and are induced under drought stress[37,38]. The transcript levels of *NcSUT4* were quantified in the samples of different developmental stages and different tissues, using two stable reference genes and two unstable reference genes as endogenous controls, respectively (Fig. 5a,b). As shown in Fig. 5a, when using the two stable reference genes (*SAMDC* or *PGK*) for normalization, the expression level of *NcSUT4* was increased in the mature leaves from March to December, with high peak in June. However, when using the least stable reference genes *ACT7* and *EF-1-α* as normalization factors, *NcSUT4* exhibited totally different expression pattern, with gradually decrease across different development stages of mature leaves. In various tissues, relative higher transcript abundance of

Ranking	Tissue	Developmental stage	photosynthetic cycle	Drought treatment	Cold treatment	Total
1	*ACT7* (1.37 ± 0.36)	*PGK* (1.83 ± 0.51)	*SAMDC* (0.35 ± 0.09)	*RPL10A* (0.61 ± 0.19)	*RPS25* (0.67 ± 0.17)	*SAMDC* (1.43 ± 0.35)
2	*RPL10A* (1.43 ± 0.45)	*RPL10A* (1.91 ± 0.58)	*ACT7* (0.64 ± 0.14)	*SAMDC* (1.04 ± 0.25)	*SAMDC* (1.35 ± 0.33)	*F-BOX* (2.71 ± 0.79)
3	*SAMDC* (1.53 ± 0.37)	*SAMDC* (2.1 ± 0.51)	*PGK* (1.32 ± 0.37)	*RPS25* (1.38 ± 0.33)	*TUA5* (1.81 ± 0.51)	*RPS25* (2.78 ± 0.68)
4	*EF-1-α* (1.96 ± 0.58)	*F-BOX* (2.67 ± 0.78)	*RPS25* (1.57 ± 0.39)	*ACT1* (1.41 ± 0.38)	*Rubisco* (1.87 ± 0.41)	*PGK* (2.85 ± 0.78)
5	*PGK* (2 ± 0.56)	*ACT7* (2.79 ± 0.68)	*ACT1* (1.6 ± 0.41)	*ACT11* (1.75 ± 0.46)	*RPL10A* (2.6 ± A0.79)	*RPL10A* (3.33 ± 1.01)
6	*F-BOX* (2.11 ± 0.62)	*TUA5* (2.94 ± 0.75)	*TUA5* (1.6 ± 0.41)	*F-BOX* (1.79 ± 0.52)	*ACT11* (2.64 ± 0.64)	*TUA5* (3.58 ± 0.96)
7	*TUA5* (2.17 ± 0.6)	*TUA2* (3.09 ± 0.76)	*RPL10A* (1.94 ± 0.55)	*TUA5* (1.97 ± 0.53)	*F-BOX* (2.94 ± 0.87)	*ACT11* (3.86 ± 0.98)
8	*ACT11* (2.26 ± 0.57)	*RPS25* (3.09 ± 0.76)	*TUA2* (2.13 ± 0.49)	*TUA4* (2.37 ± 0.59)	*TUA4* (3.1 ± 0.77)	*ACT1* (4 ± 1.06)
9	*RPS25* (2.46 ± 0.6)	*MDH* (3.45 ± 0.83)	*EF-1-α* (2.54 ± 0.61)	*PGK* (2.52 ± 0.67)	*ACT1* (3.26 ± 0.88)	*TUA4* (4.41 ± 1.07)
10	*ACT1* (2.54 ± 0.66)	*TUA4* (3.52 ± 0.86)	*ACT11* (3.11 ± 0.79)	*MDH* (3.76 ± 0.91)	*PGK* (3.61 ± 0.99)	*MDH* (4.94 ± 1.2)
11	*TUA4* (3.22 ± 0.77)	*EF-1-α* (3.97 ± 1.11)	*GAPDH* (3.17 ± 0.8)	*TUA2* (4.97 ± 1.36)	*ACT7* (3.76 ± 0.95)	*Rubisco* (5.04 ± 1.1)
12	*TUA2* (4.48 ± 1.09)	*ACT11* (4.46 ± 1.17)	*MDH* (4.11 ± 1.02)	*EF-1-α* (5.12 ± 1.37)	*EF-1-α* (3.84 ± 1.06)	*ACT7* (5.26 ± 1.32)
13	*GAPDH* (4.69 ± 1.09)	*ACT1* (4.74 ± 1.3)	*F-BOX* (4.28 ± 1.21)	*ACT7* (5.33 ± 1.36)	*GAPDH* (4.44 ± 1.02)	*GAPDH* (5.77 ± 1.35)
14	*Rubisco* (5.2 ± 1.16)	*Rubisco* (5.18 ± 1.13)	*TUA4* (5.89 ± 1.31)	*Rubisco* (6.16 ± 1.32)	*TUA2* (5.07 ± 1.32)	*TUA2* (6.21 ± 1.57)
15	*MDH* (5.28 ± 1.24)	*GAPDH* (5.31 ± 1.21)	*Rubisco* (7.17 ± 1.56)	*GAPDH* (6.23 ± 1.48)	*MDH* (6.25 ± 1.56)	*EF-1-α* (6.44 ± 1.77)

Table 1. Expression stability values for *Neolamarckia cadamba* candidate reference genes calculated by BestKeeper. Note: Fifteen candidate reference genes are evaluated by the lowest values of the coefficient of variance (CV) and standard deviation (SD). The number in the bracket indicated that CV ± SD.

Ranking	Tissue	Developmental stage	Photosynthetic cycle	Drought treatment	Cold treatment	Total
1	*RPL10A*	*PGK*	*SAMDC*	*SAMDC*	*RPS25*	*SAMDC*
2	*SAMDC*	*SAMDC*	*ACT7*	*RPS25*	*SAMDC*	*RPS25*
3	*ACT7*	*F-BOX*	*ACT1*	*RPL10A*	*Rubisco*	*F-BOX*
4	*ACT11*	*RPL10A*	*PGK*	*F-BOX*	*TUA5*	*PGK*
5	*PGK*	*ACT7*	*TUA5*	*ACT11*	*ACT11*	*RPL10A*
6	*RPS25*	*TUA2*	*RPS25*	*ACT1*	*F-BOX*	*TUA5*
7	*EF-1-α*	*MDH*	*TUA2*	*TUA4*	*GAPDH*	*ACT1*
8	*ACT1*	*TUA4*	*RPL10A*	*GAPDH*	*ACT1*	*TUA4*
9	*F-BOX*	*TUA5*	*EF-1-α*	*TUA5*	*RPL10A*	*ACT11*
10	*TUA5*	*Rubisco*	*GAPDH*	*PGK*	*PGK*	*Rubisco*
11	*TUA4*	*RPS25*	*ACT11*	*Rubisco*	*TUA4*	*MDH*
12	*GAPDH*	*GAPDH*	*MDH*	*TUA2*	*ACT7*	*ACT7*
13	*TUA2*	*ACT1*	*F-BOX*	*MDH*	*TUA2*	*GAPDH*
14	*MDH*	*EF-1-α*	*TUA4*	*EF-1-α*	*MDH*	*TUA2*
15	*Rubisco*	*ACT11*	*Rubisco*	*ACT7*	*EF-1-α*	*EF-1-α*

Table 2. Comprehensive ranking of 15 candidate reference genes integrated by RefFinder.

NcSUT4 was found in root and phloem when using the two most stable reference genes (*SAMDC* and *RPL10A*) singly or in combination. Though the expression pattern was similar when the unstable gene *Rubisco* served as internal control, the relative expression of *NcSUT4* was much higher in root, xylem and phloem than that using the most stable references. In contrast, the highest expression of *NcSUT4* was found in xylem rather than phloem when using another unstable endogenous gene *GAPDH* (Fig. 5b). The relative transcript abundance of *NcNCED3* under cold and drought stress condition was also calculated in the way similar with *NcSUT4* (Fig. 5c,d). Under cold treatment, the expression level of *NcNCED3* was not affected significantly when normalized by the most stable reference genes *SAMDC* and *RPS25*, whereas the transcript abundance was overestimated when using the least stable references *TUA2* and *EF-1-α*. With drought treatment, the relative expression level of *NcNCED3* increased to two peaks at the PEG concentration of 5% and 20%. On the contrary, normalization by the two least stable genes (*GAPDH*, *Rubisco*) led to the nearly unchanged pattern of *NcNCED3* expression level. Taken together, the substantial divergence was found in the expression levels of *NcSUT4* and *NcNCED3* when normalized by the most stable and least stable reference genes.

Discussion

Gene expression analysis has become an important aspect in the functional investigation of genes during the growth and development of various living organisms. The accuracy of genes relative expression mainly depends on the reference genes. Therefore, the selection of inappropriate reference gene can give rise to the erroneous data and misinterpretation of experimental results[39]. An ideal reference gene for normalization in qRT-PCR analysis should be stably expressed at moderate level in a variety of test samples and has similar amplification efficiency

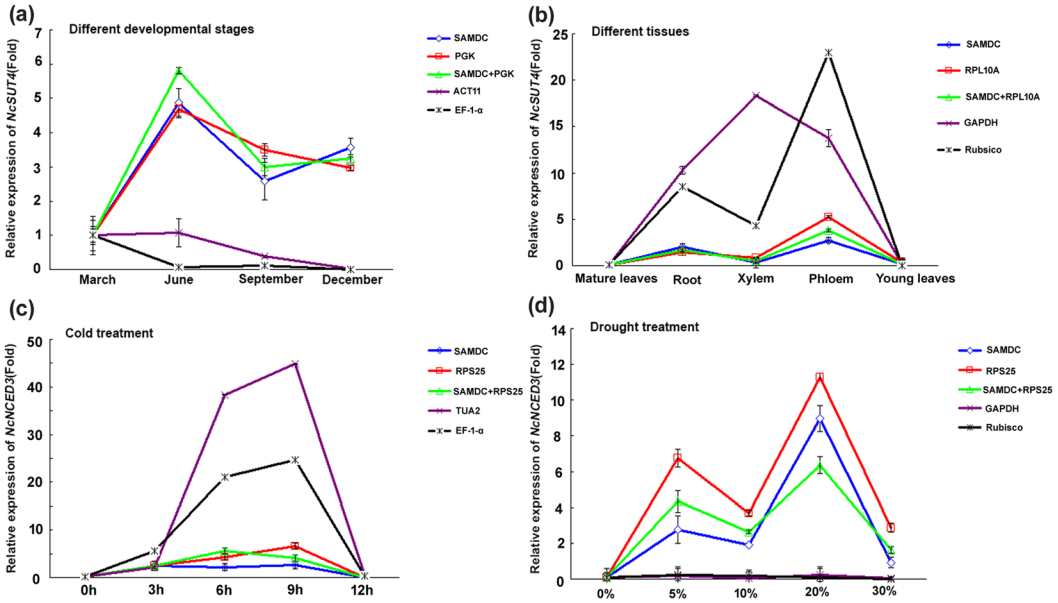

Figure 5. Relative quantification of *NcSUT4* and *NcNCED3* expression levels using the most and least stable reference genes for normalization in the given experimental conditions. (**a**) Expression level of *NcSUT4* at different developmental stages. Most stable reference genes (*SAMDC*, *PGK*) and least stable reference genes (*ACT11*, *EF-1-α*) were used, respectively; (**b**) expression level of *NcSUT4* in different tissues. Most stable reference genes (*SAMDC*, *RPL10A*) and least stable reference genes (*GAPDH*, *Rubisco*) were used, respectively; (**c**) expression level of *NcNCED3* under cold treatment. Most stable reference genes (*SAMDC*, *RPS25*) and least stable reference genes (*TUA2*, *EF-1-α*) were used, respectively; (**d**) expression level of *NcNCED3* under drought treatment. Most stable reference genes (*SAMDC*, *RPS25*) and least stable reference genes (*GAPDH*, *Rubisco*) recommended by BestKeeper were used, respectively. The error bars represent the mean of three biological replicates ± SD.

to target genes[25,40]. However, in our analysis of potential candidate reference genes in *Neolamarckia cadamba*, we determined that there is no single reference gene that exhibited constant expression level in all the samples of various tissues and under different experimental conditions, similar with the findings in cotton[41]. Even though housekeeping genes have been commonly used for normalization in qRT-PCR assay, the expression levels of several genes like *ACT*, *18S rRNA* and *GAPDH* were not always constant in the given conditions. Therefore, it is necessary to assess the expression stability of candidate reference genes systematically when performing qRT-PCR analysis for different tissue and experimental conditions.

In this study, 15 candidate genes were selected for identifying the best reference among 22 samples under different experimental conditions and a variety of various tissues from *N. cadamba*. By the use of four computational gene expression analysis programs, i.e. geNorm, NormFinder, BestKeeper and RefFinder, the expression stability of the selected candidate reference genes were evaluated. The statistical algorithms to assess the stability of references of three programs vary greatly. geNorm estimates the average pairwise variation of a reference gene versus all other genes among the given samples[1,11]. However, for NormFinder analysis, the expression stability value was calculated based on intra- and inter-group variation[19]. In BestKeeper, the CV and SD values determine the stability ranking of a candidate reference gene[20]. Owing to the different algorithms of the three software programs used in this study, the ranking order of the selected candidates showed variable degrees of agreement (Figs 2, 4, Table 1 and Supplementary Table S2). The reference genes, *SAMDC* exhibited the most stable expression based on analysis by all three programs across all 22 samples under the five given conditions (see Supplementary Table S2). In addition, *RPL10A* was one of top two most stable reference genes in various tissues by all three programs. However, *PGK*, one top ranked gene by geNorm and BestKeeper in the sample group of different developmental stages, was ranked at a medium position in NormFinder (Fig. 4). Similarly, under cold stress condition, expression of *RPS25* was the least stable according to NormFinder, whereas it was the most stable gene by geNorm and BestKeeper. Increasing evidences have demonstrated that two or three algorithms were widely used to evaluate expression stability of the reference genes for normalizing mRNA and miRNA expression[5,24,41,42]. Specially, we also noticed that the unstable reference genes identified by three programs were similar. For example, *TUA2*, *GAPDH*, *Rubisco* and *MDH* were expressed unstably in different tissues by all three algorithms. Furthermore, a web-based tool RefFinder was employed to integrate and generate the comprehensive ranking of the candidate reference genes based on the geometric mean of the weights of every gene calculating by each program[43]. The result produced by RefFinder provides us the overall ranking order, which has been widely used in the previous studies on exploring the suitable reference genes in the certain conditions[7,9,18,24].

Our study showed that *SAMDC* was the top ranked gene when all samples were analyzed, since it was recommended by all three programs as the most stable reference gene (Figs 2, 4, and Table 2). Interestingly, the integrated ranking order generated by RefFinder suggested that *SAMDC* was also the optimal reference gene

in five independent sample sets, including the samples under cold and drought stresses, which was similar with the result of *Brachypodium distachyon* plant grown under various stresses conditions[44]. *SAMDC*, encoding S-adenosylmethionine decarboxylase, is a rate-limiting enzyme in the biosynthesis of the polyamines spermidine and spermine[45,46]. *SAMDC* expressed ubiquitously in different plant organs in *Brachypodium*[44], and highly induced under various abiotic stress treatments in rice[47], indicating it might play essential roles in plant growth and tolerance response. *SAMDC* has never been used as internal reference gene for normalization *N. cadamba*, and thereby would be considered as a novel reference candidate. However, the superior stability performance of *SAMDC* was not found in some species under certain conditions. For example, *SAMDC* was considered one of the least stable reference genes in orchardgrass under various abiotic conditions and different tissues of banana[5,7]. In addition to *SAMDC*, *PGK* was also found to be the best stable candidate as reference gene in the leaves at different developmental stages in our study. PGK, encoding phosphoglycerate kinase, plays pivotal roles in the glycolytic pathway[48]. *PGK* was found to be one of the superior reference genes for normalization in chrysanthemum of cross-ploidy levels and in tomato leaves during light stress[49,50], suggesting that *PGK* had potential to be a suitable reference in certain experimental conditions., Likewise, our current study showed that *PGK* was the most stable for different stages, which will be a new reference candidate in *N. cadamba*.

Previous reports have demonstrated that using multiple reference genes rather than a single one for was more robust and accurate for normalizing qRT-PCR data[1,49]. Accordingly, more and more studies in various species were tended to apply multiple references[51–53]. In our study, the combination of two reference candidates was sufficient for normalization in the five different experimental sets (Fig. 2). Thus, additional genes were not required for gene expression normalization. However, it was not always to use multiple reference genes due to the cost, and also it would be dependent on the variability of the selected reference genes.

The housekeeping genes have long been used as internal control to quantify gene expression for their requirement in maintaining the basal cellular functions. They were supposed to be highly conserved and stably expressed under different experimental conditions and various developmental stages[15,54]. *ACTIN*, *GAPDH*, *TUB* and *EF*, considered as classical housekeeping genes, have been commonly used as reference genes in qRT-PCR analysis in the model plants, as well as the non-model species[55–58]. Unfortunately, increasing studies demonstrated the housekeeping genes would variably expressed in many species under given experimental sets, which would not be suitable to serve as reference genes for normalization. *ACT* and *GAPDH*, for instance, were not appropriate candidate reference under many experimental conditions in papaya[18], similar with the result of chicory in seedlings and cell cultures[42]. In the present study, three *ACT* genes were chosen to evaluate their stabilities in 22 samples from *N. cadamba*. When all samples were tested, *ACT7* was ranked at the bottom position while *ACT1* was ranked intermediate position, contrast with the result in samples at different developmental stages with top-ranked *ACT7* and bottom-ranked *ACT1* (Table 2). For the separate sample groups, *ACT7* and *ACT1* ranked among the top three most stable reference genes under different photosynthesis cycle, while *ACT7* had poor performance under drought stress condition. Liu *et al.*[26] have proposed that genes with similar function might have various performances in expression stability. In our work, the ribosomal protein *RPS25* and *RPL10A* were considered as the appropriate reference genes when all sample were tested, whereas they performed variably with top ranking in *RPL10A* and middle-bottom ranking in *RPS25*. Another classical housekeeping gene *TUA*, encoding one of the major components of microtubules[59], had a moderate or least stable level in most of our given experimental sets, but considered as the most stable candidate in poplar[60] and least stable reference in *Caragana korshinskii* Kom.[61]. These results further confirmed that there is no universal reference gene across all species under various experimental conditions. Accordingly, stability assessment of the traditional reference genes is necessary prior to use in qRT-PCR.

To verify the suitability of the reference genes identified in this study, the relative expression levels of *NcSUT4* and *NcNCED3* under different experimental conditions have been detected. The expression profile of *NcSUT4* and *NcNCED3* were normalized by best suitable genes as well as least unstable genes recommended by RefFinder in their own experimental sets. The results revealed that expression pattern of *NcSUT4* and *NcNCED3* were obviously over- or underestimated when using the unstable genes for normalization (Fig. 5), suggesting that selection of appropriate stable reference genes is critically important for the correct normalization for qRT-PCR data in *N. cadamba*.

In conclusion, our study presented the systematic evaluation of a set of candidate reference genes as normalization factors in qRT-PCR analysis in the samples under a wide range of experimental conditions in *N. cadamba*. Four widely used programs (geNorm, NormFinder, BestKeeper and RefFinder) were applied to estimate the expression stability of the selected candidate genes. The results of comprehensive ranking order showed that *SAMDC* displayed highest stability across the set of all samples, mature leaves at different photosynthetic cycles and under drought stress, whereas *RPL10A* had the most stable expression in various tissues. *PGK* and *RPS25* were the most stable in mature leaves at different developmental stages and under cold conditions, respectively. The expression analysis of *NcSUT4* and *NcNCED3* emphasized the importance of suitable reference gene to get accurate and reliable quantitation results by qRT-PCR. For the first time in *N. cadamba*, our study provided the optimal reference under different experimental conditions, which would be of great importance in further analysis of gene expression and facilitate the understanding of underlying mechanisms in the aspects of development and stress response.

Materials and Methods

Plant materials. Fresh young leaves, mature leaves, phloem, xylem, roots of 4–5 year-old *Neolamarckia cadamba* from South China Agricultural University Yuejin North experimental field were harvested. For samples of developmental stages, mature leaves were collected on March, June, September and December. For samples of different photosynthetic cycle, mature leaves were sampled at 7:00, 13:00 and 19:00 on October 28, 2016. For drought treatment samples, the seedlings after seven days of transplantation from tissue culture were treated with 0%, 5%, 10%, 20% and 30% concentration of PEG 6000 and the mature leaves were collected. Meanwhile,

the seedlings were also transferred to 4 °C for chilling stress, and the mature leaves were taken after 0, 3, 6, 9 and 12 h. Each sample was collected with three biological replicates. Information of all five sample sets mentioned above is summarized in Supplementary Table S3. Samples were frozen immediately in liquid nitrogen and stored at −80 °C until RNA extraction.

RNA isolation, quality control and cDNA synthesis. Total RNA was extracted from the samples using OmniPlant RNA Kit (CWBIO) with DNase I treatment to avoid genomic DNA containment. The RNA purity and integrity were estimated by calculating their A260/280 and A260/A230 absorbance ratios and agarose gel electrophoresis analysis. cDNA was synthesized from 0.5 μg of total RNA by Hiscript II Reverse Transcriptase kit (Vazyme) according to the manufacture's instruction. The cDNA were diluted 30-fold for subsequent qRT-PCR analysis.

Selection of candidate reference gene and primers design. Fifteen candidate reference genes, including Actin 1 (ACT1), Actin 7 (ACT7), Actin 11 (ACT11), Tubulin alpha 2 (TUA2), Tubulin alpha 4 (TUA4), Tubulin alpha 5 (TUA5), Elongation factor 1-alpha (EF-1-α), Ribulose bisphosphate carboxylase (Rubisco), Ribosomal protein S25 (RPS25), Ribosomal protein L10A (RPL10A), Malate dehydrogenase (MDH), Glyceraldehyde-3-phosphate dehydrogenase (GAPDH), Phosphoglycerate kinase (PGK), S-adenosylmethionine decarboxylase (SAMDC), F-Box protein (F-BOX) were selected, based on a preliminary *in silico* evaluation of gene expression stability using *in house* RNA-Seq libraries from various tissues of *N. cadamba* including leaves, xylem, cambium and phloem (unpublished data). Although gene expression study is common on plant functional genomic research, *N. cadamba* is still a less studied species. To date, only two studies on gene expression have been carried out in *N. cadamba*, and cyclophilin was used as the internal reference for normalization[31,33]. However, according to the transcriptome data of leaves, xylem, cambium and phloem, the expression of cyclophilin varied greatly in these samples (unpublished data). Therefore, cyclophilin was not selected for further evaluation of expression stability in our study. Due to lacking the genome sequence of *N. cadamba*, the primers were designed based on sequences extracted from the released transcriptome data[31]. Primers for qRT-PCR were designed using web-based Primer-BLAST tool in NCBI (https://www.ncbi.nlm.nih.gov/tools/primer-blast/) with default parameters. Gene ID, primers and the expected length of each gene were indicated in Supplementary Table S4. All the primers were designed across introns except *F-BOX* and *RPL10A*. To check the specificity of the primers, general PCR was carried out and the products was verified by electrophoresis on 1% agarose gels.

Quantitative Real-time PCR. qRT-PCR was performed on LightCycler480 (Roche Molecular Biochemicals, Mannheim, Germany) with optical 96-well plate. 10 μL of the reaction mix containing 5 μL AceQ qPCR SYBR GREEN PCR Master Mix, 0.5 μL diluted cDNA template and 0.5 μL each primer were added into each well. The thermal cycling profile was recommended by the manufacture: 95 °C for 10 min, 40 cycles of 95 °C for 15 s, 60 °C for 30 s. To confirm the specificity of the primers, melting curves were included after amplification. All the samples for qRT-PCR analysis were conducted with three biological replicates each comprising three technical replicates. To calculate the gene-specific PCR efficiency (E) and correlation coefficient (R^2) for each gene, standard curves were generated using tenfold dilution series from the mixed cDNA.

Analysis of the stabilities of reference genes. Three software tools including geNorm[1] (version 3.5, http://medgen.ugent.be/*jvdesomp/genorm/), NormFinder[19] (http://www.mdl.dk/publicationsnormfinder.htm) and BestKeeper[20] (http://www.gene-quantification.de/bestkeeper.html) were used to evaluate the stability of the 15 selected candidate reference genes across all the experimental sets. Expression levels of the candidate reference genes were determined by cycle threshold (CT) values. All the procedures of statistical analyses by the above packages were conducted according to the manufacturer's instructions.

The geNorm software calculates of gene expression stability value (M), which lower M value suggested higher gene's expression stability. Moreover, geNorm also generated a pairwise stability measurement, which can be used to evaluate the suitable number of reference genes for normalization. NormFinder focuses on finding the two genes with the least intra- and inter-group expression variation or the most stable reference gene in intra-group expression variation. The principle of the BestKeeper program is to determine the stability of the reference gene by using the two parameters to calculate the correlation coefficient (CV) and the standard coefficient of variation (SD). Finally, the stability rankings of the reference genes from the three different algorithms were integrated, generating an overall ranking according to the geometric mean by RefFinder[43].

Validation of reference genes. To evaluated the reliability of the reference genes ranked by three algorithms, we analyzed the expression profiles of two target genes *9-Cis-epoxycarotenoid dioxygenase 3* (*NcNCED3*), and *Sucrose transporter 4* (*NcSUT4*) under the two most stable and two least stable reference genes. The expression level of *NcNCDE3* was determined under drought and cold treatment with forward primer TTTCGCGATAACTGAGAACT and reverse primer ACCAAACCTCGAAACTTTGT, while *NcSUT4* was quantified in various tissues and at different developmental stages of mature leaves with forward primer GGCTTTTGTTTTAGGGTTT and reverse primer CTCGAGTCCTCCTGTGATC. The $E^{-\Delta\Delta CT}$ method was used to calculate the relative expression levels[62].

References

1. Vandesompele, J. *et al.* Accurate normalization of real-time quantitative RT-PCR data by geometric averaging of multiple internal control genes. *Genome. Biol.* **3**, (research0034). 1–0034.11 (2002).
2. Rebrikov, D. & Trofimov, D. Y. Real-time PCR: a review of approaches to data analysis. *Appl. Biochem. Micro.* **42**, 455–463 (2006).
3. Phillips, M. A., D'Auria, J. C., Luck, K. & Gershenzon, J. Evaluation of candidate reference genes for real-time quantitative PCR of plant samples using purified cDNA as template. *Plant Mol. Biol. Rep.* **27**, 407–416 (2009).
4. Bustin, S. Quantification of mRNA using real-time reverse transcription PCR (RT-PCR): trends and problems. *J. Mol. Endocrinol.* **29**, 23–39 (2002).

5. Chen, L. *et al*. Validation of reference genes for RT-qPCR studies of gene expression in banana fruit under different experimental conditions. *Planta* **234**, 377–390 (2011).
6. Hao, X. *et al*. Identification and evaluation of reliable reference genes for quantitative real-time PCR analysis in tea plant (*Camellia sinensis* (L.) O. Kuntze). *Int. J. Mol. Sci.* **15**, 22155–22172 (2014).
7. Huang, L. *et al*. Reference gene selection for quantitative real-time reverse-transcriptase PCR in orchardgrass subjected to various abiotic stresses. *Gene* **553**, 158–165 (2014).
8. Huggett, J., Dheda, K., Bustin, S. & Zumla, A. Real-time RT-PCR normalisation; strategies and considerations. *Genes Immun.* **6**, 279 (2005).
9. Duan, M. *et al*. Identification of optimal reference genes for expression analysis in Radish (*Raphanus sativus* L.) and its relatives based on expression stability. *Front. Plant Sci.* **8**, 1605 (2017).
10. Udvardi, M. K., Czechowski, T. & Scheible, W. R. Eleven golden rules of quantitative RT-PCR. *Plant Cell* **20**, 1736–1737 (2008).
11. Kou, S. J. *et al*. Selection and validation of suitable reference genes for miRNA expression normalization by quantitative RT-PCR in citrus somatic embryogenic and adult tissues. *Plant Cell Rep.* **31**, 2151–2163 (2012).
12. Pillitteri, L. J., Lovatt, C. J. & Walling, L. L. Isolation and characterization of a *TERMINAL FLOWER* homolog and its correlation with juvenility in citrus. *Plant Physiol.* **135**, 1540–1551 (2004).
13. Gamuyao, R. *et al*. The protein kinase Pstol1 from traditional rice confers tolerance of phosphorus deficiency. *Nature* **488**, 535–539 (2012).
14. Saraiva, K. D., Fernandes de Melo, D., Morais, V. D., Vasconcelos, I. M. & Costa, J. H. Selection of suitable soybean *EF1α* genes as internal controls for real-time PCR analyses of tissues during plant development and under stress conditions. *Plant Cell Rep.* **33**, 1453–1465 (2014).
15. Jain, M., Nijhawan, A., Tyagi, A. K. & Khurana, J. P. Validation of housekeeping genes as internal control for studying gene expression in rice by quantitative real-time PCR. *Biochem. Biophys. Res. Commun.* **345**, 646–651 (2006).
16. Gutierrez, L. *et al*. The lack of a systematic validation of reference genes: a serious pitfall undervalued in reverse transcription-polymerase chain reaction (RT-PCR) analysis in plants. *Plant Biotechnol. J.* **6**, 609–618 (2008).
17. Maroufi, A., Van Bockstaele, E. & De Loose, M. Validation of reference genes for gene expression analysis in chicory (*Cichorium intybus*) using quantitative real-time PCR. *BMC Mol. Biol.* **11**, 15 (2010).
18. Zhu, X. *et al*. Evaluation of new reference genes in papaya for accurate transcript normalization under different experimental conditions. *PLoS One* **7**, e44405 (2012).
19. Andersen, C. L., Jensen, J. L. & Ørntoft, T. F. Normalization of real-time quantitative reverse transcription-PCR data: a model-based variance estimation approach to identify genes suited for normalization, applied to bladder and colon cancer data sets. *Cancer Res.* **64**, 5245–5250 (2004).
20. Pfaffl, M. W., Tichopad, A., Prgomet, C. & Neuvians, T. P. Determination of stable housekeeping genes, differentially regulated target genes and sample integrity: BestKeeper–Excel-based tool using pair-wise correlations. *Biotechnol. Lett.* **26**, 509–515 (2004).
21. Czechowski, T., Stitt, M., Altmann, T., Udvardi, M. K. & Scheible, W. R. Genome-wide identification and testing of superior reference genes for transcript normalization in *Arabidopsis*. *Plant Physiol.* **139**, 5–17 (2005).
22. Manoli, A., Sturaro, A., Trevisan, S., Quaggiotti, S. & Nonis, A. Evaluation of candidate reference genes for qPCR in maize. *J. Plant Physiol.* **169**, 807–815 (2012).
23. Hu, R., Fan, C., Li, H., Zhang, Q. & Fu, Y. F. Evaluation of putative reference genes for gene expression normalization in soybean by quantitative real-time RT-PCR. *BMC Mol. Biol.* **10**, 93 (2009).
24. Galli, V. *et al*. Validation of reference genes for accurate normalization of gene expression for real time-quantitative PCR in strawberry fruits using different cultivars and osmotic stresses. *Gene* **554**, 205–214 (2015).
25. Ma, R., Xu, S., Zhao, Y., Xia, B. & Wang, R. Selection and validation of appropriate reference genes for quantitative Real-Time PCR analysis of gene expression in *Lycoris aurea*. *Front. Plant Sci.* **7**, 536 (2016).
26. Liu, Z. *et al*. Selection and validation of suitable reference genes for mRNA qRT-PCR analysis using somatic embryogenic cultures, floral and vegetative tissues in citrus. *Plant Cell Tiss. Org. Cult.* **113**, 469–481 (2013).
27. Reid, K. E., Olsson, N., Schlosser, J., Peng, F. & Lund, S. T. An optimized grapevine RNA isolation procedure and statistical determination of reference genes for real-time RT-PCR during berry development. *BMC Plant Biol.* **6**, 27 (2006).
28. Xu, M., Zhang, B., Su, X., Zhang, S. & Huang, M. Reference gene selection for quantitative real-time polymerase chain reaction in Populus. *Anal. Biochem.* **408**, 337–339 (2011).
29. Zhong, H. Y. *et al*. Selection of reliable reference genes for expression studies by reverse transcription quantitative real-time PCR in litchi under different experimental conditions. *Plant Cell Rep.* **30**, 641–653 (2011).
30. Lin, Y. L. & Lai, Z. X. Reference gene selection for qPCR analysis during somatic embryogenesis in longan tree. *Plant Sci.* **178**, 359–365 (2010).
31. Ouyang, K. *et al*. Transcriptomic analysis of multipurpose timber yielding tree *Neolamarckia cadamba* during xylogenesis using RNA-seq. *PLoS One* **11**, e0159407, https://doi.org/10.1371/journal.pone.0159407 (2016).
32. Ouyang, K., Liu, M., Pian, R., Liu, S. & Chen, X. Isolation and analysis of α-expansin genes in the tree *Anthocephalus chinensis* (Rubiaceae). *Genet. Mol. Res.* **12**, 1061–1073 (2013).
33. Li, J. *et al*. Functional identification of an *EXPA* gene (*NcEXPA8*) isolated from the tree *Neolamarckia cadamba*. *Biotechnol. Biotec. Eq.* **31**, 1116–1125 (2017).
34. Zayed, M. Z., Zaki, M. A., Ahmad, F. B., Ho, W. S. & Pang, S. L. Comparison of mimosine content and nutritive values of *Neolamarckia cadamba* and *Leucaena leucocephala* with *Medicago sativa* as forage quality index. *Int. J. Sci. Technol. Res.* **3**, 146–150 (2014).
35. Dubey, A., Nayak, S. & Goupale, D. *Anthocephalus cadamba*: A review. *Phcog. J.* **2**, 71–76 (2011).
36. Kuhn, C. & Grof, C. P. Sucrose transporters of higher plants. *Curr. Opin. Plant Biol.* **13**, 288–298 (2010).
37. Peleg, Z. & Blumwald, E. Hormone balance and abiotic stress tolerance in crop plants. *Curr. Opin. Plant Biol.* **14**, 290–295 (2011).
38. Pedrosa, A. M. *et al*. Effect of overexpression of citrus 9-cis-epoxycarotenoid dioxygenase 3 (CsNCED3) on the physiological response to drought stress in transgenic tobacco. *Genet. Mol. Res.* **16**, gmr16019292 (2017).
39. Dheda, K. *et al*. The implications of using an inappropriate reference gene for real-time reverse transcription PCR data normalization. *Anal. Biochem.* **344**, 141–143 (2005).
40. Yang, Q. *et al*. Evaluation and validation of the suitable control genes for quantitative PCR studies in plasma DNA for non-invasive prenatal diagnosis. *Int. J. Mol. Med.* **34**, 1681–1687 (2014).
41. Artico, S., Nardeli, S. M., Brilhante, O., Grossi-de-Sa, M. F. & Alves-Ferreira, M. Identification and evaluation of new reference genes in Gossypium hirsutum for accurate normalization of real-time quantitative RT-PCR data. *BMC Plant Biol.* **10**, 49 (2010).
42. Delporte, M., Legrand, G., Hilbert, J. L. & Gagneul, D. Selection and validation of reference genes for quantitative real-time PCR analysis of gene expression in Cichorium intybus. *Front. Plant Sci.* **6**, 651, https://doi.org/10.3389/fpls.2015.00651 (2015).
43. Xie, F., Xiao, P., Chen, D., Xu, L. & Zhang, B. miRDeepFinder: a miRNA analysis tool for deep sequencing of plant small RNAs. *Plant Mol. Biol.* **80**, 75–84 (2012).
44. Hong, S. Y., Seo, P. J., Yang, M. S., Xiang, F. & Park, C. M. Exploring valid reference genes for gene expression studies in *Brachypodium distachyon* by real-time PCR. *BMC Plant Biol.* **8**, 112 (2008).
45. Hu, W. W., Gong, H. & Pua, E. C. Modulation of *SAMDC* expression in Arabidopsis thaliana alters *in vitro* shoot organogenesis. *Physiol. Plant* **128**, 740–750 (2006).

46. Kumar, A., Taylor, M. A., Arif, S. A. M. & Davies, H. V. Potato plants expressing antisense and sense S-adenosylmethionine decarboxylase (SAMDC) transgenes show altered levels of polyamines and ethylene: Antisense plants display abnormal phenotypes. *Plant J.* **9**, 147–158 (1996).
47. Basu, S., Roychoudhury, A. & Sengupta, D. N. Identification of trans-acting factors regulating *SamDC* expression in *Oryza sativa*. *Biochem. Biophys. Res. Commun.* **445**, 398–403 (2014).
48. Anderson, L. E. & Carol, A. A. Enzyme co-localization in the pea leaf cytosol: 3-P-glycerate kinase, glyceraldehyde-3-P dehydrogenase, triose-P isomerase and aldolase. *Plant Sci.* **169**, 620–628 (2005).
49. Lovdal, T. & Lillo, C. Reference gene selection for quantitative real-time PCR normalization in tomato subjected to nitrogen, cold, and light stress. *Anal. Biochem.* **387**, 238–242 (2009).
50. Wang, H., Chen, S., Jiang, J., Zhang, F. & Chen, F. Reference gene selection for cross-species and cross-ploidy level comparisons in Chrysanthemum spp. *Sci. Rep.* **5**, 8094, https://doi.org/10.1038/srep08094 (2015).
51. Mahboubi, A. *et al.* Aspen SUCROSE TRANSPORTER3 allocates carbon into wood fibers. *Plant Physiol.* **163**, 1729–1740 (2013).
52. Liu, M. Y., Wu, X. M., Long, J. M. & Guo, W. W. Genomic characterization of miR156 and SQUAMOSA promoter binding protein-like genes in sweet orange (*Citrus sinensis*). *Plant Cell Tiss. Org. Cult.* **130**, 103–116 (2017).
53. Plötner, B. *et al.* Chlorosis caused by two recessively interacting genes reveals a role of RNA helicase in hybrid breakdown in Arabidopsis thaliana. *Plant J.* **91**, 251–262 (2017).
54. Jian, B. *et al.* Validation of internal control for gene expression study in soybean by quantitative real-time PCR. *BMC Mol. Biol.* **9**, 59, https://doi.org/10.1186/1471-2199-9-59 (2008).
55. de Oliveira, T. M. *et al.* Analysis of the NAC transcription factor gene family in citrus reveals a novel member involved in multiple abiotic stress responses. *Tree Genet. Genom.* **7**, 1123–1134 (2011).
56. Li, H. *et al.* ZmWRKY33, a WRKY maize transcription factor conferring enhanced salt stress tolerances in *Arabidopsis*. *Plant Growth Regul.* **70**, 207–216 (2013).
57. Lv, P., Li, N., Liu, H., Gu, H. & Zhao, W. E. Changes in carotenoid profiles and in the expression pattern of the genes in carotenoid metabolisms during fruit development and ripening in four watermelon cultivars. *Food Chem.* **174**, 52–59 (2015).
58. Vij, S. & Tyagi, A. K. Genome-wide analysis of the stress associated protein (SAP) gene family containing A20/AN1 zinc-finger(s) in rice and their phylogenetic relationship with *Arabidopsis*. *Mol. Genet. Genomics* **276**, 565–575 (2006).
59. Silflow, C. D. *et al.* Plant tubulin genes: structure and differential expression during development. *Genesis* **8**, 435–460 (1987).
60. Brunner, A. M., Yakovlev, I. A. & Strauss, S. H. Validating internal controls for quantitative plant gene expression studies. *BMC Plant Biol.* **4**, 14 (2004).
61. Yang, Q. *et al.* Reference gene selection for qRT-PCR in *Caragana korshinskii* Kom. under different stress conditions. *Mol. Biol. Rep.* **41**, 2325–2334 (2014).
62. Wong, M. L. & Medrano, J. F. Real-time PCR for mRNA quantitation. *Biotechniques* **39**, 75–85 (2005).

Acknowledgements

This research is supported by grants from the National Natural Science Foundation of China (Grant Nos 30771759, 31170636 and 31470681), the National Key Research and Development Program of China (Grant No. 2016YFD0600104), Natural Science Foundation of Guangdong Province of China (Grant No. 2016A030311032), Guangzhou Science and Technology Program (Grant No. 201607020024) and Foundation of Young Creative Talents in Higher Education of Guangdong Province(2017KQNCX017).

Author Contributions

C.P. and T.H. designed the research; T.H., S.-W.L., Z.-W.Y., Q.-J.Z. and X.-L.Z. conducted the experiment; J.L. and T.H. analyzed the data; J.L. and C.P. wrote the manuscript.

Additional Information

Supplementary information accompanies this paper at https://doi.org/10.1038/s41598-018-27633-5.

Competing Interests: The authors declare no competing interests.

Publisher's note: Springer Nature remains neutral with regard to jurisdictional claims in published maps and institutional affiliations.

Article | Open access | Published: 18 June 2018

Selection and Validation of Reference Genes for mRNA Expression by Quantitative Real-Time PCR Analysis in *Neolamarckia cadamba*

Tian Huang, Jianmei Long, Si-Wen Liu, Zi-Wei Yang, Qi-Jin Zhu, Xiao-Lan Zhao & Changcao Peng

Scientific Reports **8**, Article number: 9311 (2018) | Cite this article

3214 Accesses | **24** Citations | Metrics

Abstract

Neolamarckia cadamba is an economically-important fast-growing tree species in South China and Southeast Asia. As a prerequisite first step for future gene expression studies, we have identified and characterized a series of stable reference genes that can be used as controls for quantitative real time PCR (qRT-PCR) expression analysis in this study. The expression stability of 15 candidate reference genes in various tissues and mature leaves under different conditions was evaluated using four different algorithms, i.e., geNorm, NormFinder, BestKeeper and RefFinder. Our results showed that *SAMDC* was the most stable of the selected reference genes across the set of all samples, mature leaves at different photosynthetic cycles and under drought stress, whereas *RPL10A* had the most stable expression in various tissues. *PGK* and *RPS25* were considered the most suitable reference for mature leaves at different

Download PDF

Sections | Figures | References

Abstract
Introduction
Results
Discussion
Materials and Methods
References
Acknowledgements
Author information
Ethics declarations
Additional information
Electronic supplementary material
Rights and permissions
About this article
This article is cited by

International Journal of
Molecular Sciences

MDPI

Article

Genome-Wide Identification and Expression Analysis of WRKY Gene Family in *Neolamarckia cadamba*

Zuowei Xu [1], Yutong Liu [1], Huiting Fang [1], Yanqiong Wen [1], Ying Wang [1], Jianxia Zhang [1], Changcao Peng [1,2,*] and Jianmei Long [1,*]

[1] Guangdong Key Laboratory for Innovative Development and Utilization of Forest Plant Germplasm, College of Forestry and Landscape Architecture, South China Agricultural University, Guangzhou 510642, China; scau-zuowei@stu.scau.edu.cn (Z.X.); lyt991211@stu.scau.edu.cn (Y.L.); 18125965000@163.com (H.F.); wenwen_yq@163.com (Y.W.); wang_scau_wind@163.com (Y.W.); zhangjianxia@scau.edu.cn (J.Z.)
[2] State Key Laboratory for Conservation and Utilization of Subtropical Agro-Bioresources, South China Agricultural University, Guangzhou 510642, China
* Correspondence: ccpeng@scau.edu.cn (C.P.); longjianmei@scau.edu.cn (J.L.)

Abstract: The WRKY transcription factor family plays important regulatory roles in multiple biological processes in higher plants. They have been identified and functionally characterized in a number of plant species, but very little is known in *Neolamarckia cadamba*, a 'miracle tree' for its fast growth and potential medicinal resource in Southeast Asia. In this study, a total of 85 *WRKY* genes were identified in the genome of *N. cadamba*. They were divided into three groups according to their phylogenetic features, with the support of the characteristics of gene structures and conserved motifs of protein. The *NcWRKY* genes were unevenly distributed on 22 chromosomes, and there were two pairs of segmentally duplicated events. In addition, a number of putative cis-elements were identified in the promoter regions, of which hormone- and stress-related elements were shared in many *NcWRKYs*. The transcript levels of *NcWRKY* were analyzed using the RNA-seq data, revealing distinct expression patterns in various tissues and at different stages of vascular development. Furthermore, 16 and 12 *NcWRKY* genes were confirmed to respond to various hormone treatments and two different abiotic stress treatments, respectively. Moreover, the content of cadambine, the active metabolite used for the various pharmacological activities found in *N. cadamba*, significantly increased after Methyl jasmonate treatment. In addition, expression of *NcWRKY64/74* was obviously upregulated, suggesting that they may have a potential function of regulating the biosynthesis of cadambine in response to MeJA. Taken together, this study provides clues into the regulatory roles of the *WRKY* gene family in *N. cadamba*.

Keywords: *WRKY* gene; *Neolamarckia cadamba*; abiotic stress; expression analysis; cadambine

Citation: Xu, Z.; Liu, Y.; Fang, H.; Wen, Y.; Wang, Y.; Zhang, J.; Peng, C.; Long, J. Genome-Wide Identification and Expression Analysis of WRKY Gene Family in *Neolamarckia cadamba*. *Int. J. Mol. Sci.* **2023**, *24*, 7537. https://doi.org/10.3390/ijms24087537

Academic Editors: Chuanping Yang and Chenghao Li

Received: 23 March 2023
Revised: 15 April 2023
Accepted: 17 April 2023
Published: 19 April 2023

1. Introduction

The WRKY proteins are one of the largest families of transcriptional regulators found throughout plants [1]. They share the defining feature WRKY domain which comprises the highly conserved WRKYGQK hepta peptide sequence at the N-terminal followed by a C_2H_2- or C_2HC type of zinc-finger motif at the C-terminal. Both the WRKY domain and zinc-finger motif are required for the high binding affinity of WRKY transcription factor (TF) to the W-box cis-elements in the promoter regions of their target genes [2]. The WRKY proteins can be classified into three main groups (I–III) based on the number of WRKY domains and the category of zinc-finger motifs. Proteins with two WRKY domains belong to Group I, while Group II or III contain one WRKY domain with different zinc-finger motifs. Specifically, Group III has a zinc-finger structure of C_2HC while Group II has a zinc-finger structure of C_2H_2 and can be further divided into five subgroups: IIa, IIb, IIc, IId, and IIe [3].

Many WRKY TFs have been experimentally identified from various plant species. They play vital regulatory roles in plant defense regulatory networks, including response to various abiotic stresses, which result from an interplay between WRKYs and a variety of plant hormones [4,5]. For instance, the synergistic interaction between OsWRKY51 and OsWRKY71 genes inhibited gibberellic acid (GA) signaling in the aleurone cells of rice seeds under ABA induction in rice [6,7]. Likewise, in Arabidopsis, AtWRKY18/40/60 were shown to participate in signaling pathways that are mediated by ABA, and *AtWRKY60* might be a direct target gene of AtWRKY18 and AtWRKY40 in ABA signaling [8]. Moreover, *PoWRKY13* in *Populus tomentosa* [9], *PheWRKY86* in *Moso bamboo* [10] and *AtWRKY25/26/39* [11,12] were involved in the response to heat stress and drought stress. *DgWRKY5* in *Chrysanthemum indicum* [13], *GbWRKY1* in cotton [14], and *SlWRKY8* in *Solanum lycopersicum* [15] participated in regulating plant tolerance to salt stress.

WRKY TF also plays an activating or repressing role in the transcriptional regulation of key enzyme genes in plant secondary metabolites synthesis [4]. OpWRKY2 acted as a direct positive regulator of camptothecin biosynthesis by binding the central camptothecin pathway gene OpTDC [16]. Similarly, the total production of camptothecin was significantly upregulated in most overexpression lines of *OpWRKY3* [17]. Overexpression of *OpWRKY6* significantly reduced the accumulation of camptothecin. Conversely, camptothecin accumulation increased in *OpWRKY6* knockout lines [18]. Agarwood sesquiterpene synthase 1 (ASS1) is one of the key enzymes responsible for the biosynthesis of sesquiterpenes, and *AsWRKY44* directly binds to its promoter and represses ASS1 promoter activity [19]. Likewise, *GaWRKY1* and *AaWRKY1* activated the expression of key enzyme genes in the gossypol and artemisinin biosynthesis pathway, respectively, by binding to the W-box element in their promoter [20,21]; *PgWRKY4X* in ginseng interacted with the W-box in the squalene epoxidase (PgSE) promoter and overexpression of *PgWRKY4X* significantly upregulated PgSE and increased the accumulation of ginsenoside [22]. Paclitaxel, as a kind of terpenoid alkaloid, also has important clinical value in the treatment of cancer. Overexpression of *TcWRKY8* and *TcWRKY47* significantly increased the expression levels of genes related to paclitaxel biosynthesis [23]. Extracted from *Catharanthus roseus*, vinblastine is a monoterpenoid indole alkaloid (MIA) whose synthetic pathway has been fully resolved and is a natural antitumor drug widely used in cancer therapy. Overexpression of *CrWRKY1* in *C. roseus* hairy root activated some key genes in the MIA pathway and the transcriptional repressors (*ZCT1*, *ZCT2*, and *ZCT3)*. Interestingly, CrWRKY1 overexpression repressed the transcriptional activators *ORCA2*, *ORCA3*, and *CrMYC2*, yielding a higher level of serpentine accumulation [24]. To date, however, the regulation of WRKY in MIA synthesis is less understood.

Neolamarckia cadamba, from the *Rubiaceae* family, is widely distributed in tropical and subtropical regions of the world and is an important tree for the timber industry and traditional medicinal plants in southern China [25]. Cadambine, a kind of MIA only isolated from the *Rubiaceae* family, is the main component of total alkaloids in *N. cadamba*, accounting for about 50% of total alkalis, which has been shown to have clinical effects against malaria parasites and in the treatment of diabetes, and exhibits concentration-dependent inhibition on carcinoma cell and DNA topoisomerase [26–28]. With the completion of whole genome sequencing of *N. cadamba* [29], it enabled genome-wide identification and functional analysis of the gene families related to the development process, response to environmental change, and cadambine synthesis. Several reports suggested that WRKY participated in the regulation of MIA biosynthesis, but whether they were involved in cadambine biosynthesis was unknown. In this study, we identified 85 *WRKY* genes of *N. cadamba* at the genome-wide level and analyzed the gene structures, conserved domains, phylogenetic relationships and cis-element in the promoter of the *WRKY* genes. In addition, we performed a comprehensive analysis of spatiotemporal expression patterns of *NcWRKY* genes according to RNA-seq data and examined their expression profiles in response to hormone (MeJA, ABA, and GA) and abiotic stresses (high salinity and drought) by real time quantitative PCR (RT-qPCR). Moreover, the involvement of the NcWRKY in cadambine

synthesis was further explored. Our genome-wide results identified all *WRKY* genes in the *N. cadamba* genome and provided valuable clues for further functional study.

2. Results

2.1. Identification of WRKY Genes in Neolamarckia Cadamba

In this study, a total of 85 *WRKY* gene sequences were identified in *N. cadamba* (Supplementary File S1). They were named based on the apparently complete WRKY domains and their position on the chromosome. Gene characteristics, including the length of the protein sequence, the protein molecular weight (MW), the isoelectric point (pI), and the subcellular localization, were analyzed using ExPaSy and Plant-mPLoc. The results showed that the length of all the identified WRKY proteins in *N. cadamba* ranged from 174 to 734 amino acids (aa), in which *NcWRKY48* was the smallest protein and *NcWRKY47* was the largest one. The molecular weight (MW) of the NcWRKY proteins ranged from 20.0 to 79.3 kDa, with the predicted isoelectric point values (pI) varying from 5.04 (NcWRKY6) to 9.69 (NcWRKY61). Subcellular localization prediction indicated that all the NcWRKYs were localized to nuclear, indicating that they may function as transcription factors.

2.2. Phylogenetic Analysis and Multiple Sequence Alignment of NcWRKYs

To investigate the phylogenetic relationships among WRKY family genes, we constructed an ML phylogenetic tree using the WRKY proteins from *A. thaliana* and *N. cadamba*. The result showed that the 85 NcWRKY proteins were classified into three groups (Figure 1), based on the classification described by a previous report on *A. thaliana* [3], indicating an evolutionary conservation between these two species. Group I contained 19 NcWRKY members, while 10 NcWRKYs belonged to Group III. The largest group (Group II) consists of 56 NcWRKY proteins, which could be further divided into five subgroups, with 4, 12, 24, 7, and 9 members belonging to Group IIa–IIe, respectively. Multiple sequence alignment analysis (Figure S1) suggested that members from Group I contained two WRKY domains and C_2H_2-type zinc-finger motifs (C-X_4-C-$X_{22–23}$-H-X-H), except that NcWRKY23 only harbored two WRKY domains. All the 56 NcWRKYs from Group II contained one WRKY domain, of which six harbored mutated WRKY domains (WRKYGKK). All members in Group III contained the C_2HC-type zinc fingers (C-X_7−C-X_{23}-H-X-C).

2.3. Gene Structure and Conserved Motif Analysis

The exon–intron organizations of all the identified NcWRKYs were examined by TBtools. Another ML phylogenetic tree was constructed to align the 85 NcWRKY proteins (Figure 2a). As shown in Figure 2b, the number of introns in the *NcWRKYs* ranged from 1 to 6. Six *NcWRKY* genes from Group IIc had only one intron, and NcWRKY3 had six introns. The majority of *NcWRKY* genes contained two to five introns (37 with two introns, 13 with three introns, 17 with four introns, and 11 with five introns). Interestingly, all *NcWRKYs* in Group I contained an intron in their respective WRKY domains, but no introns existed in the N-terminal WRKY domains (Figure 2b). Genes within the same group were usually similar in structure, slightly varying in length and distribution, and most genes had UTR regions. For example, all of Group IIa genes had four introns, and there were two UTR regions in all of them except for *NcWRKY73*. Most of Group IIc contained one to three introns, but *NcWRKY40* and *NcWRKY54* contained four introns and one of them was located in 3′ UTR.

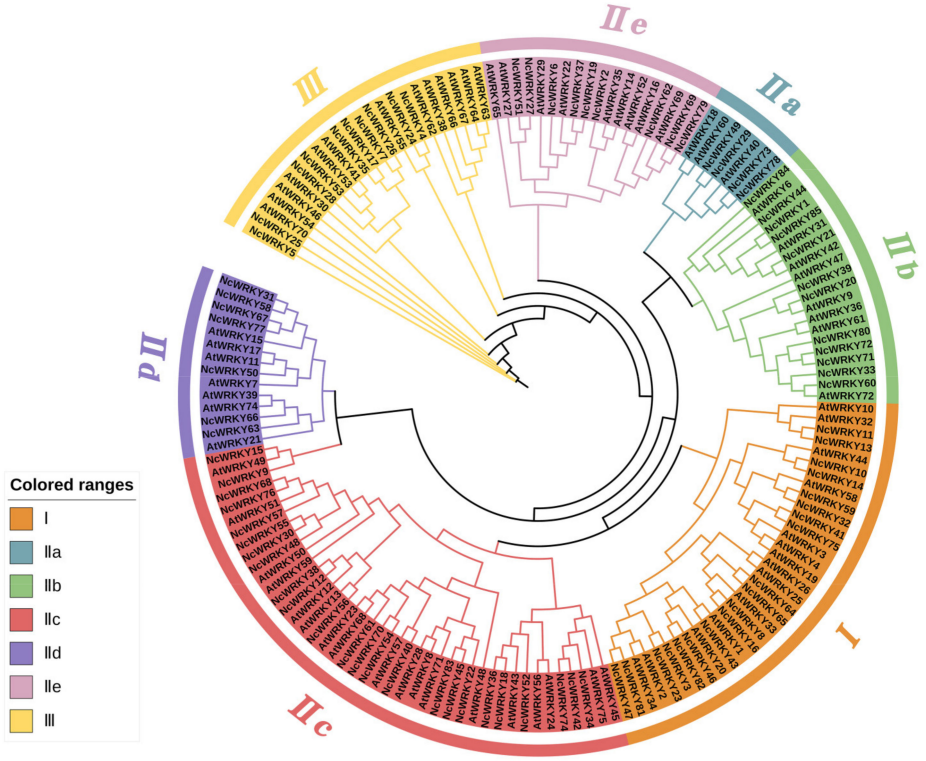

Figure 1. Unrooted phylogenetic tree representing relationships among WRKY proteins of *N. cadamba* and *A. thaliana*. A maximum likelihood (ML) phylogenetic tree was constructed with 5000 bootstrap replicates. The different-colored arcs indicate different groups (or subgroups) of WRKY proteins. WRKY proteins from *N. cadamba* and *A. thaliana* were presented with the prefix 'Nc' and 'At', respectively.

To further investigate the similarity and diversity of the motif composition of NcWRKY proteins, we annotated 10 conserved motifs predicted by MEME. As exhibited, NcWRKY members in the same subfamily were found to share similar motif profiles (Figure 2c). Motif 1 and motif 2 were highly conserved and distributed across all members of NcWRKY. Most members in Group I and Group IIb contained the highest number of motifs (n = 7), whereas three members in Group III (NcWRKY4, NcWRKY5, and NcWRKY25) only have two motifs. In addition, we also found that some motifs were specific to different groups. For example, motif 3 and motif 6 were unique to Group I, whereas motif 9 was specific to Group IIa and IIb. The distinct motif composition might be contributed to the functional diversity among NcWRKYs.

2.4. Chromosomal Distribution and Synteny Analysis of NcWRKYs

An analysis of genome chromosomal distribution revealed that 84 *NcWRKYs* were unevenly distributed on 22 chromosomes (Figure 3), while *NcWRKY85* could not map to any chromosome. There was no evidence to show a correlation relationship between the number of *NcWRKYs* and the chromosome length. The investigation of gene duplication events was also performed to obtain insight into the expansion of the *NcWRKY* family. Four *NcWRKYs* (*NcWRKY4/5* and *NcWRKY24/25*) were identified as tandem repeat gene pairs located on chr01 and chr05. In addition to tandem duplication, the fragment duplication events of the *WRKY* gene family were performed (Figure 3). The result showed that 76 segmental duplication events with 62 *NcWRKYs* were identified. All these results indicated that the *NcWRKY* family underwent an expansion in *N. cadamba* possibly generated by gene duplication, and the segmental duplication events played a major role as a driving force for *NcWRKYs* evolution. To better understand the evolutionary constraints acting on the *NcWRKY* family, the Ka/Ks ratios of the *NcWRKY* gene pairs were calculated. All segmen-

tal and tandem duplicated *NcWRKY* gene pairs had Ka/Ks < 1 (Supplementary File S2), suggesting that the *N. cadamba WRKY* gene family might have experienced strong purifying selective pressure during evolution.

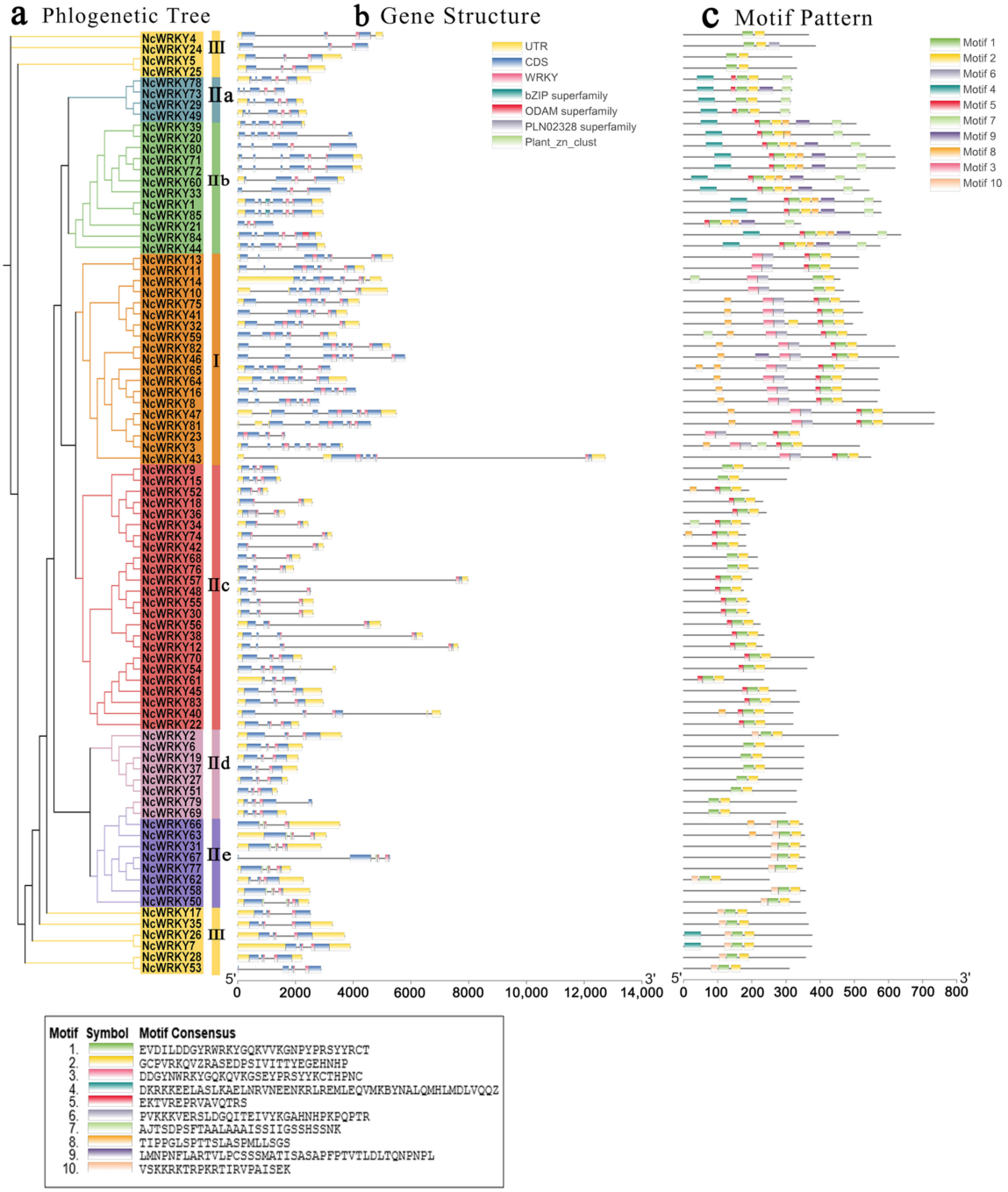

Figure 2. Phylogenetic relationships, gene structure, and architecture of conserved protein motifs in WRKY genes from *N. cadamba*. (**a**) The phylogenetic tree was constructed based on the full-length sequences of NcWRKY proteins using TBtools. Details of clusters were shown in different colors as same of Figure 1. (**b**) Exon–intron structure of NcWRKYs. Yellow boxes indicated untranslated 5′- and 3′ regions, while blue boxes indicated coding sequence (CDS) and black lines represented introns. The WRKY domains were highlighted by pink boxes and other colors indicate different conserved domains which are found in CDD. The length of genes was estimated using the scale at the bottom. (**c**) The motif composition of NcWRKY proteins. The motifs, numbers 1–10, were displayed in different-colored boxes.

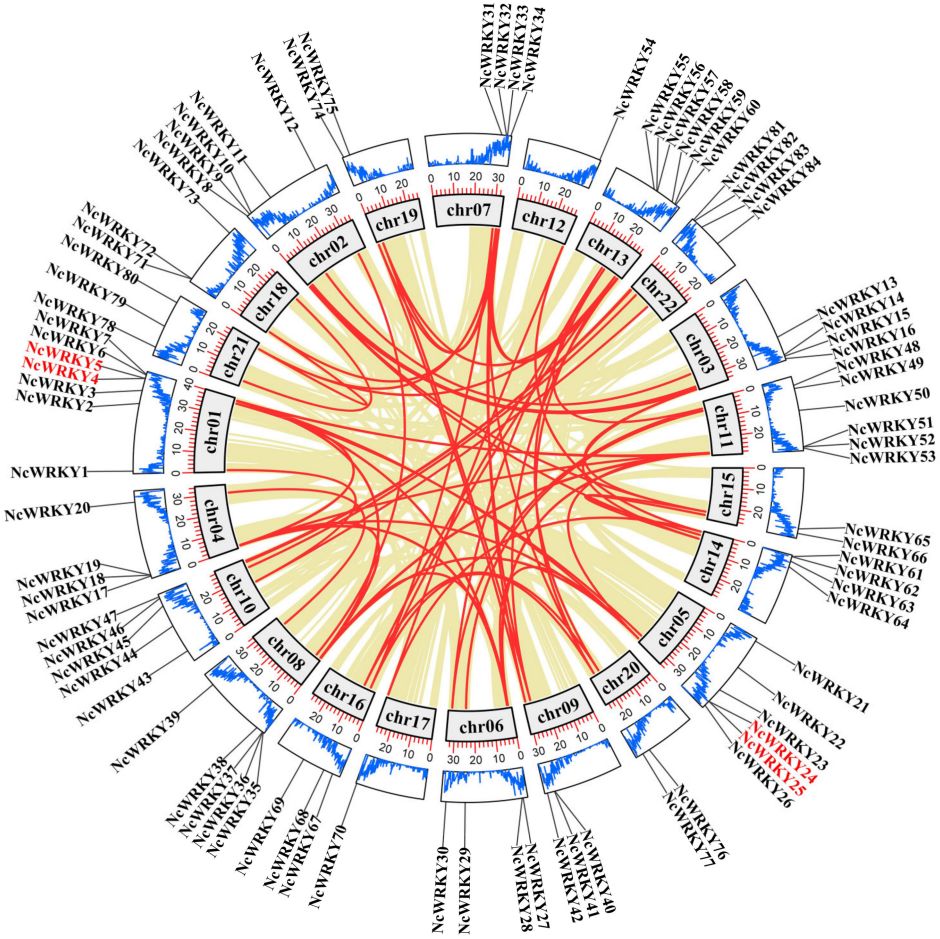

Figure 3. Chromosome location and synteny analysis of *WRKY* genes within *N. cadamba* genome. Khaki lines indicated all synteny blocks in the *N. cadamba* genome, and the red lines indicated duplicated *WRKY* gene pairs. The gray boxes indicated the chromosomes of *N. cadamba*. The blue line in the boxes represented the gene abundance at that position on the chromosome, and the height of the line was proportional to the abundance. The outermost circle indicates the chromosomal locations of *WRKY* genes in *N. cadamba*. The genes in red font indicate tandem duplication.

The phylogenetic mechanisms of the *N. cadamba* WRKY family were further explored by constructing comparative syntenic maps of *N. cadamba* associated with four representative species, including three represented dicots (*A. thaliana*, *Coffea canephora*, and *Populus trichocarpa*) and one model monocot (*O. sativa*) (Figure 4). On the whole, 78 *NcWRKYs* showed a syntenic relationship with those in *P. trichocarpa*, followed by *C. canephora* (74), *A. thaliana* (58), and *O. sativa* (30). The number of orthologous gene pairs between *N. cadamba* and the other species (*P. trichocarpa*, *C. canephora*, *A. thaliana*, and *O. sativa*) was 218, 114, 91, and 45, respectively. More than 90% of the *NcWRKYs* showed a syntenic relationship with *WRKYs* in *P. trichocarpa*, which is higher than *C. canephora* (87%), indicating that *WRKY* genes in *N. cadamba* and *P. trichocarpa* (both as tall arbor) evolved more closely related in evolution. Specifically, *NcWRKY12/38/56* were found to be associated with at least two syntenic gene pairs between *N. cadamba* and *P. trichocarpa*, respectively. *NcWRKY16* and *NcWRKY64* were found to be associated with at least two syntenic gene pairs between *N. cadamba* and *P. trichocarpa*/*A. thaliana*/*O. sativa*, speculating that they may have played an important role in the *WRKY* gene family during evolution.

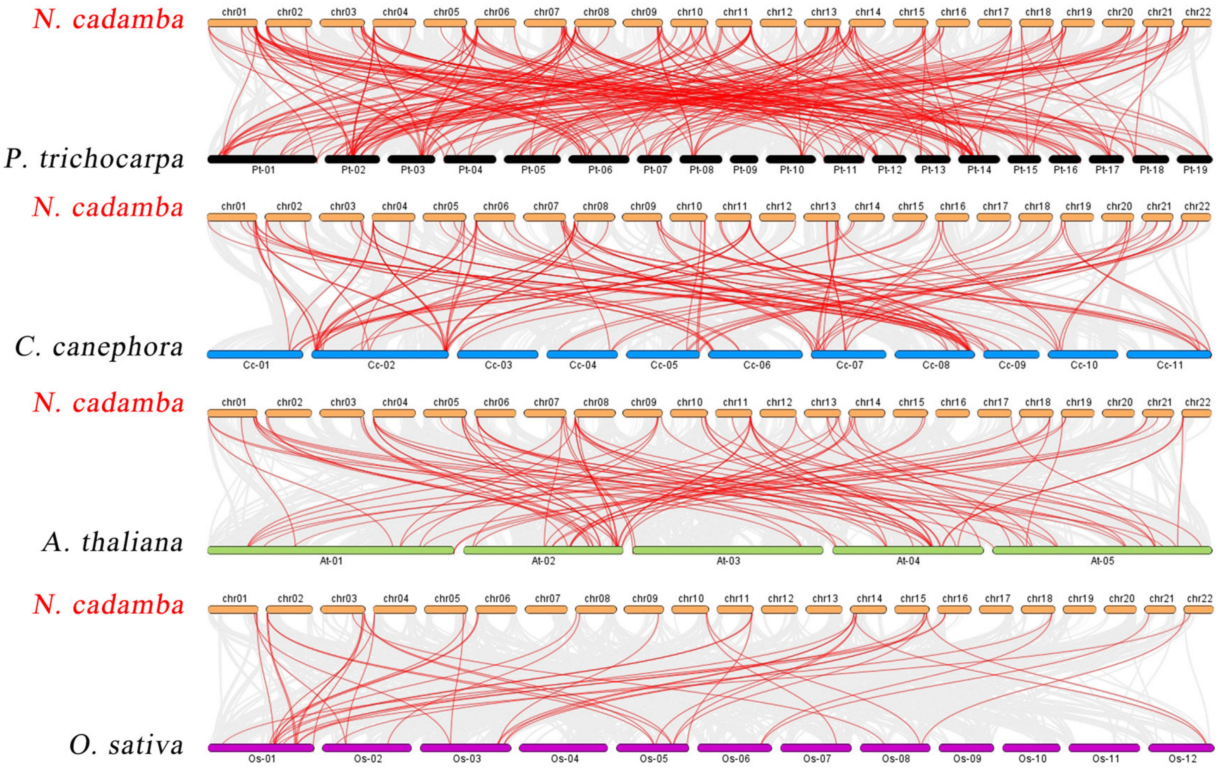

Figure 4. Synteny analysis of *WRKY* genes between *N. cadamba* and four representative plant species. Gray lines in the background indicated all synteny blocks in the genome, while the red lines indicated the duplication of *WRKY* gene pairs.

2.5. Analysis of Promoter Cis-Acting Elements

To further understand transcriptional regulation and the potential functions of *NcWRKYs* in *N. cadamba*, the *cis*-acting elements of *NcWRKY* promoters were predicted using PlantCARE. In addition to the well-characterized site-binding-related elements and promoter-related elements, three categories of cis-regulatory elements were found to be highly concentrated in the promoter region of *NcWRKYs*, including light-responsive, hormone-responsive, and environmental-stress-related elements. The most abundant elements in *NcWRKYs* promoters were hormone-responsive elements, which were represented by eight types (Figure 5a). Specifically, ABRE elements (response to ABA) were the most widely distributed and presented in over half of the identified *NcWRKYs*. Moreover, several environmental-stress-related cis-acting elements responsible for response to low-temperature (LTR), drought (MBS), wound (WUN motif), stress (TC-rich repeats and ARE), and anerobic (GC motif and ARE) were identified (Figure 5b). Specifically, ARE element was prevalent and displayed across most of the *NcWRKY* promoters, implying that *NcWRKYs* were responsive to anerobic stress. Taken together, these results suggested the potential role of *NcWRKYs* in response to stress and hormone signaling pathways. Interestingly, some *NcWRKYs* comprised more than 2 W-box (TTGACC) in their promoters, such as *NcWRKY7*, *NcWRKY24*, *NcWRKY31*, and *NcWRKY61* have four W-box, indicating that these *NcWRKYs* have the potential function to regulate plant's defensive response to stresses by self-regulating its expression and the cross-talk between different WRKY TFs.

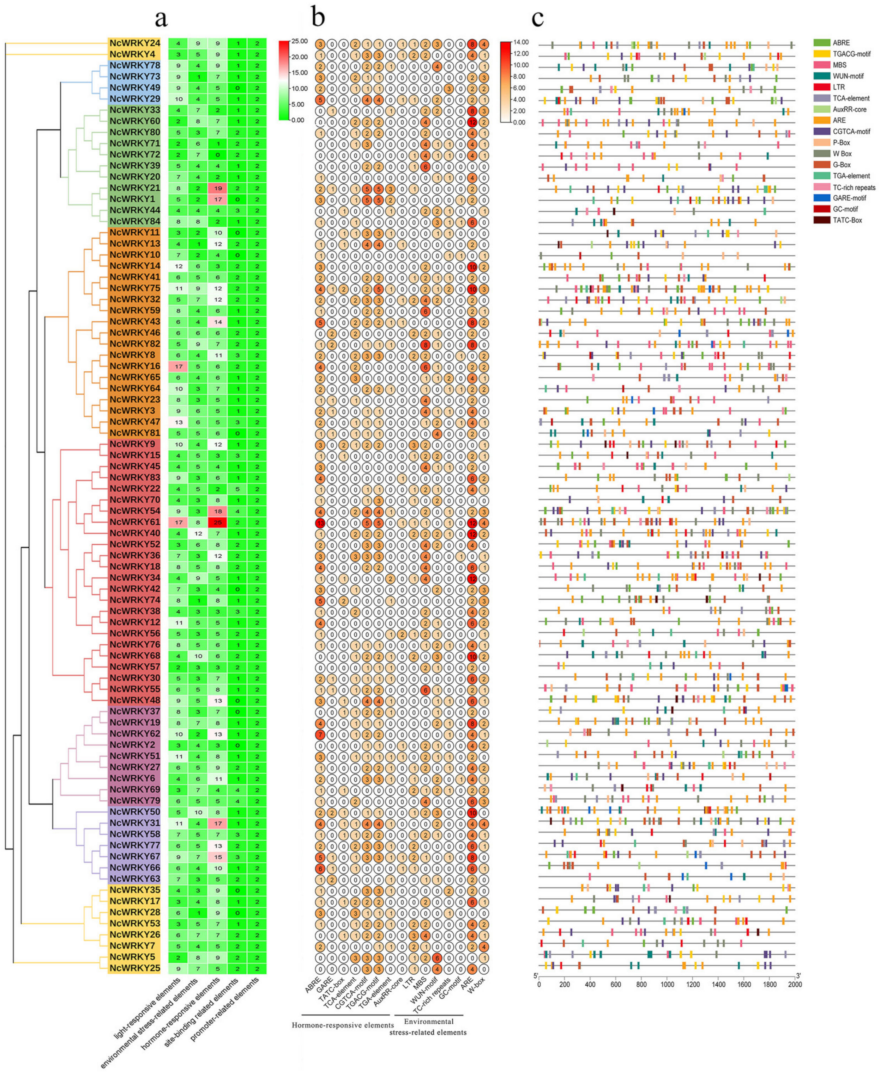

Figure 5. Prediction of cis-acting elements in promoters of *NcWRKYs*. (**a**) The number of five types of cis-acting elements in each *NcWRKYs* promoter. (**b**) The number of different elements in hormone-responsive and environmental-stress-related elements. (**c**) Visualization of environmental-stress-related and hormone-responsive elements, W-box and G-box in *NcWRKYs* promoters.

2.6. Protein Interaction Network of NcWRKY

To elucidate the biological functions and regulatory network of NcWRKY proteins, the 18 homologous WRKY proteins in *A. thaliana* were used to predict the protein–protein interaction network of NcWRKY proteins. The results of homologous similarity were shown in Supplementary File S3. The results indicated 11 AtWRKY proteins and 21 corresponding interacting functional proteins which can be divided into three groups (Figure 6). Most AtWRKY proteins interact with more than one protein, and eight proteins can interact with more than two other functional proteins. Some proteins that interact with each other in a group and only interact with one AtWRKY protein. Group 1 (EGL3, GL3, TT2, TT8, TTG1, and TTG2) only interact with AtWRKY22 by TT2 and Group 3 (CHLM, CHLI1, PPOP1, CHLI2, ALB1, and GUN5) only interact with AtWRKY40 by GUN5. According to the biological process analysis in the GO database, proteins of Group 1 were related to epidermal cell fate specification, positive regulation of anthocyanin biosynthetic process, trichome differentiation, and jasmonic-acid-mediated signaling pathway (Supplementary File S4). Proteins of Group 3 were related to the chlorophyll biosynthetic process and aromatic compound biosynthetic process. Proteins of Group 2 were mainly related to MAPK cascade which responds to abiotic and biotic stresses, such as defense and immune system pro-

cesses, and responds to osmotic and extreme temperature stresses [30–32]. This group also included positive regulation of autophagy, cellular heat acclimation, and camalexin biosynthetic process. AtWRKY33 (orthologous with NcWRKY8 and NcWRKY16), an important TF in abiotic stress [12,33] and phytoalexin biosynthesis [34], played a key role in the whole protein interaction network, especially in MAPK cascade. AtWRKY22 (orthologous with NcWRKY19) and AtWRKY25 (orthologous with NcWRKY64 and NcWRKY65) participated in aging and response to cold, respectively.

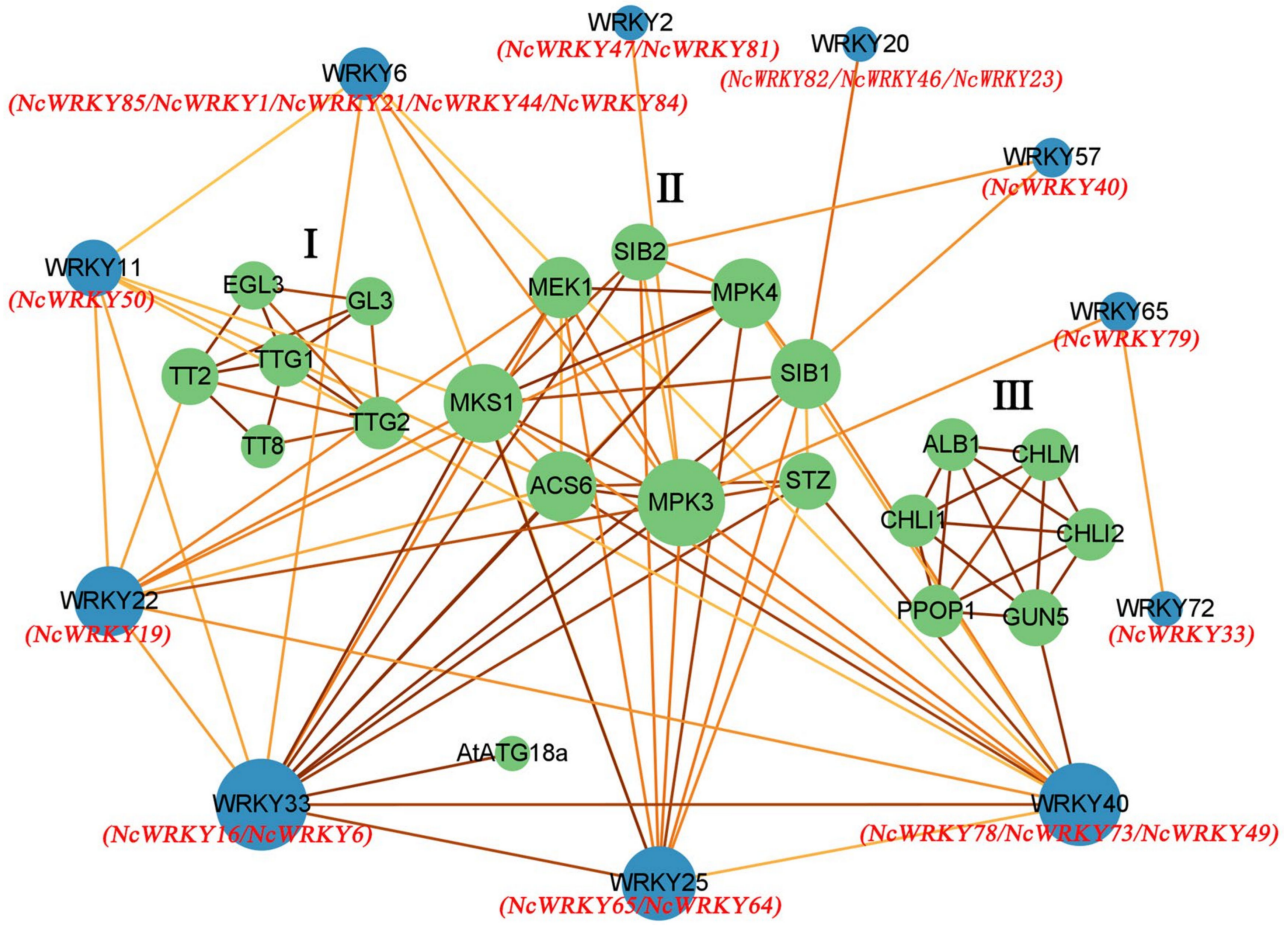

Figure 6. Protein–protein interaction network for NcWRKY proteins based on their orthologs in *A. thaliana*. The green and blue circles represented the interacting proteins found in String and orthologs proteins in *A. thaliana*, respectively. The red name below the blue circle indicates the WRKY protein orthologous to this protein in *N. cadamba*. The abbreviated names were the genes of *A. thaliana*. The color of the line represents the strength of the interaction, in which a darker line indicated higher reliability.

2.7. Expression Patterns of NcWRKYs Gene in N. cadamba Tissues by RNA-Seq

The expression patterns of all 85 *NcWRKYs* in the transcriptome data, which was derived from different tissues, including bud, young leaves, old leaves, bark, cambium, phloem, root, and young fruit, were investigated in this study (Figure S2, Supplementary File S5). The results showed that all 85 NcWRKYs were expressed in different tissues (FPKM > 0), and they were generally highly expressed in roots and old leaves. Some of the *NcWRKYs* were not expressed in the tissues we tested due to special temporal and spatial expression patterns.

Since the wood formation is of great significance for perennial trees, we further focused on the analysis of the expression patterns in different seasonal stages of cambium and phloem. *NcWRKY13/47/56/66/67/81* had high expression in both cambium and phloem in different seasons in the whole year (Figure 7). *NcWRKY12* and *NcWRKY38* had a similar expression mode, with higher expression in cambium but only expressed in phloem of June. To further explore the expression profiles of *NcWRKY* in different developmental vascular tissues, we isolated cambium, phloem, and xylem cells by laser microdissection at three stages, including primary growth, secondary growth, and the transition stage from primary to secondary growth, and the RNA-seq was subsequently carried out (data not published). The results showed that 39 *NcWRKYs* exhibited different expression levels during diverse phases of wood formation, suggesting that these *NcWRKY* genes played distinct roles during wood formation. For example, five *NcWRKYs* (*NcWRKY38/48/56/59/67*) had high expression in xylem of all three phases of wood formation, of which *NcWRKY67* exhibited the highest expression, suggesting that these genes played important roles in regulating xylem development. In cambium, *NcWRKY56*, *NcWRKY67*, and *NcWRKY58* showed the higher expression in the transition stage, while *NcWRKY81* had the highest expression in the stage of secondary growth (Figure 7b). Moreover, some *NcWRKYs* had high expression in three different wood development stages, such as *NcWRKY38/46/66/56/59/63/67*, suggesting that these genes may participate in the development of stem of *N. cadamba*. Altogether, these results indicated that *NcWRKY* genes evolved diverse biological functions that were important for wood formation.

2.8. Expression Patterns of NcWRKYs in Response to Different Treatments

To further confirm whether the expression of *NcWRKYs* was influenced by different abiotic stresses and hormonal treatments, RT-qPCR was used to examine the expression patterns of the 16 selected *NcWRKYs* in different treatments, including ABA, MeJA, GA, PEG6000, and NaCl. As to various hormone treatments (Figure 8), most of the 16 *NcWRKYs* responded to multiple treatments at the transcriptional level. For instance, *NcWRKY64* was induced by all tested treatments, except MeJA treatment. Some genes exhibited the same response pattern, such as *NcWRKY28/64/78*, which was strongly induced by ABA and GA, but slightly upregulated under MeJA treatment. On the contrary, *NcWRKY50* and *NcWRKY73* change little in different hormone treatments. In addition, several *NcWRKYs* were simultaneously induced by one treatment. For example, *NcWRKY8/19/28/65/67/74/78* were induced by ABA treatment (the fold change was more than 8), *NcWRKY8/16/28/64/65/78* were induced by GA_3 treatment (fold change > 5), and five *NcWRKY16/28/47/66/74* were induced by MeJA. Conversely, some genes were down-regulated after treatment, such as the transcript levels of *NcWRKY78* were decreased to half of the control by MeJA treatment, and *NcWRKY13* and *NcWRKY81* were repressed after ABA and GA_3 treatments.

For PEG6000 and NaCl treatments, we selected 12 *NcWRKY* genes for detecting their expression by RT-qPCR. As shown in Figure 9, most genes were more strongly responsive in leaves compared to roots, such as *NcWRKY16/19/64/65/73*. On the contrary, *NcWRKY50* had a stronger response intensity in roots. Four of the twelve genes (*NcWRKY21/28/65/78*) had little difference in expression between leaves and roots under PEG6000 and NaCl treatments. Interestingly, *NcWRKY8* only had a comparatively large response intensity in the roots of NaCl treatment.

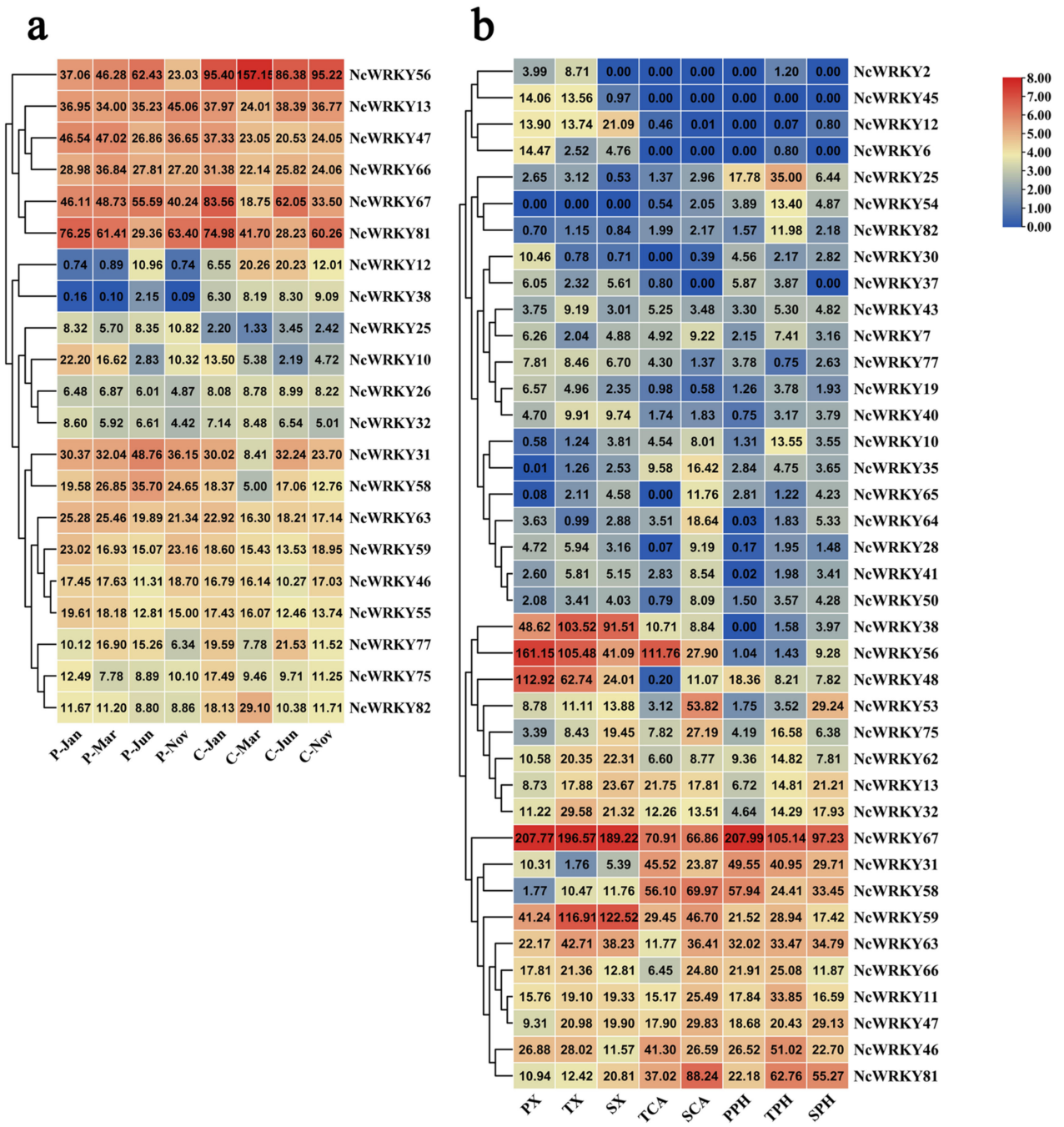

Figure 7. *NcWRKYs* transcriptional levels at different developmental stages of cambium, phloem, and xylem and combined analysis by laser capture microdissection (LCM)-RNA-seq. The heatmaps were created by TBtools based on the transformed data of log2 (FPKM+1) values, and the cluster analysis was performed on gene expression level by row. (**a**) Expression of *WRKY* genes in cambium and phloem in different months. C and P indicated cambium and phloem, respectively, and suffixes 'Jan, Mar, Jun, and Nov' indicate January, March, June, and November, respectively. (**b**) Expression of *WRKY* genes in xylem, cambium, and phloem at the stages of primary growth, secondary growth, and transitional stages from primary to secondary growth. PX, primary xylem; TX, xylem at the transitional stage from primary to secondary growth; SX, secondary xylem; TCA, cambium at the transitional stage from primary to secondary growth; SCA, secondary cambium; PPH, primary phloem; TPH, phloem at the transitional stage from primary to secondary growth; SPH, secondary phloem.

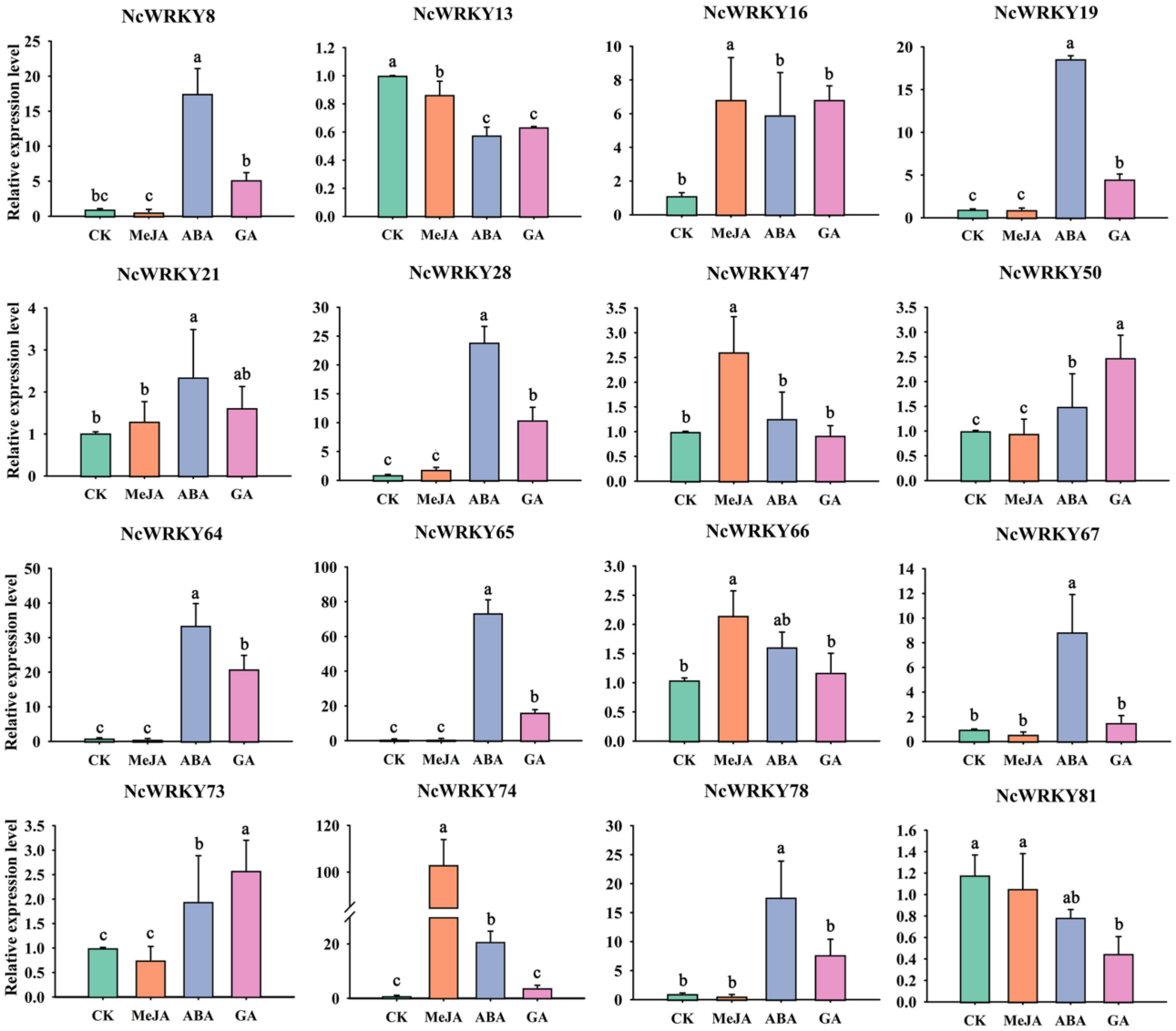

Figure 8. Expression profiles of 16 selected *NcWRKYs* in response to various hormone treatments, including MeJA, ABA, and GA. *NcUPL* was used as the endogenous control. Error bars indicated the standard deviation of three biological replicates, each containing three technical replicates. The same letters indicate groups that were not significantly different from each other according to Duncan's multiple range test, $p = 0.05$.

2.9. MeJA Promotes Cadambine Biosynthesis and NcWRKYs Expression

MeJA, as an exogenous hormone, can not only play a defensive role in plants, but also widely regulate the synthesis of a variety of secondary metabolites. The *N. cadamba* plants were treated with 0.1 mM/L and 1 mM/L of MeJA, and the contents of cadambine and tryptamine, the precursor of cadambine, were tested by UHPLC-MS-MS (Supplementary File S6). In leaves, the content of tryptamine was obviously elevated at 1 d and reached its highest at 4 d in the 1 mM/L MeJA treatment group. At 7 d after MeJA treatment, it dropped to the same level as 1 d (Figure 10a). However, the accumulation of cadambine gradually increased and reached the highest abundance at 7 d. In the stem, the content of tryptamine was slightly decreased from 1 d to 7 d. On the contrary, cadambine accumulation was obviously elevated at 4 d and slightly enhanced at 7 d (Figure 10b). As for the treatment of 0.1 mM/L, the changes of these two metabolites' accumulation were similar to that of 1 mM/L, but with gentle enhancement in both leaves and the stem.

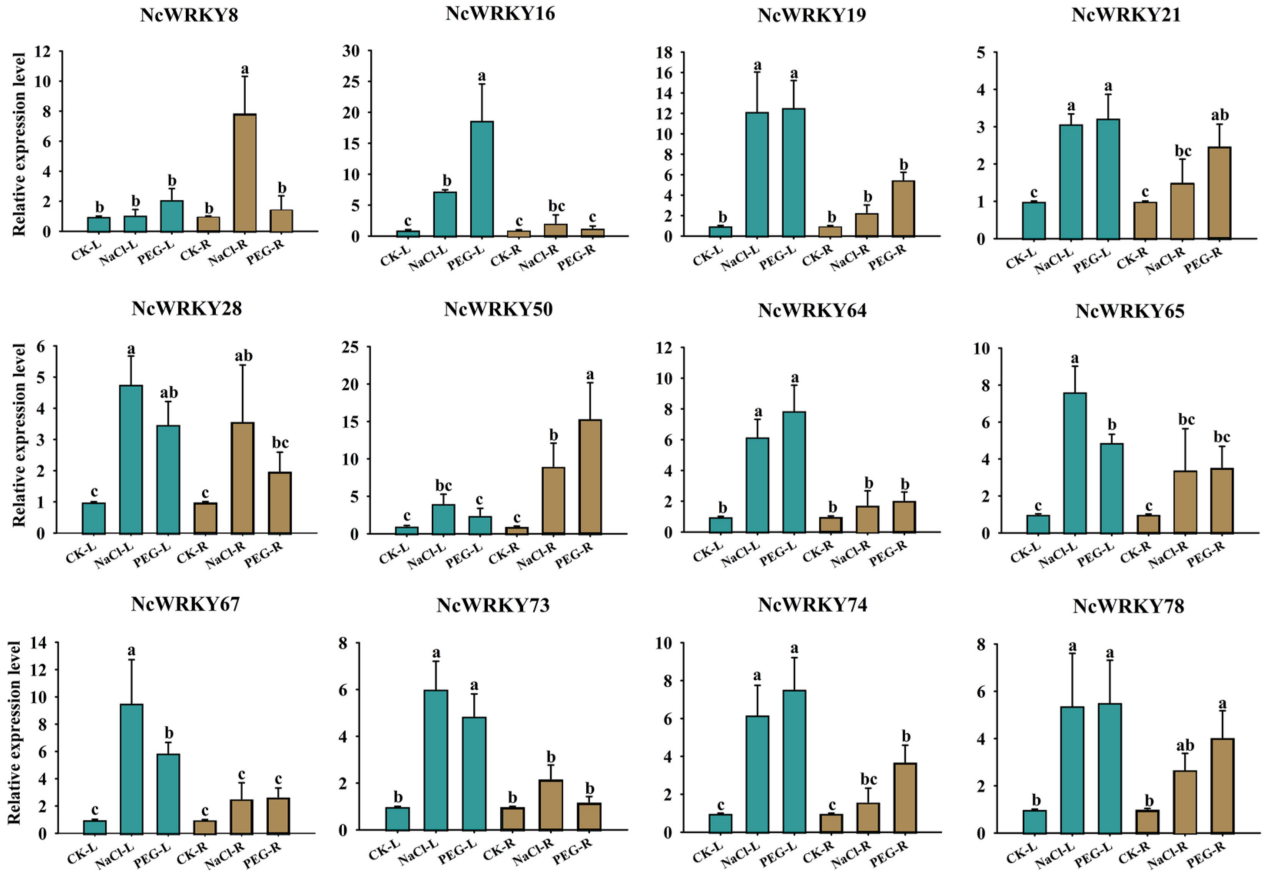

Figure 9. Expression profiles of 12 selected *NcWRKY* genes in response to NaCl and PEG6000 treatments. The leaf and root were collected after NaCl and PEG stress treatments and used for the detection of *NcWRKYs* expression. The suffix 'L' and 'R' refers to the leaf and root, respectively. *NcUPL* was used as the endogenous control. Error bars indicated the standard deviation of three biological replicates, with each comprising three technical replicates. The same letters indicate groups that were not significantly different from each other according to Duncan's multiple range test, $p = 0.05$.

As the key intermediate of the cadambine biosynthetic pathway, *NcSTR1* catalyzed the synthesis of strictosidine in *N. cadamba* [29]. Moreover, MYC is inhibited by JAZ protein, which leads to the downstream regulatory switch being turned off. When MeJA acted as an activation signal, JAZ protein would be degraded, and then the MYC transcription factor in the inhibited state was released, which thereby activates the target gene expression activity [35,36]. Accordingly, we further detected the expression patterns of *NcMYCs*, *NcSTR1* (evm. model. Contig 69.90), and *NcWRKYs* after MeJA treatment by RT-qPCR (Figure 10c). For the 1 mM/L MeJA treatment group, three *NcMYCs*' (*NcMYC2*, *7*, and *9)* expression was strongly induced by MeJA, with a peak after 1 d, and gradually decreased after 4 d and 7 d. The expression of the *STR1* gene and two *WRKY* genes (*NcWRKY64* and *NcWRKY74*) was similar to *NcMYCs*, with the same pattern. However, *NcMYC2*, *STR1*, *NcARKY64*, and *NcWRKY74* were induced at later time points (i.e., 4 d) in the 0.1 mM/L MeJA treatment group, suggesting that a higher concentration of MeJA was essential for rapid induction of expression of these genes. A control time course of treatment with the solvent ethyl alcohol showed no effect on the expression of *NcARKY64* and *NcWRKY74*, but promotes the expression of *NcMYC* and *STR1* genes. More *NcWRKYs* were upregulated significantly after treatment with 1 Mm/L MeJA (Figure S3).

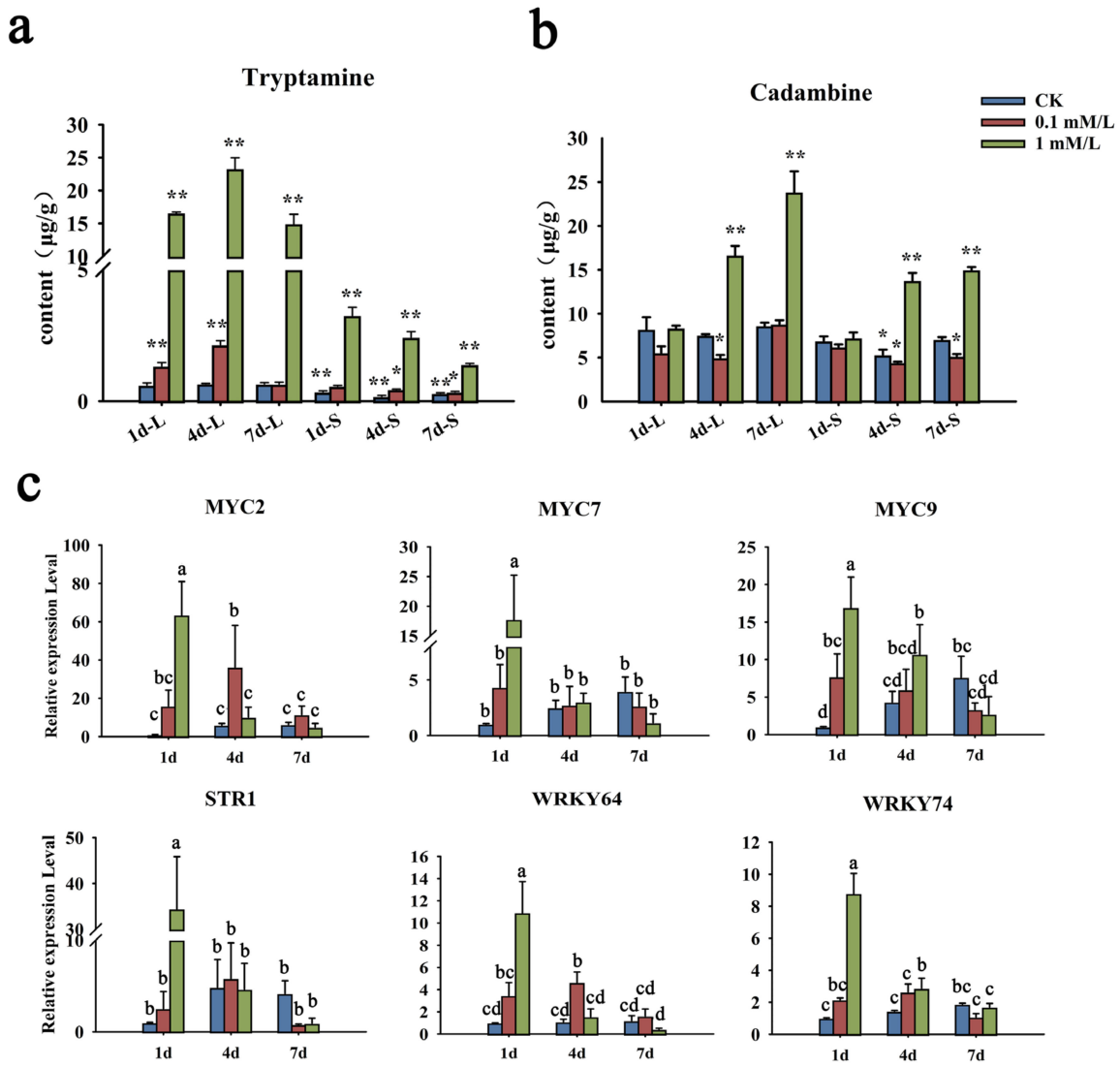

Figure 10. Changes of metabolite content and gene expression after MeJA treatment. (**a**,**b**) The content change of tryptamine and cadambine under MeJA treatment. Quantitative determination of tryptamine and cadambine was performed by UHPLC-MS-MS. (**c**) Transcript levels of *NcMYCs*, *NcSTR1*, and *NcWRKY64/74* in leaves of *N. cadamba* seedlings under MeJA treatments. The expression levels were determined by qRT-PCR. *NcMYCs*, as a kind of key transcriptional factor of MeJA signaling pathway, reflect the response of the jasmonic acid signal pathway after treatment. *NcSTR1* can catalyze the synthesis of strictosidine in *N. cadamba*, reflecting whether MeJA treatment affects the expression of synthesis pathway genes. *NcRPL* was used as the reference gene. Error bars represented the standard deviation of three biological replicates. The same letters indicate groups that were not significantly different from each other according to Duncan's multiple range test, $p = 0.05$. Statistically significant differences compared with the CK (untreated control) at 1 d were determined by *t*-tests (* $p < 0.05$, ** $p < 0.01$).

3. Discussion

The WRKY family is a large transcription factor family and plays pivotal roles in higher plants. Identification and characterization of *WRKY* genes have been performed in many plants, including the model plants, crops, and medicinal plants, such as Arabidopsis [3], corn [37], tomato [38], ginseng [39], and poplar [40]. In the present study, a total of 85 *NcWRKY* genes were identified in the genome of *N. cadamba* by bioinformatics analysis. Their features, expression patterns, and putative function were studied in detail.

3.1. Diverse Characterization of WRKY in N. cadamba

The uneven gene family size of WRKY was found in different plants. A previous report had indicated that the WRKY members ranged from 59 to 161 among seven species, of which *Z. mays* had the most prominent WRKY family members (genome size 2100 Mb), and a minor WRKY family was found in *V. vinifera* (genome size 427 Mb) [39]. *N. cadamba* had moderate WRKY family members (85), in accordance with the moderate genome size (744.5 Mb). These results indicated that the number of WRKY family members was correlated with genome size. However, an exception was found in ginseng, in which its genome size (2900 Mb) is larger than that of *Z. mays*, but with fewer WRKY family members [39]. Interestingly, *N. cadamba* possesses comparatively a greater number of *WRKY* genes compared with many dicotyledonous plants, including *Solanum lycopersicum* (81 *WRKY* genes), *A. thaliana* (72 *WRKY* genes), *D. carota* (67 *WRKY* genes), *Salvia miltiorrhiza* (61 *WRKY* genes), and *C. roseus* (47 *WRKY* genes) [41]. Gene duplication was found to play a very important role in the expansion of the *WRKY* gene family. In *N. cadamba*, a total of 76 segmental duplication events are identified in *NcWRKYs*, and the genes involved in segment duplication do not have distinct subgroup distributions, indicating that the WRKY family has no obvious evolutionary differences in the distribution of *N. cadamba*. Moreover, for all pairs, the Ka/Ks ratios are <1, indicating that the *WRKY* gene family in *N. cadamba* has undergone purifying selection rather than positive selection, and indicating that the *NcWRKYs* are highly conserved.

The WRKY domain is the key sequence that determines the specific binding of the WRKY protein to the *cis*-element W-box. According to previous studies, variations of the WRKYGQK motif in the WRKY domain might influence normal interactions of WRKY genes with downstream target genes [42]. The multiple sequence alignment results revealed that six NcWRKY proteins (NcWRKY30/48/55/57/68/76) in Group IIc had sequence variation in their WRKY domain (WRKYGKK), which binds specifically to the WK-box (TTTTCCAC) in tobacco [43]. According to transcriptome data, these six *NcWRKYs* had similar expression patterns, mainly expressed in old leaf, young fruit, and root (Additional Figure 2). The result indicated that the variation of the WRKY domain in *N. cadamba* may not affect its binding function, and the six *NcWRKYs* may have similar functions. It might be worth to further investigate whether the mutated domain confers a special function. The diversification of exon/intron patterns played a vital role in the evolution process of many gene families. We found that 85 *NcWRKYs* contained between one and six introns, consistent with that in pineapple [44], cucumber [45], and populus [46]. NcWRKY proteins from Group I have two WRKY domains, and no domain loss events were found in other NcWRKY proteins, which was similar to most of the dicotyledonous plants.

3.2. The Potential Function of NcWRKYs in Vascular Development and Response to Hormone and Abiotic Stress

Based on transcriptome data, some valuable clues about the functional role of *NcWRKYs* which are involved in the specific physiological process in *N. cadamba* were obtained. For different developmental stages of cambium, phloem, and xylem, some *WRKY* genes have high expression levels, and these genes were highly overlapping, such as *NcWRKY12/38/56* specifically expressed in different developmental stages of cambium and phloem. These genes were orthologous with the *MiWRKY12* and *PtrWRKY19*, which participate in pith secondary cell wall formation in *Miscanthus* and *P. trichocarpa*, respectively [47,48]. Moreover, in *atwrky13* mutants, lignin-synthesis-related genes were repressed, and the number of sclerenchyma cells, stem diameter, and the number of vascular bundles were reduced [49]. *NcWRKY12/38/56* were in the same subgroup as *AtWRKY13*, suggesting that they might involve in the stem development of *N. cadamba*. Accordingly, we inferred that these three *NcWRKYs* may participate in vascular development.

A variety of conserved cis-regulatory elements were shown in the promoter region of *NcWRKYs*, which were involved in a variety of functions, including hormone and abiotic stress responses (Figure 5). The response of *NcWRKYs* to hormone and abiotic stresses

can provide valuable clues to reveal the potential role of *WRKY* genes in *N. cadamba*. In this study, 16 *NcWRKYs* chosen from different groups were subjected to hormones, salt, and drought stress treatments profiled by means of RT-qPCR. The result shows that all of *NcWRKYs* can be induced by at least two hormones, implying that a single *WRKY* gene can be regulated by various hormones, similar to that in Arabidopsis, *AtWRKY18/40/60* were shown to participate in signaling pathways that were mediated by plant hormones SA, JA, and ABA [8], and Group III members of *CsWRKYs* in *Cymbidium sinense* were strongly induced in response to various hormone treatments [50]. Previous studies have revealed that WRKYs are important regulators in linking hormone signaling in response to environmental stresses [51,52]. *FcWRKY40* from *Fortunella crassifolia* was involved in ABA signaling pathways and positively regulated salt tolerance by directly binding to and activating the promoters of *FcSOS2* and *FcP5CS1*. The transcriptions of *NcWRKY8/16/64/65* were promoted simultaneously by ABA and drought stress. In addition, several stress-related transcriptional regulatory elements, including an ABA-responsive element and MYB binding site involved in drought responses, were found in these NcWRKYs. These results suggested that these NcWRKYs may regulate drought responses through ABA-dependent signaling pathways, but this remains to be elucidated in further study. Moreover, these NcWRKYs have a phylogenetically closest relationship with *AtWRKY33*, a typical ABA and drought-responsive *WRKY* gene in *A. thaliana* [53,54], supporting that they play important roles in ABA signaling pathway and response to drought stress.

3.3. The Involvement of NcWRKYs in Cadambine Biosynthesis

Jasmonic acid (JA) is an important elicitor in plant secondary metabolism at the transcriptional level by altering the expression of a set of biosynthesis genes [55,56]. It has been shown that methyl-jasmonate (MeJA) induced the expression of the terpenoid indole alkaloid (TIA) biosynthesis genes, including the strictosidine synthase (STR) gene [55], resulting in promoting TIA metabolism in *Catharanthus roseus* [57]. In this study, cadambine and the key intermediate product tryptamine were both induced under MeJA treatment, suggesting that MeJA acted as an elicitor in cadambine biosynthesis. Our results facilitated that MeJA plays a significant role in plant metabolism. In addition, the MYC gene family is a kind of key TF in the MeJA signal pathway [58]. The expression levels of *NcMYCs* were highly induced after MeJA treatment (Figure 10c), indicating that the MeJA signal pathway was activated in *N. cadamba* seedlings.

Studies have indicated that WRKY proteins participated in transcriptional regulating biosynthesis of secondary metabolites, including alkaloids [24], volatile terpenes [59], and anthocyanin [60]. It has been reported that several WRKY proteins may regulate secondary metabolism biosynthesis in response to JA elicitation. In cotton, GaWRKY1 was strongly induced by MeJA and participated in the regulation of sesquiterpene phytoalexin biosynthesis by transactivating the promoter of the (1)-δ-cadinene synthase (CAD1) gene [20]. The expression pattern of *NcWRKY64* and *NcWRKY74* was consistent with that of *NcMYCs* and *NcSTR1*, which were upregulated after MeJA treatment. In addition, there were two WRKY TF binding site W-box (TTGACC) within 2000 bp upstream of the NcSTR1 promoter (Figure S4). We proposed that NcWRKY64/74 has the potential function of positively regulating the biosynthesis of cadambine by activating NcSTR1 in response to MeJA. The interaction between NcWRKY64/74 and NcSTR1 remained to be investigated in the future study.

Furthermore, AtWRKY33, OpWRKY6, CrWRKY1, and TcWRKYs were involved in the regulation of camalexin (Indole alkaloids), camptothecin (Quinoline alkaloid), vinblastine (Indole alkaloids), and taxol (Diterpene alkaloids) biosynthesis, respectively [18,23,24,61,62]. AtWRKY33 and NcWRKY64, OpWRKY6 and NcWRKY74 were close to each other in the phylogenetic tree (Figure S5), and they have the same WRKY domain (WRKYGQK) and zinc-finger motif (C-H_4-X_{23}-H-X-H) (Figure S6). Therefore, according to the high homology between AtWRKY33, NcWRKY64, and NcWRKY74, we inferred that NcWRKY64 and NcWRKY74 were essential for MeJA-responsive TIA accumulation in *N. cadambia*. No

MeJA-responsive cis-acting element was found in the *NcWRKY74* promoter, suggesting that the expression of *NcWRKY74* was induced by MeJA in an indirect manner. Further functional characterization of *NcWRKY64* and *NcWRKY74* by overexpression or knockout of these *NcWRKY* genes may help to elucidate their function in TIA biosynthesis, which will provide crucial information for understanding the MeJA-WRKY-STR regulatory module in the cadambine biosynthesis.

4. Materials and Methods

4.1. Data Sources

All raw and processed sequencing data used in this study were derived from the previous research of our research group and can acquire in the NCBI BioProject database under accession number PRJNA650253. The raw sequencing data of the resequencing data and transcriptome were downloaded from the NCBI BioSample database under accession numbers SAMN15700860 and SAMN15700859, respectively. The genome annotation and assembled genome sequences were from the Figshare website (https://Figshare.com/s/ed20e0e82a4e7474396b) [29]. The AtWRKY protein sequences were downloaded from the *A. thaliana* Information Resource website (https://www.arabidopsis.org/index.jsp).

4.2. Identification of WRKY Genes in N. cadamba

To identify all candidate WRKY genes in *N. cadamba*, a BLASTP search with a threshold e-value of 1×10^{-5} was performed using *A. thaliana* WRKY protein sequences as query sequences. The hidden Markov model (HMM) file corresponding to the WRKY domain (PF03106) was downloaded from the Pfam database (ftp://ftp.ebi.ac.uk/pub/databases/Pfam/current_release/Pfam-A.hmm.gz). The Simple HMM Search program of TBtools [63] was used to search all the potential WRKY-domain-containing protein sequences in the *N. cadamba* genome. The unique potential WRKY proteins of *N. cadamba* based on the results of BLASTP and Simple HMM Search were further validated using the SMART (http://smart.embl.de/smart/batch.pl) and conserved domain database from NCBI (https://www.ncbi.nlm.nih.gov/cdd/) to determine that they indeed contained the core domain sequences. Eighty-five NcWRKY proteins in *N. cadamba* were finally obtained. The online tools from ExPASy (https://web.expasy.org/protparam/) were used to analyze the amino acid number, isoelectric point (pI), and MW of NcWRKY proteins. Subcellular localizations were predicted by the Plant-mPLoc website. (http://www.csbio.sjtu.edu.cn/bioinf/plant-multi/).

4.3. Phylogenetic Analysis of WRKY Family Members and Sequence Alignment

A phylogenetic tree with 72 AtWRKY protein sequences and the identified NcWRKY proteins sequences was constructed by One Step Bulid, an ML Tree program from TBtools [63] with default parameters, followed by visualization and optimization in iTOL [64]. The WRKY family members from *A. thaliana* were used as a reference for the classification of the WRKY family members in *N. cadamba*. All WRKY domain sequences of candidate NcWRKY proteins were aligned using DNAMAN software.

4.4. Analysis of Conserved Motifs, Conserved Domains, and Gene Structures

The conserved motifs of the NcWRKY proteins were analyzed using Simple MEME Wrapper from TBtools [63] with the following parameters: Num of Motifs was 10, Min Motif Width was 6, Max Motif Width was 50, and Max E-value was 10. The conserved domains of NcWRKY proteins were searched by CDD (https://www.ncbi.nlm.nih.gov/cdd/). The conserved motifs, conserved domains, and gene structures which were obtained from the gene structure annotation file were visualized by TBtools.

4.5. Promoter Cis-Regulatory Element Analysis and Chromosomal Localization

The 2000 bp gene sequence upstream of the initiation codon (ATG) of *NcWRKYs* was considered as the gene promoter sequence and deprived of the *N. cadamba* genome by TBtools [63]. *Cis*-acting elements in the promoter region were analyzed using the

online software PlantCARE [65] and subsequently visualized using TBtools [63]. Location Visualize from GTF/GFF of TBtools was used to determine the chromosomal position of the identified *NcWRKYs*.

4.6. Colinear Analysis and Selective Pressure

To identify the pattern of gene duplication, One Step MCScanX from TBtools [63] with default parameters (E-value cut-off < 1×10^{-10} and Num of BlastHits with 5) was used to analyze *WRKY* genes in *N. cadamba* vs. itself and *N. cadamba* vs. *A. thaliana*/*Coffea canephora*/*Populus trichocarpa*/rice, respectively. The results were visualized using TBtools. To assess the selection pressure of genes encoding WRKY proteins, the ratio of nonsynonymous (Ka)/synonymous (Ks) (Ka/Ks is an indicator of selective pressure) was used to evaluate its evolutionary pressure. The values of Ka, Ks, and Ka/Ks were calculated by Simple KaKs Calculator in TBtools [63].

4.7. Homology Analyses and Protein Interaction Network Analysis

In order to obtain the orthologous gene pairs and paralogous gene pairs, all the individual NcWRKYs protein sequences were compared against AtWRKY protein sequences using BLASTP (https://blast.ncbi.nlm.nih.gov/Blast.cgi) with the following settings: Total Score >200, Query Cover >than 60%, E-value cut-off < 1×10^{-10}, and Identity >45%. Using homolog *A. thaliana* WRKYs as a template, the WRKY protein interaction network of *N. cadamba* was analyzed using STRING (https://string-db.org/) with a threshold required score >0.4. The interaction network was further visualized and analyzed using the software Cytoscape 3.9.1.

4.8. Plant Material and Stress Treatments

For salinity and drought treatments, 7-week-old clonal plants of *N. cadamba* with uniform height were transferred into MS liquid medium supplied with 100 mM/L NaCl and 10% PEG6000 solution, respectively. The leaves and roots were collected at 8 h. For phytohormone analysis, the seedlings that were transplanted outdoors and grow up to 60 cm after 3 months were respectively sprayed 10 mg/L ABA, GA_3, and MeJA 50 mL. Then wrap the leaves in fresh-keeping bags. The young leaves were collected 2 d after treatments. All the collected samples were immediately frozen in liquid nitrogen and stored at −80 °C for subsequent analysis.

The 4-month-old *N. cadamba* plants (about 100 cm in height) were sprayed with different MeJA concentrations (0.1 and 1 mM/L) that were mixed with pure water. The mother liquor is 1 mM/mL, which is prepared from MeJA stock solution and absolute ethanol. At about 8:30 every morning, the MeJA was sprayed on the leaf's front and back surface till dripping for 7 consecutive days. The roots, stems, and leaves of the plants were sampled and stored at −80 °C on the first (1 d), the fourth (4 d), and the seventh (7 d) days after spraying was stopped. Each sample contained three biological replicates.

4.9. Expression Patterns of NcWRKYs

The transcriptome sequencing data of young leaves, old leaves, bud, bark, phloem, cambium, young fruit, and root from 5-year-old *N. cadamba* were collected for RNA extraction for RNA-seq in our previous study [29]. The vascular cells, including cambium, phloem, and xylem cells, at three developmental stages (primary growth, secondary growth, and the transition from primary to secondary growth) were captured by laser microdissection and used for subsequent RNA-seq [66]. The transcript abundance of *N. cadamba WRKY* genes was calculated as fragments per kilobase of exon model per million mapped reads (FPKM). The HeatMap program in TBtools was used to visualize the expression of the target gene obtained from the transcriptome. The HeatMap program in TBtools was used to visualize the expression of the target gene obtained from the transcriptome. Total RNA was isolated from each sample using the E.Z.N.A®Plant RNA Kit (Omega, GA, USA). RNA integrity was evaluated by 1% (v/v) agarose gel electrophoresis, and

RNA purity was quantified using an IMPLEN NanoPhotometer. Total RNA was used to synthesize cDNA by using HiScript III RT SuperMix for qPCR (+gDNA wiper) (Vazyme, Nanjing, China). The quantitative RT-qPCR was carried out with the Roche Lightcyler® 480 instrument using SYBR Green chemistry. The housekeeping *UPL* and *RPL* genes were used as an internal control of different treatments and MeJA treatment with different concentrations, respectively [67,68]. The RT-qPCR program was set as follows: 95 °C for 30 s, followed by 40 cycles of 95 °C/10 s, 60 °C/30 s, and the fluorescence signal was then read. Subsequently, the procedure was conducted as follows: 95 °C for 15 s, 60 °C for 60 s, and warming up to 95 °C then 50 °C for 30 s; after the fluorescence signal was read, the dissolution curve was analyzed. There were three biological replicates for each sample, and each biological replicate had three technical repetitions. Sequences of the primers used in this study were shown in detail in Supplementary File S7. The data obtained were visualized using SigmaPlot.

4.10. Extraction and Quantitative Determination of Tryptamine and Cadambine

The samples were ground at −80 °C using liquid nitrogen. We weighed 0.12 g of sample and added 5 mL of 70% ethanol, and the mixture was held overnight at −20 °C, followed by ultrasonic crushing for 30 min, vibrating every 5 min. After ultrasonic crushing, and centrifugation at 4 °C for 10 min at 7000 rpm, samples were filtered through 0.22 μm membrane filters before liquid chromatography–mass spectrometry (LC-MS) analysis.

Samples were analyzed by reversed-phase chromatography on an Agilent 1290 HPLC, using a 3.0 × 50 mm ECLIPS PLUS C18 column. Water with 0.1% formic acid (A) and methanol (B) was used as the mobile phase component at a flow rate of 0.3 mL/min with the following gradient: 0–3 min, 50% B; 3–6 min, 90% B; 5–6 min, 90% B; 6–10 min, 10% B. A coupled Agilent 6470 MS-QQQ mass spectrometer with ESI and Agilent Jet Stream was used to collect MS data in positive ion mode (parameters: Gas: 300 °C, 8 L/min; Nebulizer: 45 psi; Sheath Gas: 350 °C, 10 L/min; Capillary: 4000 V; VCharging: 1000). Scan type was MRM.

4.11. Statistical Analysis

Data from three biological and three technical replicates were used for statistical analysis. All data were indicated by an average of three biological replicate measurements and standard deviation. As for RT-qPCR, the relative gene expression levels were analyzed using the $2^{-\Delta\Delta Ct}$ method. Significance was determined by pairwise comparison using *t*-tests or multiple comparison using Duncan's multiple range test in SPSS software 26 ($p = 0.05$).

5. Conclusions

Overall, a total of 85 *WRKY* genes were identified from *N. cadamba* and divided into seven subfamilies according to their phylogenetic relationships, and members of the same subfamily had similar gene structures and conserved motifs and domains. The analyses of expression patterns based on RNA-seq data revealed their probable functions in different tissues and vascular development. In addition, the detection of remarkable expression profiles of NcWRKYs under hormones and abiotic stresses will provide clues for exploring the signaling pathways in *N. cadambia* in response to hormone and abiotic stresses. It is worth noting that MeJA promoted cadambine accumulation and induced the expression of the key intermediate gene *STR1*, *NcWRKY64*, and *NcWRKY74*, implying the MeJA-WRKY-STR regulatory module in the cadambine biosynthesis. This study suggests a basis for further functional research of the regulatory mechanism of *NcWRKYs* in hormone and stress responses and provides promising candidate genes for regulating cadambine synthesis in *N. cadamba*.

Supplementary Materials: The following supporting information can be downloaded at https://www.mdpi.com/article/10.3390/ijms24087537/s1.

Author Contributions: C.P. and J.L. conceived the project; Z.X., Y.L. and H.F. performed the experiments and analyzed the data; Y.W. (Yanqiong Wen), Y.W. (Ying Wang) and J.Z. helped to prepare the plant materials and extracted metabolites; Z.X., J.L. and C.P. wrote and revised the manuscript. All authors have read and agreed to the published version of the manuscript.

Funding: This work was supported by funds from the National Natural Science Foundation of China (Grant No. 32271908); Natural Science Foundation of Guangdong Province of China (Grant Nos 2021A1515010816, 2023A1515030250, and 2023A1515010341); and Guangzhou Science and Technology Program (Grant No. 202102020505).

Institutional Review Board Statement: Not applicable.

Informed Consent Statement: Not applicable.

Data Availability Statement: Data are provided within the article and Supplementary Materials.

Conflicts of Interest: The authors declare no conflict of interest.

References

1. Ulker, B.; Somssich, I.E. WRKY transcription factors: From DNA binding towards biological function. *Curr. Opin. Plant Biol.* **2004**, *7*, 491–498. [CrossRef]
2. Brand, L.H.; Fischer, N.M.; Harter, K.; Kohlbacher, O.; Wanke, D. Elucidating the evolutionary conserved DNA-binding specificities of WRKY transcription factors by molecular dynamics and in vitro binding assays. *Nucleic Acids Res.* **2013**, *41*, 9764–9778. [CrossRef] [PubMed]
3. Eulgem, T.; Rushton, P.J.; Robatzek, S.; Somssich, I.E. The WRKY superfamily of plant transcription factors. *Trends Plant Sci.* **2000**, *5*, 199–206. [CrossRef]
4. Jingjing, J.; Shenghui, M.; Nenghui, Y.; Ming, J.; Jiashu, C.; Jianhua, Z. WRKY transcription factors in plant responses to stresses. *J. Integr. Plant Biol.* **2017**, *59*, 86–101. [CrossRef]
5. Rushton, P.J.; Somssich, I.E.; Ringler, P.; Shen, Q.J. WRKY transcription factors. *Trends Plant Sci.* **2010**, *15*, 247–258. [CrossRef] [PubMed]
6. Xie, Z.; Zhang, Z.L.; Zou, X.; Yang, G.; Komatsu, S.; Shen, Q.J. Interactions of two abscisic-acid induced *WRKY* genes in repressing gibberellin signaling in aleurone cells. *Plant J.* **2006**, *46*, 231–242. [CrossRef] [PubMed]
7. Hwang, S.H.; Kwon, S.I.; Jang, J.Y.; Fang, I.L.; Lee, H.; Choi, C.; Park, S.; Ahn, I.; Bae, S.C.; Hwang, D.J. OsWRKY51, a rice transcription factor, functions as a positive regulator in defense response against *Xanthomonas oryzae* pv. oryzae. *Plant Cell Rep.* **2016**, *35*, 1975–1985. [CrossRef] [PubMed]
8. Chen, H.; Lai, Z.; Shi, J.; Xiao, Y.; Chen, Z.; Xu, X. Roles of Arabidopsis WRKY18, WRKY40 and WRKY60 transcription factors in plant responses to abscisic acid and abiotic stress. *BMC Plant Biol.* **2010**, *10*, 281. [CrossRef] [PubMed]
9. Shixiong, R.; Kaibiao, M.; Zhaogeng, L.; Gang, C.; Jiawen, C.; Peixi, T.; Li, W.; Nianjun, T.; Biao, J. Transcriptomic and metabolomic analysis of the heat-stress response of *Populus tomentosa Carr*. *Forests* **2019**, *10*, 383. [CrossRef]
10. Wu, M.; Zhang, K.; Xu, Y.; Wang, L.; Liu, H.; Qin, Z.; Xiang, Y. The moso bamboo WRKY transcription factor, PheWRKY86, regulates drought tolerance in transgenic plants. *Plant Physiol. Biochem.* **2022**, *170*, 180–191. [CrossRef] [PubMed]
11. Chan, Y.P.; Ju, H.L.; Jae, H.Y.; Byeong, C.M.; Man, S.C.; Yun, H.K.; Sang, M.L.; Ho, S.K.; Kyu, Y.K.; Woo, S.C.; et al. WRKY group IId transcription factors interact with calmodulin. *FEBS Lett.* **2005**, *579*, 1545–1550. [CrossRef]
12. Li, S.; Fu, Q.; Chen, L.; Huang, W.; Yu, D. *Arabidopsis thaliana WRKY25*, *WRKY26*, and *WRKY33* coordinate induction of plant thermotolerance. *Planta* **2011**, *233*, 1237–1252. [CrossRef] [PubMed]
13. Liang, Q.; Wu, Y.; Wang, K.; Bai, Z.; Liu, Q.; Pan, Y.; Zhang, L.; Jiang, B. Chrysanthemum WRKY gene *DgWRKY5* enhances tolerance to salt stress in transgenic chrysanthemum. *Sci. Rep.* **2017**, *7*, 4799. [CrossRef] [PubMed]
14. Luo, X.; Li, C.; He, X.; Zhang, X.; Zhu, L. ABA signaling is negatively regulated by *GbWRKY1* through JAZ1 and ABI1 to affect salt and drought tolerance. *Plant Cell Rep.* **2020**, *39*, 181–194. [CrossRef]
15. Yong, F.G.; Ji, K.L.; Feng, M.Y.; Guo, Y.Z.; Dan, W.; Lin, Z.; Yong, B.O.; Yin, A.Y. The WRKY transcription factor WRKY8 promotes resistance to pathogen infection and mediates drought and salt stress tolerance in *Solanum lycopersicum*. *Physiol. Plant.* **2020**, *168*, 98–117. [CrossRef]
16. Hao, X.; Xie, C.; Ruan, Q.; Zhang, X.; Wu, C.; Han, B.; Qian, J.; Zhou, W.; Nutzmann, H.W.; Kai, G. The transcription factor OpWRKY2 positively regulates the biosynthesis of the anticancer drug camptothecin in *Ophiorrhiza pumila*. *Hortic. Res.* **2021**, *8*, 7. [CrossRef] [PubMed]

17. Can, W.; Chao, W.; Yao, W.; Chenhong, X.; Min, S.; Shivraj, N.; Zhigang, Z.; Guoyin, K. Transcription factor OpWRKY3 is involved in the development and biosynthesis of camptothecin and its precursors in *Ophiorrhiza pumila* hairy roots. *Int. J. Mol. Sci.* **2019**, *20*, 3996. [CrossRef]
18. Wang, C.; Hao, X.; Wang, Y.; Maoz, I.; Zhou, W.; Zhou, Z.; Kai, G. Identification of WRKY transcription factors involved in regulating the biosynthesis of the anti-cancer drug camptothecin in *Ophiorrhiza pumila*. *Hortic. Res.* **2022**, *9*, uhac099. [CrossRef]
19. Sun, P.W.; Xu, Y.H.; Yu, C.C.; Lv, F.F.; Tang, X.L.; Gao, Z.H.; Zhang, Z.; Wang, H.; Liu, Y.; Wei, J.H. *WRKY44* represses expression of the wound-induced sesquiterpene biosynthetic gene ASS1 in *Aquilaria sinensis*. *J. Exp. Bot.* **2020**, *71*, 1128–1138. [CrossRef]
20. Xu, Y.H.; Wang, J.W.; Wang, S.; Wang, J.Y.; Chen, X.Y. Characterization of GaWRKY1, a cotton transcription factor that regulates the sesquiterpene synthase gene (+)-delta-cadinene synthase-A. *Plant Physiol.* **2004**, *135*, 507–515. [CrossRef]
21. Ma, D.; Pu, G.; Lei, C.; Ma, L.; Wang, H.; Guo, Y.; Chen, J.; Du, Z.; Wang, H.; Li, G.; et al. Isolation and characterization of AaWRKY1, an *Artemisia annua* transcription factor that regulates the amorpha-4,11-diene synthase gene, a key gene of artemisinin biosynthesis. *Plant Cell Physiol.* **2009**, *50*, 2146–2161. [CrossRef] [PubMed]
22. Lu, Y.; Juan, W.; Jiachen, S.; Junping, H.; Kee-Yoeup, P.; So-Young, P.; Luqi, H.; Wenyuan, G. A WRKY transcription factor, PgWRKY4X, positively regulates ginsenoside biosynthesis by activating squalene epoxidase transcription in *Panax ginseng*. *Ind. Crops Prod.* **2020**, *154*, 112671. [CrossRef]
23. Zhang, M.; Chen, Y.; Nie, L.; Jin, X.; Liao, W.; Zhao, S.; Fu, C.; Yu, L. Transcriptome-wide identification and screening of WRKY factors involved in the regulation of taxol biosynthesis in *Taxus chinensis*. *Sci. Rep.* **2018**, *8*, 5197. [CrossRef] [PubMed]
24. Suttipanta, N.; Pattanaik, S.; Kulshrestha, M.; Patra, B.; Singh, S.K.; Yuan, L. The transcription factor CrWRKY1 positively regulates the terpenoid indole alkaloid biosynthesis in *Catharanthus roseus*. *Plant Physiol.* **2011**, *157*, 2081–2093. [CrossRef]
25. Pandey, A.; Negi, P.S. Traditional uses, phytochemistry and pharmacological properties of *Neolamarckia cadamba*: A review. *J. Ethnopharmacol.* **2016**, *181*, 118–135. [CrossRef] [PubMed]
26. Isao, K.; Hong, W.; Sanae, N.; Taifo, M.; Kazuyuki, H.; Motomasa, K.; Tahan, U.; Hirotaka, S. Indonesian Medicinal Plants. XIV. Characterization of 3′-0-Caffeoylswerosicle, a new secoiridoid glucoside, and kelampayosides A and B, two new phenolic apioglucosides, from the bark of *Anthocephalus chinensis* (*Rubiaceae*). *Chem. Pharm. Bull.* **1996**, *44*, 1162–1167. [CrossRef]
27. Ashish, K.; Somenath, R.C.; Kumar, K.J.; Tulika, C.; Hemanta, K.M.; Tarun, J.; Sibabrata, M. Anthocephaline, a new indole alkaloid and cadambine, a potent inhibitor of DNA topoisomerase IB of leishmania donovani (LdTOP1LS), isolated from *Anthocephalus cadamba*. *Nat. Prod. Commun.* **2015**, *10*, 297–299. [CrossRef]
28. Deepak, K.; Chilukuri, T.; Saiprasanna, R.; Sumana, M.; Bikas, C.P. Bio-assay guided isolation of anti-cancer compounds from *Anthocephalus cadamba* bark. *Nat. Prod. Commun.* **2015**, *10*, 1349–1350. [CrossRef]
29. Zhao, X.; Hu, X.; OuYang, K.; Yang, J.; Que, Q.; Long, J.; Zhang, J.; Zhang, T.; Wang, X.; Gao, J.; et al. Chromosome-level assembly of the *Neolamarckia cadamba* genome provides insights into the evolution of cadambine biosynthesis. *Plant J.* **2022**, *109*, 891–908. [CrossRef] [PubMed]
30. He, X.; Wang, C.; Wang, H.; Li, L.; Wang, C. The function of MAPK cascades in response to various stresses in horticultural Plants. *Front. Plant Sci.* **2020**, *11*, 952. [CrossRef] [PubMed]
31. Meng, X.; Zhang, S. MAPK cascades in plant disease resistance signaling. *Annu. Rev. Phytopathol.* **2013**, *51*, 245–266. [CrossRef] [PubMed]
32. Pitzschke, A.; Schikora, A.; Hirt, H. MAPK cascade signalling networks in plant defence. *Curr. Opin. Plant Biol.* **2009**, *12*, 421–426. [CrossRef] [PubMed]
33. Krishnamurthy, P.; Vishal, B.; Ho, W.J.; Lok, F.; Lee, F.; Kumar, P.P. Regulation of a cytochrome P450 gene *CYP94B1* by WRKY33 transcription factor controls apoplastic barrier formation in roots to confer salt tolerance. *Plant Physiol.* **2020**, *184*, 2199–2215. [CrossRef] [PubMed]
34. Mao, G.; Meng, X.; Liu, Y.; Zheng, Z.; Chen, Z.; Zhang, S. Phosphorylation of a WRKY transcription factor by two pathogen-responsive MAPKs drives phytoalexin biosynthesis in Arabidopsis. *Plant Cell* **2011**, *23*, 1639–1653. [CrossRef]
35. Hu, P.; Zhou, W.; Cheng, Z.; Fan, M.; Wang, L.; Xie, D. JAV1 controls jasmonate-regulated plant defense. *Mol. Cell* **2013**, *50*, 504–515. [CrossRef]
36. Wasternack, C. Action of jasmonates in plant stress responses and development—Applied aspects. *Biotechnol. Adv.* **2014**, *32*, 31–39. [CrossRef]
37. Tang, Y.; Guo, J.; Zhang, T.; Bai, S.; He, K.; Wang, Z. Genome-wide analysis of WRKY gene family and the dynamic responses of key WRKY genes involved in *Ostrinia furnacalis* attack in *Zea mays*. *Int. J. Mol. Sci.* **2021**, *22*, 13045. [CrossRef]
38. Huang, S.; Gao, Y.; Liu, J.; Peng, X.; Niu, X.; Fei, Z.; Cao, S.; Liu, Y. Genome-wide analysis of WRKY transcription factors in *Solanum lycopersicum*. *Mol. Genet. Genom.* **2012**, *287*, 495–513. [CrossRef]
39. Di, P.; Wang, P.; Yan, M.; Han, P.; Huang, X.; Yin, L.; Yan, Y.; Xu, Y.; Wang, Y. Genome-wide characterization and analysis of WRKY transcription factors in *Panax ginseng*. *BMC Genom.* **2021**, *22*, 834. [CrossRef]
40. Jiang, Y.; Duan, Y.; Yin, J.; Ye, S.; Zhu, J.; Zhang, F.; Lu, W.; Fan, D.; Luo, K. Genome-wide identification and characterization of the Populus WRKY transcription factor family and analysis of their expression in response to biotic and abiotic stresses. *J. Exp. Bot.* **2014**, *65*, 6629–6644. [CrossRef]
41. Yang, Z.; Wang, X.; Xue, J.; Meng, L.; Li, R. Identification and expression analysis of WRKY transcription factors in medicinal plant *Catharanthus roseus*. *Sheng Wu Gong Cheng Xue Bao Chin. J. Biotechnol.* **2013**, *29*, 785–802.

42. Baillo, E.H.; Kimotho, R.N.; Zhang, Z.; Xu, P. Transcription factors associated with abiotic and biotic stress tolerance and their potential for crops improvement. *Genes* **2019**, *10*, 771. [CrossRef] [PubMed]
43. Van Verk, M.C.; Pappaioannou, D.; Neeleman, L.; Bol, J.F.; Linthorst, H.J. A novel WRKY transcription factor is required for induction of PR-1a gene expression by salicylic acid and bacterial elicitors. *Plant Physiol.* **2008**, *146*, 1983–1995. [CrossRef] [PubMed]
44. Xie, T.; Chen, C.; Li, C.; Liu, J.; Liu, C.; He, Y. Genome-wide investigation of WRKY gene family in pineapple: Evolution and expression profiles during development and stress. *BMC Genom.* **2018**, *19*, 490. [CrossRef] [PubMed]
45. Chen, C.; Chen, X.; Han, J.; Lu, W.; Ren, Z. Genome-wide analysis of the WRKY gene family in the cucumber genome and transcriptome-wide identification of WRKY transcription factors that respond to biotic and abiotic stresses. *BMC Plant Biol.* **2020**, *20*, 443. [CrossRef]
46. He, H.; Dong, Q.; Shao, Y.; Jiang, H.; Zhu, S.; Cheng, B.; Xiang, Y. Genome-wide survey and characterization of the WRKY gene family in *Populus trichocarpa*. *Plant Cell Rep.* **2012**, *31*, 1199–1217. [CrossRef]
47. Yu, Y.; Hu, R.; Wang, H.; Cao, Y.; He, G.; Fu, C.; Zhou, G. MlWRKY12, a novel Miscanthus transcription factor, participates in pith secondary cell wall formation and promotes flowering. *Plant Sci.* **2013**, *212*, 1–9. [CrossRef]
48. Yang, L.; Zhao, X.; Yang, F.; Fan, D.; Jiang, Y.; Luo, K. PtrWRKY19, a novel WRKY transcription factor, contributes to the regulation of pith secondary wall formation in *Populus trichocarpa*. *Sci. Rep.* **2016**, *6*, 18643. [CrossRef]
49. Li, W.; Tian, Z.; Yu, D. WRKY13 acts in stem development in *Arabidopsis thaliana*. *Plant Sci.* **2015**, *236*, 205–213. [CrossRef]
50. Wei, Y.; Jin, J.; Liang, D.; Gao, J.; Li, J.; Xie, Q.; Lu, C.; Yang, F.; Zhu, G. Genome-wide identification of *Cymbidium sinense* WRKY gene family and the importance of its Group III members in response to abiotic stress. *Front. Plant Sci.* **2022**, *13*, 969010. [CrossRef]
51. Li, S.; Zhou, X.; Chen, L.; Huang, W.; Yu, D. Functional characterization of *Arabidopsis thaliana* WRKY39 in heat stress. *Mol. Cells* **2010**, *29*, 475–483. [CrossRef] [PubMed]
52. Rushton, D.L.; Tripathi, P.; Rabara, R.C.; Lin, J.; Ringler, P.; Boken, A.K.; Langum, T.J.; Smidt, L.; Boomsma, D.D.; Emme, N.J.; et al. WRKY transcription factors: Key components in abscisic acid signalling. *Plant Biotechnol. J.* **2012**, *10*, 2–11. [CrossRef] [PubMed]
53. Jiang, Y.; Deyholos, M.K. Functional characterization of Arabidopsis NaCl-inducible WRKY25 and WRKY33 transcription factors in abiotic stresses. *Plant Mol. Biol.* **2009**, *69*, 91–105. [CrossRef] [PubMed]
54. Fu, Q.; Yu, D. Expression profiles of *AtWRKY25*, *AtWRKY26* and *AtWRKY33* under abiotic stresses. *Heredity* **2010**, *32*, 848–856. [CrossRef]
55. Van der Fits, L.; Memelink, J. The jasmonate-inducible AP2/ERF-domain transcription factor ORCA3 activates gene expression via interaction with a jasmonate-responsive promoter element. *Plant J.* **2001**, *25*, 43–53. [CrossRef]
56. De Geyter, N.; Gholami, A.; Goormachtig, S.; Goossens, A. Transcriptional machineries in jasmonate-elicited plant secondary metabolism. *Trends Plant Sci.* **2012**, *17*, 349–359. [CrossRef]
57. Sibéril, Y.; Benhamron, S.; Memelink, J.; Giglioli-Guivarc'H, N.; Thiersault, M.; Boisson, B.; Doireau, P.; Gantet, P. *Catharanthus roseus* G-box binding factors 1 and 2 act as repressors of strictosidine synthase gene expression in cell cultures. *Plant Mol. Biol.* **2001**, *45*, 477–488. [CrossRef]
58. Chini, A.; Boter, M.; Solano, R. Plant oxylipins: COI1/JAZs/MYC2 as the core jasmonic acid-signalling module. *FEBS J.* **2009**, *276*, 4682–4692. [CrossRef]
59. Skibbe, M.; Qu, N.; Galis, I.; Baldwin, I.T. Induced plant defenses in the natural environment: *Nicotiana attenuata* WRKY3 and WRKY6 coordinate responses to herbivory. *Plant Cell* **2008**, *20*, 1984–2000. [CrossRef]
60. Duan, S.; Wang, J.; Gao, C.; Jin, C.; Li, D.; Peng, D.; Du, G.; Li, Y.; Chen, M. Functional characterization of a heterologously expressed Brassica napus WRKY41-1 transcription factor in regulating anthocyanin biosynthesis in *Arabidopsis thaliana*. *Plant Sci.* **2018**, *268*, 47–53. [CrossRef]
61. Kishi-Kaboshi, M.; Takahashi, A.; Hirochika, H. MAMP-responsive MAPK cascades regulate phytoalexin biosynthesis. *Plant Signal. Behav.* **2010**, *5*, 1653–1656. [CrossRef] [PubMed]
62. Qiu, J.L.; Fiil, B.K.; Petersen, K.; Nielsen, H.B.; Botanga, C.J.; Thorgrimsen, S.; Palma, K.; Suarez-Rodriguez, M.C.; Sandbech-Clausen, S.; Lichota, J.; et al. Arabidopsis MAP kinase 4 regulates gene expression through transcription factor release in the nucleus. *EMBO J.* **2008**, *27*, 2214–2221. [CrossRef] [PubMed]
63. Chen, C.; Chen, H.; Zhang, Y.; Thomas, H.R.; Frank, M.H.; He, Y.; Rui, X. TBtools: An integrative toolkit developed for interactive analyses of big biological data. *Mol. Plant.* **2020**, *13*, 1194–1202. [CrossRef] [PubMed]
64. Letunic, I.; Bork, P. Interactive Tree of Life (iTOL) v4: Recent updates and new developments. *Nucleic Acids Res.* **2019**, *47*, W256–W259. [CrossRef]
65. Higo, K.; Ugawa, Y.; Iwamoto, M.; Korenaga, T. Plant cis-acting regulatory DNA elements (PLACE) database: 1999. *Nucleic Acids Res.* **1999**, *27*, 297–300. [CrossRef]
66. Wang, X.; Long, J.; Dong, T.; Zheng, D.; Zhang, L.; Peng, C. Establishment of vascular tissue cells capture system by laser microdissection in *Neolamarckia cadamba*. *Guihaia* **2021**, *41*, 1226–1236. (In Chinese with English abstract).

67. Huang, T.; Long, J.; Liu, S.W.; Yang, Z.; Zhu, Q.; Zhao, X.; Peng, C. Selection and validation of reference genes for mRNA expression by quantitative Real-Time PCR analysis in *Neolamarckia cadamba*. *Sci. Rep.* **2018**, *8*, 9931. [CrossRef]
68. Zhang, D.; Li, J.J.; Zhang, M.J.; Bao, Y.T.; Yang, X.; Xu, W.Y.; Quyang, K.X.; Chen, X.Y. Selection and validation of reference genes for quantitative RT-PCR analysis in *Neolamarckia cadamba*. *Chin. Bull. Bot.* **2018**, *53*, 829–839. [CrossRef]

International Journal of Molecular Sciences

Open Access Article

Genome-Wide Identification and Expression Analysis of WRKY Gene Family in *Neolamarckia cadamba*

by Zuowei Xu [1], Yutong Liu [1], Huiting Fang [1], Yanqiong Wen [1], Ying Wang [1], Jianxia Zhang [1], Changcao Peng [1,2,*] and Jianmei Long [1,*]

[1] Guangdong Key Laboratory for Innovative Development and Utilization of Forest Plant Germplasm, College of Forestry and Landscape Architecture, South China Agricultural University, Guangzhou 510642, China

[2] State Key Laboratory for Conservation and Utilization of Subtropical Agro-Bioresources, South China Agricultural University, Guangzhou 510642, China

* Authors to whom correspondence should be addressed.

Int. J. Mol. Sci. **2023**, *24*(8), 7537; **https://doi.org/10.3390/ijms24087537**

Submission received: 23 March 2023 / Revised: 15 April 2023 / Accepted: 17 April 2023 / Published: 19 April 2023

(This article belongs to the Special Issue **Molecular Mechanisms of Abiotic Stress Responses in Trees**)

Abstract

The WRKY transcription factor family plays important regulatory roles in multiple biological processes in higher plants. They have been identified and functionally characterized in a number of plant species, but very little is known in *Neolamarckia cadamba*, a 'miracle tree' for its fast growth and potential medicinal resource in Southeast Asia. In this study, a total of 85 *WRKY* genes were identified in the genome of *N. cadamba*. They were divided into three groups according to their phylogenetic features, with the support of the characteristics of gene structures and conserved motifs of protein. The *NcWRKY* genes were unevenly distributed on 22 chromosomes, and there were two pairs of segmentally duplicated events. In addition, a number of putative cis-elements were identified in the promoter regions, of which hormone- and stress-related elements were shared in many *NcWRKYs*. The transcript levels of *NcWRKY* were analyzed using the RNA-seq data, revealing distinct expression patterns in various tissues and at

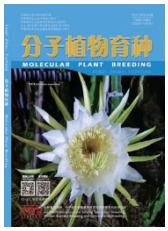

分子植物育种
Molecular Plant Breeding
ISSN 1672-416X,CN 46-1068/S

《分子植物育种》网络首发论文

题目：黄梁木蔗糖转运蛋白 NcSUT4 和 NcSUT5 的表达与功能分析

作者：梁正炫，冯佳乐，陈鑫，唐琳涵，彭昌操，龙健梅

网络首发日期：2024-07-22

引用格式：梁正炫，冯佳乐，陈鑫，唐琳涵，彭昌操，龙健梅. 黄梁木蔗糖转运蛋白 NcSUT4 和 NcSUT5 的表达与功能分析[J/OL]. 分子植物育种.
https://link.cnki.net/urlid/46.1068.S.20240719.1235.006

网络首发时间：2024-07-22 10:08:26
网络首发地址：https://link.cnki.net/urlid/46.1068.S.20240719.1235.006

研究报告
Research Report

黄梁木蔗糖转运蛋白 NcSUT4 和 NcSUT5 的表达与功能分析

梁正炫　冯佳乐　陈鑫　唐琳涵　彭昌操　龙健梅*
华南农业大学林学与风景园林学院, 广东省森林植物种质创新与利用重点实验室, 广州, 510642
*通信作者, longjianmei@scau.edu.cn

摘　要　蔗糖转运蛋白(sucrose transporter, SUT)介导光合作用产物蔗糖的长距离运输，在植物的生长发育及逆境响应中发挥重要作用。黄梁木(*Neolamarckia cadamba*)是华南地区重要的速生用材树种，探讨黄梁木 SUTs 的序列特征、表达模式和蔗糖转运活性，可为揭示其生物学功能奠定基础。本研究成功克隆黄梁木两个蔗糖转运蛋白基因 *NcSUT4* 和 *NcSUT5*，通过生物信息学分析这两个基因编码蛋白的特征与系统进化，采用转录组及荧光实时定量 PCR 分析 *NcSUT4* 和 *NcSUT5* 的表达模式，并利用酵母功能互补系统验证其蔗糖转运活性。结果表明，*NcSUT4* 和 *NcSUT5* 基因编码序列(coding sequences, CDS)全长分别为 1 515 bp 和 1 518 bp，编码 514 和 515 个氨基酸。二者均包含 12 个跨膜结构域，且定位在细胞膜上。系统进化树分析表明 NcSUT4 和 NcSUT5 隶属于 SUT4 分支，其转录本在树皮、形成层和韧皮部中表达较高，并且受外源蔗糖诱导。酵母功能互补实验证明 NcSUT4 和 NcSUT5 具有转运蔗糖能力。本研究对黄梁木 *NcSUT4* 和 *NcSUT5* 基因序列分析、表达模式与功能进行初步分析，为阐明 NcSUT4 和 NcSUT5 在黄梁木维管发育中的功能奠定重要基础。

关键词　黄梁木; 蔗糖转运蛋白; 表达分析; 功能分析

Expression and Functional Analysis of the Sucrose Transporter NcSUT4 and NcSUT5 in *Neolamarckia cadamba*

Liang Zhengxuan　Feng Jiale　Chen Xin　Tang Linhan　Peng Changcao　Long Jianmei *
Guangdong Key Laboratory for Innovative Development and Utilization of Forest Plant Germplasm, College of Forestry and Landscape Architecture, South China Agricultural University, Guangzhou, 510642
* Corresponding author, longjianmei@scau.edu.cn

Abstract　Sucrose transporter (SUT) mediates the long-distance transport of sucrose, which is the major form of photosynthetic products. It plays important roles in plant growth and development and stress response. *Neolamarckia cadamba* is an important fast-growing timber tree in South China, and study on the sequence characteristics, expression patterns and sucrose transport activity of SUTs from *Neolamarckia cadamba* would lay foundation for revealing their biological function. In this study, two sucrose transporter genes *NcSUT4* and *NcSUT5* of *Neolamarckia cadamba* were successfully cloned. The characteristics and phylogenetic evolution of the proteins encoded by these two genes were analyzed through bioinformatic method. Expression pattern of *NcSUT4* and *NcSUT5* was detected by RNA-Seq and quantitative real-time PCR. The sucrose transport activity of NcSUT4 and NcSUT5 was verified using yeast functional complementation assay. The results showed that the CDS of *NcSUT4* and *NcSUT5* genes were 1 515 bp and 1 518 bp, respectively, encoding 514 and 515 amino acids, respectively. They both contained 12 transmembrane domains and localized to the plasma membrane. Phylogenetic analysis indicated that both NcSUT4 and NcSUT5 belong to the SUT4 clade. Their transcripts were highly expressed in bark, cambium and phloem and were induced by exogenous sucrose. Yeast functional complementation experiments demonstrated that NcSUT4 and NcSUT5 were able to transport sucrose. Our study laid an important foundation for elucidating the functions of NcSUT4 and NcSUT5 in vascular development in *Neolamarckia cadamba*.

Keywords　*Neolamarckia cadamba*; Sucrose transporter; Expression analysis; Functional analysis

蔗糖是高等植物中源器官和库器官之间光合作用同化物的主要运输形式，为植物的生长发育提供能量和底物；同时作为信号分子参与植物生长代谢及逆境胁迫响应(Hackel et al., 2005)。蔗糖的长距离运输主要有共质体途径或质外体途径，其中质外体途径为蔗糖经过跨膜运输在韧皮部的筛管和伴胞复合体中转运，这种跨膜运输需要位于质膜上的 H^+同向蔗糖转运载体协助，即蔗糖转运蛋白(sucrose transporter, SUT 或者 SUC) (Sun et al., 2022)。SUT 具有与亲水循环相连接的 12 个跨膜结构域，根据系统发育分析将 SUT 划分为 5 个分支：SUT1～SUT5，其中 SUT1 为双子叶植物特有，而 SUT3 和 SUT5 为单子叶植物所特有(Kühn and Grof, 2010)。随着许多物种基因组测序的完成，已经在多个植物中鉴定并克隆了蔗糖转运蛋白基因，除了在模式植物拟南芥和水稻中的研究较为深入外，其他物种的蔗糖转运蛋白基因的功能研究也逐渐展开。

不同 SUT 分支成员表现出不同的功能，且与其亚细胞定位密切相关。SUT1 分支成员定位于细胞质膜中，负责将蔗糖装载到韧皮部或将蔗糖卸载到库组织细胞中(Kühn and Grof, 2010; Geiger, 2011)。SUT1 分支基因还在植物的不同发育和生理过程中发挥着重要作用，调控花粉发育和开花等(Sivitz et al., 2008;

Iftikhar et al., 2020)。大多数 SUT2 成员位于细胞质膜中，最初被认为充当蔗糖传感器(Barker et al., 2000)，但后续研究证实 SUT2 成员作为蔗糖转运蛋白参与韧皮部装载(Meyer et al., 2004)。同时，也有少量 SUT2 成员，如苹果(*Malus domestica*) MdSUT2.2 定位在液泡膜中，其超量表达导致液泡中蔗糖积累增加(Ma et al., 2019)。SUT4 分支成员定位于液泡膜中，它们参与蔗糖从液泡流出到细胞质中(Kühn and Grof, 2010)。也有部分物种 SUT4 蛋白如番茄(*Solanum lycopersicum*) SlSUT4 和马铃薯(*Solanum tuberosum*) StSUT4 定位于细胞质膜，负责蔗糖从叶片运输库器官，影响植物开花或避阴反应等过程(Chincinska et al., 2007; Liang et al., 2023a)。SUT4 分支成员的双重定位赋予其不同的功能，且其定位的特征具有物种特异性，因此，对 SUT4 成员展开研究对解析其功能具有重要的意义,。

SUT4 分支的基因在植物的生长发育和逆境响应中发挥重要作用。大豆(*Glycine max*)中超量表达 *GmSUT4.2* 促进蔗糖刺激的毛状根生长并提高蔗糖吸收能力，*GmSUT4.2* 超表达的拟南芥莲座叶和分枝增多，而 CRISPR/Cas9 基因编辑的 *GmSUT4.2* 大豆叶片变小，导致大豆产量和生物量降低，说明 *GmSUT4.2* 在植物生长发育和产量形成的调控中发挥着关键作用(Wu et al., 2024)。番茄 *SlSUT4* 参与开花调控(Liang et al., 2023a)，同时影响了植物对干旱胁迫的响应(Liang et al., 2023b)；苹果 *MdSUT4.1* 和梨(*Pyrus bretschneideri*) *PbSUT2* 均促进果实中糖的积累(Wang et al., 2016; Peng et al., 2020)；抑制马铃薯 *StSUT4* 表达诱导提前开花、提高块茎产量和降低对遮荫反应的敏感性(Chincinska et al., 2007)。拟南芥(*Arabidopsis thaliana*) *AtSUC4* 通过脱落酸(abscisic acid, ABA)途径参与非生物逆境胁迫响应(Gong et al., 2014)，同时参与高糖条件下根的伸长(Liu et al., 2022)。在林木植物中，RNAi 抑制 *PtaSUT4* 的转基因杨树(*Populus tremula* ×*Populus alba*)表现出叶茎生物量比增加、源叶和茎中蔗糖含量增加以及苯丙烷代谢改变(Payyavula et al., 2011)，同时 *PtaSUT4* 参与调控整株植物的水分关系、对水分胁迫的反应和光合作用(Frost et al., 2012)。超量表达 *PagSUT4* 的转基因杨树(*Populus alba*×*Populus glandulosa*)光合作用增强，木质部的宽度增加，促进了杨树的次生生长(张利, 2016)。由此可见，SUT4 与木材发育密切相关，在木材的遗传改良中具有潜在的应用价值，但目前 SUT 参与木材形成的报道较少，仍需进一步挖掘。

黄梁木(*Neolamarckia cadamba*)隶属茜草科团花属，常绿高大乔木，是中国华南地区重要的乡土用材树种，因其生长极其迅速被称为“奇迹树”(邓小梅等, 2012)。黄梁木叶片巨大肥厚，光合作用强，能够贮藏与运输大量蔗糖等营养物质满足迅速生长的需求。已有研究表明，蔗糖可从韧皮部通过径向运输途径经射线细胞进入木质部，射线细胞与木质部纤维或导管之间没有胞间连丝(van Bel, 1990)，只能通过依赖蔗糖转运蛋白的质外体途径完成该过程。因此，蔗糖转运蛋白对黄梁木的速生性和木材形成过程中可能具有重要作用。本研究基于基因组和转录组数据，通过同源序列法比对获得黄梁木 SUT4 分支两个成员 NcSUT4 和 NcSUT5，对其氨基酸序列进行分析，并对其基因表达模式、蔗糖转运活性和亚细胞定位等方面进行深入研究，为阐明 NcSUT4 和 NcSUT5 的生物学功能奠定基础。

1 结果与分析

1.1 黄梁木 *NcSUT4* 和 *NcSUT5* 基因的克隆

根据获得的 *NcSUT4* 和 *NcSUT5* 基因序列设计特异引物，以黄梁木叶片和各维管组织的混合 cDNA 为模板，进行 PCR 扩增。经琼脂糖凝胶电泳显示(图 1)，分别获得清晰明亮的条带，经测序获得黄梁木 *NcSUT4* 和 *NcSUT5* 基因的 ORF 序列信息，大小分别为 1 515 bp 和 1 518 bp，测序序列与基因组参考序列一致，说明这两个基因已成功克隆。

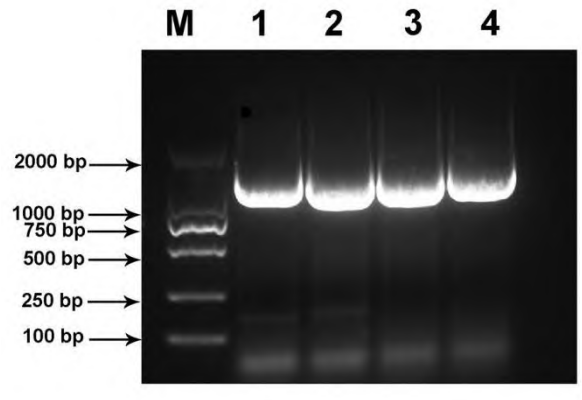

图 1 黄梁木 *NcSUT4* 和 *NcSUT5* 基因的 PCR 扩增

注: M: DL 2000 bp DNA Marker; 1 和 2: *NcSUT4* 基因的 PCR 产物; 3 和 4: *NcSUT5* 基因的 PCR 产物

Figure 1 PCR amplification product of *NcSUT4* and *NcSUT5* in *Neolamarckia cadamba*
Note: M: DL 2000 bp DNA Marker; 1 and 2: PCR amplification product of *NcSUT4;* 3 and 4: PCR amplification product of *NcSUT5*

1.2 NcSUT4 和 NcSUT5 蛋白的理化性质和结构域分析

黄梁木 *NcSUT4* 和 *NcSUT5* 基因编码的氨基酸序列理化性质分析结果表明，NcSUT4 与 NcSUT5 氨基酸长度分别为 504、505 aa，推测 NcSUT4 和 NcSUT5 基因编码的蛋白分子量分别为 55 210 Da 和 55 257 Da；理论等电点分别为 9.31 和 9.16，均为碱性蛋白(理论等电点>7)。不稳定系数分别为 42.05 和 41.67，脂肪系数分别为 109.88、112.39，两个成员蛋白的总平均疏水指数分别为 0.49 和 0.47，均为疏水蛋白。跨膜结构域预测结果显示 NcSUT4 和 NcSUT5 均含有 12 个 TMH 跨膜螺旋，两蛋白中间都有 1 个大的亲水胞质环，且这两个蛋白的前、后两个半区均具 6 个跨膜结构，且 N 端和 C 端均在细胞质内(图 2)，符合 SUT 家族蛋白的结构特征，与报道的其他物种 SUT 蛋白结构一致。

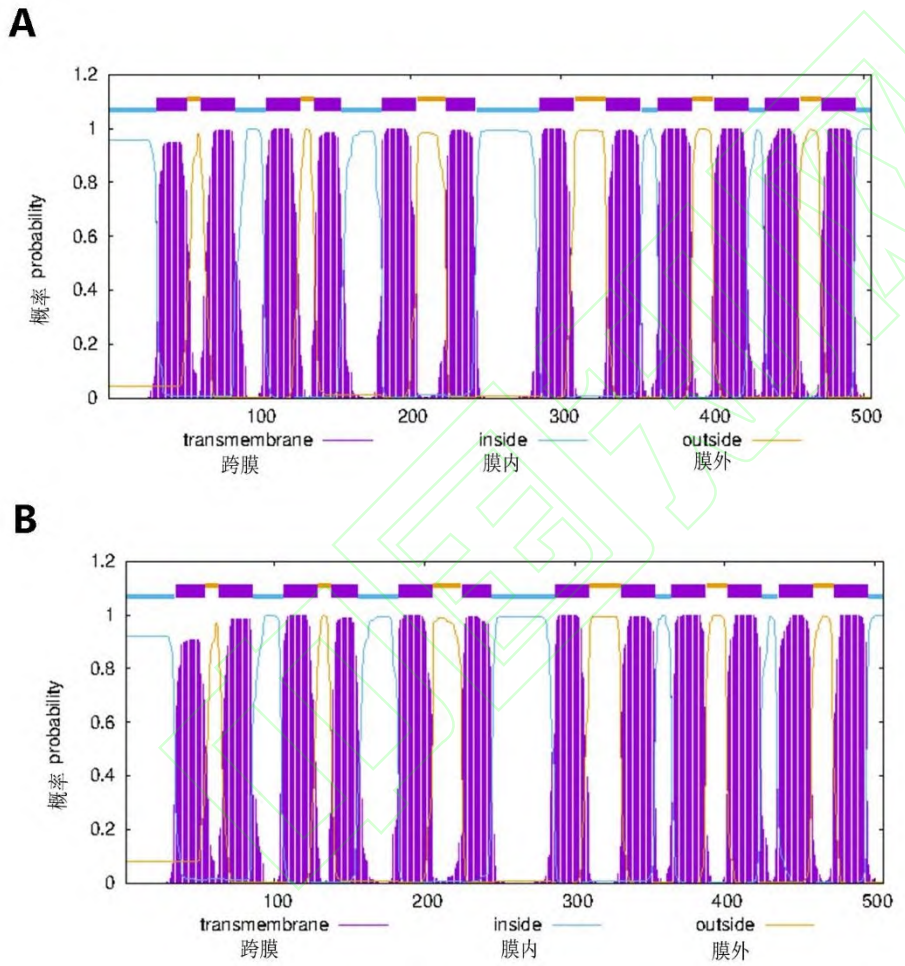

图 2 黄梁木 NcSUT4 和 NcSUT5 跨膜结构域的预测
注: A: NcSUT4 跨膜结构域预测; B: NcSUT5 跨膜结构域预测
Figure 2 Prediction of transmembrane structure of NcSUT4 and NcSUT5 in *Neolamarckia cadamba*
Note: A: Prediction of transmembrane structure of NcSUT4; B: Prediction of transmembrane structure of NcSUT5

通过 NCBI 网站上的 CD-search 分析黄梁木 NcSUT4 和 NcSUT5 蛋白结构域，发现这两个蛋白均具有典型的 GPH 结构域(图 3A)，表明 NcSUT4 和 NcSUT5 属于 SUT 家族成员。利用 MEME 程序分析 NcSUT4、NcSUT5 和其他物种 SUT4 成员的 motif，结果显示，这些 SUT4 蛋白均含有保守的 10 个 motif，并且这些 motif 排序相似(图 3B)，说明这些 SUT4 分支成员的 motif 高度保守。

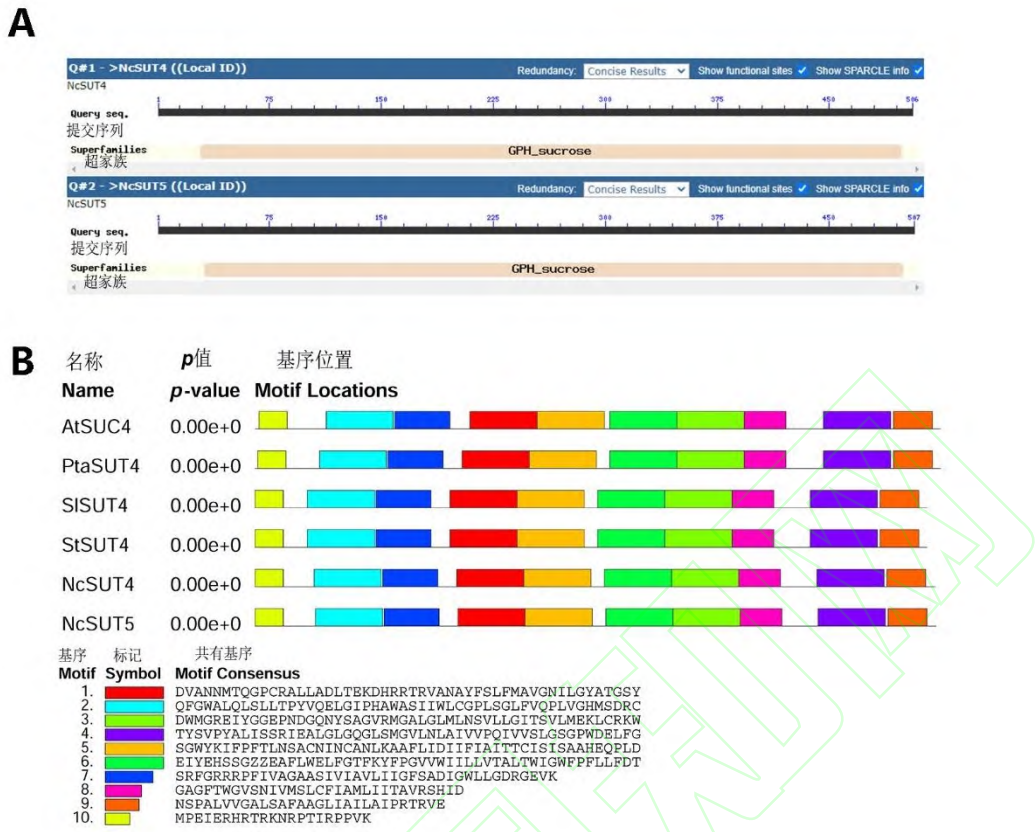

图 3 NcSUT4 和 NcSUT5 蛋白结构分析。
注: A: 蛋白质保守结构域分析; B: 蛋白质基序(motif)分析; At: 拟南芥; Pta: 杨树; Sl: 番茄; St: 马铃薯
Figure 3 Protein structure of NcSUT4 and NcSUT5
注: A: conserved domain of NcSUT4 and NcSUT5; B: motif of NcSUT4 and NcSUT5 and other SUT4 from different species; At: *Arabidopsis thaliana*; Pta: *Populus tremula*×*Populus alba*; Sl: *Solanum lycopersicum*; St: *Solanum tuberosum*

1.3 NcSUT4 和 NcSUT5 蛋白同源性和系统进化

将 NcSUT4 与 NcSUT5 编码蛋白的氨基酸序列进行比对(图 4)。通过 BioAider 软件，计算可得氨基酸同一性值为 97.63，说明黄梁木 NcSUT4 和 NcSUT5 结构序列高度相似。

```
                    *         20        *         40        *         60        *         80        *
NcSUT4 : MPEIERHSKDKPRTTTR--HPVREPVRPCRVPLRLLLRVSSIACGIQFGWALQLSLLTPYVQELGIPHAWASIIWLCGPVSGFFVQPLVGHM :  90
NcSUT5 : MPDAERHFKNKCRTTNRPPPPVREPVRP-RVPLRLLLRVSSVACGIQFGWALQLSLLTPYVQELGIPHAWASIIWLCGPISGFFVQPLAGHM :  91
         MP  ERH K1K R T R   PVREPVRP RVPLRLLLRVSS6ACGIQFGWALQLSLLTPYVQELGIPHAWASIIWLCGP6SGFFVQPL GHM

              100       *       120       *       140       *       160       *       180
NcSUT4 : SDRCRSRLGRRRPFIIAGAASIVVAVVVIGFSADIGWLFGDRGKVKLRAIAAFVLGFWLLDVANNMTQGPCRALLADLTGKDHRRTRVANAY : 182
NcSUT5 : SDRCRSRLGRRRPFIIAGAASIVVAVIVIGFSADIGWLFGDRGKVKLRAIAAFVLGFWLLDVANNMTQGPCRALLADLTEKDHRRTRVANAY : 183
         SDRCRSRLGRRRPFIIAGAASIVVAV6VIGFSADIGWLFGDRGKVKLRAIAAFVLGFWLLDVANNMTQGPCRALLADLT KDHRRTRVANAY

         *       200       *       220       *       240       *       260       *
NcSUT4 : FSLWMAVGNILGYATGAYSGWFKILPFTRSSACNVNCANLKAAFLIDIIFITITTYISISAAHEQPLDSLHSSPASIEERFBESSHEQEAFL : 274
NcSUT5 : FSLWMAVGNILGYATGAYSGWFKILPFTLNSACNINCANLKAAFLIDIIFIAITTCISISGAHEQPLDSLHNSPASMEERYEQSSHEQEAFL : 275
         FSLWMAVGNILGYATGAYSGWFKILPFT  SACN6NCANLKAAFLIDIIFI ITT ISIS AHEQPLDSLH SPAS6EER5E SSHEQEAFL

          280       *       300       *       320       *       340       *       360
NcSUT4 : WEMFGTFKYFTGVIWIILLAIALTWIGWFPFLLFDTDWMGREIYGGQPNDGQNYSVGVRMGAFGLMSNSVVLGITSVLMEKLCRKWGAGFTW : 366
NcSUT5 : WEMFGTFKYFTGVIWIILLAIALTWIGWFPFLLFDTDWMGREIYGGEPNDGQNYSVGVRMGALGLMLNSVVLGITSVLMEKLCRKWGAGFTW : 367
         WEMFGTFKYFTGVIWIILLAIALTWIGWFPFLLFDTDWMGREIYGG PNDGQNYSVGVRMGA GLM NSVVLGITSVLMEKLCRKWGAGFTW

          *       380       *       400       *       420       *       440       *       460
NcSUT4 : GVSNIVMSLCFVAMLIITAVRTHMDIGDRLPPDGVVIAALVVFAVLGFPLAVTYSVPYALISSRIEALGLGQGLSMGVLNLAIVVPQILVSL : 458
NcSUT5 : GVSNIIMSLCFVAMLIITAVRPHMDLGNRLPPDGVVIAALVTFSILGIPLAITYSVPYALISSRIEALGLGQGLSMGVLNLAIVVPQILVSV : 459
         GVSNI6MSLCFVAMLIITAVR HMD6G1RLPPDGVVIAALV F 6LG PLA6TYSVPYALISSRIEALGLGQGLSMGVLNLAIVVPQILVS6

              *       480       *       500
NcSUT4 : GSGPWDELFGGGNSPALAVGAVSAFASGLIAILAIPRTRVEKSRIIP* : 505
NcSUT5 : GSGPWDELFGGGNSPALVVGAVSAFASGLIAILAIPRTRVEKSRIIH* : 506
         GSGPWDELFGGGNSPAL VGAVSAFASGLIAILAIPRTRVEKSRIL
```

图 4 NcSUT4 和 NcSUT5 蛋白序列比对
Figure 4 Protein alignment between NcSUT4 and NcSUT5

通过进化分析表明黄梁木大约 80.4 mya (million years ago，百万年前)从茄科(*Solanaceae*)分化出来。为进一步确定黄梁木 NcSUT4 和 NcSUT5 与其他植物基因的关系，将 NcSUT4 和 NcSUT5 与茄科两个代表物种番茄(*Solanum lycopersicum*)和马铃薯(*Solanum tuberosum*)，以及模式植物拟南芥和杨树等 4 个物种 SUT 氨基酸序列进行 NJ 法系统聚类分析(图 5)，所有的 SUT 可分为 3 个分支，分别是 SUT1、SUT2 和 SUT4，其中 NcSUT4 和 NcSUT5 均属于 SUT4 分支分支，并且与番茄和马铃薯 SUT4 亲缘关系最近。以上结果也进一步验证了黄梁木与茄科植物具有较近的亲缘关系。

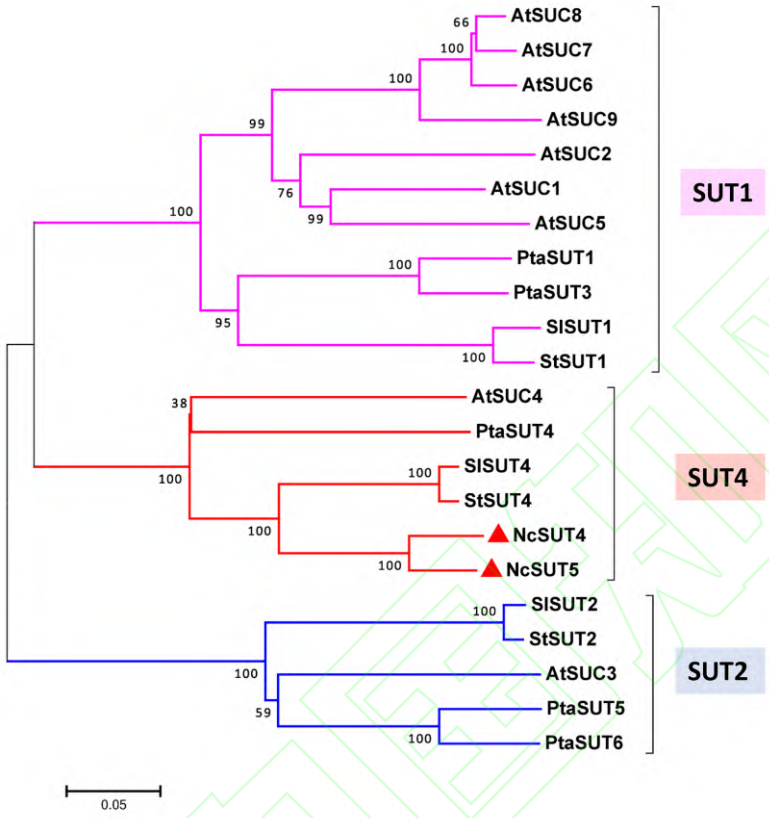

图 5 黄梁木 NcSUT4, NcSUT5 与其他物种 SUT 蛋白序列的系统进化树
注: At: 拟南芥; Pta: 杨树; Sl: 番茄; St: 马铃薯
Figure 5 Phylogenetic tree of NcSUT4, NcSUT5 and other SUTs from four species.
Note: At: *Arabidopsis thaliana;* Pta: *Populus tremula*×*Populus alba*; Sl: *Solanum lycopersicum*; St: *Solanum tuberosum.*

1.4 NcSUT4 和 NcSUT5 蛋白的亚细胞定位

为确定黄梁木 NcSUT4 和 NcSUT5 蛋白的亚细胞定位情况，构建 pAN580-NcSUT4/NcSUT5-GFP 融合蛋白表达载体，以细胞膜定位 marker AtPIP2-mCherry 作为阳性对照，共转入拟南芥原生质体中。结果表明，在原生质体的细胞膜中观察到明显的绿色荧光信号，与阳性对照的红色荧光重叠(图 6)，说明 NcSUT4 和 NcSUT5 蛋白均定位在细胞膜中。

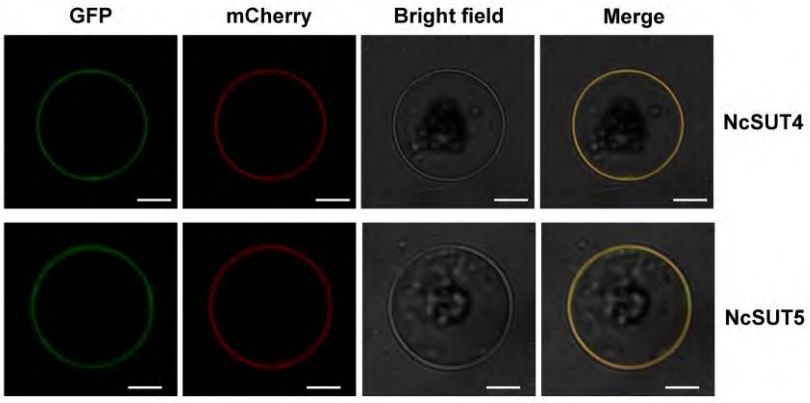

图 6 NcSUT4 和 NcSUT5 蛋白的亚细胞定位分析。
注：细胞膜定位的 marker AtPIP2-mCherry 作阳性对照；GFP：绿色荧光蛋白；mCherry：红色荧光蛋白；Bright field：明场；Merge：叠加
Figure 6 Subcellular localization of NcSUT4 and NcSUT5
Note: The plasma membrane marker of AtPIP2-mCherry was used as positive control; GFP: Green fluorescent protein; mCherry: Red fluorescent protein.

1.5 NcSUT4 和 NcSUT5 表达模式分析

为研究 NcSUT4 和 NcSUT5 在黄梁木生长发育中的作用，基于黄梁木不同组织及不同发育时期维管组织细胞 RNA-Seq 数据，对 *NcSUT4* 和 *NcSUT5* 基因表达模式进行分析，得到其表达热图(图 7)。结果显示，*NcSUT4* 和 *NcSUT5* 在不同组织的表达模式比较相似，均为在树皮、形成层与韧皮部呈现高表达，在芽和嫩叶中表达较低(图 7A)。*NcSUT4* 在初生韧皮部(primary phloem, PPH)和次生形成层(secondary cambium, SCA)表达最显著，而 *NcSUT5* 在 SCA 表达最高，其次为次生韧皮部(secondary phloem, SPH)。值得注意的是，*NcSUT4* 在 PPH、转换时期的韧皮部(transitional stage of phloem, TPH)、转换时期的木质部(transitional stage of xylem, TX)高表达，但 *NcSUT5* 却相反，在这 3 个组织中呈现低表达模式(图 7B)。

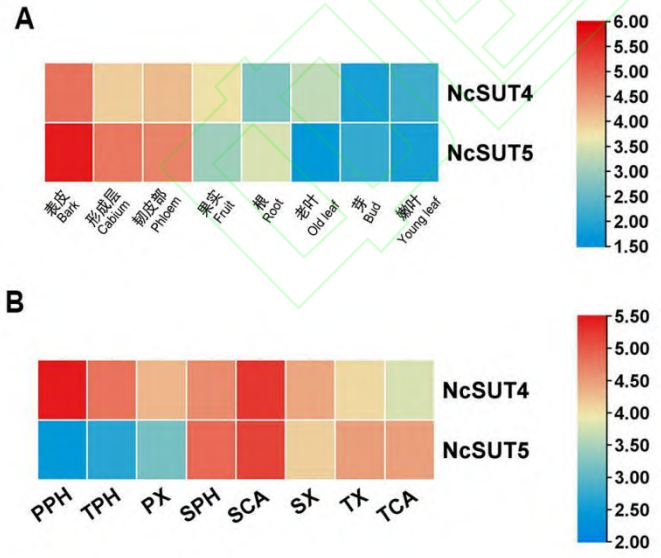

图 7 *NcSUT4* 和 *NcSUT5* 在黄梁木不同组织和维管细胞不同发育时期表达分析
注：A：不同组织；B：维管细胞不同发育时期；PPH：初生韧皮部；TPH：转换阶段韧皮部；SPH：次生韧皮部；TCA：转换阶段形成层；SCA：次生形成层；PX：初生木质部；TX：转换转换阶段木质部；SX：次生木质部
Figure 7 Expression analysis of *NcSUT4* and *NcSUT5* in different tissues and developmental stages of vascular cells in *Neolamarckia cadamba*
Note: A: Different tissues; B: Different developmental stages of vascular cells; A: different tissues; B: different developmental stages of vascular cells. PPH: primary phloem; TPH: transitional stage of phloem; SPH: secondary phloem; TCA: transitional stage of cambium; SCA: secondary cambium; PX: primary xylem; TX: transitional stage of xylem; SX: secondary xylem

为探究 *NcSUT4* 和 *NcSUT5* 在不同外源蔗糖浓度下的表达模式，利用 RT-qPCR 对 4 种不同蔗糖浓度(0, 1%, 3%和 6%)处理后根、茎、叶的表达进行检测。结果表明(图 8)，随着蔗糖浓度升高，*NcSUT4* 和 *NcSUT5* 在 3 个不同组织的表达呈现先升后降的趋势。在根和叶中，*NcSUT4* 和 *NcSUT5* 在 1%的蔗糖浓度下表达最高，在 3%和 6%蔗糖浓度下逐渐降低；而在茎中，这两个基因的最高表达量出现在 3%蔗糖浓度处理下，说明在 3%蔗糖浓度内蔗糖可以诱导 *NcSUT4* 和 *NcSUT5* 的表达。

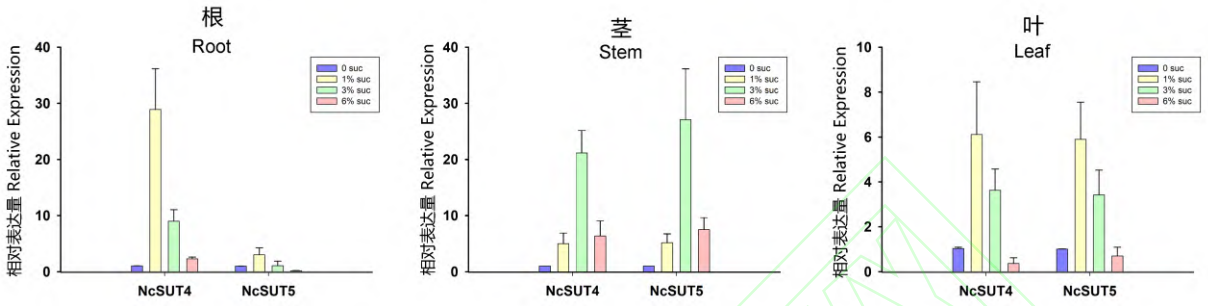

图 8 *NcSUT4* 和 *NcSUT5* 在不同外源蔗糖浓度下的表达模式
注: 0 suc, 1% suc, 3% suc 和 6% suc 分别代表蔗糖浓度为 0, 1%, 3%和 6%
Figure 8 Expression pattern of *NcSUT4* and *NcSUT5* under different concentration of exogenous sucrose conditions.
Note: 0 suc, 1% suc, 3% suc 和 6% suc indicated the sucrose concentration of 0, 1%, 3% and 6%, respectively

1.6 NcSUT4 和 NcSUT5 的蔗糖转运功能验证

为验证 NcSUT4 和 NcSUT5 蛋白的蔗糖转运功能，本研究通过构建酵母表达载体 pDR196-NcSUT4/NcSUT5，并将其与空载体和阳性对照 pDR196-AtSUC2 分别转化至缺陷型酵母 SEY6210 中，进行蔗糖类似物七叶苷的吸收实验。结果显示(图 9A)，表达空载体 PDR196 的酵母细胞没有观察到荧光，表达 AtSUC2、NcSUT4 和 NcSUT5 的酵母细胞均观察到蓝色荧光。进一步利用酶标仪对吸收的七叶苷进行荧光强度定量检测(图 9B)，结果显示表达阳性对照 AtSUC2 的酵母细胞，荧光强度超过了 100，显著高于表达空白载体的酵母细胞的荧光强度；表达 NcSUT4 的和 NcSUT5 酵母的荧光强度约是阴性对照的 4 倍以上，显著高于阴性对照，说明 NcSUT4 和 NcSUT5 对七叶苷有明显的吸收，证实了两者具有蔗糖转运的活性。

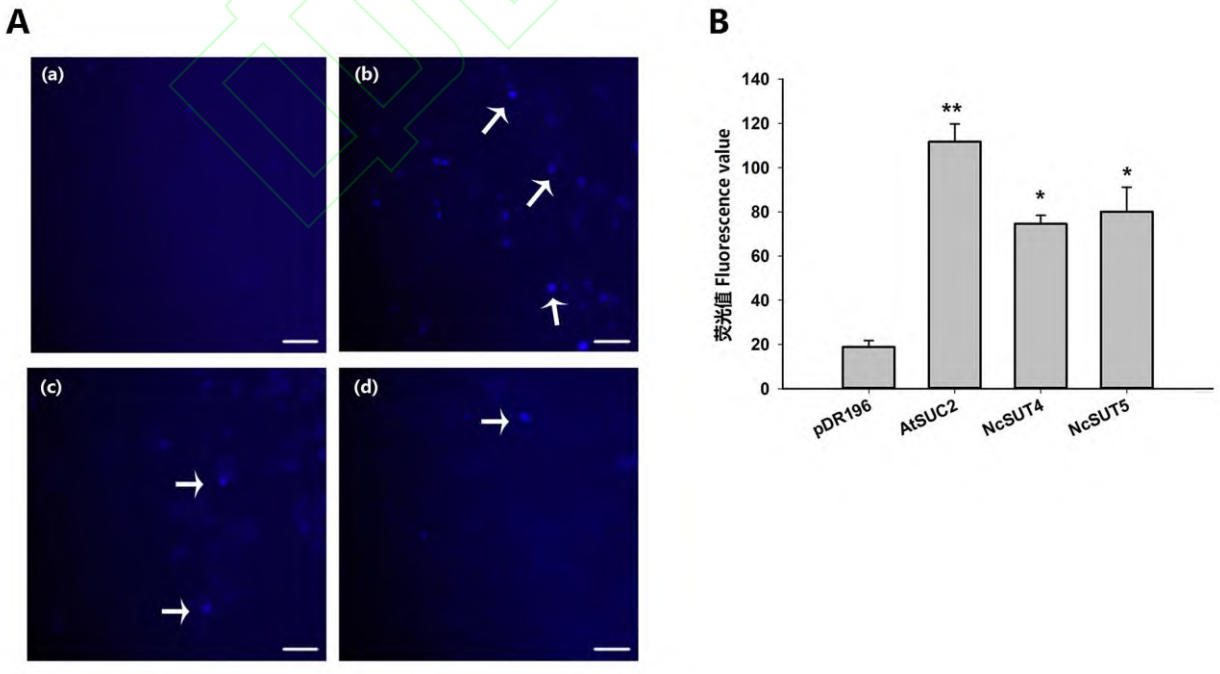

图 9 NcSUT4 和 NcSUT5 吸收七叶苷的荧光观察与检测

注: A: 七叶苷的荧光观察, (a): pDR196; (b): AtSUC2: (c): NcSUT4; (d): NcSUT5; 标尺: 20 μm; B: 七叶苷的荧光检测, 误差线代表 SD, *:P<0.05, **: P<0.001

Figure 9 Esculin uptake assay for NcSUT4 and NcSUT5

Note: A: Fluorescence detection of esculin by microscope, (a): pDR196; (b): AtSUC2: (c): NcSUT4; (d): NcSUT5; Scale bars=20 μm; B: Detection of the fluorescence value, SD represented the standard derivation, *: P<0.05, **: P<0.001

2 讨论

蔗糖转运蛋白 SUT 是植物体内重要的糖转运蛋白家族，通过介导蔗糖在植物体内的长距离运输参与了植物生长发育与逆境胁迫。本研究成功克隆了黄梁木 NcSUT4 和 NcSUT5 两个蔗糖转运蛋白基因序列，保守结构域预测这两个基因编码的氨基酸序列中含有 GPH domain，并且具有 12 个跨膜结构，说明 NcSUT4 和 NcSUT5 属于典型的蔗糖转运蛋白。双子叶植物 SUT 家族可分为 3 个分支，分别是 SUT1、SUT2 和 SUT4，大多数物种 SUT4 分支仅一个成员，如拟南芥、番茄、马铃薯、烟草和苜蓿等(Reinders et al., 2008; 高蕾等, 2011; Reinders et al., 2012)，而在黄梁木中鉴定并克隆了两个 SUT4 分支成员，说明 SUT4 分支在黄梁木中发生了基因扩张。但 NcSUT4 和 NcSUT5 功能是否冗余仍需进一步做功能验证。

SUT1 和 SUT2 分支一般定位于细胞膜，而 SUT4 家族成员除了细胞膜定位，有的成员还可定位在液泡膜上，也有少数成员具有细胞膜和液泡膜双重定位，比如天麻 SUT4、苜蓿 LjSUT4 和马铃薯 StSUT4 等(Reinders et al., 2008; Chincinska et al., 2013; Ho et al., 2020)，说明 SUT4 分支成员定位具有多样性，且具有物种差异性。SUT4 家族成员定位于细胞膜或者液泡膜可能与蔗糖运输机制密切相关。具有液泡膜定位的 SUT4 参与蔗糖从液泡外排至细胞质，如桃 PpSUT4 和苹果 MdSUT4 (Zanon et al., 2015; 许海峰等, 2017)。而定位于质膜上的 SUT4 可能与细胞质内蔗糖进出的调控有关，如梨 PbSUT2 定位在细胞质膜上，功能分析推测 PbSUT2 促进蔗糖叶片运输至果实，提高果实蔗糖含量(Wang et al., 2016)。黄梁木 NcSUT4 和 NcSUT5 均定位于细胞膜上，可能通过调控细胞质内蔗糖运输影响黄梁木的生长发育及对外源蔗糖的响应。利用瞬时转化体系证明 AtSUC4 定位在液泡膜上(Schneider et al., 2011)，但是 AtSUC4-GFP 稳定转化拟南芥发现其定位在细胞质膜上(Liu et al., 2022)，说明不同的检测方法可能会有不同的定位结果。本研究利用原生质体的瞬时转化体系去检测黄梁木 NcSUT4 和 NcSUT5 的亚细胞定位，结果表明两者均定位在细胞膜(图 6)，但是否还存在液泡膜定位，未来仍需利用黄梁木的稳定转化体系或者其他体系去验证。已有报道提出一种基于 I 型 SUTs 能够转运荧光物质七叶苷(蔗糖类似物)能力，来测定蔗糖转运蛋白是否具有转运蔗糖的功能(Gora et al., 2012)，本研究利用该系统验证了 NcSUT4 和 NcSUT5 能够转运蔗糖(图 9)，与其他 SUT4 分支成员(如 IbSUT4 和 SlSUT4)类似均具有蔗糖转运活性(Wang et al., 2020; Liang et al., 2023a)。根据 SUT 对蔗糖的亲和性和转运能力，可将 SUT 分成两种类型，分别为高亲和/低转运能力(high-affinity/low-capacity, HALC)和低亲和/高转运能力(low-affinity/high-capacity, LAHC)，其中 HALC 类型的底物动力学参数(michaelis-menten kinetics, Km)处在 0.3~2.0 mmol/L 之间，而 LAHC 类型的 Km 则为 6.0~11.70 mmol/L (Weise et al., 2000)。大部分的 SUT4 分支成员属于 LAHC 类型，该类型的 SUT 主要作用为在蔗糖浓度高条件下依然可以转运蔗糖到库组织，以保证库组织的能量需求。拟南芥 AtSUC4 和番茄 LeSUT4 的 Km 分别为 6.0 mmol/L 和 11.6 mmol/L，而苹果 MdSUT1 的 Km 为 0.63 mmol/L，说明其对蔗糖的转运具有高亲和性，在功能上属于 HALC，但序列的同源性分析其属于 SUT4 分支(Fan et al., 2009)。本研究已证实黄梁木 NcSUT4 和 NcSUT5 具有转运蔗糖的能力，但其属于 HALC 还是 LAHC 还有待下一步验证。

蔗糖转运蛋白与木材的形成密切相关。蔗糖作为主要碳源之一，不仅为树木的生长发育提供能量，也为木材形成过程中的细胞壁合成如木质素与纤维素的合成等代谢过程提供相关底物。在木材形成过程中，由于射线细胞与木质部纤维或导管之间缺乏胞间连丝，需要 SUT 将蔗糖从韧皮部运输至木质部。超量表达银腺杨 *PagSUT4* 增加木质部宽度(张利, 2016)，白杨 *PttSUT3* 在次生生长的茎中表达，功能分析表明 *PttSUT3* 影响碳源的分配进而影响木材纤维的形成(Mahboubi et al., 2013)。*NcSUT4* 和 *NcSUT5* 在树皮、形成层与韧皮部表达较高(图 7)，表明这两个基因可能对维管发育具有重要作用，后续可利用遗传转化对其具体生物学功能进行深入研究。外源蔗糖影响 *SUT4* 的表达。拟南芥 *AtSUC4* 启动子驱动下添加外源蔗糖促进 GUS 表达，说明 *AtSUC4* 受蔗糖诱导表达(Liu et al., 2022)。在本研究中，在低浓度蔗糖条件下(<3%) *NcSUT4* 和 *NcSUT5* 表达上升，但随着蔗糖浓度提高，*NcSUT4* 和 *NcSUT5* 的表达降低(图 8)，说明低浓度蔗糖促进这两个基因的表达，可将外源的蔗糖高效转入细胞内利用；而高浓度蔗糖造成渗透压的改变则会抑制其表达，这可能是植物适应外界条件变化的结果。

本研究从黄梁木中克隆出两个 SUT4 分支成员 *NcSUT4* 和 *NcSUT5* 基因，初步验证了这两个基因编码的蛋白具有蔗糖转运能力，并且都定位在细胞质膜上。*NcSUT4* 和 *NcSUT5* 在维管组织中高表达，表明二者可能参与黄梁木维管发育过程。本研究为后期进一步研究 *NcSUT4* 和 *NcSUT5* 基因调控黄梁木生长发育

奠定重要基础。

3 材料与方法

3.1 实验材料

本实验所用到的植物材料是黄梁木组培苗。黄梁木种子采集于华南农业大学启林北校区苗圃地(E: 113°22', N: 23°9')。取种子于 1.5 mL 离心管中，加入 ddH_2O 浸没种子，于 200 r/min 摇床 37 ℃的环境春化 36 h 左右；用 5% HClO 浸泡消毒 5~10 min；无菌水漂洗 6 次，每次于管中停留 1 min；加入 0.1%琼脂适量，均匀涂播于 MS 培养基上。其中黄梁木的生长条件：16 h 光照与 8 h 黑暗，培养室温度约为 25 ℃。培养月 2 个月获得幼苗后，切取茎段再生扩繁成苗。

大肠杆菌 DH5*α* 购于上海唯地生物公司；酵母菌株 SEY6210 是转化酶突变体，它可以在以葡萄糖为唯一碳源的培养基上生长，不能在以蔗糖为唯一碳源的培养基上生长，由海南大学唐朝荣教授惠赠。酵母表达载体 pDR196 由本实验室保存。

3.2 *NcSUT4* 和 *NcSUT5* 基因克隆

从拟南芥 TAIR 网站(https://www.arabidopsis.org/)上获得拟南芥 *AtSUC4* 基因(At1G09960)的蛋白序列，通过 Blast 比对黄梁木基因组数据(Zhao et al., 2022)筛选出黄梁木 NcSUT4 和 NcSUT5 的蛋白序列及其对应的 CDS 序列。设计扩增黄梁木 *NcSUT4* 和 *NcSUT5* 基因 CDS 全长序列的引物已列出(表 1)。以黄梁木叶片和各维管组织混合 cDNA 为模板，利用高保真酶 PhantaMax super-Fidelity DNA Polymerase (诺唯赞, 南京)进行 PCR 扩增。PCR 反应体系(50 μL)组分为：2×Phanta Max Buffer 25 μL、dNTP Mix 1 μL、正向引物 2 μL、反向引物 2 μL (反应引物为 10 pmol/μL)、 Phanta Max super-Fidelity DNA Polymerase 1 μL、cDNA 2 μL、ddH_2O 17 μL。PCR 反应程序为：95 ℃，3 min；95 ℃，15 sec；55 ℃，15 sec；72 ℃，2 min，共 34 个循环；72 ℃，5 min。

表 1 黄梁木 *NcSUT4* 和 *NcSUT5* 基因扩增与表达分析引物

Table 1 Primer sequences used for *NcSUT4* and *NcSUT5* amplification and expression analysis

引物名称 Primer name	引物序列(5'-3') Primer sequence (5'-3')	目的 Objective
NcSUT4-F	ATGCCGGAAATCGAGAGGC	基因扩增 Gene amplification
NcSUT4-R	TCAGGGGAGGATTCTTGATTTTT	
NcSUT5-F	ATGCCGGACGCCGAAAGA	
NcSUT5-R	TCAGTGGAGGATCCTTGATTTCTC	
qNcUPL-F	GGTTGGTGGTAGAGTTGTGACTC	qRT-PCR
qNcUPL-R	CGAGCACTACCACGACACG	
qNcSUT4-F	AGACAAACCGAGAACAACAACTCGC	
qNcSUT4-R	GTAGGGAGTCAGCAACGACAACTGC	
qNcSUT5-F	TAAACAGAGAATAACAAACCGGC	
qNcSUT5-R	GTATGGGGTGAGTAATGAGAGCTGT	

3.3 NcSUT4 和 NcSUT5 生物信息学分析

通过软件 Clustal 和 GeneDoc 将黄梁木 SUT4 和 SUT5 编码蛋白的氨基酸进行序列比对分析，设置参数为系统默认。利用 NCBI CDD search (https://www.ncbi.nlm.nih.gov/Structure/cdd/wrpsb.cgi)查看两个蛋白的保守结构域。从 NCBI (https://www.ncbi.nlm.nih.gov)网站下载杨树(*Populus tremula*×*Populus alba*)、番茄(*Solanum lycopersicum*)、马铃薯(*Solanum tuberosum*)和拟南芥(*Arabidopsis thaliana)*的 SUT 家族的蛋白质序列，序列号分别为：PtaSUT1 (ADW94615)、PtaSUT3 (ADW94616)、PtaSUT4 (ADW94617)、PtaSUT5 (ADW94618)、PtaSUT6 (ADW94619)、SlSUT1 (CAA57726)、SlSUT2 (AAG12987)、SlSUT4 (AAG09270)、StSUT1 (NP_001305553)、StSUT2 (NP_001275438)、StSUT4 (NP_001275070)、AtSUC1 (CAA53147)、AtSUC2 (AAC25515)、AtSUC3 (AAC32907)、AtSUC4 (CAB92308)、AtSUC5 (AAG27852)、AtSUC6 (BAB11624)、

AtSUC7 (AAG27852)、AtSUC8 (AAC69375)、AtSUC9 (BAB09682)。利用软件 MEGA7 中的 Neighbor-joining 方法将 NcSUT4、NcSUT5 及上述物种 SUT 家族蛋白序列构建系统进化树，设置参数为系统默认。使用在线网站 The MEME Suite (https://meme-suite.org/meme/)对 NcSUT4、NcSUT5 以及上述物种的 SUT4 氨基酸序列的 Motif 结构进行分析：利用 ExPAsy 网站的 ProtParam tool 工具(https://web.expasy.org/protparam/)预测分析黄梁木 NcSUT4 和 NcSUT5 蛋白的理化性质。利用 DeepTMHMM 网站(https://dtu.biolib.com/DeepTMHMM)预测跨膜结构域。

3.4 NcSUT4 和 NcSUT5 表达模式分析

利用前期已发表的 RNA-Seq 数据(Zhao et al., 2022)获取 *NcSUT4* 与 *NcSUT5* 在不同组织部位、不同维管细胞、韧皮部和形成层不同发育时期的表达 FPKM (fragments per kilobase of exon model per million mapped fragments)值，再利用 TBtools 绘制表达热图(Chen et al., 2020)。选择生长一致，株高 7~8 cm 的黄梁木组培苗转移至分别含有 0% Suc(sucrose, 蔗糖)、1% Suc、3% Suc、6% Suc 液体培养基中，在光照条件下处理 8 h 后取样，分别取根、茎、叶三部分，液氮速冻，于-80 ℃保存。提取上述样品 RNA，采用植物 RNA 提取试剂盒(OMEGA)，取检测完整性好的 RNA 作为模板，并使用 Vazyme 公司的试剂盒 Hiscript III RT superMix for qPCR 进行逆转录反应。利用 RT-qPCR 检测黄梁木 *NcSUT4* 和 *NcSUT5* 基因在不同蔗糖浓度处理下的表达量，引物已列出(表 1)，内参基因为 *NcUPL* (张登等, 2018)。

3.5 荧光底物七叶苷吸收检测蔗糖转运活性

根据酵母表达载体 PDR196 图谱，选择酶切位点 PstI 和 SalI，设计引物，NcSUT4-F_PstI：AGTGGATCCCCCGGGCTGCAGATGCCGGAAATCGAGAGGC；NcSUT4-R_salI：GGGCCCCCCCTCGAGGTCGACTCAGGGGAGGATTCTTGATTTTT；NcSUT5-F_PstI：AGTGGATCCCCCGGGCTGCAGATGCCGGACGCCGAAAGA；NcSUT5-R_salI：GGGCCCCCCCTCGAGGTCGACTCAGTGGAGGATCCTTGATTTCTC，构建 NcSUT4 和 NcSUT5 的酵母表达载体，使用一步克隆法将目的片段连接到载体上(诺唯赞, 南京)。采用 PEG-LiAc 介导转化的方法，将构建好的重组载体、空载体及阳性对照(AtSUC2)分别转化酵母菌株 SEY6210，获得阳性单克隆。荧光物质七叶苷的吸收检测方参考(Gora et al., 2012)。将酵母阳性单克隆在 SD-Ura+2%葡萄糖的液体培养基中培养至 OD_{600} 约为 0.8~1，离心收集酵母菌株，加入 200 μL 含有 2 mmol/L 七叶苷的 25 mmol/L NaH_2PO4 (pH=5.0)缓冲液重新悬浮酵母细胞，30 ℃中水浴 2~3 h，再次离心收集酵母细胞，加入 25 mmol/L NaH_2PO4 (pH=5.0)缓冲液进行冲洗后重悬酵母细胞；将重悬的酵母细胞转移至黑色的酶标仪平板上，使用酶标仪(Vaioskan LUX, Thermo Scientific)测定其在激发波长 367 nm 和发射波长 454 nm 下的吸光值。同时将重悬的酵母细胞稀释 5 倍后，在激发波长 367 nm 和发射波长 454 nm 的荧光显微镜(Eclipse Ni-U, Nikon)下观察荧光发光情况。

3.6 NcSUT4 和 NcSUT5 亚细胞定位

利用 PCR 扩增 *NcSUT4* 和 *NcSUT5* 基因 CDS 全长，连入 pAN580 载体，构建 NcSUT4/NcSUT5-GFP 融合蛋白，使用 QIAGEN Plasmid Midi Kit (QIAGEN)试剂盒提取高纯度高浓度质粒。制备拟南芥原生质体方法参照 Wu 等(2009)。使用细胞质膜定位 marker AtPIP2-mCherry 作为阳性对照，分别与 NcSUT4/NcSUT5-GFP 质粒共转化原生质体，3 天后使用激光共聚焦共聚焦显微镜(LSM880, ZESISS)观察原生质体荧光发光情况并拍照。

作者贡献

梁正炫是本研究的实验研究执行人，完成数据分析及论文初稿写作；冯佳乐、陈鑫和唐琳涵参与实验设计和实验结果分析；彭昌操给予实验设计建议；龙健梅是项目的构思者及负责人，指导实验设计、数据分析、论文写作与修改。全体作者都阅读并同意最终的文本。

致谢

本研究由国家自然科学基金(31800560)、广东省基础与应用基础研究基金项目(2021A1515010816；2023A1515030250)和广州市科技计划项目(202102020505)共同资助。

参考文献

Barker L., Kühn C., Weise A., Schulz A., Gebhardt C., Hirner B., Hellmann H., Schulze W., Ward J.M., and Frommer W.B., 2000, SUT2, a putative sucrose sensor in sieve elements, Plant Cell, 12(7): 1153-1164.

Chen C.J., Chen H., Zhang Y., Thomas H.R., Frank M.H., He Y.H., and Xia R., 2020, TBtools: an integrative toolkit developed for interactive analyses of big biological data, Mol. Plant, 13(8): 1194-1202.

Chincinska I., Gier K., Krügel U., Liesche J., He H.X., Grimm B., Harren F.J.M., Cristescu S.M., and Kühn C.,

2013, Photoperiodic regulation of the sucrose transporter StSUT4 affects the expression of circadian-regulated genes and ethylene production, Front. Plant Sci., 4: 26.
Chincinska I.A., Liesche J., Krügel U., Michalska J., Geigenberger P., Grimm B., and Kühn C., 2007, Sucrose transporter StSUT4 from potato affects flowering, tuberization, and shade avoidance response, Plant Physiol., 146(2): 515-528.
Deng X.M., Zhan Y.L., Zhang Q., Huang H., and Chen X.Y., 2012, Study on tissue culture of *Neolamarckia cadamba*, Huanan Nongye Daxue Xuebao (Journal of South China Agricultural University), 33(2): 216-219, 224. (邓小梅, 詹艳玲, 张倩, 黄浩, 陈晓阳, 2012, 黄梁木组培快繁技术研究, 华南农业大学学报, 33(2): 216-219, 224.)
Fan R.C., Peng C.C., Xu Y.H., Wang X.F., Li Y., Shang Y., Du S.Y., Zhao R., Zhang X.Y., Zhang L.Y., and Zhang D.P., 2009, Apple sucrose transporter SUT1 and sorbitol transporter SOT6 interact with cytochrome b5 to regulate their affinity for substrate sugars, Plant Physiol., 150 (4): 1880-1901.
Frost C.J., Nyamdari B., Tsai C.J., and Harding S.A., 2012, The tonoplast-localized sucrose transporter in *populus* (PtaSUT4) regulates whole-plant water relations, responses to water stress, and photosynthesis, PLoS ONE, 7(8): e44467.
Gao L., Xiao W.F., Li W.Y., and Peng C.C., 2011, Progress on functions of sucrose transporters (SUTs) in *Arabidopsis thaliana*, Fenzi Zhiwu Yuzhong (Molecular Plant Breeding), 9(2): 251-255. (高蕾, 肖文芳, 李文燕, 彭昌操, 2011, 拟南芥蔗糖转运蛋白(SUTs)的功能研究进展, 分子植物育种, 9(2): 251-255.)
Geiger D., 2011, Plant sucrose transporters from a biophysical point of view, Mol. Plant, 4(3): 395-406.
Gong X., Liu M.L., Zhang L.J., Ruan Y.Y., Ding R., Ji Y.Q., Zhang N., Zhang S.B., Farmer J., and Wang C., 2014, Arabidopsis AtSUC2 and AtSUC4, encoding sucrose transporters, are required for abiotic stress tolerance in an ABA-dependent pathway, Physiol. Plantarum, 153(1): 119-136.
Gora P.J., Reinders A., and Ward J.M., 2012, A novel fluorescent assay for sucrose transporters, Plant Methods, 8: 13.
Hackel A., Schauer N., Carrari F., Fernie A.R., Grimm B., and Kühn C., 2005, Sucrose transporter LeSUT1 and LeSUT2 inhibition affects tomato fruit development in different ways, Plant J., 45(2): 180-192.
Ho L.H., Lee Y.I., Hsieh S.Y., Lin I.S., Wu Y.C., Ko H.Y., Klemens P.A., Neuhaus H.E., Chen Y.M., Huang T.P., Yeh C.H., and Guo W.J., 2020, GeSUT4 mediates sucrose import at the symbiotic interface for carbon allocation of heterotrophic *Gastrodia elata* (*Orchidaceae*), Plant Cell Environ., 44(1): 20-33.
Iftikhar J., Lyu M., Liu Z.Y., Mehmood N., Munir N., Ahmed M.A.A., Batool W., Aslam M.M., Yuan Y., and Wu B.H., 2020, Sugar and hormone dynamics and the expression profiles of SUT/SUC and SWEET sugar transporters during flower development in *Petunia axillaris*. Plants, 9(12): 1770.
Kühn C., and Grof C.P., 2010, Sucrose transporters of higher plants, Curr. Opin. Plant Biol.,13: 287-297.
Liang Y.F., Bai J.Y., Xie Z.L., Lian Z.Y., Guo J., Zhao F.Y., Liang Y., Huo H.Q., and Gong H.J., 2023a, Tomato sucrose transporter SlSUT4 participates in flowering regulation by modulating gibberellin biosynthesis, Plant Physiol., 192(2): 1080-1098.
Liang Y.F., Chen S.R., Liu S.H., Cai R., Hu W.X., Jia J.H., Lian Z.Y., Huo H.Q., and Gong H.J., 2023b, Alteration in the expression of tomato sucrose transporter gene SlSUT4 modulates sucrose subcellular compartmentation and affects responses of plants to drought stress, Environ. Exp. Bot., 215: 105506.
Liu S.W., Long J.M., Zhang L.D., Gao J.Y., Dong T.T., Wang Y., and Peng C.P., 2022, *Arabidopsis* sucrose transporter 4 (AtSUC4) is involved in high sucrose-mediated inhibition of root elongation, Biotechnol. Biotec. Eq., 36: 561-574.
Ma Q.J., Sun M.H., Lu J., Kang H., You C.X., and Hao Y.J., 2019, An apple sucrose transporter MdSUT2.2 is a phosphorylation target for protein kinase MdCIPK22 in response to drought, Plant Biotec. J., 17: 625-637.
Mahboubi A., Ratke C., Gorzsás A., Kumar M., Mellerowicz E.J., and Niittyla T., 2013, Aspen SUCROSE TRANSPORTER3 allocates carbon into wood fibers, Plant Physiol., 163: 1729-1740.
Meyer S., Lauterbach C., Niedermeier M., Barth I., Sjolund R.D., and Sauer N., 2004, Wounding enhances expression of AtSUC3, a sucrose transporter from Arabidopsis sieve elements and sink tissues, Plant Physiol.,134: 684-693.
Payyavula R.S., Tay K.H.C., Tsai C.J., and Harding S.A., 2011, The sucrose transporter family in *Populus*: the importance of a tonoplast PtaSUT4 to biomass and carbon partitioning, Plant J., 65(5): 757-770.
Peng Q., Cai Y.M., Lai E.H., Nakamura M., Liao L., Zheng B.B., Ogutu C., Cherono S., and Han Y.P., 2020, The sucrose transporter MdSUT4.1 participates in the regulation of fruit sugar accumulation in apple, BMC Plant Biol., 20(1): 191.
Reinders A., Sivitz A.B., and Ward J.M., 2012, Evolution of plant sucrose uptake transporters, Front. Plant Sci.,3:

22.
Reinders A., Sivitz A.B., Starker C.G,. Gantt J.S., and Ward J.M., 2008, Functional analysis of LjSUT4, a vacuolar sucrose transporter from *Lotus japonicus*, Plant Mol. Bio., 68(3): 289-299.
Schneider S., Hulpke S., Schulz A., Yaron I., Höll J., Imlau A., Schmitt B., Batz S., Wolf S., Hedrich R., and Sauer N., 2011, Vacuoles release sucrose via tonoplast-localised SUC4-type transporters, Plant Bio., 14(2): 325-336.
Sivitz A.B., Reinders A., and Ward J.M., 2008, Arabidopsis sucrose transporter AtSUC1 is important for pollen germination and sucrose-induced anthocyanin accumulation, Plant Physiol., 147(1): 92-100.
Sun L.X., Deng R.L., Liu J.W., Lai M.Y., Wu J.W., Liu X.D., and Shahid M.Q., 2022, An overview of sucrose transporter (SUT) genes family in rice, Mol. Biol. Rep., 49(6): 5685-5695.
van Bel A.J.E., 1990, Xylem-phloem exchange via the rays: the undervalued route of transport, J. Exp. Bot., 41(6): 631-644.
Wang D.D., Liu H.J., Wang H.X., Zhang P., and Shi C.Y., 2020, A novel sucrose transporter gene IbSUT4 involves in plant growth and response to abiotic stress through the ABF-dependent ABA signaling pathway in Sweetpotato, BMC Plant Biol., 20(1): 157.
Wang L.F., Qi X.X., Huang X.S., Xu L.L., Jin C., Wu J., and Zhang S.L., 2016, Overexpression of sucrose transporter gene PbSUT2 from *Pyrus bretschneideri*, enhances sucrose content in *Solanum lycopersicum* fruit, Plant Physiol. Biochem., 105: 150-161.
Weise A., Barker L., Kühn C., Lalonde S., Buschmann H., Frommer W. B., and Ward J. M., 2000, A new subfamily of sucrose transporters, SUT4, with low affinity/high capacity localized in enucleate sieve elements of plants, Plant Cell, 12 (8): 1345-1355.
Wu F.H., Shen S.C., Lee L.Y., Lee S.H., Chan M.T., and Lin C.S., 2009, Tape-*Arabidopsis* Sandwich - a simpler *Arabidopsis* protoplast isolation method, Plant Methods, 5(1): 16.
Wu X., Mubeen S., Luo D.J., Cao S., Wang C.J., Yue J., Wu Q.J., Zhang H., Nie J.Z., Chen C.N., Wang M., Li R., and Chen P., 2024, Function characterization of a soybean sucrose transporter GmSUT4.2 involved in plant growth, development, and crop yield, Plant Growth Regul., 102: 529-543.
Xu H.F., Qu C.Z., Liu J.X., Wang Y.C., Wang D.Y., Zuo W.F., Jiang S.H., Wang N., Zhang Z.Y., and Chen X.S., 2017, Expression analysis and functional identification of a vacuolar sucrose transporter gene *MdSUT4* in apple, Yuanyi Xuebao (Acta Horticulturae Sinica), 44(7): 1235-1243. (许海峰, 曲常志, 刘静轩, 王意程, 王得云, 左卫芳, 姜生辉, 王楠, 张宗营, 陈学森, 2017, 苹果液泡膜蔗糖转运蛋白基因 *MdSUT4* 的表达分析与功能鉴定, 园艺学报, 44(7): 1235-1243.)
Zanon L., Falchi R., Hackel A., Kühn C., and Vizzotto G., 2015, Expression of peach sucrose transporters in heterologous systems points out their different physiological role, Plant Sci., 238: 262-272.
Zhang D., Li J.J., Zhang M.J., Bao Y.T., Yang X., Xu W.Y., OuYang K.X., and Chen X.Y., 2018, Selection and validation of reference genes for quantitative RT-PCR analysis in *Neolamarckia cadamba*, Zhiwu Xuebao (Chinese Bulletin of Botany), 53(6): 829-839. (张登, 李景剑, 张梦洁, 包钰韬, 杨霄, 徐武云, 欧阳昆唏, 陈晓阳, 2018, 黄梁木实时荧光定量 PCR 分析中内参基因的选择, 植物学报, 53(6): 829-839.)
Zhang L., Xu X.D., Wang L.J., Lu M.Z., 2016, Identification and functional analysis of the *Populus* sucrose transporter gene *PagSUT4*, Linye Kexue (Scientia Silvae Sinicae), 52(8): 21-28. (张利, 徐向东, 王丽娟, 卢孟柱, 2016, 杨树蔗糖转运体基因 *PagSUT4* 的鉴定及功能分析, 林业科学, 52(8): 21-28.)
Zhao X.L., Hu X.D., OuYang K.X., Yang J., Que Q.M., Long J.M., Zhang J.X., Zhang T., Wang X., Gao J.Y., Hu X.Q., Yang S.Q., Zhang L.S., Li S.F., Gao W.J., Li B.P., Jiang W.K., Nielsen E., Chen X.Y., and Peng C.C., 2022, Chromosome-level assembly of the *Neolamarckia cadamba* genome provides insights into the evolution of cadambine biosynthesis, Plant J., 109(4): 891-908.

证书编号：2024071945524

中国知网学术期刊网络首发论文出版证书

《中国学术期刊（网络版）》是教育部主管、清华控股有限公司主办、国家新闻出版广电总局 2015 年 8 月 14 日批准的网络版连续出版物（国际标准连续出版物号 ISSN 2096-4188；国内统一连续出版物号 CN 11-6037/Z），在《中国学术期刊（光盘版）》电子杂志社有限公司的互联网出版网站中国知网（www.cnki.net，新出网证（京）字 008 号）上进行出版。

《分子植物育种》与《中国学术期刊（光盘版）》电子杂志社有限公司合作，在中国知网创办了与《分子植物育种》内容一致的网络版，以单篇或整期出版形式，在印刷版出版之前刊发纸质期刊已正式录用定稿的论文，著作权受法律保护。论文发表时间按中国知网的网络出版时间确认。

兹有，梁正炫，冯佳乐，陈鑫，唐琳涵，彭昌操，龙健梅同志的题为《黄梁木蔗糖转运蛋白 NcSUT4 和 NcSUT5 的表达与功能分析》的论文

链接地址：https://link.cnki.net/urlid/46.1068.S.20240719.1235.006

已于 2024 年 7 月 22 日在中国知网出版，出版证书验证地址 www.cnki.net，特此证明。

《分子植物育种》编辑部（签章）

《中国学术期刊（光盘版）》
电子杂志社有限公司（签章）

2024 年 7 月 22 日

技术与方法 Techniques and Methods

激光显微切割分离黄梁木不定根原基的技术体系建立

董甜甜#, 王雪#, 刘思雯, 张立定, 龙健梅*, 彭昌操*

华南农业大学林学与风景园林学院, 广州510642

摘要: 为挖掘黄梁木不定根原基发生的关键基因, 获取特异性高的根原基起始细胞群是分析根原基表达图谱的重要前提。激光显微切割是目前获取特异细胞群的一种常用手段。本研究通过分析石蜡切片过程中固定剂、脱水时间、渗透剂、切片厚度、粘片试剂和烘片温度等对RNA质量的影响, 以及对激光显微切割参数的调试, 建立了采用激光显微切割技术分离黄梁木不定根原基细胞的体系, 获得的RNA可以满足后续RNA-seq文库构建的要求, 为揭示黄梁木不定根原基发生的分子机制奠定了关键基础。

关键词: 黄梁木; 不定根原基; 激光显微切割; 石蜡切片; RNA完整性

无性繁殖是一种大量繁殖遗传性状相同的植物材料的重要技术方法。木本植物通常用茎扦插繁殖, 而不定根的形成是扦插繁殖成活的前提(王荣等2018)。不定根的形成主要经历4个过程: (1)细胞脱分化; (2)细胞分裂形成不定根原基; (3)不定根原基分化伸长; (4)突破表皮(Jun等2015)。然而, 在大多数双子叶植物的茎段中没有潜在的特异细胞分化成根原基, 因此细胞分裂、分化是形成不定根原基必不可少的过程(Lin等2014; Klerk等1999)。

激光显微切割技术(laser microdissection, LMD)通过显微操作系统从异质群体中有效分离特定的目标细胞群(Simone等1998)。LMD结合高通量测序已成为一种重要的手段来研究植物中特定的细胞类群的功能。已利用LMD分离的细胞组织有生殖器官、分生组织、茎和根等, 并且进行了转录组分析(Fang和Schneider 2013)。Cassson等(2005)使用冰冻切片联合LMD分离拟南芥(*Arabidopsis thaliana*)胚胎发育过程中的球形胚和心形胚, 研究拟南芥胚胎发育过程中基因的表达模式。冰冻切片制备流程简单, 在一定程度上可以提高RNA质量, 但是由于植物细胞中有大的液泡, 冰冻切片过程会产生冰晶(王英旗等2013)。含水量高或木质素含量较高的植物材料使用冰冻切片容易导致切片破碎, 不能提供很好的视觉效果, 甚至导致目标细胞破碎(Spencer等2007)。然而石蜡切片包括固定、脱水、渗蜡等繁琐的步骤, 可能会导致RNA降解(Takahashi等2010)。既要保证组织切片的完整性, 又要提高RNA的质量, 需要在这双方之间取得平衡。有文献报道了石蜡切片流程中固定剂和切片厚度对于RNA质量的影响, 主要针对拟南芥、玉米(*Zea mays*)、番茄(*Solanum lycopersicum*)等草本植物(Zhang等2012; Kerk等2003; Shibutani等2000; Brooks等2009), 石蜡切片各个流程对木本植物RNA质量的影响相关报道较少, 而且石蜡切片中的其他步骤如脱水流程、渗透剂、粘片试剂等方面对RNA质量的影响目前还未详细介绍。

黄梁木(*Neolamarckia cadamba*), 又称团花树, 属茜草科团花属, 是亚热带和热带地区常绿阔叶乔木, 分布广泛, 生长迅速, 躯干通直, 成林快, 将成为华南地区人工造林的一种速生树种(阙青敏等2017)。但黄梁木枝条扦插生根较难, 难以利用扦插繁殖方式保持其优良性状。为了研究黄梁木不定根发生的分子机理, 我们通过获取黄梁木组培苗不定根原基, 进行转录组分析, 以期获得参与不定根起始相关的关键基因, 初步探究不定根发生的分子机理, 为促进黄梁木扦插生根提供重要理论基础。

收稿 2018-09-03 **修定** 2019-04-25

资助 国家重点研发计划(2016YFD0600104)、国家自然科学基金(31470681)、广东省自然科学基金(2016A030311032)、广州市科技计划(201607020024)、广东省教育厅人才计划(2017KQNCX017)和广东省林业科技创新(2016KJCX003)。

并列第一作者。

* 共同通讯作者: 龙健梅(longjianmei@scau.edu.cn)、彭昌操(ccpeng@scau.edu.cn)。

本论文主要从固定剂、脱水步骤、渗透剂、切片厚度、粘片试剂和烘片温度等方面研究其对黄梁木组培苗茎段RNA质量的影响, 建立了黄梁木不定根原基LMD分离的最佳石蜡切片制片方法, 并对LMD参数进行了调适。本研究为后续黄梁木以及其他木本植物使用LMD分离特异性细胞提供了技术支持和参考价值。

1 材料与方法

1.1 试验材料

采集黄梁木[*Neolamarckia cadamba* (Roxb.) Bosser]优势树种的种子, 50%次氯酸钠消毒10 min, 无菌水反复洗涤4次, 再用70%酒精快速消毒30 s, 立即吸去酒精, 用无菌水洗涤4次, 消毒后播种于MS培养基。待长出子叶后, 挑选其中一棵苗接种于增殖培养基(MS+1 mg·L^{-1} 6-BA+0.1 mg·L^{-1} NAA), 扩繁无性系。30 d后, 转至生根培养基(MS+0.1 mg·L^{-1} NAA)促进幼苗茎伸长变粗。待其茎粗为3~4 mm, 剪切顶端第二茎节处, 重新接种在生根培养基中。取接种第4天的苗茎基1 cm做石蜡切片, 用于激光显微切割。温室培养生长条件为: 光照强度60~70 μmol·m^{-2}·s^{-1}, 光照时间12 h·d^{-1}, 培养温度25~27°C (邓小梅等2012)。

1.2 石蜡制片流程的不同处理

1.2.1 不同固定液处理

用3种不同的新鲜预冷固定液处理: EA (乙醇:乙酸=3:1)、丙酮、FAA (70%酒精90 mL+冰乙酸5 mL+甲醛5 mL)。将固定液倒入15 mL离心管置于冰上, 取黄梁木组培苗第二茎节基部1 cm, 切成每段2 mm, 投入固定液中。冰上抽真空20 min, 更换固定液, 重复2次, 4°C保存12 h, 每种处理3个重复。固定后, 用Plant RNA Kit (OMEGA)试剂盒提取RNA, 琼脂糖凝胶电泳检测RNA完整性。

1.2.2 不同脱水处理

根据脱水梯度和脱水时间的不同, 分为以下3个处理(表1)。每种处理3个重复, 脱水流程均在4°C。脱水完成后, 提取RNA, 琼脂糖凝胶电泳检测RNA完整性。

1.2.3 不同渗透剂处理

根据最佳的固定剂和脱水流程, 使用3种渗透剂处理(表2), 每种处理3个重复, 渗透过程均在4°C。渗透完成后, 提取RNA, 琼脂糖凝胶电泳检测RNA完整性(Schroeder等2006)。

1.2.4 不同蜡块储藏温度处理

将制备好的蜡块分别在4和–20°C存放12 h后切片。将蜡带在2 mL离心管中脱蜡10 min, 1 500×*g*离心5 min, 重复2次。用RNAt Rneasy Micro Kit (Qiagen)试剂盒提取RNA。用Agilent RNA 6000 Pico Kit检测RNA的完整性(Schroeder等2006)。

1.2.5 不同切片厚度处理

采用Leica石蜡切片机, 切片厚度设置2个梯

表1 3种不同的脱水处理

Table 1 Three treatments of different dehydrations

脱水处理编号	脱水步骤		
	第一步	第二步	第三步
1	75%酒精处理20 min	100%酒精处理20 min	
2	75%酒精处理20 min	90%酒精处理20 min	100%酒精处理20 min
3	75%酒精处理30 min	90%酒精处理30 min	100%酒精处理1 h

表2 3种不同的渗透剂处理

Table 2 Three treatments of different penetrating agents

渗透剂处理	第一步		第二步	
	试剂配比	时间/min	试剂配比	时间/min
异丙醇	异丙醇:乙醇(1:1)	30	100%异丙醇	30
二甲苯	二甲苯:乙醇(1:1)	30	100%二甲苯	30
To透明剂(优质松节油)	To透明剂:乙醇(1:1)	30	100% To透明剂	30

度, 分别为10和14 μm。切片后脱蜡, 提取RNA并检测质量。

1.2.6 不同粘片试剂处理

将蜡带黏贴在经过1%焦碳酸二乙酯(DEPC)水处理的载玻片上, 分别用DEPC水、RNA酶抑制剂黏贴。粘片后烘干, 用解剖针从载玻片上刮取植物组织, 提取RNA并检测质量。

1.2.7 不同烘片温度和时间处理

将黏贴好的载玻片分别在40°C烘干20 min、38°C烘干40 min和4°C烘干2 h。烘干后, 刮取植物组织, 提取RNA并检测质量。

1.3 激光显微切割

采用Leica AS LMD 7000对目标细胞进行收集, 主要对以下几个参数进行调试: 激光能量(Power)、激光切割孔径(Aperture)、切割速度(Speed)、发射强度(Head Current)和脉冲频率(Pulse Frequency)等参数, 最终建立黄梁木不定根原基的最佳切割参数。

2 实验结果

2.1 不同固定液对RNA质量的影响

固定剂的作用是稳定细胞内容物, 并在组织切片和细胞切割期间保持组织形态的完整性(Kerk等2003)。植物细胞包括不同硬度的细胞壁和很大的中央液泡, 组织需要被固定在合适的固定液中, 才能使材料保持很好的形态和RNA的完整性(Barcala等2012)。但是, 固定剂对目标细胞的RNA有一定的降解, 该步骤是决定RNA命运的关键。为了保证组织切片的完整性, 又降低固定剂对RNA质量的影响, 本文比较了这三种不同的固定剂对黄梁木组培苗茎段RNA回收率的影响。表3显示, 丙酮固定后RNA的回收率最高, 比EA固定要高10 $ng \cdot mg^{-1}$左右。FAA固定的RNA回收率非常低, 说明用FAA固定的组织RNA易降解。琼脂糖凝胶电泳检测结果(图1)表明, EA固定后的组织RNA 28 S和18 S处为明亮的条带, 并且28 S比18 S条带亮, 无杂带; 丙酮固定后组织RNA的条带, 有明显的弥散拖带现象, 28 S的亮度弱于18 S, 说明RNA有部分降解; FAA回收的RNA在28 S和18 S没有亮带, 几乎全部降解。总上所述, 适用于黄梁木组培苗LMD切割的最佳固定剂是EA。

表3 不同固定液处理后黄梁木的RNA回收率

Table 3 The RNA concentrations of *N. cadamba* treated with different fixed solutions

固定液	RNA回收率/$ng \cdot mg^{-1}$
EA	32[a]
丙酮	43[a]
FAA	4[b]

不同小写字母表示差异达到显著水平(P<0.05, n=3), 下表同此。

2.2 不同脱水处理对RNA质量的影响

酒精梯度脱水用于交换出植物组织中的水分, 化学脱水也可能损害RNA的质量(Polster等2006)。脱水流程中酒精梯度对保持细胞完整性至关重要, 稍有不慎会导致细胞破碎, 内容物溢出, 无法收集RNA, 并且会造成LMD切割时不能识别目标细胞。本文检测了3种不同的脱水步骤对黄梁木组培苗RNA回收率的影响。结果(表4)显示, 处理1的时间

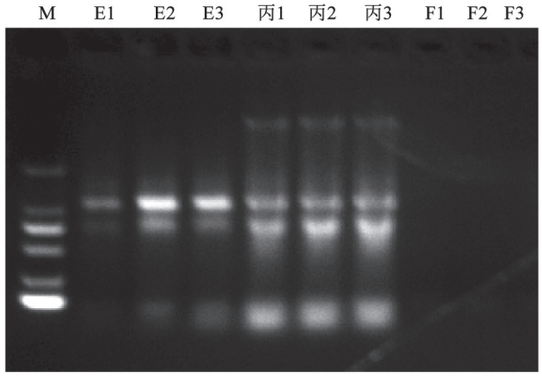

图1 不同固定液处理后RNA电泳图

Fig.1 The electrophoresis of RNA treated with different fixed solutions

M: DNA marker 2000; E1~3: EA固定液; 丙1~3: 丙酮固定液; F1~3: FAA固定液。

表4 不同脱水处理后黄梁木的RNA回收率

Table 4 The RNA concentrations of *N. cadamba* treated with different dehydrations

脱水处理	RNA回收率/$ng \cdot mg^{-1}$
处理1	28[a]
处理2	11[b]
处理3	31[a]

最短, RNA回收率较高; 处理2的RNA回收率最低; 处理3脱水步骤时间较长, 但RNA回收率较高。对RNA进行琼脂糖凝胶电泳检测, 3种脱水处理的上样量均在1 μg左右, 处理1的28 S明显比另外两个处理更亮, 并且28 S比18 S亮很多, 无杂带; 处理2和处理3的28 S条带要微弱一些, 18 S条带很微弱, 几乎看不到(图2)。

综上所述, 脱水时间越长, 步骤越繁琐, RNA酶降解RNA的可能性就越大。所以, 在保证植物组织中的水分完全被替换的前提下, 尽量缩短脱水时间, 减少脱水步骤, 但同时要避免细胞缩水, 影响激光切割时组织形态的观察。经处理1脱水后, 细胞形态完整(图3), 并且RNA质量较高, 因此是针对黄梁木组培苗用于LMD石蜡制片最优的脱水处理。

2.3 不同渗透剂对RNA质量的影响

渗透剂的作用是辅助石蜡渗透到植物组织内部, 起到过渡作用。常用的渗透剂主要有异丙醇、二甲苯和To透明剂(Ohtsu等2007; Cai和Lashbrook 2006)。表5显示, 异丙醇的RNA回收率较低; 二甲苯的回收率最高。琼脂糖凝胶电泳检测, 异丙醇在28 S比18 S条带更亮, 并且在小分子处无降解。二甲苯和To透明剂在18 S处亮带都很强, 在小分子处有明显的亮带, 说明RNA有部分降解(图4)。综上所述, 异丙醇的回收率较低, 但是RNA质量是最好的, 因此是适用于黄梁木组培苗最佳的渗透剂。

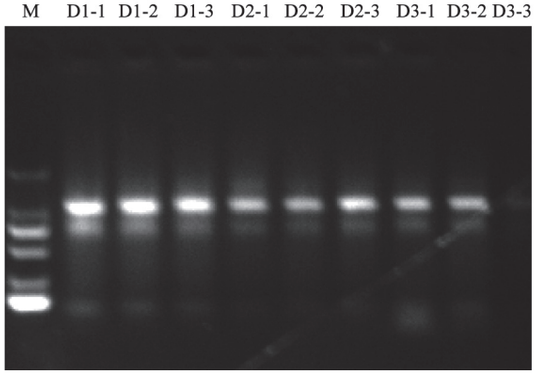

图2 不同脱水处理后RNA电泳图

Fig.2 The electrophoresis of RNA treated with deifferent dehydrations

M: DNA marker 2000; D1-1~3: 脱水处理1; D2-1~3: 脱水处理2; D3-1~3: 脱水处理3。

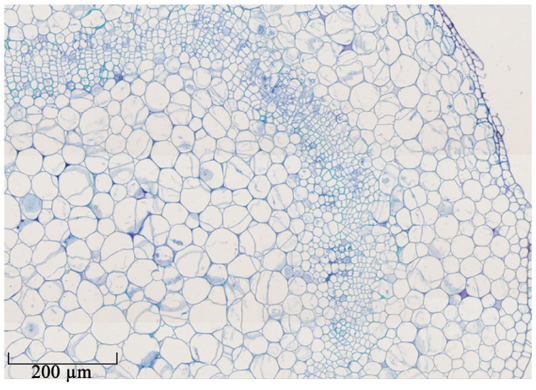

图3 第一种脱水处理后黄梁木组培苗横切效果图

Fig.3 Cross-sectional diagram of tissue culture seedlings of *N. cadamba* treated with the first dehydration

表5 不同渗透剂处理后黄梁木的RNA回收率

Table 5 The RNA concentrations of *N. cadamba* treated with different infiltrations

透明试剂	RNA回收率/ng·mg^{-1}
异丙醇	38^{c}
二甲苯	116^{a}
To透明剂	72^{b}

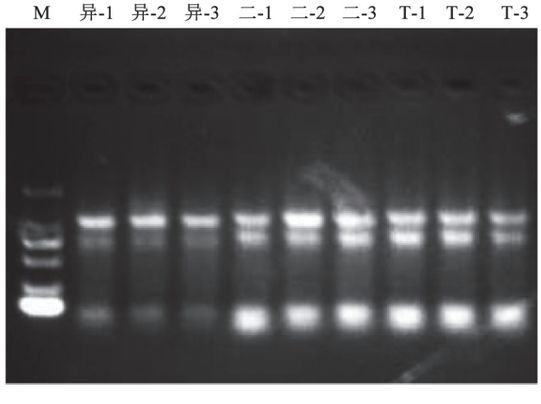

图4 不同渗透剂处理后RNA电泳图

Fig.4 The electrophoresis of RNA treated with different infiltrations

M: DNA marker 2000; 异-1~3: 异丙醇; 二-1~3: 二甲苯; T-1~3: To透明剂。

2.4 不同蜡块储藏温度对RNA质量的影响

石蜡包埋的组织制备用于LMD切片, 除了为细胞收集提供清晰的视觉辅助之外, 该方法还具

有以下优点: 嵌入蜡块的组织RNA可稳定保存, 不需要立即切割(Takahashi等2010)。对制备好的蜡块进行储藏保存, 这样可以节省制备蜡块的时间。因此我们针对蜡块储藏温度设置了4和–20°C。Agilent 2100生物分析仪检测RNA质量结果(图5)显示, 4°C储存的RIN (RNA Integrity Number)=5.8 (图5-A), 28 S和18 S峰形高; 电泳图28 S和18 S条带清晰(图5-C)。–20°C储存的RIN=5.0 (图5-B), 28 S峰非常低, 25 nt处有明显峰形, 有小分子降解, 电泳图28 S模糊(图5-D)。相比于4°C储存, –20°C储藏的RIN值较低, RNA有明显降低。可能由于从–20°C到室温, 有明显的温差变化, 导致RNA降解。因此, 蜡块的最佳储藏温度为4°C。

2.5 不同切片厚度对RNA质量的影响

切片厚度通常要大于目标细胞群直径(Casson等2005)。通过对黄梁木组培苗3个区域不定根原基细胞的平均直径计算(图6-A), 发现其细胞直径平均为9.54 μm。针对黄梁木组培苗不定根原基的切片厚度最小值为10 μm, 可以适当增加切片厚度以提高RNA质量。因此设置了2个切片厚度10 μm (图6-B)和14 μm (图6-C)。这两个切片厚度均可获得清晰的组织学观察。Agilent 2100生物分析仪检测RNA质量结果(图7)表明, 切片厚度为14 μm的RIN=6.0 (图7-A), 28 S和18 S峰形高, 电泳图条带明显(图7-C)。而切片厚度为10 μm的RIN=5.5 (图7-B), 28 S峰形较低, 25 nt处有较大峰值, 电泳图28 S条带不明显, 有拖带现象(图7-D)。因此, 选用14 μm的切片厚度既可提供清晰的组织图片, 所获得RNA的RIN值较高, 适合于黄梁木不定根原基细胞的激光显微切割。

2.6 粘片试剂的最佳选择

1% DEPC水能破坏RNase的结构, 从而使其失活。因此我们检测了DEPC水和RNase抑制剂溶液在粘片过程中对RNA的保护作用。DEPC水粘片RIN=6.1 (图8-A), 28 S和18 S有明显的峰形, 电泳图条带明显(图8-C)。RNase抑制剂溶液粘片RIN=5.4 (图8-B), 从200 nt到18 S之间峰值较高, RNA有降解, 电泳图有明显的拖带(图8-D)。1% DEPC水对RNase的抑制作用要优于RNA酶抑制剂, 因此粘片剂选用1% DEPC水。

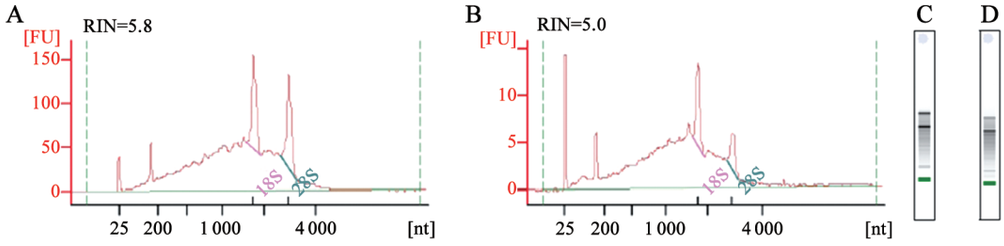

图5 不同蜡块储藏温度的RNA质检图

Fig.5 The electrophoresis images of RNA under different storage temperatures of paraffin blocks

A: 4°C储藏峰图; B: –20°C储藏峰图; C: 4°C储藏电泳图; D: –20°C储藏电泳图。

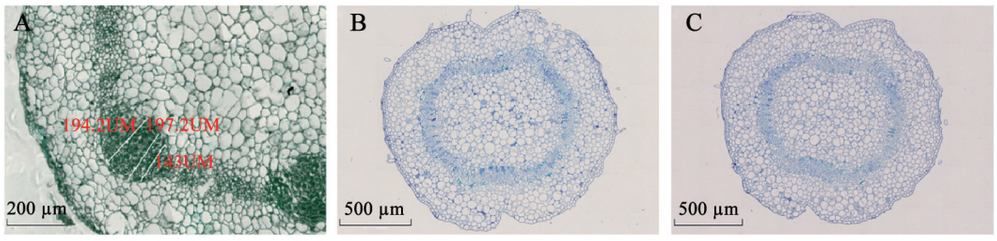

图6 不定根原基细胞直径测量和切片厚度效果图

Fig.6 Measurement of diameter of adventitious root primordial cells and slice thickness

A: 不定根原基细胞直径大小计算; B: 切片厚度10 μm; C: 切片厚度14 μm。

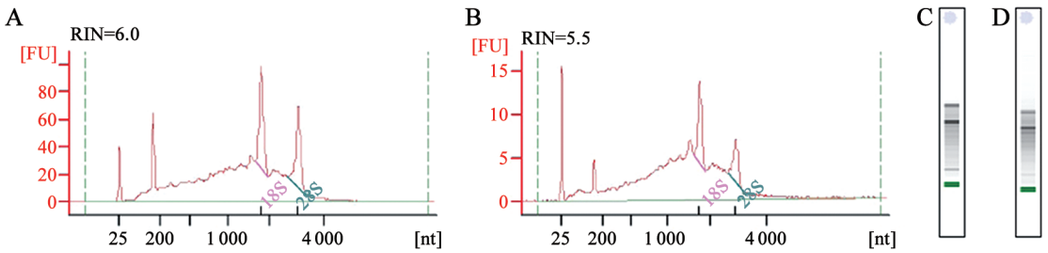

图7 不同切片厚度的RNA质检图

Fig.7 The electrophoresis images of RNA with different slice thickness

A: 切片厚度14 μm峰图; B: 切片厚度10 μm峰图; C: 切片厚度14 μm电泳图; D: 切片厚度10 μm电泳图。

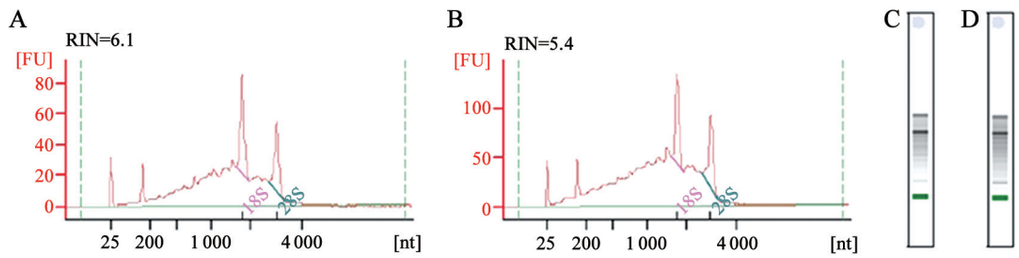

图8 不同粘片试剂的RNA质检图

Fig.8 The electrophoresis images of RNA using different floating media

A: DEPC水峰图; B: RNase抑制剂溶液峰图; C: DEPC水电泳图; D: RNase抑制剂溶液电泳图。

2.7 最佳的烘片温度

我们设置了3个温度梯度: 42、38和4°C。烘片时间按照水分全部挥发完, 蜡带紧紧贴在载玻片上的最少时间来计算。为了减少烘片时间, 用枪头把多余的水分吸干。42°C烘干需要20 min, 38°C烘干至少需要40 min, 4°C冰箱风干至少2 h以上。结果(图9)显示, 42°C烘干后RIN=6.6 (图9-A), 基线较平整, 28 S和18 S峰形都很高, 电泳图28 S和18 S非常明显(图9-D, 泳道1); 38°C烘干后RIN=4.0 (图9-B), 28 S和18 S没有峰值, 几乎全部降解, 电泳图28 S和18 S条带很弱(图9-D, 泳道2); 4°C风干后RIN=4.9 (图9-C), 略比38°C高一点, 28 S和18 S没有峰值, 电泳图18 S没有条带, 28 S有微弱的条带(图9-D, 泳道3)。综上所述, 烘片的最佳温度和时间为42°C烘干20 min。

2.8 激光显微切割参数调适

激光显微切割的参数具有物种和组织特异性, 并且各个参数并不是单独决定, 而是相互影响和制约。切割收集目标细胞所经历的时间是决定RNA质量的关键, 所以在整个实验过程中应尽量缩短切割时间, 保证样品在1 h内收集完成。在10×物镜下, 经反复试验, 得到切割黄梁木不定根原基细胞的最佳参数(表6)。在该参数下激光显微切割样品时, 收集根原基细胞效果图(图10), 镜检管盖上收集到的目标细胞(图10-C)。

2.9 不定根原基LMD的最佳石蜡制片方法

综上所述, 用于黄梁木组培苗不定根原基LMD的最佳石蜡制片方法如下。预冷的EA固定, 冰上抽真空20 min, 重复2次, 更换溶液, 在4°C存放12 h。4°C下脱水, 75%乙醇20 min, 100%乙醇20 min。4°C条件下渗透, 乙醇:异丙醇(1:1) 30 min, 100%异丙醇30 min。65°C下浸蜡, 异丙醇:石蜡40min, 100%石蜡40 min, 100%石蜡2 h (重复2次)。切片厚度为14 μm; 粘片用1% DEPC水滴在leica膜玻片300 μL, 贴4条蜡带, 不要产生气泡, 用枪头吸走多余水分。烘片条件为42°C处理20 min; 脱蜡使用二甲苯10 min共2次; 通风橱风干10 min。为了保证RNA质量的完整性, 一般不进行染色处理,

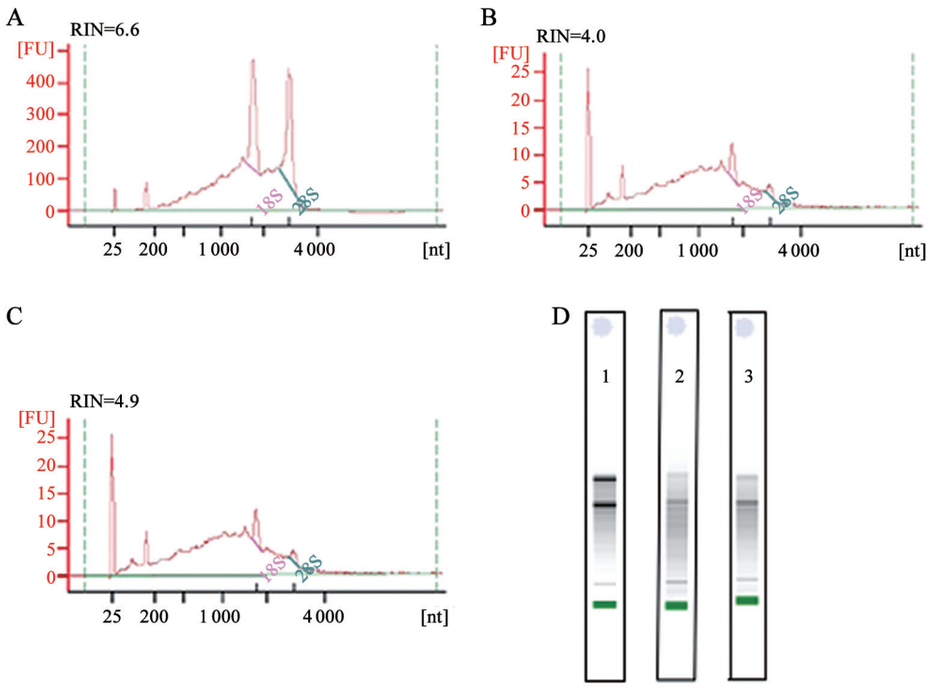

图9 不同烘片温度处理的RNA质检图

Fig.9 The electrophoresis images of RNA under different drying temperature

A: 42°C峰图; B: 38°C峰图; C: 4°C峰图; D: 电泳图, 1: 42°C, 2: 38°C, 3: 4°C。

表6 分离不定根原基的主要激光显微切割参数

Table 6 Main parameters of LMD for adventitious root primordia

物镜	激光能量	切割孔径	切割速度	发射强度/%	脉冲频率	样品平衡
10×	38	6	10	100	555	25

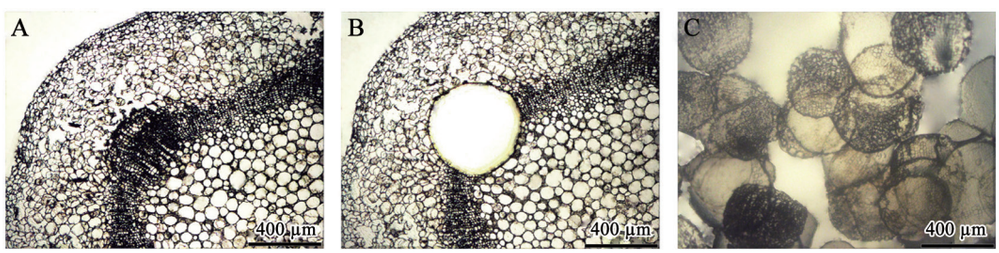

图10 激光显微切割效果图

Fig.10 Laser microdissection of adventitious root primordia

A: 切割前; B: 切割后剩余组织; C: 管盖上收集到的细胞。

染色中的脱水复水过程及染料会对RNA质量造成严重影响, 因此脱蜡通风干燥后, 可上激光显微切割机操作。

根据上述流程获得的植物组织切片形态结构完整清晰(图11-A), 为LMD显微观察提供了良好的视觉效果, RIN值达到7.5 (图11-B), 基线平整, 只在

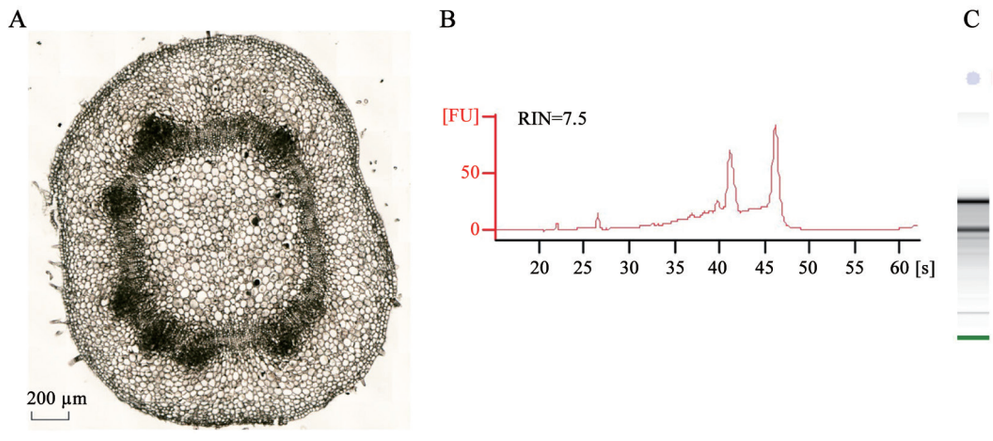

图11 组织切片和RNA质检结果图

Fig.11 Histological anatomy and the RNA electrophoresis images

A: 黄梁木组培苗组织学观察; B: 根据最佳石蜡制片流程获得的RNA质检峰图; C: 电泳图。

28 S和18 S起峰, 28 S峰值比18 S高, 电泳图28 S和18 S条带清晰(图11-C), 无杂带, 满足后续RNA-seq的要求。

3 讨论

LMD结合RNA-seq已成为分析植物基因特异性表达的有力工具, 可以深入了解调控植物发育或生理过程的关键基因(Ohyama等2000; Breyne和Zabeau 2001)。然而, 这种方法对于很多植物细胞类型的适用性取决于细胞形态的完整性。为了获得RIN值较高并且可重复的结果, LMD要求一些基本的预防措施: 应尽量保证最短的取材时间和起始固定时间, 可以在适当的步骤使用RNA酶抑制剂来提高RNA的产量。LMD运用在植物细胞的最大难点是切片的制作, 一般用于LMD的切片方式有石蜡切片和冰冻切片, 石蜡切片相比于冰冻切片来说更适用于植物材料。

固定质量取决于组织中固定剂穿透的时间长度, 固定温度和组织大小(Inada等2005)。常用的固定剂有FAA、卡诺(乙醇:乙酸=3:1), 在LMD中丙酮也是一种常用的固定剂, 例如Ohtsu等(2007)采用丙酮固定的方法进行组织制片, 用LMD分离玉米的芽、花序分生组织、叶原基。有两种类型的化学固定剂广泛用于组织的保存。第一种类型是凝固型固定剂(例如醇和丙酮)。另一种是交联(非凝固)固定剂(例如醛), 交联固定剂更好地保留细胞结构。用37%~40%甲醛:冰乙酸:95%乙醇(10%:5%:50%) (FAA)固定的组织切片的形态优于75%乙醇和25%乙酸固定的。然而, 用凝固固定剂(75%乙醇和25%乙酸)固定比用FAA固定产生更好的RNA产量。从FAA固定的组织中提取的RNA被降解(Chandran等2003), 与本文的结果一致。在本文中采用EA (75%乙醇和25%乙酸)固定, 组织切片结构清晰, 细胞形态完整, 足够提供给LMD过程的目标细胞识别。

石蜡包埋的材料可提供完整的细胞形态, 并且RNA较稳定(Su等2004)。如果干燥剂存在, 且储藏于4°C, 未切片的石蜡包埋块仍可切片, 可储藏至少2周仍适用于后续LMD切片(Kerk等2003)。本文结果也提出了最佳的蜡块储藏温度为4°C。Kerk等(2003)测试了切片厚度是否影响细胞RNA的质量。切片厚度是石蜡制片中较关键的一个参数, 文献中报道的厚度通常为10~60 μm (Hölscher等2009), 该参数应根据具体材料和目标细胞的大小确定。用于LMD的石蜡切片厚度通常为6~10 μm, 尽管较薄的切片通常会提供更好的结构分辨率, 但较厚的切片可以获得更高质量的RNA (Fang和Schneiider 2013)。对于切取单个细胞而言, 如果切片厚度大于或小于平均细胞厚度, 则细胞壁可能成为从组织表面释放单个细胞的屏障。他们比

较了萝卜(*Raphanus sativus*)皮层薄壁组织的厚度从3 μm到10 μm变化的部分, 发现该范围内的切片厚度对从收获的细胞中回收RNA几乎没有影响。本论文中不同的切片厚度对RNA质量有轻微影响, 在保证组织结构清晰的前提下, 可适当增加切片厚度来提高RNA质量。

将蜡带漂浮在水上, 然后在载玻片上展平, 该过程中组织暴露在水中会激活石蜡切片组织中的RNase活性, 因此被认为可能会导致RNA严重降解。在粘片过程中会拉伸蜡带, 也会导致RNA降解(Cai和Lashbrook 2006)。Takahashi等(2010)检测了采用不含RNase的水或RNase抑制剂粘片, 表明两者没有明显的差异。Cai和Lashbrook (2006)描述了使用胶带转移系统以在粘片过程中会产生更好的RNA质量, 然而, 这在制备载玻片期间增加了额外的耗时步骤, 并且还需要特殊设备。在载玻片上涂上少量甲醇, 足以润湿表面, 用滤纸吸走多余的水, 在该步骤中使用甲醇确实改善了RNA质量(Florez Rueda等2016)。

烘片过程主要是使蜡带牢牢粘在载玻片, 防止脱蜡的时候蜡带滑落。Florez Rueda等(2016)将载玻片在加热板上42°C下干燥过夜约12 h。有文献报道在, 42°C烘片条件下, 时间越久, RNA越容易降解。也可在较低的干燥温度即4°C, 至少1 h (Takahashi等2010)。在烘片过程中, 4°C干燥会导致空气水分凝结在载玻片上, 导致RNA降解严重, 应该尽量把制备好的载玻片当天LMD切割收集完成, 待用的载玻片放在干燥盒内密封。38°C烘片, RNA降解严重, 可能是给RNA酶提供很好的温度条件, 应该尽量避开38°C附近。42°C温度较高, 抑制RNA酶活性, 干燥时间更短, 避免载玻片长期暴露在空气中。

LMD结合微矩阵(LMD-M)或者二代测序(LMD-NGS)已经应用于鉴定特殊的发育过程中相关的基因。由于LMD-NGS成本降低、技术提高, 更频繁应用于基因组功能分析、比较基因组, 植物病原体互作。Casson等(2005)使用LMD-M研究了与拟南芥胚胎发育相关的表达基因, 研究表明65%的拟南芥基因组都参与了胚胎发育过程。Spencer等(2007)使用LMD-M分析了拟南芥胚胎发育过程中每个阶段的相关基因。LMD不仅局限于拟南芥的应用, 已经广泛应用于很多模式植物, 例如玉米、大豆(*Glycine max*)、苜蓿(*Medicago sativa*)、水稻(*Oryza sativa*)等。Emrich等(2007)使用LMD-454测序技术在玉米中得到了几种特殊细胞类型的转录组。Takacs等(2012)使用LMD-NGS已经鉴定了在玉米中SAM (shoot apical meristem)早期和晚期的基因表达。今天, 很多先进的技术在植物生物学领域已经开始蔓延, LMD仍然扮演一个关键的工具分析植物学领域的科学问题, 例如生物学发育、植物-病原体相互作用、组织特异性蛋白分析。并且, LMD方法已经广泛应用于植物和各种各样的组织类型去研究基因表达模式和基因组功能。在未来, 它仍然是一种不可缺少的工具去研究细胞自噬、营养物质运输、转录组分析、细胞壁修复和防御病原体。因此建立适合于特定植物的特定组织细胞的LMD体系是至关重要的。

本文建立了适合于分离黄粱木不定根原基细胞的激光显微切割技术体系, 该体系操作过程较简单, 短时间内可获得大量特异类型细胞, 所提取的RNA也满足后续实验的要求, 因此该技术可以推广到黄粱木其他组织中, 也为其他植物精细分离特异性细胞群提供了参考价值。

参考文献(References)

Barcala M, Fenoll C, Escobar C (2012). Laser microdissection of cells and isolation of high-quality RNA after cryosectioning. Methods Mol Biol, 883: 87–95

Breyne P, Zabeau M (2001). Genome-wide expression analysis of plant cell cycle modulated genes. Plant Biol, 4: 136–142

Brooks L, Strable J, Zhang X, et al (2009). Microdissection of shoot meristem functional domains. PLoS Genet, 5: 513–520

Cai S, Lashbrook CC (2006). Laser capture microdissection of plant cells from tape-transferred paraffin sections promotes recovery of structurally intact RNA for global gene profiling. Plant J, 48: 628–637

Casson S, Spencer M, Walker K, et al (2005). Laser capture microdissection for the analysis of gene expression during embryogenesis of *Arabidopsis*. Plant J, 42: 111–123

Chandran D, Scanlon MJ, Ohtsu K, et al (2009). Laser microdissection-mediated isolation and *in vitro* transcriptional amplification of plant RNA. Curr Protoc Mol Biol, 25:

23–25

Deng XM, Zhan YL, Zhang Q, et al (2012). Stuay on tissue culture of *Neolamarckia cadamba*. J South China Agric Univ, 33: 216–224 (in Chinese with English abstract) [邓小梅, 詹艳玲, 张倩等(2012). 黄梁木组培快繁技术研究. 华南农业大学学报, 33: 216–224]

Emrich SJ, Barbazuk WB, Li L, et al (2007). Gene discovery and annotation using LCM-454 transcriptome sequencing. Genome Res, 17: 69–73

Fang JJ, Schneiider B (2013). Laser microdissection: a sample preparation technique for plant micrometabolic profiling. Phytochem Anal, 25: 307–313

Florez Rueda AM, Grossniklaus U, Schmidt A (2016). Laser-assisted microdissection (LAM) as a tool for transcriptional profiling of individual cell types. J Vis Exp, 111: 1–10

Hölscher D, Shroff R, Knop K, et al (2009). Matrix-free UV-laser desorption/ ionization (LDI) mass spectrometric imaging at the single-cell level: distribution of secondary metabolites of *Arabidopsis thaliana* and *Hypericum* species. Plant J, 60: 907–918

Inada N, Wildermuth MC (2005). Novel tissue preparation method and cell-specific marker for laser microdissection of *Arabidopsis* mature leaf. Planta, 211: 9–16

Kerk NM, Ceserani T, Tausta SL, et al (2003). Laser capture microdissection of cells from plant tissues. Plant Physiol 132: 27–35

Klerk GJ, Krieken W, Jong JC (1999). Review the formation of adventitious roots: new concepts, new possibilities. In Vitro Cell Dev Biol, 35: 189–99

Lin Y, Zhang W, Qi F, et al (2014). Hydrogen-rich water regulates cucumber adventitious root development in a heme oxygenase-1/carbon monoxide-dependent manner. J Plant Physiol, 171: 1–8

Ohtsu K, Smith MB, Emrich SJ, et al (2007). Global gene expression analysis of the shoot apical meristem of maize (*Zea mays* L.). Plant J, 52: 391–404

Ohyama H, Zhang X, Kohno Y, et al (2000). Laser capture microdissection-generated target sample for high-density oligonucleotide array hybridization. Biotechniques, 29: 530–536

Polster J, Dithmar H, Burgemeister R, et al (2006). Flavonoids in plant nuclei: detection by laser microdissection and pressure catapulting (LMPC), in vivo staining, and UV-visible spectroscopic titration. Physiol Plantarum, 128: 163–174

Que QM, Li P, Ouyang KX, et al (2017). Genetic variation of young forest growth traits of *Neolamarckia cadamba.* Subtropics Plant Sci, 46: 248–253 (in Chinese with English abstract) [阙青敏, 李培, 欧阳昆唏等(2017). 幼苗期黄梁木生长形状的种源间变异. 亚热带植物科学, 46: 248–253]

Schroeder A, Mueller O, Stocker S, et al (2006). The RIN: an RNA integrity number for assigning integrity values to RNA measurements. BMC Mol Biol, 7: 3–8

Shibutani M, Uneyama C, Miyazaki K, et al (2000). Methacarn fixation: a novel tool for analysis of gene expressions in paraffin-embedded tissue specimens. Lab Invest, 80: 199–208

Simone NL, Bonner RF, Gillespie JW, et al (1998). Laser-capture microdissection: opening the microscopic frontier to molecular analysis. Trends Genet, 14: 272–276

Spencer MW, Casson SA, Ondsey K (2007). Transcriptional profiling of the *Arabidopsis* embryo. Plant physiol, 143: 924–940

Su JM, Perlaky L, Li XN, et al (2004). Comparison of ethanol versus formalin fixation on preservation of histology and RNA in laser capture microdissected brain tissues. Brain Pathol, 14: 175–182

Takacs EM, Li J, Du C, et al (2012). Ontogeny of the maize shoot apical meristem. Plant Cell, 24: 3219–3234

Takahashi H, Kamakura H, Sato Y, et al (2010). A method for obtaining high quality RNA from paraffin section of plant tissues by laser microdissection. J Plant Res, 123: 807–813

Wang R, Wang ZH, Mao YF, et al (2018). Variance analysis of endogenous hormones in self-rooted rootstock cutting f apple with different adventitious root gravitropic setpoint angles. Plant Physiol J, 54: 483–490 (in Chinese with English abstract) [王荣, 王增辉, 毛云飞等(2018). 不定根向重力性定点角不同的苹果自根砧插穗内源激素差异分析. 植物生理学报, 54: 483–490]

Wang YQ, Yao Y, Chen BL, et al (2013). Effects of different fixing methods on isolation of ovules in female gametophyte of *Pinus tabulaeformis* Carr. by laser capture microdissection. Plant Physiol J, 49: 195–199 (in Chinese with English abstract) [王英旗, 姚阳, 陈彬丽等(2013). 不同的固定方法对激光显微切割分离油松胚珠雌配子体的影响. 植物生理学报, 49: 195–199]

Zhang X, Douglas RN, Strable J, et al (2012). Punctate vascular expression is a novel maize gene required for leaf pattern formation that functions downstream of the trans-acting small interfering RNA pathway. Plant Physiol, 159: 1453–1462

Establishment of adventitious root primordia cells capture system by laser microdissection in *Neolamarckia cadamba*

DONG Tian-Tian[#], WANG Xue[#], LIU Si-Wen, ZHANG Li-Ding, LONG Jian-Mei[*], PENG Chang-Cao[*]

College of Forestry and Landscape Architecture, South China Agricultural University, Guangzhou 510642, China

Abstract: In order to explore the key genes involved in the root primordia initiation of *Neolamarckia cadamba*, gene expression profile of root primordia initiation cells will be a prerequisite. Laser microdissection (LMD) is a common method which allows for location and isolation of specific tissues or cells from heterogeneous tissues. In this study, comparisons of the effect on RNA quality from samples with different treatment during paraffin sections were conducted, including fixing, dehydration, penetrant, slice thickness, floating medium. In addition, the parameters of LMD were optimized for root primordia cells. Accordingly, adventitious root primordia cells capture system by LMD was established. The RNA from adventitious root primordia cells by LMD could be used for construction of cDNA library for RNA-seq. Taken together, our study provide the basis for the rapid acquisition of adventitious root primordia cells, which thus facilitate our research towards the molecular mechanism of adventitious root primordia initiation and formation in *N. cadamba*.

Key words: *Neolamarckia cadamba*; adventitious root primordia; laser microdissection; paraff in section; RNA integrigy number

Received 2018-09-03 Accepted 2019-04-25

This work was supported by the National Key Research and Development Program of China (2016YFD0600104), the National Natural Science Foundation of China (31470681), the Natural Science Foundation of Guangdong Province (2016A030311032), the Science and Technology Project of Guangzhou (201607020024), the Talents Program of Guangdong Education Department (2017KQNCX017), and the Forestry Science and Technology Innovation of Guangdong Province (2016KJCX003).

#Co-first authors.

*Co-corresponding authors: Long JM (longjianmei@scau.edu.cn), Peng CC (ccpeng@scau.edu.cn).

中文核心期刊·中国科技核心期刊·CSCD核心期刊

ISSN 2095-1108
CN 31-2055/Q

植物生理学报

Plant Physiology Journal

2019 年第 55 卷第 5 期
Vol. 55, No.5, 2019

中国植物生理与植物分子生物学学会
中国科学院上海生命科学研究院植物生理生态研究所 主办
Sponsored by Chinese Society for Plant Biology
and Institute of Plant Physiology and Ecology, SIBS, CAS

科学出版社 Science Press 出版

植物生理学报
第五十五卷 第五期 二〇一九年五月
科学出版社

植 物 生 理 学 报

ZHIWU SHENGLI XUEBAO

(原刊名《植物生理学通讯》, 1951年创刊)

第55卷 第5期(总第375期) 2019年5月

目 次

封面图片: 由第642~648页陈志伟等的论文《不同低氮胁迫对大麦地方品种苗期耐低氮性的影响》提供

PLANT PHYSIOLOGY JOURNAL

Vol. 55 No. 5 May 2019

(Formerly PLANT PHYSIOLOGY COMMUNICATIONS, Publication Started in 1951)

CONTENTS

第11届《植物生理学报》编辑委员会名单

植物生理学报(原刊名《植物生理学通讯》)(月刊, **1951**年创刊)　　第**55**卷　第**5**期　　**2019**年**5**月**20**日出版

编 辑 部　地址: 上海市岳阳路319号31B楼, 邮政编码: 200031
电话/传真: 021-54922836
电子邮箱: zstx@sibs.ac.cn
网址: http://www.plant-physiology.com

主　　编　何祖华

主　　管　中国科学技术协会

主　　办　中国植物生理与植物分子生物学学会
上海市岳阳路319号31A楼, 邮政编码: 200031
中国科学院上海生命科学研究院植物生理生态研究所
上海市枫林路300号, 邮政编码: 200032

出　　版　科 学 出 版 社
北京市东黄城根北街16号, 邮政编码: 100717

印　　刷　上海盛通时代印刷有限公司
上海市金山区广业路568号, 邮政编码: 201506

发行范围　公开

国内发行　上海市邮政局报刊发行局

订　　阅　全国各地邮政局

国外发行　中国国际图书贸易总公司
北京市399信箱, 邮政编码: 100044

广告经营许可证号　3100420080068

ISSN 2095-1108
CN 31-2055/Q

国内邮发代号: 4-267
国外发行代号: M-1364
定价: 120.00元

ISSN 2095-1108

购书可扫描上方二维码

基因组学与应用生物学, 2022 年, 第 41 卷, 第 8 期, 第 1754-1766 页

研究报告
Research Report

黄梁木 *WOX* 基因家族的鉴定与表达分析

王明俊[1,2] 许佐威[1,2] 刘宇彤[1,2] 王莹[1,2] 朱裕灵[1,2] 杨姝琦[1,2] 龙健梅[1,2*] 彭昌操[1,2*]
1 华南农业大学林学与风景园林学院, 广州, 510642; 2 广东省森林植物种质创新与利用重点实验室, 广州, 510642
* 共同通信作者, longjianmei@scau.edu.cn; ccpeng@scau.edu.cn

摘 要 WOX (WUSCHEL-related homebox)转录因子在调节植物生长发育和响应非生物胁迫中起着重要作用。为揭示华南地区重要速生树种黄梁木(*Neolamarckia cadamba*) *WOX* 基因家族的功能, 本研究利用生物信息学方法对黄梁木 *WOX* 基因进行全基因组鉴定, 并对其理化性质、蛋白质结构、染色体定位、系统进化、基因表达模式以及启动子顺式元件进行分析。结果表明: 黄梁木中共有 19 个 *WOX* 基因, 分布在 14 条染色体上; NcWOX 家族成员分为 WUS 进化支、中间进化支和古代进化支, 均具有高度保守的同源结构域。基因表达模式分析表明, *NcWOX4. 1*、*NcWOX4. 2*、*NcWOX13. 1* 以及 *NcWOX13. 2* 在茎的维管组织中表达量较高, 其中 *NcWOX4. 1*、*NcWOX4. 2* 在初生生长向次生生长转换期的形成层表达量最高, 推测 *NcWOX4. 1*、*NcWOX4. 2*、*NcWOX13. 1* 和 *NcWOX13. 2* 参与黄梁木维管发育。启动子顺式作用元件分析表明, *NcWOX* 基因家族成员的启动子具有丰富的光应答、激素应答以及逆境反应元件。本研究为深入研究 *NcWOX* 基因在黄梁木生长发育及逆境响应中的作用奠定了重要基础。

关键词 黄梁木; *WOX* 基因家族; 生物信息学分析; 表达模式

Identification and Expression Analysis of *WOX* Gene Family in *Neolamarckia cadamba*

Wang Mingjun[1,2] Xu Zuowei[1,2] Liu Yutong[1,2] Wang Ying[1,2] Zhu Yuling[1,2] Yang Shuqi[1,2] Long Jianmei[1,2*] Peng Changcao[1,2*]
1 College of Forestry and Landscape Architecture, South China Agricultural University, Guangzhou, 510642; 2 Guangdong Key Laboratory for Innovative Development and Utilization of Forest Plant Germplasm, Guangzhou, 510642
* Co-corresponding authors, longjianmei@scau.edu.cn; ccpeng@scau.edu.cn
DOI: 10. 13417/j.gab.041.001754

Abstract WOX (WUSCHEL-related homebox), an unique type of transcription factors in plant, plays significant roles in regulating plant growth and development and the response to abiotic stress. *Neolamarckia cadamba* is an important fast-growing tree species in South China with high economic value. In order to characterize the functions of *WOX* in *N. cadamba*, genome-wide analysis of *WOX* gene family was conducted in this study using bioinformatic method. The results showed that a total of 19 *NcWOX* genes was identified and their protein-related information, gene structure, chromosome distribution, phylogenetic relationship and gene expression patterns were subsequently analyzed. The *NcWOX* genes were distributed across 14 chromosomes, and their proteins were divided into three groups by phylogenetic tree, including WUS clade, intermediate clade and ancient clade. Multiple sequence analysis of the *NcWOX* gene family reveals a highly conserved homeodomain. Expression profile analysis shows that *NcWOX4. 1*、*NcWOX4. 2*、*NcWOX13. 1* and *NcWOX13. 2* have high ex-

基金项目: 本研究由广东省林业科技创新重点项目(2019KJCX001)、国家自然科学基金项目(31800560)和广州市科技计划项目(201607020024)共同资助
引用格式: Wang M.J., Xu Z.W., Liu Y.T., Wang Y.,Zhu Y.L., Yang S.Q., Long J.M., and Peng C.C., 2022, Identification and expression analysis of *WOX* gene family in *Neolamarckia cadamba*, Genomics and Applied Biology, 41(8): 1754-1766. (王明俊, 许佐威, 刘宇彤, 王莹, 朱裕灵, 杨姝琦, 龙健梅, 彭昌操, 2022, 黄梁木 *WOX* 基因家族的鉴定与表达分析, 基因组学与应用生物学,41(8): 1754-1766.)

pression levels in vascular. Particularly, *NcWOX4. 1*、*NcWOX4. 2* exhibited the highest expression levels in TCA (transition phase of cambium). These results indicated that *NcWOX4. 1*、*NcWOX4. 2*、*NcWOX13. 1* and *NcWOX13. 2* might be involved in vascular development in *N. cadamba*. Analysis of the promoter elements of the *NcWOXs* showed that there were rich ele-ments in response to light, hormone and stress. Collectively, identification and preliminarily analysis of *WOX* gene family members in *N. cadamba* has been conducted in present study, which lay a theoretical basis for the further functional investigation of *NcWOX* genes in *N. cadamba*.
Keywords *Neolamarckia cadamba*; *WOX* gene family; Bioinformatics analysis; Expression pattern

WOX (WUSCHEL-related homebox)基因家族是植物中独特的转录因子家族，属于同源域（Homeodomain）超家族的一个亚分支，其成员均具有 60~66 个氨基酸残基的 DNA 结合同源域（Kamiya et al., 2003; Park et al., 2005）。通过对不同植物 *WOX* 基因的系统发育分析，发现 *WOX* 基因家族可以被分为 3 个分支，即古代进化支、中间进化支和 WUS 进化支（Yang et al., 2017; Zhou et al., 2018）。低等植物（绿藻、苔藓等）的 *WOX* 基因仅属于古代进化支，而高等植物的 *WOX* 基因则存在于 3 个进化支中（van der Graaff et al., 2009）。

已有研究表明，WOX 转录因子在调节植物生长发育中起着重要作用，包括胚胎发育、胚胎极化、分生干细胞的维持、侧向器官的发育、种子形成和离体组织器官的再生等（Jha et al.,2020; Tvorogova et al., 2021）。模式植物拟南芥（*Arabidopsis thaliana*）中有 15 个 *WOX* 基因，其中 *AtWUS* 在胚珠、花药和茎尖分生组织中表达，已被证明在分生组织维持中起着关键作用（Laux et al., 1996）。*AtWOX1* 在子叶和新生叶片的初生维管组织中高表达，过量表达导致叶片小、植株矮化和生育力降低（Vandenbussche et al., 2009; Zhang et al., 2011）。*AtWOX2* 和 *AtWOX8* 在早期胚胎发育中起着关键作用（Haecker et al., 2004; Ueda et al., 2011）。*AtWOX3* 是托叶、花中侧萼片和雄蕊发育所必需的（Matsumoto and Okada., 2001; Shimizu et al., 2009）。位于受体激酶（phloem intercalated with xylem, PXY）调控下游通路的 *AtWOX4* 是调控拟南芥原形成层/形成层干细胞增殖的重要调控因子（Ji et al., 2010; Etchells et al., 2013）。杨树（*Populus przewalskii*）*PtrWOX4* 还被发现参与维管的次生生长，对维管发育有着重要的影响（Kucukoglu et al., 2017）。*AtWOX5* 受生长素诱导，在根尖分生组织中发挥重要作用（Gonzali et al., 2005）。*AtWOX6* 参与调节胚珠发育并影响胚珠模式（Park et al., 2005）。在侧根中表达的 *AtWOX7* 被证实以糖依赖的方式抑制侧根的发育（Kong et al., 2016）。*AtWOX9* 整合发育信号和调节细胞周期，以维持细胞分裂并调节根部的分化（Wu et al., 2005）。*AtWOX11* 以及其同源基因 *AtWOX12* 参与调控根器官的发生（Liu et al., 2014a）。*AtWOX13* 促进胚座框的形成以及调控果实的发育（Romera-Branchat et al., 2013）。*AtWOX14* 在调控维管细胞分裂中与 *AtWOX4* 发挥冗余作用，在干细胞形成中发挥关键作用（Etchells et al., 2013）。此外，还有报道 *AtWOX14* 与促进赤霉素的合成以及花序茎中的维管细胞分化和木质化有关（Denis et al., 2017）。目前，关于 *WOX* 家族基因功能研究在木本植物黄梁木（*Neolamarckia cadamba*）中尚未报道。

此外，已有研究表明多个物种中 WOX 转录因子参与非生物胁迫的响应。如拟南芥 *AtWOX6* 参与调节冷胁迫耐受性（Zhu et al., 2004）；杨树 *PagWOX11* 和 *PagWOX12a* 参与盐胁迫抗性反应，以及通过参与诱导根生物量的增加从而提高干旱胁迫的耐受性（Wang et al., 2019; Liu et al., 2021; Wang et al., 2021）；棉花（*Gossypium hirsutum*）*GhWOX4* 和 *GhWOX13* 在盐胁迫下于叶片中上调表达，*GhWOX13* 在 PEG6000 处理后于叶片中上调表达（Yang et al., 2017）；多个水稻（*Oryza sativa* L.）*OsWOX* 基因如 *OsWUS*、*OsWOX3*、*OsWOX4*、*OsWOX5*、*OsWOX9*、*OsWOX11* 和 *OsWOX12* 分别在盐、干旱以及低温胁迫后不同程度地上调表达（Cheng et al., 2014）；水稻 *OsWOX13* 具有增强干旱耐受性同时促进早花的作用（Minh-Thu et al., 2018）；小麦（*Triticum aestivum*）*TaWOX3* 和 *TaWOX8* 在干旱胁迫下上调表达，*TaWOX3*、*TaWOX6*、*TaWOX8*、*TaWOX10* 和 *TaWOX12* 在盐胁迫下上调表达（Rathour et al., 2020）等。

黄梁木属于茜草科（Rubiaceae）团花属（*Neolamarckia*）的常绿阔叶乔木，是南方地区重要的速生树种，其树皮富含单宁、类固醇、生物碱、团花酸、奎诺酸和卡丹宾等活性物质（Pandey and Nige, 2016），树叶中含有生物碱类、黄酮类、类固醇和糖苷等（李晓琳等, 2019），药用价值高。本研究通过全基因组鉴定了黄梁木 19 个 *NcWOX* 基因，并开展了进化关系分析、编码蛋白的结构特征和理化性质分析以及基因表

达模式分析，为深入研究 *NcWOX* 基因的功能及其对林木生长发育和抗逆的影响奠定理论基础。

1　结果

1.1　黄梁木 *WOX* 基因家族鉴定与进化关系分析

基于黄梁木全基因组测序数据（Zhao et al.，2022），结合 BlastP 和保守结构域鉴定的结果，初步得到黄梁木 WOX 蛋白序列，并使用在线网站 Pfam 分析其蛋白结构域，排除不含保守结构域的序列，最后鉴定出 19 个 *NcWOX* 基因。使用 MEGA11.0 软件中的近邻相接法（Neighbor joining method，NJ）对 15 个拟南芥 AtWOX、18 个毛果杨（*Populus trichocarpa*）PtrWOX 以及 19 个 NcWOX 进行系统发育树分析。结果显示，与拟南芥类似，NcWOX 家族也分为 3 个分支（图 1）。NcWOX 家族按照与拟南芥同源的基因命名，Ⅰ组的 WUS 进化支包括 NcWOX1.1～NcWOX1.4、NcWOX2.1、NcWOX2.2、NcWOX3.1、NcWOX3.2、NcWOX4.1、NcWOX4.2、NcWOX5、NcWUS1.1 以及 NcWUS1.2，Ⅱ组中间进化支包括 NcWOX8、NcWOX9 和 NcWOX11，Ⅲ组古代进化支包括 NcWOX13.1～NcWOX13.3，其中黄梁木和毛果杨很多 *WOX* 基因均出现 2 个或以上的拟南芥同源基因，如 *WOX1*～*WOX4* 以及 *WOX13*。

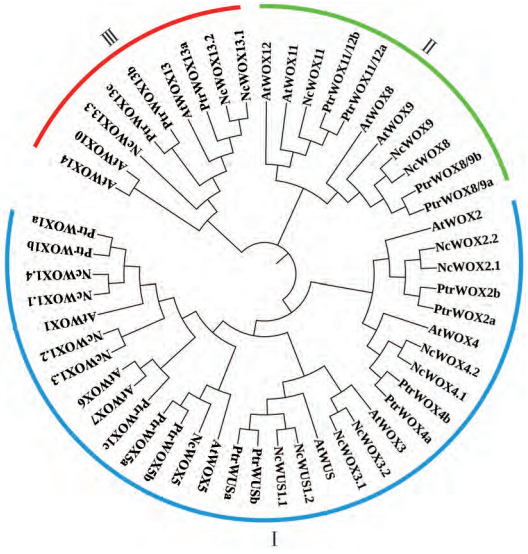

图 1　黄梁木 WOX 家族蛋白系统进化分析

注：At：拟南芥；Nc：黄梁木；Ptr：毛果杨；Ⅰ：WUS 进化支；Ⅱ：中间进化支；Ⅲ：古代进化支

Figure 1　Phylogenetic tree of WOX family proteins in *Neolamarckia cadamba*

Note：At：*Arabidopsis thaliana*；Nc：*Neolamarckia cadamba*；Ptr：*Populus trichocarpa*；Ⅰ：WUS clade；Ⅱ：Intermediate clade；Ⅲ：Ancient clade

1.2　黄梁木 *WOX* 共线性分析

黄梁木基因组的共线性分析结果表明（图 2A），黄梁木 *WOX* 基因家族成员中没有串联复制的基因对，有 8 个基因对来源于片段复制事件，说明片段复制事件在黄梁木 *WOX* 基因家族的扩张中起着重要作用。为了进一步阐明 *WOX* 基因在拟南芥和黄梁木间的进化关系，我们对拟南芥和黄梁木的基因组进行了共线性分析，结果表明，5 个拟南芥染色体与 22 个黄梁木染色体存在大量共线性区块，且每个拟南芥染色体均与多个不同的黄梁木染色体存在共线性区块（图 2B）。黄梁木与拟南芥共线性 *WOX* 基因为 15 对，其中有 6 个拟南芥 *WOX* 基因分别对应两个不同的黄梁木 *WOX* 基因，以上结果说明所鉴定的黄梁木 *WOX* 基因与拟南芥 *WOX* 基因

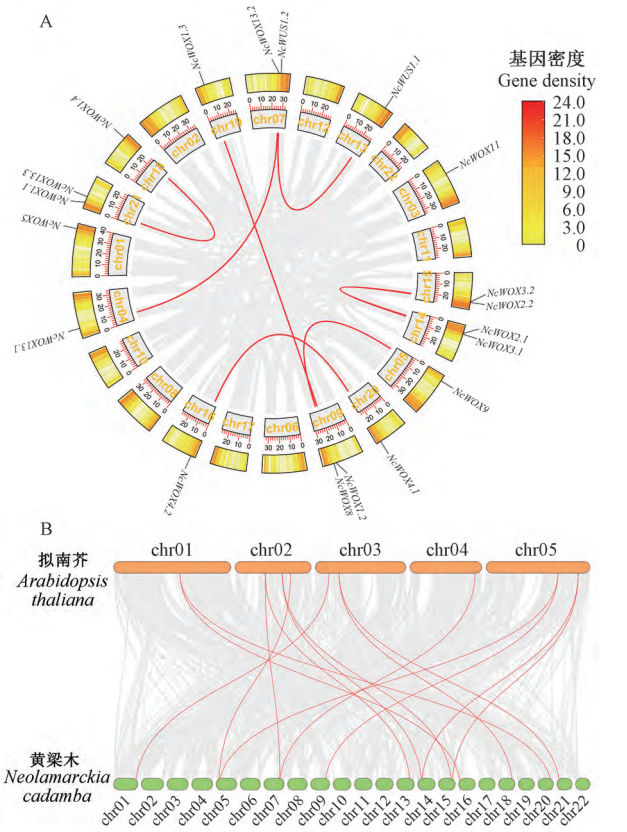

图 2　黄梁木 *NcWOX* 基因的共线性分析

注：A：黄梁木基因组内共线性分析；B：拟南芥与黄梁木基因组间共线性分析；灰色线条代表黄梁木/两个物种间的共线性基因对，红色线条代表 *WOX* 基因的共线性基因对

Figure 2　Collinearity analysis of *NcWOXs* in *Neolamarckia cadamba*

Note：A：Collinearity analysis within *Neolamarckia cadamba* genomes；B：Collinearity analysis between *Arabidopsis thaliana* and *Neolamarckia cadamba* genomes；The gray line represents all gene pairs that have collinearity within *Neolamarckia cadamba* or between the two species，and the red highlight line represents *WOX* collinearity gene pairs

直系同源，在进化的过程中黄梁木可能发生了基因组复制以及染色体节段重复事件。

1.3 黄梁木 WOX 蛋白性质分析

NcWOX 蛋白序列理化性质的分析结果显示（表 1），NcWOX 蛋白序列长度在 165～396 aa，分子量范围为 18.85～43.27 kDa，等电点范围为 5.56～9.46。其中，蛋白等电点小于 7 的酸性蛋白包括 7 个 NcWOX 蛋白（NcWOX1.1、NcWOX1.4、NcWOX8、NcWOX11、NcWOX13.1、NcWOX13.2 和 NcWUS1.1），蛋白等电点大于 7 的碱性蛋白包括 12 个 NcWOX 蛋白（NcWOX1.2、NcWOX1.3、NcWOX2.1、NcWOX2.2、NcWOX3.1、NcWOX3.2、NcWOX4.1、NcWOX4.2、NcWOX5、NcWOX9、NcWOX13.3 和 NcWUS1.2）。NcWOX 蛋白的不稳定指数均较高，范围为 42.71～75.22。NcWOX 蛋白的脂肪系数在 52.20～69.49，其中 NcWOX9 的脂肪系数最高，蛋白最稳定。NcWOX 蛋白的总平均疏水指数在−1.042～−0.417，均为负值，属于亲水性蛋白。

NcWOX 蛋白二级结构的分析结果显示（表 2），NcWOX 蛋白均有 α-螺旋、β-转角、延伸链和无规则卷曲，其中 NcWOX 蛋白均以 α-螺旋和无规则卷曲为主，除 NcWOX8 和 NcWOX11 外，NcWOX 二级结构组成占比均为无规则卷曲>α-螺旋>延伸链>β-转角。NcWOX 家族成员的亚细胞定位预测显示，19 个 NcWOX 均定位于细胞核，符合转录因子的亚细胞定位特性。

1.4 黄梁木 *WOX* 基因家族染色体定位分析

基于黄梁木基因组数据，对 19 个 *NcWOX* 基因进行染色体定位。结果显示（图 3），19 个 *NcWOX* 基因映射到 14 条染色体上。黄梁木染色体 chr07、chr09、chr14、chr15 和 chr21 各有 2 个 *NcWOX* 基因，而其他染色体只有 1 个。

1.5 黄梁木 *WOX* 基因家族保守结构域、保守基序与基因结构分析

使用 DNANAN 和 MEME 软件对 19 个 NcWOX 蛋白的结构域和保守基序进行分析。结果显示（图 4；图 5），NcWOX 蛋白序列均包含 1 个高度保守的“螺旋-环-螺旋-转角-螺旋”同源结构域（图 4A）。WUS-box 基序（TLXLTP）仅存在于组Ⅰ的 WUS 进化支（图 4B）。在 NcWOX 蛋白保守基序分析中（图 5A），基序 1 和基序 2 为同源结构域，存在于所有的 NcWOX 蛋白中；基序 3 为 WUS-box 基序（TLXLTP），存在于组Ⅰ所有 NcWOX 蛋白中。*NcWOX* 基因家族结构分析结果（图 5B）表明，在该基因家族中外显子和内含子结构存在差异，但亲缘关系较近的基因中含有相似的外显子-内含子结构。所有基因的内含子相位为 0 和 1，没有相位为 2 的内含子，其中 *NcWOX13.3* 不具有内含子。

表 1 黄梁木 WOX 蛋白理化性质

Table 1 Information of WOX proteins in *Neolamarckia cadamba*

蛋白名称 Protein name	基因号 Gene ID	氨基酸数目（aa） No. of amino acids (aa)	分子量（kDa） Molecular mass (kDa)	等电点 Isoelectric point	不稳定指数 Instability index	脂肪族氨基酸指数 Aliphatic index	总平均疏水指数 Grand average of hydrophobicity
NcWOX1.1	evm.model.Contig21.449	358	40.44	6.08	58.29	56.48	−0.879
NcWOX1.2	evm.model.Contig230.3	286	32.44	8.13	59.70	52.20	−0.973
NcWOX1.3	evm.model.Contig371.72	338	38.72	9.14	58.45	66.36	−0.763
NcWOX1.4	evm.model.Contig45.151	357	40.65	6.24	64.83	58.77	−0.901
NcWOX2.1	evm.model.Contig207.274	259	29.46	8.96	75.22	62.55	−0.714
NcWOX2.2	evm.model.Contig583.204	261	29.81	9.10	63.17	60.96	−0.679
NcWOX3.1	evm.model.Contig207.192	224	25.66	9.05	61.67	54.87	−0.877
NcWOX3.2	evm.model.Contig583.143	220	25.47	9.28	42.71	54.59	−0.836
NcWOX4.1	evm.model.Contig12.525	221	25.48	9.46	49.51	56.06	−1.042
NcWOX4.2	evm.model.Contig555.419	232	26.73	9.28	48.80	53.92	−1.000
NcWOX5	evm.model.Contig96.218	165	18.85	9.12	63.63	66.18	−0.716
NcWOX8	evm.model.Contig481.32	396	43.27	6.86	55.97	67.47	−0.484
NcWOX9	evm.model.Contig565.25	393	43.11	8.29	48.09	69.49	−0.487
NcWOX11	evm.model.Contig28.288	259	28.68	5.81	74.23	69.27	−0.417
NcWOX13.1	evm.model.Contig483.17	269	30.07	5.70	54.44	60.22	−0.800
NcWOX13.2	evm.model.Contig45.634	274	30.66	5.56	60.06	61.97	−0.815
NcWOX13.3	evm.model.Contig16.50	252	28.66	7.10	59.72	62.70	−0.862
NcWUS1.1	evm.model.Contig45.514	274	30.85	6.00	57.61	53.07	−0.883
NcWUS1.2	evm.model.Contig394.345	286	32.44	8.13	59.70	52.20	−0.973

表 2　黄梁木 WOX 蛋白二级结构预测

Table 2　Prediction of secondary structure of WOX proteins in *Neolamarckia cadamba*

蛋白名称 Protein name	α-螺旋(%) Alpha-helix(%)	β-转角(%) Beta-turn(%)	延伸链(%) Extended strand (%)	无规则卷曲(%) Random coil (%)
NcWOX1. 1	27. 93	2. 51	11. 17	58. 38
NcWOX1. 2	29. 50	2. 36	10. 91	57. 23
NcWOX1. 3	25. 15	2. 07	10. 36	62. 43
NcWOX1. 4	26. 61	2. 80	11. 20	59. 38
NcWOX2. 1	16. 99	3. 09	6. 59	72. 97
NcWOX2. 2	14. 94	3. 83	11. 88	69. 35
NcWOX3. 1	26. 79	3. 12	8. 04	62. 05
NcWOX3. 2	26. 36	3. 64	13. 18	56. 82
NcWOX4. 1	28. 51	4. 07	8. 14	59. 28
NcWOX4. 2	28. 88	4. 74	5. 60	60. 78
NcWOX5	36. 97	4. 85	13. 94	44. 24
NcWOX8	13. 13	3. 54	13. 13	70. 20
NcWOX9	13. 49	3. 56	12. 21	70. 74
NCWOX11	15. 06	6. 56	16. 99	61. 39
NCWOX13. 1	30. 48	2. 23	3. 72	63. 57
NcWOX13. 2	36. 13	4. 38	3. 65	55. 84
NcWOX13. 3	37. 70	3. 97	5. 95	52. 38
NcWUS1. 1	18. 61	4. 01	8. 03	69. 34
NcWUS1. 2	21. 33	3. 85	6. 99	67. 83

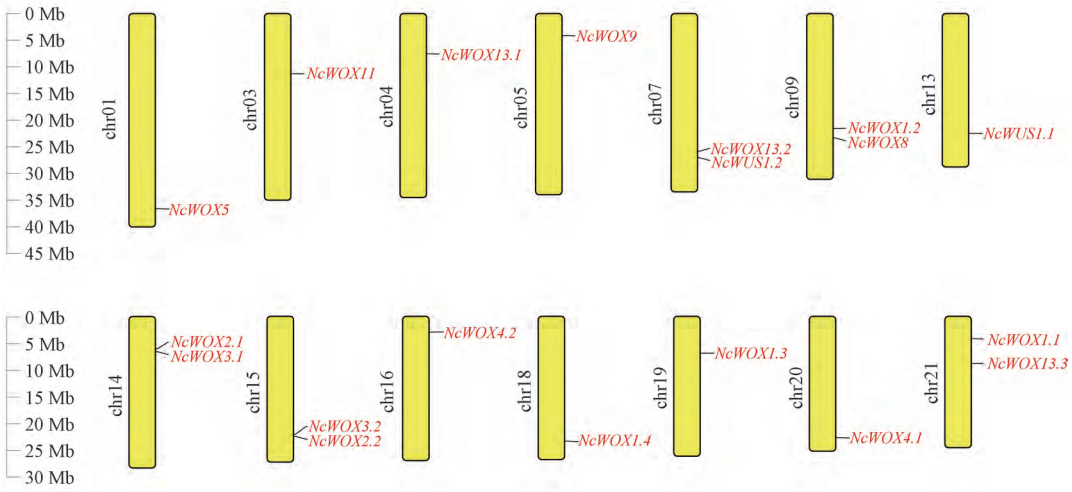

图 3　黄梁木 *NcWOX* 基因染色体定位

Figure 3　Chromosome location of *NcWOXs* in *Neolamarckia cadamba*

1.6　黄梁木 *WOX* 基因家族表达模式分析

为了研究 *NcWOX* 基因家族在黄梁木生长发育中的作用，我们基于黄梁木转录组数据（Zhao et al.，2022）对 19 个 *NcWOX* 基因在黄梁木不同组织部位以及不同维管组织发育时期的表达模式进行分析。结果显示(图 6)，*NcWOX* 基因家族在不同部位都有一定的表达量，其中 *NcWOX4. 1*、*NcWOX4. 2*、*NcWOX13. 1* 和 *NcWOX13. 2* 的表达量最为显著，且在维管组织中的表达量最高。*NcWOX4. 1* 与 *NcWOX4. 2*，*NcWOX13. 1* 与 *NcWOX13. 2* 均为同源基因，其表达模式相似，相似度分别为 79. 9% 和 86. 5%，其中 *NcWOX4. 1* 与 *NcWOX13. 2* 表达量相对较高，因此推测 *NcWOX4. 1* 与 *NcWOX4. 2*，*NcWOX13. 1* 与 *NcWOX13. 2* 可能存在功能冗余，且 *NcWOX4. 1* 与 *NcWOX13. 2* 发挥主要功能。值得注意的是，在维管组织 3 个不同发育时期（初生生长、次生生长和初生生长向次生生长转换期）的茎节中，*NcWOX4. 1* 和 *NcWOX4. 2* 在转换期的形成层(TCA)表达量最高且显著差异表达，表明其可能参与黄梁木初生生长向次生生长发育转换的调控。

为了进一步验证 *NcWOX4* 和 *NcWOX13* 基因的表达模式，对 *NcWOX4* 和 *NcWOX13* 基因进行实时荧

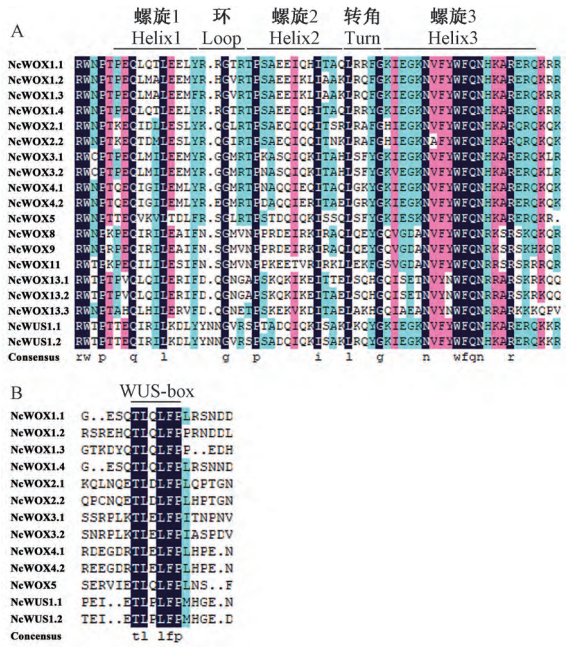

图 4　黄梁木 WOX 蛋白序列保守结构域分析

注：A：黄梁木 WOX 蛋白“螺旋-环-螺旋-转角-螺旋”结构域（HD 结构域）分析；B：黄梁木 WOX 蛋白 WUS-box 基序（TLXLFP）

Figure 4　The conserved domain analysis of NcWOX proteins sequence in *Neolamarckia cadamba*

Note：A：The Helix1-Loop-Helix2-Turn-Helix3 domain (HD domain) analysis of NcWOX proteins in *Neolamarckia cadamba*；B：The WUS-box domain (TLXLFP) of NcWOX proteins in *Neolamarckia cadamba*

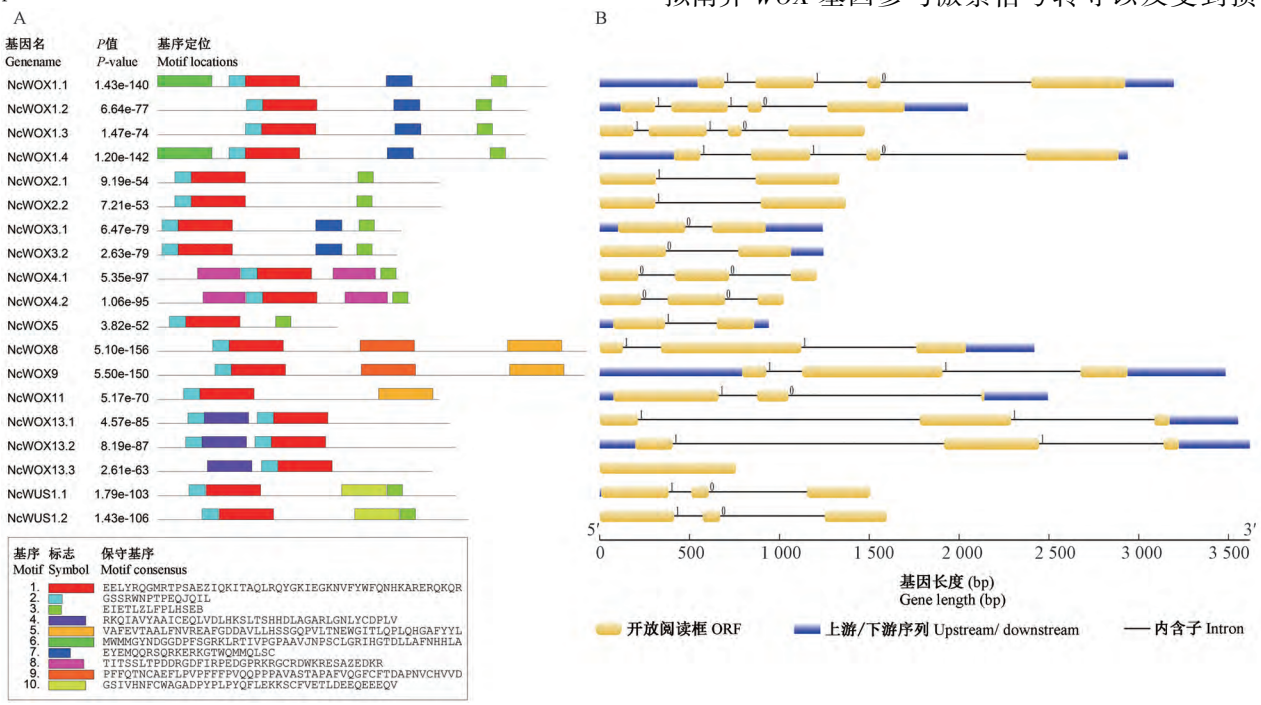

图 5　黄梁木 WOX 家族保守基序及其基因的结构

注：A：黄梁木 WOX 家族保守基序分析；B：黄梁木 WOX 基因结构分析；0、1、2 为内含子相位

Figure 5　The conserved motif of NcWOXs and gene structure of *WOX* gene family in *Neolamarckia cadamba*

Note：A：The conserved motif analysis of NcWOXs in *Neolamarckia cadamba*；B：The gene structure analysis of WOX gene family in *Neolamarckia cadamba*；0，1，2 is intiron phasa

光定量 PCR（RT-qPCR）分析。结果表明，在 8 个不同组织部位中 *NcWOX4. 1*、*NcWOX4. 2* 以及 *NcWOX13. 2* 在韧皮部和形成层均高量表达（图 7A）；在初生生长向次生生长转换的茎节，*NcWOX4. 1* 和 *NcWOX4. 2* 在转换时期形成层（TCA）表达量最高，*NcWOX13. 2* 在转换时期形成层和韧皮部（TCA 和 TPH）表达量较高（图 7B），而 *NcWOX13. 1* 在所有组织部位的表达量都较低，这与转录组的基因表达结果一致，说明转录组测序结果的准确性较高。总之，根据转录组以及荧光定量验证的基因表达结果显示，*NcWOX4. 1*、*NcWOX4. 2* 和 *NcWOX13. 1*、*NcWOX13. 2* 在茎维管组织高量表达，可能和参与黄梁木茎维管组织发育的调控有关。

1. 7　黄梁木 *WOX* 基因启动子序列顺式作用元件分析

基于黄梁木基因组数据，提取 *NcWOX* 基因起始密码子（ATG）上游 2 000 bp 序列并使用 PlantCARE 网站（http://bioinformatics.psb.ugent.be/webtools/plantcare/html/）分析，在 *NcWOX* 基因家族的启动子中发现了大量与逆境、光以及激素响应相关的顺式元件（图 8），其中激素响应元件包括茉莉酸甲酯、生长素、脱落酸、水杨酸以及赤霉素等，逆境响应元件包括防御、损伤以及低温等。已经有研究表明拟南芥 *WOX* 基因参与激素信号转导以及受到损伤

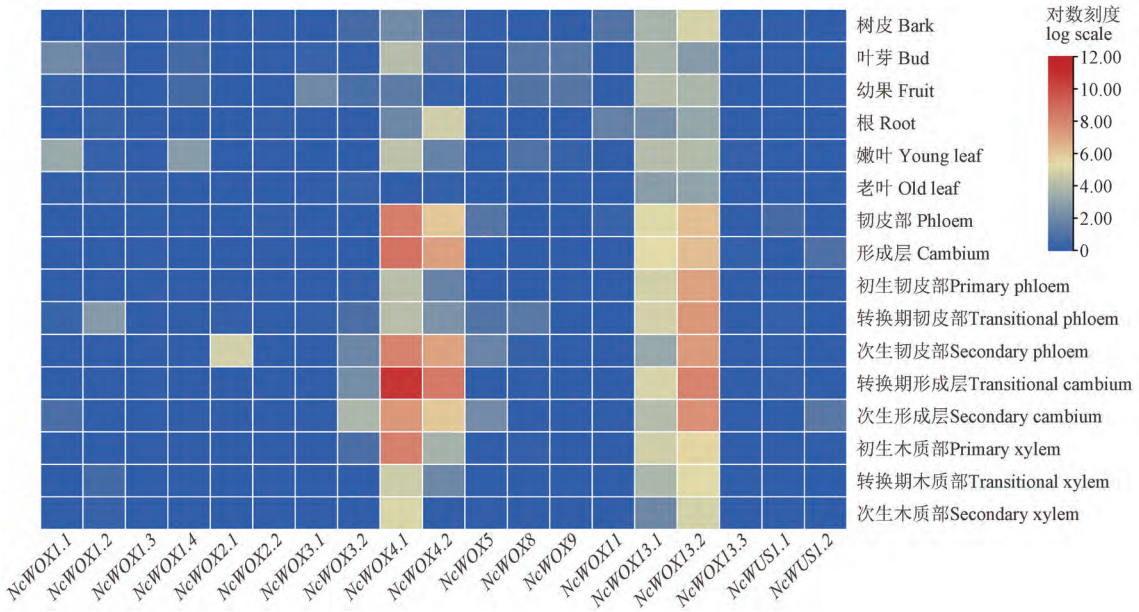

图 6　黄梁木 *NcWOX* 基因组织表达模式

Figure 6　Tissue expression profiles of *NcWOXs* in *Neolamarckia cadamba*

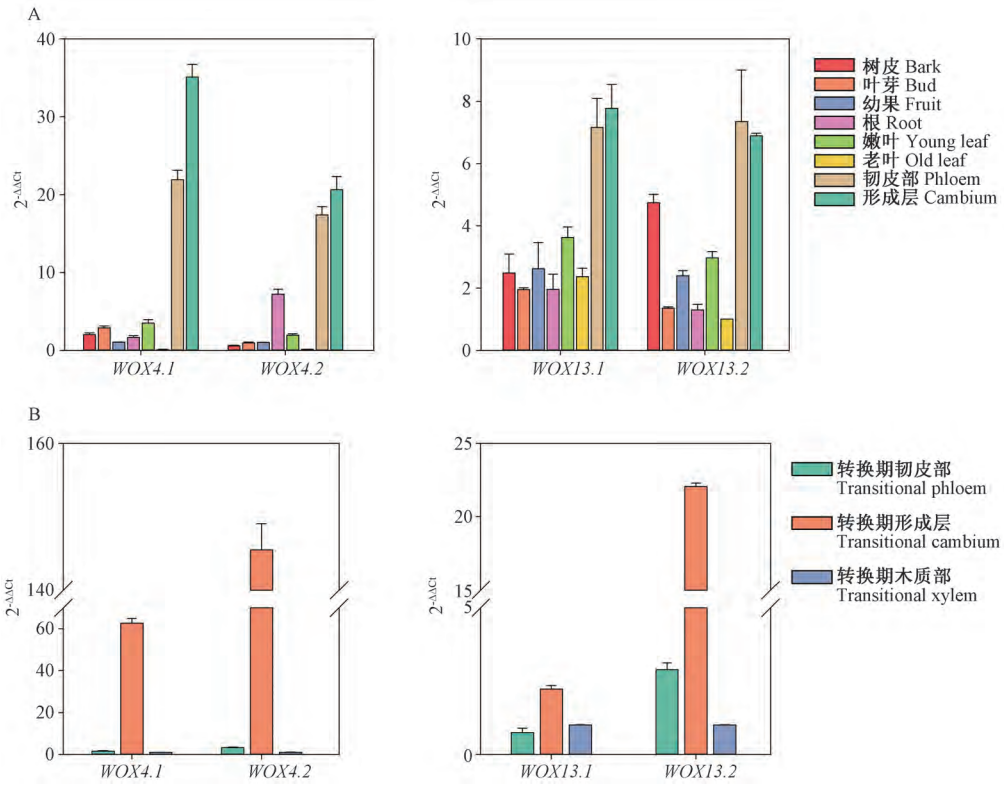

图 7　RT-qPCR 验证不同组织部位中 *NcWOX4* 和 *NcWOX13* 的相对表达量

注：A：*NcWOX*4 和 *NcWOX13* 在 8 个不同组织部位的相对表达量；B：*NcWOX*4 和 *NcWOX13* 在转换期茎节的相对表达量

Figure 7　Analysis of relative expression level of *NcWOX4* 和 *NcWOX13* at different tissues by RT-qPCR

Note：A：The relative expression of *NcWOX*4 和 *NcWOX13* in 8 different tissues；B：The relative expression of *NcWOX*4 和 *NcWOX13* in stem nodes at transition period

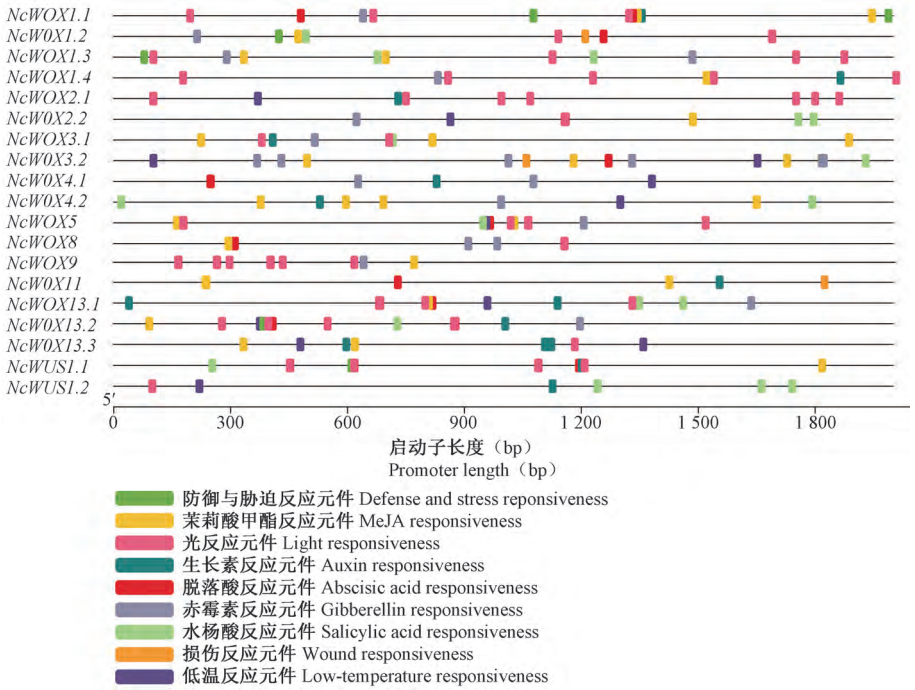

图 8　黄梁木 *NcWOX* 家族基因启动子序列顺式作用元件分析

Figure 8　Analysis of cis-acting elements in promoters sequence of *NcWOXs* family genes in *Neolamarckia cadamba*

诱导，如生长素诱导 *AtWOX4* 表达参与拟南芥的生长发育（Suer et al.，2011）；受伤口诱导表达的 *AtWOX13* 基因对于拟南芥愈伤组织生长和器官重建十分关键（Ikeuchi et al.，2022）。丰富的光应答、激素应答以及逆境反应元件表明，*NcWOX* 基因家族可能参与激素信号转导、昼夜节律调控、对生物和非生物胁迫的响应以及防御信号转导。

2　讨论

随着高通量测序的迅速发展和测序成本的降低，许多物种已完成基因组测序，植物研究进入了基因组学全新时代，为基因家族的鉴定以及基因结构、表达模式和功能分析等相关研究奠定了基础。对于木本植物而言，由于大部分木质生物量取决于维管形成层的活动，因此，研究形成层活动和细胞分化的机制对木质生物量的调控显得尤为关键。然而，尽管目前模式植物拟南芥形成层发育的调控机制已有深入研究，但关于木本植物次生生长和形成层活动的调控机理还有待拓展。在植物中，*WOX* 作为一个重要的基因家族，其编码的蛋白质参与植物生长发育的多个过程（Breuninger et al.，2008；Costanzo et al.，2014；Dolzblasz et al.，2016）。本研究基于黄梁木全基因组以及转录组数据，通过多种生物信息学方法鉴定了 19 个 *NcWOX* 基因，并对 NcWOX 家族的蛋白理化性质、二级结构、亚细胞定位预测、系统发育树、保守基序、保守结构域，以及其基因结构、染色体定位、表达模式以及启动子顺式作用元件等进行全面分析，为后续深入研究 *NcWOXs* 在黄梁木生长发育及逆境响应中的功能奠定基础。

同源结构域（HD）和 WUS-box 结构域是 WOX 家族的两个保守结构域。HD 的功能是将转录因子结合到 DNA 链上，作为转录因子的一个标志特征（Keleher et al.，1989；Hayashi and Scott，1990；Jiang et al.，1991）。目前关于 WUS-box 结构域的研究主要是在 *WUS* 基因上，在 *WUS* 参与维持植物茎分生组织中干细胞特性的过程中，WUS-box 主要发挥抑制活性的作用，并维持干细胞增殖调控的动态平衡。另外，WUS-box 与其他因子的相互作用会将其从抑制因子转变为激活因子。研究表明，WUS-box 对干细胞特性的维持发挥着重要的作用（Ikeda et al.，2009；Dolzblasz et al.，2016）。NcWOX4 属于 WUS 进化支，拥有保守的 WUS-box 结构域，且其在维管形成层中显著表达，因此，NcWOX4 可能参与调控黄梁木茎维管形成层干细胞的发育。

相比于拟南芥，杨树与黄梁木 WOX 家族距离较近，说明木本植物 WOX 序列具有较高的保守性。已有研究表明，杨树 *PtoWOX4* 和 *PtoWOX13* 在形成层和韧皮部以及未成熟的木质部均有相对较高的表

达量（Liu et al., 2014b），本研究中黄梁木 *NcWOX4. 1*、*NcWOX4. 2*、*NcWOX13. 1* 和 *NcWOX13. 2* 在维管组织中表达量较高，说明 *WOX4* 和 *WOX13* 在杨树和黄梁木中的表达模式相似。进一步研究发现杨树 *PtrWOX4a*、*PtrWOX4b* RNAi 植株的形成层宽度明显减小，次生木质部常出现较大的间隙，维管次生生长受到严重的影响，植株无法正常直立生长，但次生韧皮部的生长没有明显下降（Kucukoglu et al., 2017），因此我们推测黄梁木 *NcWOX4* 也可能参与黄梁木维管次生生长过程。系统进化分析表明，*AtWOX14* 是拟南芥 *WOX* 基因家族特有的基因，其促进拟南芥花序茎中维管细胞的分化和木质化，且与 *AtWOX4* 具有功能冗余作用（Etchells et al., 2013; Zhang et al., 2019）。而在黄梁木和杨树中都没有 *AtWOX14* 同源基因，却包含 2 个 *AtWOX4* 同源基因，且 *NcWOX4. 1* 在初生木质部（PX）有明显表达，因此推测 *NcWOX4. 1* 在进化过程中替代了 *WOX14* 的功能，参与促进维管细胞的分化和木质化，且与 *NcWOX4. 2* 存在功能冗余。目前关于木本植物 *WOX13* 基因功能的研究少有报道。在苔藓植物（*Physcomitrella patens*）中，*WOX13* 在干细胞发生过程中的细胞重编程发挥着重要作用（Sakakibara et al., 2014），而 *NcWOX13* 在黄梁木维管组织中高量表达，因此研究 *NcWOX13* 对丰富 *WOX13* 的功能具有重要意义。

植物的维管发育受到植物激素的严格调控，如生长素诱导 *WOX4* 表达参与拟南芥形成层的发育（Suer et al., 2011）；杨树 ARF7（AUXIN RESPONSE FACTOR7）直接与 *WOX4* 的启动子结合并调节其表达，从而整合生长素和赤霉素信号以调节形成层活性（Hu et al., 2022）；据报道，赤霉素（GAs）参与木材的形成，特别是木质部纤维的分化（Digby and Wareing, 1966; Wolbang et al., 2004; Israelsson et al., 2005）。在棉花中，*WOX13* 基因在纤维中特异性表达，且分别受生长素和赤霉素诱导表达，表明 *GhWOX13* 基因可能在植物激素介导的棉花纤维伸长中起重要作用（He et al., 2019）。而 *NcWOX4* 和 *NcWOX13* 基因在茎维管组织高量表达且其启动子上均存在生长素和赤霉素响应元件，表明其可能也通过生长素和赤霉素的介导而参与黄梁木茎维管组织的发育。

拟南芥顺式作用元件 DRE（Dehydration-responsive element）“TACCGACAT”已被发现响应于干旱、低温以及盐胁迫（Yamaguchi-Shinozaki et al., 1994）。杨树 *PagWOX11* 和 *PagWOX12a* 的启动子中也存在脱水反应元件（DRE），其核心序列为“ACCGAGA”。也已证明转录因子 PagERF35 与 *PagWOX11* 和 *PagWOX12a* 启动子的 DRE 元件结合，响应干旱胁迫（Wang et al., 2019）。本研究在黄梁木中发现 *NcWOX1. 1* 的启动子包含“TACCGACAT” DRE 作用元件，*NcWOX1. 4* 的启动子也含有“ACCGAGA”DRE 核心序列，于是我们推测 *NcWOX1. 1* 和 *NcWOX1. 4* 可能与干旱、低温以及盐胁迫响应有关。此外，启动子元件分析亦显示多个 *NcWOX* 基因启动子存在茉莉酸甲酯的响应元件，这说明 *NcWOX* 在植物防御中可能扮演着重要的角色。因此，开展 *NcWOX* 启动子胁迫反应元件的发掘以及相关 *WOX* 的抗逆性功能研究，将成为木本植物抗逆性研究方面一个有趣的话题。目前我们正在利用黄梁木进行激素处理和逆境处理，以检测处理后 *NcWOX* 表达量的变化，并通过 *NcWOX* 的遗传转化和基因编辑等反向遗传学方法来验证其功能，为阐明 NcWOX 在黄梁木次生生长以及激素或逆境响应中的分子机制奠定基础。

3 材料与方法

3.1 *WOX* 基因家族的鉴定与进化关系分析

本课题组前期已经对黄梁木（2011 年种植于华南农业大学）开展全基因组测序，原始测序数据已提交至 NCBI BioProject 数据库，索引号为 PRJNA650253（Zhao et al., 2022）。从 Tair 数据库（https://www.arabidopsis.org/）中获得 15 个拟南芥 WOX 蛋白序列，以拟南芥 WOX 蛋白序列为 query，使用 TBTOOLS 软件（Chen et al., 2020）本地检索 NcWOX 蛋白序列。同时，从 Pfam 数据库网站（http://pfam.xfam.org/）下载 *WOX* 家族的隐马尔科夫模型文件（ID：PF00046），利用 HMMER（V3. 2. 1）软件对 NcWOX 蛋白序列进行基于保守结构域的搜索鉴定。结合 BlastP 和保守结构域鉴定的结果初步筛选出 NcWOX 家族成员，并使用在线网站 Pfam 分析其蛋白结构域，排除不含保守结构域的序列，并根据拟南芥 WOX 蛋白的同源性与进化关系命名。构建进化树所使用的毛果杨 WOX 家族成员索引号参照 Liu 等（2014b）的方法，并从 NCBI 数据库（https://www.ncbi.nlm.nih.gov/）获取相应的蛋白序列。使用 MEGA11. 0 软件的 MUSCLE 方法对 NcWOX、AtWOX 和 PtrWOX 蛋白序列进行比对，使用近邻相接方法构建系统发育树，选择 Complete Deletion 和 P-distance 模式，Bootstrap 设置为 1 000 次。

3.2 染色体共线性分析

基于黄梁木和拟南芥基因组序列文件以及基因结构注释信息文件,其中拟南芥序列文件从网站 phytozome13（https://phytozome-next.jgi.doe.gov/）下载，使用 TBTOOLS 软件的 One Step MCScanX 功能分别进行黄梁木种内、黄梁木与拟南芥种间基因组共线性分析，其中参数 Num of BlastHits 分别设置为 5 和 4，*E*-value 设置为 1e-10。

3.3 WOX 蛋白生物信息学分析

使用在线网站 ExPASy Proteomics（https://web.expasy.org/protparam/）分析 NcWOX 蛋白的理化性质，包括氨基酸数目、分子量、等电点、不稳定指数、脂肪系数以及总平均疏水指数。使用在线网站 SOPMA（https://npsa-prabi.ibcp.fr/cgi-bin/npsa_automat.pl?page=npsa_sopma.html）分析 NcWOX 蛋白二级结构。通过在线网站 Plant-mPLoc（http://www.csbio.sjtu.edu.cn/bioinf/plant-multi/）对 NcWOX 蛋白进行亚细胞定位预测。

3.4 *WOX* 基因家族的染色体定位分析

基于黄梁木基因组 gff 文件，使用 TBTOOLS 软件对 *NcWOX* 基因家族成员进行染色体定位分析。

3.5 WOX 家族保守结构域、保守基序与基因结构分析

使用 DNAMAN 软件对 NcWOX 蛋白序列进行多序列比对，并分析 NcWOX 蛋白所具有的 HD 结构域和 WUS-box 结构域。使用网站分析工具 MEME（http://meme-suite.org/tools/me）分析 NcWOX 蛋白的保守基序，设定保守基序鉴定数为 10 个，命名为基序 1~基序 10，并将分析结果保存为 XML 文件用于后续绘图。基于黄梁木基因组 gff 文件，使用 TBTOOLS 软件分析 *NcWOX* 基因家族的基因结构。

3.6 *WOX* 基因的表达模式分析

本课题组前期已获得黄梁木树皮、叶芽、幼果、根、嫩叶、老叶、韧皮部以及形成层的转录组数据。采用激光显微切割获取 3 个不同发育时期（初生生长、次生生长及初生向次生生长转换时期）的维管细胞（王雪等，2021），每个样品均设置 3 个生物学重复，送测转录组（北京诺禾致源公司测序）。以上原始测序数据已提交至 NCBI BioSample 数据库，索引号为 SAMN15700859（Zhao et al.，2022）。采用 FPKM（expected number of fragments per kilobase of transcript sequence per millions base pairs sequenced）对基因表达水平标准化，并使用 TBTOOLS 软件绘制 *NcWOX* 基因表达热图。荧光定量实验使用的仪器为罗氏 LightCycler480；试剂盒为诺维赞公司的 SYBR qPCR Master Mix；*NcUPL* 作为内参基因（张登等，2018），使用相对定量 $2^{-\Delta\Delta Ct}$ 方法计算基因的表达量。

3.7 *WOX* 基因启动子的顺式作用元件分析

利用黄梁木基因组信息，提取 *NcWOX* 基因起始密码子（ATG）上游 2 000 bp 启动子序列；使用网站分析工具 PlantCARE（http://bioinformatics.psb.ugent.be/webtools/plantcare/html/），预测 *WOX* 基因启动子的顺式作用元件，对预测结果数据进行处理并使用 TBTOOLS 软件进行启动子元件的可视化。

作者贡献

王明俊是本研究的实验设计和实验研究的执行人，完成数据分析、论文初稿的写作；许佐威、杨姝琦、刘宇彤、王莹和朱裕灵参与实验设计和实验结果分析；彭昌操和龙健梅指导实验设计、数据分析和论文写作与修改。全体作者都阅读并同意最终的文本。

参考文献

Breuninger H., Rikirsch E., Hermann M., Ueda M., and Laux T., 2008, Differential expression of *WOX* genes mediates apical-basal axis formation in the *Arabidopsis* embryo, Dev. Cell, 14(6): 867-876.

Chen C.J., Chen H., Zhang Y., Thomas H.R., Frank M.H., He Y.H., and Xia R., 2020, TBtools: an integrative toolkit developed for interactive analyses of big biological data, Mol. Plant, 13(8): 1194-1202.

Cheng S.F., Huang Y.L., Zhu N., and Zhao Y., 2014, The rice *WUSCHEL*-related homeobox genes are involved in reproductive organ development, hormone signaling and abiotic stress response, Gene, 549(2): 266-274.

Costanzo E., Trehin C., and Vandenbussche M., 2014, The role of *WOX* genes in flower development, Ann. Bot., 114(7): 1545-1553.

Denis E., Kbiri N., Mary V., Claisse G., Silva N.C.E., Kreis M., and Deveaux Y., 2017, *WOX14* promotes bioactive gibberellin synthesis and vascular cell diffe-

rentiation in Arabidopsis, Plant J., 90(3): 560-572.

Digby J., and Wareing P.F., 1966, The effect of applied growth hormones on cambial division and the differentiation of the cambial derivatives, Ann. Bot., 30(3): 539-548.

Dolzblasz A., Nardmann J., Clerici E., Causier B., van der Graaff E., Chen J.H., Davies B., Werr W., and Laux T., 2016, Stem cell regulation by *Arabidopsis WOX* genes, Mol. Plant, 9(7): 1028-1039.

Etchells J.P., Provost C.M., Mishra L., and Turner S.R., 2013, *WOX4* and *WOX14* act downstream of the PXY receptor kinase to regulate plant vascular proliferation independently of any role in vascular organisation, Development, 140(10): 2224-2234.

Gonzali S., Novi G., Loreti E., Paolicchi F., Poggi A., Alpi A., and Perata P., 2005, A turanose-insensitive mutant suggests a role for *WOX5* in auxin homeostasis in *Arabidopsis thaliana*, Plant J., 44(4): 633-645.

Haecker A., Gross-Hardt R., Geiges B., Sarkar A., Breuninger H., and Herrmann M., 2004, Expression dynamics of *WOX* genes mark cell fate decisions during early embryonic patterning in *Arabidopsis thaliana*, Development, 131: 657-668.

Hayashi S., and Scott M.P., 1990, What determines the specificity of action of *Drosophila* homeodomain proteins? Cell, 63(5): 883-894.

He P., Zhang Y.Z., Liu H., Yuan Y., Wang C., Yu J.N., and Xiao G.H., 2019, Comprehensive analysis of *WOX* genes uncovers that *WOX13* is involved in phytohormone-mediated fiber development in cotton, BMC Plant Biol., 19(1): 312.

Hu J., Su H.L., Cao H., Wei H.B., Fu X.K., Jiang X.M., Song Q., He X.H., Xu C.Z., and Luo K.M., 2022, AUXIN RESPONSE FACTOR7 integrates gibberellin and auxin signaling *via* interactions between DELLA and AUX/IAA proteins to regulate cambial activity in poplar, Plant Cell, 34(7):2688-2707.

Ikeda M., Mitsuda N., and Ohme-Takagi M., 2009, *Arabidopsis* WUSCHEL is a bifunctional transcription factor that acts as a repressor in stem cell regulation and as an activator in floral patterning, Plant Cell, 21(11): 3493-3505.

Ikeuchi M., Iwase A., Ito T., Tanaka H., Favero D.S., Kawamura A., Sakamoto S., Wakazaki M., Tameshige T., Fujii H., Hashimoto N., Suzuki T., Hotta K., Toyooka K., Mitsuda N., and Sugimoto K., 2022, Wound-inducible *WUSCHEL RELATED HOMEOBOX 13* is required for callus growth and organ reconnection, Plant Physiol., 188(1): 425-441.

Israelsson M., Sundberg B., and Moritz T., 2005, Tissue-specific localization of gibberellins and expression of gibberellin-biosynthetic and signaling genes in wood-forming tissues in aspen, Plant J., 44(3): 494-504.

Jha P., Ochatt S.J., and Kumar V., 2020, WUSCHEL: a master regulator in plant growth signaling, Plant Cell Rep., 39(4): 431-444.

Ji J.B., Strable J., Shimizu R., Koenig D., Sinha N., and Scanlon M.J., 2010, WOX4 promotes procambial development, Plant Physiol., 152(3): 1346-1356.

Jiang J., Hoey T., and Levine M., 1991, Autoregulation of a segmentation gene in *Drosophila*: combinatorial interaction of the even-skipped homeo box protein with a distal enhancer element, Genes Dev., 5(2): 265-277.

Kamiya N., Nagasaki H., Morikami A., Sato Y., and Matsuoka M., 2003, Isolation and characterization of a rice *WUSCHEL*-type homeobox gene that is specifically expressed in the central cells of a quiescent center in the root apical meristem, Plant J., 35(4): 429-441.

Keleher C.A., Passmore S., and Johnson A.D., 1989, Yeast repressor alpha 2 binds to its operator cooperatively with yeast protein Mcm1, Mol. Cell Biol., 9(11): 5228-5230.

Kieffer M., Stern Y., Cook H., Clerici E., Maulbetsch C., Laux T., and Davies B., 2006, Analysis of the transcription factor WUSCHEL and its functional homologue in *Antirrhinum* reveals a potential mechanism for their roles in meristem maintenance, Plant Cell, 18(3): 560-573.

Kong D.Y., Hao Y.L., and Cui H.C., 2016, The WUSCHEL related homeobox protein WOX7 regulates the sugar response of lateral root development in *Arabidopsis thaliana*, Mol. Plant, 9(2): 261-270.

Kucukoglu M., Nilsson J., Zheng B., Chaabouni S., and Nilsson O., 2017, *WUSCHEL-RELATED HOMEOBOX*4 (*WOX*4)-like genes regulate cambial cell division activity and secondary growth in *Populus* trees, New Phytol., 215(2): 642-657.

Laux T., Mayer K.F., Berger J., and Jürgens G., 1996, The *WUSCHEL* gene is required for shoot and floral meristem integrity in *Arabidopsis*, Development., 122(1): 87-96.

Li X.L., Chen T., Xi Q.Y., and Zhang Y.L., 2019, Research progress on antibacterial and anti-inflammatory effects of *Neolamarckia cadamba*, Chinese Journal of Animal Nutrition, 31(3): 1061-1071. (李晓琳, 陈婷, 习欠云, 张永亮, 2019, 黄梁木的抗菌消炎作用研究进展, 动物营养学报, 31(3): 1061-1071.)

Liu B.B., Wang L., Zhang J., Li J.B., Zheng H.Q., Chen J., and Lu M.Z., 2014b, *WUSCHEL*-related Homeobox genes in *Populus tomentosa*: diversified expression patterns and a functional similarity in adventitious root formation, BMC Genom., 15: 296.

Liu J.C., Sheng L.H., Xu Y.Q., Li J.Q., Yang Z.N., Huang H., and Xu L., 2014a, WOX11 and 12 are involved in the first-step cell fate transition during *de novo* root organogenesis in *Arabidopsis*, Plant Cell, 26(3): 1081-1093.

Liu R., Wang R., Lu M.Z., and Wang L.Q., 2021, *WUSCHEL*-related homeobox gene *PagWOX11/12a* is involved in drought tolerance through modulating reactive oxygen species scavenging in poplar, Plant Signal. Behav., 16(3): 1866312.

Matsumoto N., and Okada K., 2001, A homeobox gene, *PRESSED FLOWER*, regulates lateral axis-dependent development of *Arabidopsis* flowers, Genes Dev., 15(24): 3355-3364.

Minh-Thu P.T., Kim J., Chae S., Jun K.M., Lee G.S., Kim D.E., Cheong J., Song S., Nahm B., and Kim Y.K., 2018, A WUSCHEL homeobox transcription factor, OsWOX13, enhances drought tolerance and triggers early flowering in rice, Mol. Cells, 41(8): 781-798.

Pandey A., and Negi P.S., 2016, Traditional uses, phytochemistry and pharmacological properties of *Neolamarckia cadamba*: a review, J. Ethnopharmacol., 181: 118-135.

Park S.O., Zheng Z.G., Oppenheimer D.G., and Hauser B.A., 2005, The *PRETTY FEW SEEDS2* gene encodes an *Arabidopsis* homeodomain protein that regulates ovule development, Development, 132(4): 841-849.

Rathour M., Sharma A., Kaur A., and Upadhyay S.K., 2020, Genome-wide characterization and expression and co-expression analysis suggested diverse functions of *WOX* genes in bread wheat, Heliyon., 6(12): e05762.

Romera-Branchat M., Ripoll J.J., Yanofsky M.F., and Pelaz S., 2013, The *WOX13* homeobox gene promotes replum formation in the *Arabidopsis thaliana* fruit, Plant J., 73(1): 37-49.

Sakakibara K., Reisewitz P., Aoyama T., Friedrich T., Ando S., Sato Y., Tamada Y., Nishiyama T., Hiwatashi Y., Kurata T., Ishikawa M., Deguchi H., Rensing S., Werr W., Murata T., Hasebe M., and Laux T., 2014, *WOX13*-like genes are required for reprogramming of leaf and protoplast cells into stem cells in the moss *Physcomitrella patens*, Development, 141(8): 1660-1670.

Shimizu R., Ji J., Kelsey E., Ohtsu K., Schnable P.S., and Scanlon M.J., 2009, Tissue specificity and evolution of meristematic WOX3 function, Plant Physiol., 149(2): 841-850.

Suer S., Agusti J., Sanchez P., Schwarz M., and Greb T., 2011, *WOX4* imparts auxin responsiveness to cambium cells in *Arabidopsis*, Plant Cell, 23(9): 3247-3259.

Tvorogova V.E., Krasnoperova E.Y., Potsenkovskaia E.A., Kudriashov A.A., Dodueva I.E., and Lutova L.A., 2021, What does the WOX say? review of regulators, targets, partners, Mol. Biol. (Mosk), 55(3): 362-391.

Ueda M., Zhang Z.J., and Laux T., 2011, Transcriptional activation of *Arabidopsis* axis patterning genes *WOX8/9* links zygote polarity to embryo development, Dev. Cell, 20(2): 264-270.

van Der Graaff E., Laux T., and Rensing S.A., 2009, The WUS homeobox-containing (WOX) protein family, Genome Biol., 10(12): 248.

Vandenbussche M., Horstman A., Zethof J., Koes R., Rijpkema A.S., and Gerats T., 2009, Differential recruitment of WOX transcription factors for lateral development and organ fusion in *Petunia* and *Arabidopsis*, Plant Cell, 21(8): 2269-2283.

Wang L.Q., Li Z., Wen S.S., Wang J.N., Zhao S.T., and Lu M.Z., 2019, *WUSCHEL*-related homeobox gene *PagWOX11/12a* responds to drought stress by enhancing root elongation and biomass growth in poplar, J. Exp. Bot., 71(4): 1503-1513.

Wang L.Q., Wen S.S., Wang R., Wang C., Gao B., and Lu M.Z., 2021, *PagWOX11/12a* activates *PagCYP736A12* gene that facilitates salt tolerance in poplar, Plant Biotechnol. J., 19(11): 2249-2260.

Wang X., Long J.M., Dong T.T., Zheng D.J., Zhang L.D., and Peng C.C., 2021, Establishment of vascular ti-

ssue cells capture system by laser microdissection in *Neolamarckia cadamba*, Guihaia, 41(8): 1226-1236. (王雪, 龙健梅, 董甜甜, 郑丹菁, 张立定, 彭昌操, 2021, 黄梁木维管组织细胞激光显微切割技术体系建立, 广西植物, 41(8): 1226-1236.)

Wolbang C.M., Chandler P.M., Smith J.J., and Ross J.J., 2004, Auxin from the developing inflorescence is required for the biosynthesis of active gibberellins in barley stems, Plant Physiol., 134(2): 769-776.

Wu X.L., Dabi T., and Weigel D., 2005, Requirement of homeobox gene *STIMPY/WOX9* for *Arabidopsis* meristem growth and maintenance, Curr. Biol., 15(5): 436-440.

Yamaguchi-Shinozaki K., and Shinozaki K., 1994, A novel *cis*-acting element in an *Arabidopsis* gene is involved in responsiveness to drought, low-temperature, or high-salt stress, Plant Cell, 6(2): 251-264.

Yang Z.E., Gong Q., Qin W.Q., Yang Z.R., Cheng Y., Lu L.L., Ge X.Y., Zhang C.J., Wu Z.X., and Li F.G., 2017, Genome-wide analysis of *WOX* genes in upland cotton and their expression pattern under different stresses, BMC Plant Biol., 17(1): 1-17.

Zhang D., Li J.J., Zhang M.J., Bao Y.T., Yang X., Xu W.Y., Ouyang K.X., and Chen X.Y., 2018, Selection and validation of reference genes for quantitative RT-PCR analysis in *Neolamarckia cadamba*, Chinese Bulletin of Botany, 53(6): 829-839. (张登, 李景剑, 张梦洁, 包钰韬, 杨霄, 徐武云, 欧阳昆唏, 陈晓阳, 2018, 黄梁木实时荧光定量 PCR 分析中内参基因的选择, 植物学报, 53(6): 829-839.)

Zhang J., Eswaran G., Alonso-Serra J., Kucukoglu M., Xiang J.L., Yang W.B., Elo A., Nieminen K., Damén T., Joung J.G., Yun J.Y., Lee J.H., Ragni L., Barbier de Reuille P., Ahnert S.E., Lee J.Y., Mähönen A.P., and Helariutta Y., 2019, Transcriptional regulatory framework for vascular cambium development in *Arabidopsis* roots, Nat. Plants, 5(10): 1033-1042.

Zhang Y.X., Wu R.H., Qin G.J., Chen Z.L., Gu H.Y., and Qu L.J., 2011, Over-expression of *WOX1* leads to defects in meristem development and polyamine homeostasis in *Arabidopsis*, J. Integr. Plant Biol., 53(6): 493-506.

Zhao X.L., Hu X.D., Ouyang K.X., Yang J., Que Q.M., Long J.M., Zhang J.X., Zhang T., Wang X., Gao J.Y., Hu X.Q., Yang S.Q., Zhang L.S., Li S.F., Gao W.J., Li B.P., Jiang W.K., Nielsen E., Chen X.Y., and Peng C.C., 2022, Chromosome-level assembly of the *Neolamarckia cadamba* genome provides insights into the evolution of cadambine biosynthesis, Plant J., 109(4): 891-908.

Zhou X.M., Guo Y.Y., Zhao P., and Sun M.X., 2018, Comparative analysis of *WUSCHEL*-related homeobox genes revealed their parent-of-origin and cell type-specific expression pattern during early embryogenesis in tobacco, Front. Plant Sci., 9: 311.

Zhu J.H., Shi H.Z., Lee B.H., Damsz B., Cheng S.E., Stirm V., Zhu J.K., Hasegawa P.M., and Bressan R.A., 2004, An *Arabidopsis* homeodomain transcription factor gene, *HOS9*, mediates cold tolerance through a *CBF*-independent pathway, Proc. Natl. Acad. Sci. USA, 101(26): 9873-9878.

(责任编辑 甘凤琼)
(实习编辑 李金妮)

中国科学引文数据库(CSCD)核心库入选期刊
北大《中文核心期刊要目总览》核心期刊
中国科技期刊全文数据库(CNKI)核心期刊
中国科技论文统计源核心期刊

ISSN 1674-568X
CN 45-1369/Q

基因组学与应用生物学

GENOMICS AND APPLIED BIOLOGY

Jiyinzuxue Yu Yingyong Shengwuxue

澄黄滨珊瑚 /*Porites lutea*

微信公众号
genomics1982

官方网站
gxnb.cbpt.cnki.net

扫一扫，获取更多资讯

为基因组时代的理论与应用生物学提供服务的高品质学术期刊
A High-Quality Scientific Periodical Dedicated to Theoretical and Applied Biology in the Genomic Era

2022 年 8 月
第 41 卷 第 8 期
Vol.41 No.8

基因组学与应用生物学
ISSN 1674-568X
CN 45-1369/Q
1982年创刊，月刊
第41卷，第8期，2022年8月25日
主管
广西大学
主办
广西大学
主编
冯家勋 博士
名誉主编
朱玉贤 院士
执行主编
陈玲玲 博士
出版
广西西大传媒有限公司
地址：广西南宁市大学东路100号广西大学西校园
邮编：530004
电话：0771-3239102
网址：https://gxnb.cbpt.cnki.net
邮箱：571388455@qq.com
责任编辑：甘凤琼 庞晓鑫
蹇 慧 罗厚枚
实习编辑：李金妮 王伟莉
封面：庞芳洲
印刷
广西民族印刷包装集团有限公司
国内发行
邮发代号：48-213
国内定价：￥60.00
国外发行
国外定价：$60.00

Genomics and Applied Biology
ISSN 1674-568X
CN 45-1369/Q
Started in 1982, Monthly
Vol.41, No.8, August 25th, 2022
Authorities-in-Charge
Guangxi University
Sponsored by
Guangxi University
Editor-in-Chief
Feng J.X., Ph.D.
Honorary Editor-in-Chief
Zhu Y.X., Academician
Executive Editor-in-Chief
Chen L.L., Ph.D.
Published by
Guangxi Xida Media Co., Ltd
Address: The Western Campus, Guangxi University, 100 Daxue East Road, Nanning, Guangxi
Postcode: 530004
Telephone: 0771-3239102
Website: https://gxnb.cbpt.cnki.net
E-mail: 571388455@qq.com
Chief editor: Gan F.Q., Pang X.X.
Jian H., Luo H.M.
Internship editor: Li J.N., Wang W.L.
Cover: Pang F.Z.
Printed by
Guangxi Minzu Printing and Packing Group Co., Ltd
Circulated by Domestic
Postal distributing code: 48-213
Domestic subscription price: RMB ￥60.00
Circulated by Abroad
International subscription price: US$60.00

＊＊

版权转让与文责声明

投稿论文必须注明谁是通信作者。本刊视通信作者为投稿论文的责任作者，保证所有的作者都看过并同意论文的内容，都同意在论文上的署名及其排序，也同意将其投给《基因组学与应用生物学》刊物。如编辑部需要，同意提供有关验证论文的试验结果所必需的材料和方法。

在投稿论文发表之前，投稿稿件是编辑部的特权文件。通信作者要保证该论文内容未在其它任何期刊、报纸、电子网络等媒介发表过，也不得向新闻界或大众公开，没有知识产权争议。

投稿论文的全部作者同意并确认自将本论文手稿投至《基因组学与应用生物学》之时起，该论文的全部署名作者及其所在单位同意将其版权(包括电子版权)转让给《基因组学与应用生物学》编辑部。并同意《基因组学与应用生物学》期刊中约定的作者投稿指南中涉及的关于版权与文责的全部内容。

本刊已被中国知网等数据库全文收录，并已加入中国知网优先数字出版平台。论文一经录用后，如无特别声明，将视为作者许可本刊使用此文的发表权、复制权、发行权、信息网络传播权，同时许可本刊转授第三方使用。

《基因组学与应用生物学》编辑部

基因组学与应用生物学
Genomics and Applied Biology

第41卷，第8期，2022年8月
Vol.41，No.8，August，2022

基因组学与应用生物学 第41卷，第8期，2022年8月
Genomics and Applied Biology Vol.41，No.8，August，2022

目 次

基因组学与应用生物学 第41卷，第8期，2022年8月
Genomics and Applied Biology Vol.41，No.8，August，2022

欢迎订阅 2022 年
《基因组学与应用生物学》

连续7次被CSCD核心库收录、
连续5次入编北大《中文核心期刊要目总览》

澄黄滨珊瑚
Porites lutea

■ 图片 / 文字：黄雯 / 冯逸
Picture / Text：Huang Wen / Feng Yi

澄黄滨珊瑚（*Porites lutea*）是滨珊瑚科（Poritidae）的造礁石珊瑚。群体为团块状、半球状或钟状，常显现奶油色或褐色，其表面常见不规则的块状或瘤状突起。珊瑚杯浅，网眼状，杯间共骨薄，直径1~1.5 mm。雌雄异体，生殖方式为产卵排放型，扩散能力较强，一般在春季产卵。作为团块状的造礁石珊瑚，它相对于分枝状珊瑚具有更宽的生态位，可以适应较为恶劣的生存环境，分布范围十分广泛，遍布热带和亚热带的印度 - 太平洋珊瑚礁区，是我国大部分珊瑚礁分布海域的优势种之一。澄黄滨珊瑚作为理想的研究材料常被用于开展珊瑚群体遗传学和环境适应能力的研究，同时也被广泛应用于高分辨率古气候反演和海平面变化规律的记录，因此备受国内外生态学和地质学研究人员的关注。

Porites lutea, a scleractinian coral of Poritidae family, forms massive, hemispherical mounds or helmet-shaped colonies. The color is usually cream or brown. The surface has blocky or tuberculate protrusions irregularly. The corallites are shallow and have thin walls, 1~1.5 mm in diameter. It is dioecious spawning coral with strong larval dispersal ability, and its spawning typically occurs in spring. As a massive coral, it has a wider ecological niche than branching coral and can adapt to harsh environment. *P. lutea* is widely distributed throughout the tropical and subtropical Indo-Pacific coral reef area, and it is one of the dominant species in most coral reef distribution areas of China. *P. lutea* is usually used for the study on population genetics and environmental adaptability, as well as for high-resolution paleoclimatic reconstruction and record of sea-level fluctuations. As an ideal research material, it has attracted a lot of attention from ecologists and geologists at home and abroad.

ISSN 1674 – 568X
CN 45 – 1369/Q
邮发代号：48–213
海外发行：DK45010
国内定价：￥60.00
国际定价：$60.00

ISSN 1674-568X
08>
9 771674 568226